

**The Effects of Perfluoroalkyl Compounds on In Ovo Toxicity and Hepatic mRNA
Expression in the Domestic Chicken (*Gallus gallus domesticus*)**

Jason O'Brien

Thesis submitted to the
Faculty of Graduate and Postdoctoral Studies
in partial fulfilment of the requirements for the
Ph.D. degree in Biology, Specialization in Chemical and Environmental Toxicology

Department of Biology
Faculty of Science
University of Ottawa

April 28, 2011

Abstract

Perfluoroalkyl compounds (PFCs) are a group of chemical surfactants most notably used in non-stick and stain-resistance applications. Due to their wide-spread use and inherent resistance to degradation, several PFCs have become persistent environmental contaminants. Despite the high concentrations of PFCs reported in wild birds and their eggs, very little is known about the toxicological effects they have on avian species.

This thesis investigates the developmental toxicity of PFCs in an avian model species: the domestic chicken (*Gallus gallus domesticus*). Egg injection experiments were performed to assess the *in ovo* toxicity of perfluorooctane sulfonate (technical grade, T-PFOS), perfluorooctanoic acid (PFOA), perfluorodecane sulfonate (PFDS) and perfluoroundecanoic acid (PFUDA). Real-time RT-PCR was then used to measure the transcription of candidate biomarker genes in the liver tissue of day 20 embryos. Candidate genes were selected based on their responsiveness to PFC exposure in previously conducted *in vitro* screening assays. *In ovo* exposure to PFOS resulted in a dose-dependent decrease in embryo pipping success (a measure of hatching success) with an LD₅₀ of 93 µg/g (3.54 µg/g-672,910 µg/g, 95% confidence interval), however the expression of peroxisome proliferator-activated receptor alpha (PPAR α)-regulated genes was not affected in liver tissue as hypothesized. PFOA, PFDS and PFUDA had no effect on the pipping success of chicken embryos. The expression of cytochrome P450 1A4 (CYP1A4) and liver fatty acid binding protein (L-FABP) mRNA increased in embryo liver tissue following *in ovo* exposure to PFUDA but was only statistically significant at 10 µg/g, which is several orders of magnitude higher than concentrations reported in wild bird eggs.

The isomer-specific accumulation of PFOS in chicken embryo livers was also investigated using an in-port derivatization gas-chromatography/mass spectrometry (GC-MS)

method. Prior to incubation, chicken eggs were injected with T-PFOS, composed of 63% linear isomer (L-PFOS) and 37.3% branched isomers. The isomer profiles in day-20 embryo liver tissue showed up to 20% enrichment in the proportion of L-PFOS, compared to T-PFOS, with a corresponding decrease in the proportion of branched isomers. This enrichment was inversely proportional to dose.

Finally, the transcriptional profiles of cultured chicken embryonic hepatocytes (CEH) exposed to either T-PFOS or L-PFOS were compared using Agilent 4x44k Chicken (V2) Gene Expression microarrays. At equal concentrations (10 μ M), T-PFOS altered the expression of significantly more genes (340 genes, >1.5 fold change, false discovery rate adjusted $p < 0.05$) compared to L-PFOS (130 genes). Functional analysis showed that L-PFOS and T-PFOS affected genes involved in lipid metabolism, cellular growth and proliferation, and cell-cell signaling. Pathway and interactome analysis suggested that gene expression may be affected through RXR, oxidative stress response, TP53 signaling, MYC signaling, Wnt/ β -catenin signaling and PPAR γ and SREBP receptors. In all functional categories and pathways examined, T-PFOS had a more pronounced disruptive effect on transcriptional regulation than L-PFOS.

In summary, egg injection experiments showed that T-PFOS (but not linear PFOA, PFDS or PFUDA) may affect the hatching success of the chicken at environmentally relevant concentrations. It was also demonstrated that the accumulation of PFOS in embryonic liver is isomer specific, and leads to an enrichment of L-PFOS. The increased transcriptional disruption caused by T-PFOS in cultured hepatocytes over L-PFOS suggests that the branched isomers may be largely responsible for the toxicological effects of PFOS. Combined, the results from this thesis demonstrate the importance of considering PFOS isomer burdens during risk assessment. In addition, gene expression analysis identified several candidate mechanisms for PFOS toxicity.

Résumé

Les composés perfluoroalkylés (PFC) sont un groupe de surfactants chimiques souvent utilisés dans des produits antiadhésifs et résistants aux taches. Comme ils sont largement utilisés et qu'ils résistent à la dégradation, plusieurs PFC sont devenus des contaminants persistants dans l'environnement. Malgré les concentrations élevées de PFC signalées chez les oiseaux sauvages et leurs œufs, leurs effets toxiques chez les espèces aviaires sont très peu connus.

La présente thèse traite de la toxicité des PFC au cours du développement d'une espèce aviaire modèle : le poulet domestique (*Gallus gallus domesticus*). Nous avons procédé à des injections dans des œufs pour évaluer la toxicité *in ovo* du perfluorooctanesulfonate (qualité technique, PFOS-T), de l'acide perfluorooctanoïque (APFO), du sulfonate de perfluorodécane (SPFD) et de l'acide perfluoroundécanoïque (APFUD). Nous avons alors mesuré la transcription de gènes biomarqueurs candidats dans le tissu hépatique d'embryons de 20 jours par RT-PCR. Nous avons choisi les gènes candidats en fonction de leur sensibilité à une exposition aux PFC dans le cadre d'essais de criblage *in vitro*. L'exposition *in ovo* au PFOS entraînait une réduction dose-dépendante du bêcheage (mesure du succès d'éclosion), avec une DL₅₀ de 93 µg/g (3,54 µg/g-672 910 µg/g, intervalle de confiance à 95 %), mais, contrairement à l'hypothèse que nous avons formulée, l'expression du récepteur alpha activé par les proliférateurs des peroxisomes (PPARα) n'était pas modifiée dans le tissu hépatique. L'APFO, le SPFD et l'APFUD n'avaient pas d'effet sur le bêcheage des embryons de poulet. L'expression des ARNm du cytochrome P450 1A4 (CYP1A4) et de la protéine liant les acides gras du foie (L-FABP) augmentait dans le tissu hépatique embryonnaire après une exposition *in ovo* à l'APFUD, mais cette augmentation n'était statistiquement significative qu'à la concentration de 10 µg/g, une

concentration de plusieurs ordres de grandeur plus élevée que celles signalées dans les œufs des oiseaux sauvages.

Nous avons également étudié l'accumulation des isomères du PFOS dans le foie des embryons de poulet à l'aide de la chromatographie en phase gazeuse couplée à la spectrométrie de masse (CG-SM) avec dérivation dans la chambre d'injection. Avant l'incubation, nous avons injecté des PFOS-T, composés de 63 % d'isomères linéaires (PFOS-L) et de 37,3 % d'isomères ramifiés, dans les œufs de poulet. Le profil d'isomères dans 20 échantillons de tissu hépatique embryonnaire présentait un enrichissement jusqu'à 20 % en la proportion des PFOS-L, comparativement aux PFOS-T, et une diminution correspondante des isomères ramifiés. Cet enrichissement était inversement proportionnel à la dose.

Enfin, à l'aide de micropuces Agilent *4x44k Chicken (V2) Gene expression* servant à déterminer l'expression génique chez le poulet, nous avons comparé le profil de transcription des hépatocytes d'embryon de poulet cultivés exposés aux PFOS-T ou aux PFOS-L. À concentrations égales (10 μ M), les PFOS-T modifiaient l'expression d'un nombre significativement plus élevé de gènes (340 gènes, >1,5 fois plus, taux de faux positifs fixé à $p < 0,05$) que les PFOS-L (130 gènes). Une analyse fonctionnelle a montré que les PFOS-L et les PFOS-T modifiaient l'expression de gènes intervenant dans le métabolisme des lipides, la croissance et la prolifération cellulaires et la signalisation cellule-cellule. L'analyse des voies en jeu et des interactomes a indiqué que l'expression génique pourrait être influencée par les récepteurs suivants : RXR, réponse au stress oxydatif, signalisation TP53, signalisation MYC, signalisation Wnt/ β -caténine, PPAR γ et SREBP. Dans toutes les catégories fonctionnelles et voies examinées, les réponses induites par les PFOS-T étaient plus robustes que celles induites par les PFOS-L.

En résumé, les expériences par injection dans les œufs ont montré que les PFOS-T (mais non l'APFO, le SPFD ou l'APFUD linéaires) peuvent avoir un effet sur le succès d'éclosion des poulets à des concentrations semblables à celles observées dans l'environnement. Nous avons également montré que l'accumulation des PFOS dans le tissu hépatique embryonnaire varie en fonction des isomères et se solde par un enrichissement en PFOS-L. Le fait que les PFOS-T soient responsables d'une augmentation plus élevée de l'activité transcriptionnelle dans les hépatocytes cultivés que les PFOS-L indique que les isomères ramifiés sont probablement largement responsables des effets toxiques des PFOS. Dans l'ensemble, les résultats présentés dans la thèse illustrent l'importance d'étudier le profil des isomères de PFOS dans le cadre d'une évaluation du risque. En outre, l'analyse de l'expression génique a permis de signaler plusieurs mécanismes pouvant intervenir dans la toxicité des PFOS.

Table of Contents

	Page
Abstract	
English.....	ii
French.....	iv
Table of Contents.....	vii
List of Tables.....	x
List of Figures.....	xii
List of Abbreviations.....	xiv
Statement of Contributions	xvii
Acknowledgements.....	xix
Chapter 1: Introduction.....	1
1.1. General introduction to PFCs.....	1
1.2. Structure and properties of PFCs.....	1
1.3. PFC production.....	2
1.4. PFCs are environmentally persistent.....	3
1.4.1. PFCs in the environment.....	3
1.4.2. PFCs in wildlife.....	4
1.4.3. Replacement PFCs.....	6
1.5. Toxicology of PFCs.....	6
1.5.1. Pharmacokinetics.....	6
1.5.2. Toxicity of PFCs in mammals.....	7
1.5.3. Toxicity of PFCs in birds.....	8
1.6. Mechanisms of Toxicity.....	9
1.6.1. PFCs and PPAR α activation.....	9
1.6.2. PPAR α -independent mechanisms.....	10
1.7. Thesis overview.....	13
1.7.1. Rationale.....	13
1.7.2. Research objectives.....	14
Chapter 2: Perfluorooctane Sulfonate (PFOS) Toxicity in the Domestic Chicken (<i>Gallus gallus domesticus</i>) Embryos in the Absence of Effects on Peroxisome Proliferator Activated Receptor Alpha (PPARα)-Regulated Genes.....	17
2.1. Abstract.....	17
2.2. Introduction.....	18
2.3. Materials and methods.....	21
2.3.1. Chemicals.....	21

2.3.2. Egg injection and tissue collection.....	21
2.3.3. Hepatic PFOS concentration.....	23
2.3.4. RNA extraction and cDNA preparation.....	24
2.3.5. Real-time RT-PCR.....	25
2.3.6. Statistical analysis.....	26
2.4. Results.....	27
2.4.1. Effects on pipping success.....	27
2.4.2. Hepatic PFOS concentrations.....	27
2.4.3. PPAR α -regulated genes.....	28
2.5. Discussion.....	28
Chapter 3: Pipping Success and Liver mRNA Expression in Chicken Embryos Exposed <i>in ovo</i> to C₈ and C₁₁ Perfluorinated Carboxylic Acids and C₁₀ Perfluorinated Sulfonate...	37
3.1. Abstract.....	37
3.2. Introduction.....	38
3.3. Materials and methods.....	40
3.3.1. Chemicals.....	40
3.3.2. Egg injection and tissue collection.....	41
3.3.3. Hepatic PFC concentration determination by HPLC/MS/MS.....	42
3.3.4. Sex determination by PCR.....	43
3.3.5. Real-time RT-PCR.....	43
3.4. Results.....	45
3.4.1. Effect of PFCs on pipping success.....	45
3.4.2. Hepatic PFC concentrations.....	45
3.4.3. mRNA expression.....	46
3.5. Discussion.....	46
Chapter 4: Isomer-Specific Accumulation of Perfluorooctane Sulfonate in the Liver of Chicken Embryos Exposed <i>in ovo</i> to a Technical Mixture.....	56
4.1. Abstract.....	56
4.2. Introduction.....	57
4.3. Materials and methods.....	59
4.3.1. Chemicals.....	59
4.3.2. Tissues.....	60
4.3.3. Isomer-specific PFOS determination.....	60
4.3.4. Statistics.....	62
4.4. Results.....	62
4.5. Discussion.....	64
Chapter 5: Technical Grade PFOS is More Transcriptionally Disruptive in Cultured Chicken Embryonic Hepatocytes than Linear PFOS.....	73
5.1. Abstract.....	73
5.2. Introduction.....	74

5.3. Materials and methods.....	76
5.3.1. Chemicals.....	76
5.3.2. Preparation of hepatocyte cultures and dosing.....	76
5.3.3. RNA isolation and quantification.....	77
5.3.4. Microarray hybridization.....	78
5.3.5. Microarray data analysis.....	78
5.3.6. Real-time RT-PCR.....	80
5.4. Results and discussion.....	82
5.4.1. Differentially expressed genes.....	82
5.4.2. PCA and clustering analysis.....	86
5.4.3. Mapping gene IDs to IPA.....	87
5.4.4. Functional analysis.....	87
5.4.5. Canonical pathway mapping.....	90
5.4.6. Interaction networks and potential regulatory molecules.....	91
5.5. Conclusions.....	96
Chapter 6: General Conclusions and Future Directions.....	111
6.1. General Conclusions.....	111
6.2. Future Directions.....	117
References.....	120
Appendix: Supplementary Material.....	137

List of Tables

Table		Page
2.1	Primer and probe nucleotide sequences and their final concentrations in each reaction for real-time reverse transcription polymerase chain reactions	34
2.2	The effect of injecting PFOS into the air cell of chicken embryos prior to incubation on pipping success and hepatic PFOS concentration	35
3.1	Retention time, transitions and compound dependent operation parameters for target compounds and internal standards	51
3.2	Nucleotide sequence and final reaction concentration of each primer and probe used for real-time RT-PCR assays	52
3.3	Hepatic concentration of PFOA, PFUdA and PFDS in day 20 chicken embryos that were exposed to PFCs via egg injection prior to incubation	53
4.1	Abbreviations and chemical formulas of all eleven isomers identified in technical grade PFOS	70
5.1	Number of genes that were differentially expressed in CEH exposed to L-PFOS or T-PFOS	99
5.2	Enriched functional categories for genes differentially expressed due to L-PFOS or T-PFOS exposure in CEH	100
5.3	Significantly enriched canonical pathways for genes that were differentially expressed due to L-PFOS or T-PFOS exposure in CEH	101
5.4	Functional enrichment of interaction networks generated for genes differentially expressed following exposure to L-PFOS or T-PFOS	102
5.5	Molecules from IPA-generated networks that had interactions with four or more PFOS-disregulated genes and were considered to have potential regulatory activity	103
S5.1	List of genes examined for real-time RT-PCR and their gene symbols, accession numbers, and primer and probe sequences	138
S5.2	Detailed list of genes that were differentially expressed following exposure to L-PFOS or T-PFOS	139

List of Tables Continued

Table		Page
S5.3	Comparison of real-time RT-PCR results for changes in mRNA transcription in cultured chicken embryonic hepatocytes for genes determined by microarray analysis to be significantly affected by exposure to L-PFOS or T-PFOS	146
S5.4A	Detailed list of functional enrichment categories, function and their genes, for genes differentially expressed following exposure to L-PFOS 10 μ M	147
S5.4B	Detailed list of functional enrichment categories, function and their genes, for genes differentially expressed following exposure to T-PFOS 10 μ M	152
S5.5A	Detailed list of enriched canonical pathways for genes that were differentially expressed following exposure to L-PFOS 10 μ M	166
S5.5B	Detailed list of enriched canonical pathways for genes that were differentially expressed following exposure to T-PFOS 10 μ M	167
S5.6	Detailed list of potential regulatory molecules and their interactions with genes that were dysregulated by exposure to L-PFOS or T-PFOS	170

List of Figures

Figure		Page
1.1	Perfluorinated compounds (PFCs) have long completely fluorinated carbon chains and various functional groups at the terminal end. A) Perfluorooctane sulfonate (PFOS) and B) perfluorooctanoic acid (PFOA) are the most environmentally prevalent PFCs	16
2.1	Mean fold induction of PPAR α regulated transcripts in chicken embryos exposed in ovo to PFOS prior to incubation	36
3.1	The effect of injecting PFOA, PFUdA and PFDS into chicken eggs prior to incubation on embryonic pipping success	54
3.2	Expression of CYP1A4, CYP1A5, CYP4B1, HMGR, and L-FABP mRNA in liver tissue of chicken embryos exposed to increasing concentrations of A) PFUdA and B) PFDS	55
4.1	Perfluorooctane sulfonate (PFOS) isomer profiles in liver tissue from chicken embryos exposed prior to incubation to various concentrations of technical grade PFOS (T-PFOS)	71
4.2	Profile of branched perfluorooctane sulfonate (PFOS) isomers normalized to total branched isomer content in chicken embryos exposed to various concentrations of technical grade PFOS (T-PFOS)	72
5.1	Venn diagram illustrating the number of genes that were uniquely dysregulated by either L-PFOS or T-PFOS or genes that were affected by both L-PFOS and T-PFOS	104
5.2	Expression of Acs11, Acsbg2, Areg and Gsta3 in sub-pooled CEH following exposure to L-PFOS or T-PFOS	105
5.3	The expression profile of L-PFOS- and T-PFOS-treated samples plotted on three principal components compared to the DMSO control group	106
5.4	Hierarchical Clustering of expression profiles of CEH exposed to L-PFOS, T-PFOS or DMSO vehicle control	107
5.5	One of two IPA-generated interaction networks for genes dysregulated by exposure to T-PFOS 10 μ M	108
5.6	All documented direct (solid line) and indirect (dashed line) interactions from Ingenuity's Knowledge Base between TP53 and genes that were differentially expressed due to exposure to A) L-PFOS or B) T-PFOS at 10 μ M	109

List of Figures continued

Figure		Page
5.7	Direct (solid line) and indirect (dashed line) interactions between genes that were differentially expressed following exposure to PFOS and A) PPAR γ or B) PPAR α .	110
S4.1	Proportion of each perfluorooctane sulfonate (PFOS) isomer recovered in chicken embryo livers relative to the administered dose of technical grade PFOS (T-PFOS)	137
S5.1	Part of the LPS/IL-1 mediated inhibition of RXR function canonical pathway	176
S5.2	IPA generated interaction network for genes that were differentially expressed following L-PFOS 10 μ M	177
S5.3	IPA generated interaction network for genes that were differentially expressed following T-PFOS 10 μ M (1 of 2)	178
S5.4	IPA generated interaction network for genes that were differentially expressed following T-PFOS 10 μ M (2 of 2)	179
S5.5	Expression of HDAC1 in sub-pooled CEH (N=2-3 sub-pools, 6 livers/pool) following exposure to L-PFOS or T-PFOS	180

List of Abbreviations

ACOX	acyl-CoA oxidase
<i>Acat1</i>	acetyl-Coenzyme A acetyltransferase 1
<i>Acsbg2</i>	acyl-CoA synthetase bubble gum family member 2
<i>Acs11</i>	acyl-CoA synthetase long-chain family member 1
AHR	aryl hydrocarbon receptor
<i>Ahsg</i>	alpha-2-HS-glycoprotein
<i>Akr1b1</i>	aldo-keto reductase family 1, member B1
<i>Apoa4</i>	apolipoprotein A-IV
<i>Areg</i>	amphiregulin
BIEN	bifunctional enzyme
<i>Cadm1</i>	cell adhesion molecule 1
CAR	constitutive androstane receptor
CDK4	cyclin-dependent kinase 4
<i>Cdkn2A</i>	cyclin-dependent kinase inhibitor 2A
CEH	chicken embryonic hepatocytes
CFIA	Canadian Food Inspection Agency
CTNNB1	catenin beta 1
<i>Ccng2</i>	cyclin G2
CYP1A4	cytochrome P450 1A4
CYP1A5	cytochrome P450 1A5
CYP4B1	cytochrome P450 4B1
<i>Cyp8B1</i>	cytochrome P450 8B1
DEPC	diethylpyrocarbonate
<i>Dio2</i>	type II iodothyronine deiodinase
DMSO	dimethyl sulfoxide
ECF	electrochemical fluorination
ESI	electrospray ionization
EST	expression sequence tag
FDR	false discovery rate
<i>Fzd4</i>	frazzled 4
GC	gas chromatograph
<i>Gjb1</i>	gap junction protein beta 1
GJIC	gap junctional intercellular communication
GSH	glutathione
GST	glutathione-S-transferase
<i>Gsta3</i>	glutathione-S-transferase alpha 3
<i>Gsta4</i>	glutathione-S-transferase alpha 4
<i>Gsto1</i>	glutathione-S-transferase omega 1
<i>Hdac1</i>	Histone deacetylase 1
HMGCR	3-hydroxy-3-methyl-glutaryl-Coenzyme A reductase
HNF4A	hepatocyte nuclear factor 4 alpha
HPLC	high-performance liquid chromatography
<i>Idi1</i>	isopentenyl-diphosphate delta isomerase 1
<i>Inhba</i>	inhibin, beta A

IPA	Ingenuity Pathway Analysis (software)
L-FABP	liver fatty acid binding protein
L-PFOS	linear perfluorooctane sulfonate
LD ₅₀	median lethal dose
LOAEL	lowest observed adverse effect level
LSI	liver somatic index
LXR	liver X receptor
MDL	method detection limit
<i>Mdm2</i>	murine double minute 2
MPFDS	perfluoro-1-[1,2,3,4- ¹³ C ₄]decane sulfonate
MPFOA	perfluoro- <i>n</i> -[1,2,3,4- ¹³ C ₄]octanoic acid
MPFUdA	perfluoro- <i>n</i> -[1,2- ¹³ C ₂]undecanoic acid
MRM	multiple reaction monitoring
MS	mass spectrometer
<i>Myh6</i>	myosin heavy chain 6
MYC	v-myc myelocytomatosis viral oncogene homolog
N-EtFOSE	N-ethyl-(2-hydroxyethyl)-perfluorooctane sulfonamide
OAT3	organic anion transporter 3
OATP1	organic anion transporting polypeptide 1
P1MHpS	perfluoro-1-methyl-heptane sulfonate
P2MHpS	perfluoro-2-methyl-heptane sulfonate
P3MHpS	perfluoro-3-methyl-heptane sulfonate
P4MHpS	perfluoro-4-methyl-heptane sulfonate
P5MHpS	perfluoro-5-methyl-heptane sulfonate
P6MHpS	perfluoro-6-methyl-heptane sulfonate
P35DMHxS	perfluoro-3,5-dimethyl-hexane sulfonate
P44DMHxS	perfluoro-4,4-dimethyl-hexane sulfonate
P45DMHxS	perfluoro-4,5-dimethyl-hexane sulfonate
P55DMHxS	perfluoro-5,5-dimethyl-hexane sulfonate
PC1	principal component 1
PC2	principal component 2
PC3	principal component 3
PCA	principal component analysis
PCB 126	3,3',4,4',5-pentachlorobiphenyl
PFBS	perfluorobutane sulfonate
PFC	perfluoroalkyl compound
PFCA	perfluorinated carboxylates
PFDA	perfluorodecanoic acid
PFDS	perfluorodecane sulfonate
PFHxS	perfluorohexane sulfonate
PFNA	perfluorononanoic acid
PFOA	perfluorooctanoic acid
PFOS	perfluorooctane sulfonate
PFSA	perfluorinated sulfonates
PFTriA	perfluorotridecanoic acid
PFUdA	perfluoroundecanoic acid

PKT	peroxisomal 3-ketoacyl thiolase
PPAR	peroxisome proliferator activated receptor
PPAR α	peroxisome proliferator-activated receptor alpha
PPAR γ	peroxisome proliferator-activated receptor gamma
PXR	pregnane X receptor
RT-PCR	real-time reverse-transcription polymerase chain reaction
RXR	retinoid X receptor
SPE	solid phase extraction
SREBP1	Sterol Regulatory Element Binding Protein 1
T-PFOS	technical-grade perfluorooctane sulfonate
T3	triiodothyronine
T4	thyroxine
TBAH	tetrabutylammonium hydroxide 30 hydrate
TP53	tumor protein p53

Statement of Contributions

Chapter 2

Experimental design, results analysis and manuscript preparation

Performed by:

Jason O'Brien
Robert Letcher
Sean Kennedy

Egg injections, dissections and real-time RT-PCR

Jason O'Brien
Amanda Carew

HPLC-MS/MS preparation and analysis

Jason O'Brien
Shaogang Chu

Chapter 3

Experimental design, results analysis and manuscript preparation

Jason O'Brien
Doug Crump
Robert Letcher
Sean Kennedy

Egg Injections and dissections

Jason O'Brien
Kristina McLaren
Viengtha Vongphachan

Real-time RT-PCR

Jason O'Brien
Lukas Mundy

Sexing PCR

Jason O'Brien

HPLC-MS/MS preparation and analysis

Lukas Mundy
Shaogang Chu

Chapter 4

Experimental design, results analysis and manuscript preparation

Jason O'Brien
Robert Letcher
Sean Kennedy

GC-MS preparation and analysis

Shaogang Chu

Statement of Contributions Continued

Chapter 5

Experimental design, results analysis and manuscript preparation	Jason O'Brien Carole Yauk Sean Kennedy
Chicken embryonic hepatocyte culture	Jason O'Brien Doug Crump Stephanie Jones Lukas Mundy Aislynn Austin
Microarray hybridizations	Jason O'Brien
Microarray data pre-processing	Andrew Williams
RT-PCR	Jason O'Brien Aislynn Austin Viengtha Vongphachan Suzanne Chiu

Acknowledgements

Environment Canada's National Wildlife Research Centre is filled to the brim with many kind and intelligent people. I'd like to thank everyone there who I've had the pleasure of meeting for their friendship and support. I would especially like to express my appreciation to all the members of the Kennedy lab, past and present who made it fun and interesting to work (and play): Cristina Cassone, Matt Cwinn, Caroline Egloff, Reza Farmahin, Jessica Head, Jessica Hervé, Nathan Hickey, Gillian Manning, Michio Watanabe and Kim Williams. I'd especially like to acknowledge Aislynn Austin for her assistance with RT-PCR assay optimizations, Kristina McLaren and Amanda Carew for their efforts on the differential display project (that unfortunately didn't make it into this thesis), Stephanie Jones and Suzanne Chiu for their technical advice and support, Lukas Mundy for his help with the HPLC prep work and several RT-PCR experiments, Viengtha Vongphachan for her contributions to the egg injection experiments and microarray validation, and a very special thank you to Doug Crump for sharing his thoughts and advice on countless occasions. I would also like to apologize to the staff of Popcorn Karaoke Bar for all of the previously mentioned people. To the members of the Letcher lab: thanks for being great office- and lab-mates. Thanks to Shaogang Chu for his chromatography and mass spec work. I also would like to extend my gratitude to Brian Collins for sharing his statistical expertise. I'm very grateful to our collaborators at Health Canada's Environmental Health Centre in the Yauk lab, Andrew Williams, Lynn Berndt-Weis, Andrea Rowan Carroll, and Julie Buick, for training me and allowing me to use their microarray facility and expertise.

Thank you to all of my friends and family, particularly my parents Fay and Larry O'Brien, for your love, encouragement and support. I'd especially like to thank Joanna James, whose understanding, encouragement and companionship helped me endure the many long days and nights of study. Thanks for being my homework lady.

I'd like to thank my committee members, Tom Moon, and Paul White, for their guidance, Carole Yauk for her help with the microarray analysis and manuscript prep, and Rob Letcher for his many collaborations and encouragements. Finally, and most importantly, to my supervisor Sean Kennedy: Without your endless support, patience, faith in me, and your friendship, I surely would not have come this far. Words cannot express my gratitude.

Chapter 1

Introduction

1.1. General introduction to PFCs

Perfluoroalkyl compounds (PFCs) are a class of fluorochemicals used for a variety of commercial and industrial products including stain and soil repellents, paper coatings, semi-conductors, metal plating, fire fighting foams and insecticides (Kissa, 2001; Lau *et al.*, 2007). Large-scale use of PFCs is a relatively new phenomenon, with PFC production steadily increasing over the last fifty years, particularly in the last two decades. Wide-spread PFC use has led to an increase in the detection of these compounds in the environment as well as in human and wildlife tissues. Due to this increased presence, much research has been carried out in recent years to understand the environmental fate of PFCs and the toxicological effects caused by exposure to this class of chemical.

1.2. Structure and properties of PFCs

Structurally, PFCs are composed of a completely fluorinated carbon backbone, generally four to fourteen carbon atoms long, and have a variety of functional groups at the terminal end (Figure 1.1). The fluorocarbon tail gives PFCs their hydrophobic characteristics, whereas the charged or highly polar functional group grants oleophobic properties to the end of the molecule. This amphipathic nature gives these chemicals very low surface tensions, making them ideal surfactants for a multitude of applications.

PFCs are highly stable compounds. The extreme electronegativity of fluorine makes the carbon-fluorine bond one of the strongest in organic chemistry. As a result, the PFC fluorocarbon tail is extremely resistant to degradation by acids, bases, or oxidizing agents (Prescher *et al.*,

1985), and is dehalogenated only in very rare conditions (Chen & Zhang, 2006; Hori *et al.*, 2006; Ochoa-Herrera *et al.*, 2008). The non-fluorocarbon functional groups, however, are susceptible to nucleophilic, oxidative or reductive attack and are often terminally degraded to either carboxylate or sulfonate moieties (Dimitrov *et al.*, 2004).

1.3. PFC production

PFCs are synthesized by two main processes; electrochemical fluorination (ECF) and telomerization. In the ECF process all of the hydrogen atoms of a hydrocarbon precursor are replaced by fluorine atoms by applying an electric current. The high input of energy needed for this reaction can lead to fragmentation and rearrangement of the original carbon skeleton causing the end product of this method to be a mixture of linear and branched isomers as well as shorter and longer carbon-chain impurities. The second method involves the telomerization of tetrafluoroethylene sub-units. The end products of this method are always linear, even-chained alcohols. The terminal alcohol can then be replaced by other functional groups as required.

Because PFCs with carbon chain-lengths of eight have optimal surfactant properties, perfluorooctane sulfonate (PFOS) and perfluorooctanoic (PFOA) acid, and their related precursors, were the primary components of most PFC products. Estimated global production for PFOS reached 3,500 metric tons in 2000 and 1,200 tons in 2004 for PFOA (Lau *et al.*, 2007). However, due largely to the detection of high levels in environmental media, wildlife samples and even human tissue, the leading manufacturer of PFOS and PFOA, 3M Company, announced the voluntary phase-out of these two compounds beginning in 2000. Global output of PFOS and PFOA has since declined, although several international suppliers continue to produce these PFCs (OECD, 2002).

To fill the market demand following the phase-out of PFOS and PFOA, perfluorochemical manufacturers have turned to similarly structured PFCs as replacements. The most immediate replacements have been shorter or longer chained equivalents to the phased out products. For example the four-carbon perfluorobutane sulfonate (PFBS) has been used instead of PFOS in several products and the six-carbon perfluorohexanoic acid (PFHxA) as a replacement for PFOA (Van de Vijver *et al.*, 2005).

1.4. PFCs are environmentally persistent

1.4.1. PFCs in the environment

PFCs have been found in various environmental matrices. Detectable levels of PFCs were reported in surface waters, drinking water, rain water, air, dust in homes and workplaces, sewer sludge, soil and sediments from various locations around the world (Boulanger *et al.*, 2004; Emmett *et al.*, 2006; Hansen *et al.*, 2002; Houde *et al.*, 2006). Although typically detected in the parts per trillion range, concentrations in the parts per million level have been reported in regions near manufacturing facilities, areas of accidental release and sites where fire-fighting foams have been used (Bao *et al.*, 2010; Boulanger *et al.*, 2004; Moody *et al.*, 2002).

As expected, PFCs are detected in urban areas where there is high degree of commercial and industrial PFC product use. However, many PFCs have also been found in more remote regions of the globe, including in distant ocean waters and in the Arctic (Yamashita *et al.*, 2005). There are several hypotheses for why these anthropogenic compounds are observed in locations so far from where they are produced and used. Water is believed to be the primary environmental compartment in which PFCs reside and therefore thought to be the main media by which they are globally transported. Evidence that PFCs are globally transported by ocean currents includes the

detection of PFCs in ocean waters in decreasing concentrations from coastal to offshore areas and trace amounts being detected in deep sea waters (Yamashita *et al.*, 2005; Prevedouros *et al.*, 2006). Another theory for global PFC transportation involves atmospheric transportation of volatile precursor compounds. Most of the dominant PFCs detected in the environment, such as PFOS and PFOA, have low volatility at normal temperature and air pressure. In contrast, some of their precursors are highly volatile at normal conditions and have been detected in the troposphere (D'eon *et al.*, 2006; Ellis *et al.*, 2004; Martin *et al.*, 2006). In the atmosphere, precursors can be oxidized by hydroxyl radicals to form less volatile compounds or can be degraded by abiotic or biotic means once they are precipitated (Dinglasan *et al.*, 2004; Ellis *et al.*, 2004). For example, the highly volatile N-ethyl-(2-hydroxyethyl)-perfluorooctane sulfonamide (N-EtFOSE) can be aerobically reduced to form PFOS (Rhoads *et al.*, 2008).

1.4.2. PFCs in wildlife

Some PFCs are known for their ability to bioaccumulate in wildlife and are suspected of biomagnify up food chains (Conder *et al.*, 2008). PFCs have been reported in organisms at all levels of food webs, particularly in aquatic environments. Generally, low concentrations are found in organisms at low trophic levels. Concentrations in the low ng/g (all tissue concentrations in this chapter are reported in wet weight) level were reported for benthic algae, zooplankton, and small invertebrates (Kannan *et al.*, 2005; Tomy *et al.*, 2004; Martin *et al.*, 2004b). For higher invertebrates, PFOS concentrations as high as 437 ng/g have been reported in molluscs, 530 ng/g in shrimp and 877 ng/g in crab (Kannan *et al.*, 2002b; Van de Vijver *et al.*, 2003).

Moderate PFC concentrations have been reported for various species of freshwater and saltwater fish. PFOS and PFOA levels near 100 ng/g were found in fish from various locations around the world, alewife from Lake Ontario, Canada (Martin *et al.*, 2004b), rainbow smelt from the North American Great Lakes (Martin *et al.*, 2004b), Chinook salmon from Michigan, USA (Kannan *et al.*, 2005), bib from the North Sea (Hoff *et al.*, 2003), blue fin tuna from the Mediterranean Sea (Giesy & Kannan, 2001), and bluegill in Lake Biwa, Japan (Taniyasu *et al.*, 2003). Low ng/g levels of PFCs have also even been detected in fish from arctic waters (Tomy *et al.*, 2004). More highly elevated concentrations have also been reported from several locations. Carp in Belgium were found to have PFOS levels as high as 934 ng/g (Hoff *et al.*, 2005; Taniyasu *et al.*, 2003). Eels in Tokyo Bay, Japan, had 1387 ng/g PFOS in the liver (Taniyasu *et al.*, 2003). One of the highest PFOS concentration ever reported, 3250 ng/g, was found in ornate jobfish in Okinawa, Japan, near an electric power plant and a military base, where fire-fighting exercises are performed (Taniyasu *et al.*, 2003).

Due to their high trophic level, fish eating animals are at particular risk of PFC exposure. The highest concentrations reported in mammals were found in the plasma and liver of bottlenose dolphins in the USA coast and Arctic polar bears. The highest concentration found in bottlenose dolphins was 1,315 ng/g of PFOS (Houde *et al.*, 2005). Polar bears are the top predator of the Arctic food web. Their diets consist mostly of seals and fish. Arctic seals, which mainly feed on fish, also have reportedly high PFC concentrations in their tissues (mostly liver, >100 ng/g in many cases) (Houde *et al.*, 2006). The highest level reported in polar bear tissue was 3,100 ng/g of PFOS in the liver (Martin *et al.*, 2004a).

Fish-eating birds are also very susceptible to high concentrations of PFCs through dietary exposure. Some of the highest concentrations in birds from the literature were 650 ng/g PFOS in

the liver of common cormorants (Taniyasu *et al.*, 2003), 1625 ng/g PFOS in whole blood of great tits in Europe (Dauwe *et al.*, 2007) and 2570 ng/g PFOS in the plasma of American bald eagles (Giesy & Kannan, 2001). PFOS levels as high as 196, 220 and 669 ng/g have also been reported in glaucous gull, cormorant and guillemot eggs, respectively suggesting that PFCs are transferred during egg laying (Holmstrom *et al.*, 2005; Kannan *et al.*, 2001; Verreault *et al.*, 2005).

1.4.3. Replacement PFCs

Short and long chain PFCs have also been detected in wild bird tissue, although concentrations are not as high as those reported for PFOS and PFOA. Herring gull eggs from the North America Great Lakes had approximately 30 ng/g of each the eleven-carbon perfluoroundecanoic acid (PFUdA) and the thirteen-carbon perfluorotridecanoic acid (PFTriA) (Gebbinck *et al.*, 2009). Glaucous gulls from Arctic Norway had 74.4 ng/g of PFUdA and 15.1 ng/g of the PFTriA in the plasma (Verreault *et al.*, 2005). Gulls from Japan contained 34 ng/g of the six-carbon perfluorohexane sulfonate (PFHxS) in liver tissue (Kannan *et al.*, 2002a). Mallards from Tokyo bay were found to have hepatic PFBS concentrations of 45 ng/g (Taniyasu *et al.*, 2003). The highest concentrations reported for long- or short-chain PFCs in birds was 675 ng/g PFUdA in the eggs of parrotbills from Korea (Yoo, 2008) followed by 140 ng/g PFUdA in the eggs of herring gulls from Norway (Lofstrand *et al.*, 2008).

1.5. Toxicology of PFCs

1.5.1. Pharmacokinetics

Most PFCs are easily absorbed orally, are not metabolized and are poorly eliminated (Andersen *et al.*, 2008). In the body, PFCs are primarily distributed to the liver, then the blood

serum and kidneys. They have also been detected in brain tissues following laboratory exposure, providing evidence that they can cross the blood-brain barrier (Austin *et al.*, 2003; Sato *et al.*, 2009). In these tissues they bind primarily to proteins, particularly to fatty acid binding proteins, lipoproteins and albumin (Jones *et al.*, 2003; Luebker *et al.*, 2002). The accumulation rates of PFCs appear to be dose-dependent. Kudo *et al.* (2007) observed that higher proportions of the total administered PFOA accumulated in the liver at low doses, and suggested that saturation of binding sites or activation of binding components may be responsible for this dose-dependency. Kinetic rates also seem to be dependent on the chain-length of the PFC. Short-chain molecules have shorter elimination half-lives than long-chain PFCs (Ohmori *et al.*, 2003). There are also large inter-species differences in elimination rates. For example, the elimination half-life of PFOS in rats is 100 days whereas in humans it is 5.4 years (Lau *et al.*, 2007) and in mallard ducks it is a mere 20 days (Newsted *et al.*, 2006). Sex dependent differences in elimination rates for some PFCs have also been observed. In female rats the elimination half-life of PFOA is only 2-4 hours. In males it is 4-6 days (Kemper & Jepson, 2003). The mechanism for the different uptake and elimination rates of PFCs between species and sexes is unclear but may involve the organic anion transporters OATP1 and OAT3, which have been shown to affect PFC transport (Katakura *et al.*, 2007), and are differentially expressed between sexes in rats (Buist *et al.*, 2002).

1.5.2. Toxicity of PFCs in mammals

Exposure to PFOS in rodent and primate studies resulted in reduced body weight, increased liver weight, reduced serum cholesterol and triiodothyronine (T3) levels, hepatocellular and thyroid follicular adenomas, and mortality (Kennedy *et al.*, 2004; Lau *et al.*, 2007; OECD, 2002; Seacat *et al.*, 2002; Seacat *et al.*, 2003). Similar effects were seen in

mammals exposed to PFOA, with the addition of Leydig cell and pancreatic tumors, although decreased cholesterol was not observed (Biegel *et al.*, 1995; Butenhoff *et al.*, 2002; Kennedy *et al.*, 2004). Several of these adverse toxic effects such as hepatocyte hypertrophy or reduced serum cholesterol and T3 levels were observed in rats and cynomolgus monkeys with liver PFOS burdens of 21.4 and 23.8 µg/g, respectively; concentrations that are within one order of magnitude of the highest concentrations reported in wild animals.

Reproductive studies with rodent models show that gestational exposure to PFOS causes an increase in the occurrence of cleft palate, edema, and cardiac abnormalities as well as slight reductions in fetal weight and fetal survival (Lau *et al.*, 2004; OECD, 2002). The most notable effect, however, was the sharp decrease in neonate survival observed during the first week following birth. Lau *et al.* (2003) observed that although many fetuses from their high dose-group (maternal exposure of 10 mg/kg/day during gestation) survived to term, all neonate rats died within the first day after birth. This trend was also observed, although not as severe, in animals from lower dose-groups that had associated liver PFOS concentrations of 86.5 µg/g, which is between one to two orders of magnitude of wildlife levels.

1.5.3. Toxicity of PFCs in birds

Acute and chronic exposure to PFOS in mallards and bobwhite quails caused decreased body weight, increased liver mass and mortality, although liver and serum concentrations associated with mortality and other adverse toxic effects were much greater than what has been reported in avian wildlife (Newsted *et al.*, 2006; Newsted *et al.*, 2007). Reproductive toxicity, however, was observed at relatively low concentrations in several avian studies. Both Molina *et al.* (2006) and Yanai *et al.* (2008) reported reduced hatching success of domestic chicken eggs

injected with PFOS or PFOA at concentrations comparable to or less than what has been reported in wild bird eggs. Reduced hatching success was accompanied by histological aberrations including periportal inflammation, bile duct hyperplasia and hepatocyte necrosis at doses as low as 1.0 µg/g. Newsted *et al.* (2007) also noted a significant reduction in the survival of hatchling quails with liver PFOS burdens of 5.5 µg/g during their reproductive study. Other egg injection studies performed using the domestic chicken as a model species suggest that PFCs may also be developmentally immunotoxic or neurotoxic to birds. Peden-Adams *et al.* (2008) reported an inhibited immune response and an increase in the frequency and severity of brain asymmetry in chicken hatchlings exposed *in ovo* to 1.0 µg/g PFOS. Pinkas *et al.* (2010) further demonstrated the developmental neurotoxicity of both PFOS and PFOA when they showed that *in ovo* exposure to either compound impaired imprinting behaviour in hatchling chickens.

1.6. Mechanisms of toxicity

1.6.1. PFCs and PPAR α activation

One of the primary mechanisms by which PFCs can cause toxicity has been proposed to be through agonism of the peroxisome proliferator-activated receptor alpha (PPAR α). PPAR α is a lipid sensing nuclear receptor that is responsible for regulating the transcription of genes involved in peroxisome proliferation, lipid metabolism, cholesterol metabolism and cell cycle. Due to the structural resemblance of PFOS to fatty acids, PFOS is thought to bind to PPAR α and disturb this regulatory activity (Vanden Heuvel *et al.*, 2006). Several studies with rats and mice have shown that PFOS and PFOA can cause peroxisome proliferation (Berthiaume & Wallace, 2002; Ikeda *et al.*, 1985). Activation of PPAR α is one of the first key steps required for peroxisome proliferation to occur. Once initiated, peroxisome proliferation leads to increased

oxidative metabolism of fatty acids, and therefore increased oxidative stress within the cell and ultimately to DNA damage, mutation and cancer. Luciferase reporter assays have also shown that PFOS and PFOA are able to activate PPAR α , although they are relatively weak activators compared to the native ligands for this receptor (Vanden Heuvel *et al.*, 2006).

The ability of short and long chain PFCs to induce peroxisome proliferation via PPAR α has also been explored. Rats treated with PFBS, PFHxS or PFOS all had significantly increased acyl-CoA oxidase (ACOX) activity. ACOX catalyzes the first rate limiting step in peroxisomal β -oxidation, the primary lipid metabolizing process within the membrane of the peroxisome. ACOX is also known to be transcriptionally regulated by PPAR α . The PFBS dose required to induce ACOX activity, however, was 50 times higher than that required for PFOS (Ehresman *et al.*, 2007). This might be due to the faster elimination rate of the smaller PFBS molecule. Another study monitored changes in peroxisomal β -oxidation activity in rats in response to treatment with different chain length perfluoroalkyl carboxylic acids (Kudo *et al.*, 2000). PFOA, perfluorononanoic acid (PFNA) and perfluorodecanoic acid (PFDA) treatment caused an increase in peroxisomal β -oxidation. Only PFHA was unable to increase β -oxidation.

1.6.2. PPAR α -independent mechanisms

Some evidence is not consistent with PPAR α activation as the sole mechanism of toxicity, suggesting that PPAR α independent modes of action also exist. The doses required to induce hepatotoxicity and hepatocellular adenomas are much lower than required to induce peroxisome proliferation in rats (Seacat *et al.*, 2003). Hepatic lesions have also been seen in Cynomolgus monkeys treated with PFOS (Seacat *et al.*, 2002). This was surprising as these animals are known to have weak peroxisome proliferative responses. The developmental toxicity

of PFOS may also be independent of PPAR α in some species as impaired neonate survival was still observed in PPAR α knock-out mice (Abbott *et al.*, 2009). Interestingly, PFOAs developmental toxicity appears to be dependent on PPAR α expression in mice (Abbott *et al.*, 2007), highlighting that PFOS and PFOA may have very different modes of action. PFCs may also partially induce peroxisome proliferation independently of PPAR α by disrupting lipid transportation and metabolism in a more direct fashion. PFOS and PFOA have been shown to bind strongly to liver fatty acid binding protein (L-FABP). PFCs may compete with fatty acids for binding sites on L-FABP, leading to an increase in free fatty acids that are free to up-regulate lipid metabolizing activity within the cell.

Meta-analysis of gene expression data from experiments performed across various species revealed that several other nuclear receptors may be involved in the toxic response to PFCs (Ren *et al.*, 2009). A high incidence of perturbed transcriptional activity of genes involved in xenobiotic metabolism insinuated the activation of the constitutive androstane receptor (CAR) and the pregnane X receptor (PXR). Another recent report showed that many genes involved in lipid and xenobiotic metabolism were upregulated by PFOS exposure in PPAR α -null mice, which further supported the activation of CAR, PXR and other receptors such as PPAR γ (Rosen *et al.*, 2010). The involvement of CAR and PXR is further supported by activation of several cytochrome P450 isoforms following exposure to PFOA (Elcombe *et al.*, 2007).

PFCs also appear to have detrimental effects on hormonal regulation. Decreases in T3 and thyroxine (T4) levels were first noted in rats exposed to the ten carbon chained carboxylic acid PFDA (Gutshall *et al.*, 1988). This was also accompanied by lowered body temperature and depressed heart rate. Interestingly, the activity of thyroid hormone responsive enzymes in the liver was increased due to PFDA exposure. More recent studies have shown similar decreases in

serum thyroid hormones due to exposure to PFOS (Yu *et al.*, 2008). Several reports have also shown changes in sex hormone levels upon PFC treatment. Male rats treated with PFOA for 14 days experienced decreased levels of testicular and serum testosterone and an increase in serum estradiol (Bookstaff *et al.*, 1990; Lau *et al.*, 2007).

Several non-receptor mediated modes of toxicity have also been proposed. Due to their amphiphilic nature, it has been proposed that PFCs can directly interfere with cell membrane physiology. One study showed that PFOS increased the fluidity of the cell membrane using flow cytometry (Hu *et al.*, 2003). This same study also showed that PFOS increased the permeability of the cell membrane to hydrophobic molecules. Furthermore, these effects were observed at concentrations lower than those associated with other adverse effects, such as PPAR α activation. However, these membrane effects were not observed in cells treated with PFHxS or PFBS, so it is uncertain if these properties are unique to PFOS.

PFCs have also been shown to interfere with gap junctional intercellular communication (GJIC) (Hu *et al.*, 2002). GJIC is the major pathway by which adjacent cells exchange ions, second messengers and other small molecules and is important for tissue homeostasis and proper cellular differentiation and development. Loss of GJIC can lead to tumor formation (Ruch & Trosko, 2001; Trosko & Ruch, 1998). Experiments were performed with cultured rat and dolphin liver epithelial cells, as well as in liver tissues from rats orally exposed to PFOS. Reductions in GJIC activity were neither tissue nor species-dependent, suggesting that GJIC interference may be a common mechanism of PFC toxicity across species.

Differences in lung histology and morphology have been noted in neonate rats that were exposed *in utero* to PFOS (Grasty *et al.*, 2003) suggesting that PFOS can inhibit or delay

perinatal lung development. This may partially explain why rodent and avian embryos are able to survive *in utero* or *in ovo* but often die shortly after birth (Lau *et al.*, 2004; Newsted *et al.*, 2006).

The effects of PFOA and PFOS on the immune response have become a concern as more and more evidence of their immunotoxicity are reported. Their effects on the immune system were first evident when mice fed a diet containing PFOA were observed to have dose dependent reductions in thymus and spleen weight (Yang *et al.*, 2000). The number of thymocytes and spleenocytes also decreased by approximately 90% and 50%, respectively. Inhibited inflammatory response (De Witt *et al.*, 2007), altered immunoglobulin levels (Fairley *et al.*, 2007), and cytokine levels (De Witt *et al.*, 2008) have since been reported due to PFC exposure. These effects, however, seem to be partially dependent on PPAR α activation as thymus and spleen weight and thymocyte and spleenocyte number are not affected in PPAR α knock-out mice exposed to PFOA (Yang *et al.*, 2002a).

1.7. Thesis overview

1.7.1. Rationale

The consequences of PFC exposure have been studied extensively in mammalian models. However, despite the high levels of some PFCs reported in wild bird species, and the low concentrations at which toxic effects are observed, very few studies have characterized the toxicity of PFCs in an avian model in the laboratory. As previously described, recent evidence shows that PFOS and PFOA can be developmentally toxic to birds, with LOAEL values lower than what has been reported in wild bird eggs (Molina *et al.*, 2006; Peden-Adams *et al.*, 2008; Yanai *et al.*, 2008). Furthermore, very little is known about the mechanisms of toxicity specific to the developing avian embryo. In order to make well informed regulatory decisions regarding

emerging PFCs, a better understanding of their toxicity in species that are at high risk of exposure, such as birds, is required.

1.7.2. Research objectives

Experiments were designed to investigate the effects of various PFCs on an avian model species, the white leghorn chicken (*Gallus gallus domesticus*). The specific hypotheses and objectives for the four experimental chapters of this Ph.D. thesis are as follows:

Chapter 2

Hypothesis: PFOS can reduce the hatching success of chicken embryos exposed *in ovo* at environmentally relevant concentrations. Because PPAR α is a proposed target for PFOS induced toxicity, changes in PPAR α -regulated genes can be observed in chicken embryos exposed *in ovo* to PFOS.

Objectives: To assess the overt *in ovo* toxicity of PFOS in chicken embryos via egg injection exposure experiments and measure the transcriptional activity of PPAR α -regulated genes in liver tissue using real-time RT-PCR.

Chapter 3

Hypothesis: PFOA, PFUdA and PFDS can reduce the hatching success of chicken embryos at environmentally relevant concentrations. Several genes involved in xenobiotic metabolism, cholesterol synthesis and lipid transportation were recently reported to be induced by PFUdA or PFDS exposure in cultured chicken embryonic hepatocytes (CEH) (Hickey *et al.*, 2009). It is

hypothesized that these genes will also be affected in the liver tissue of developing chicken embryos following *in ovo* PFUdA or PFDS exposure.

Objectives: To assess the overt *in ovo* toxicity of PFOA, PFUdA and perfluorodecane sulfonate (PFDS) in chicken embryos by egg injection exposure experiments and to measure the transcriptional response of genes involved in xenobiotic metabolism, cholesterol synthesis and lipid transportation in liver tissue using real-time RT-PCR.

Chapter 4

Hypothesis: The accumulation of PFOS isomers in the livers of developing chicken embryos is isomer specific.

Objectives: To investigate PFOS isomer accumulation in the liver tissue of chicken embryo exposed *in ovo* to a technical mixture of PFOS (T-PFOS) containing branched and linear isomers using gas-chromatography/mass spectrometry.

Chapter 5

Hypothesis: T-PFOS, which contains branched and linear PFOS isomers, causes a greater disruption of transcriptional regulation than purely linear PFOS (L-PFOS) in liver cells.

Objectives: To compare the system-wide transcriptional response of cultured CEH exposed to either T-PFOS or L-PFOS using gene expression microarrays.

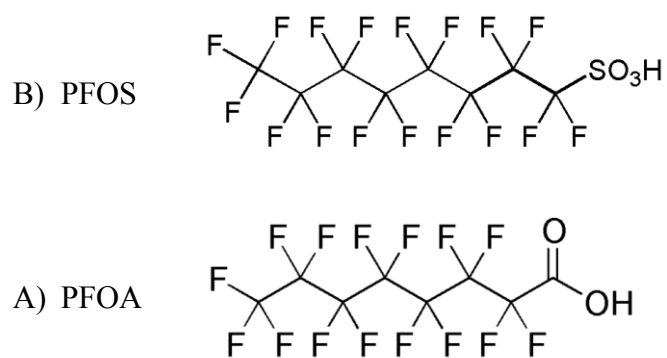


Figure 1.1: Perfluorinated compounds (PFCs) have long completely fluorinated carbon chains and various functional groups at the terminal end. A) Perfluorooctane sulfonate (PFOS) and B) perfluorooctanoic acid (PFOA) are the most environmentally prevalent PFCs.

Chapter 2

Perfluorooctane Sulfonate (PFOS) Toxicity in the Domestic Chicken (*Gallus gallus domesticus*) Embryos in the Absence of Effects on Peroxisome Proliferator Activated Receptor Alpha (PPAR α)-Regulated Genes

(Modified from O'Brien, J.M., Carew, A.C., Chu, S., Letcher, R.J. & Kennedy, S.W. 2009. *Comp.Biochem.Physiol.C.Toxicol.Pharmacol.*, **149**, 524-530)

2.1. Abstract

Perfluorooctane sulfonate (PFOS) is a widely distributed industrial compound that has been detected in the eggs of various wild avian species. Laboratory studies have indicated that PFOS is embryotoxic to domestic chickens (*Gallus gallus domesticus*), but the mechanisms of toxicity in the developing avian embryo remain unknown. We recently demonstrated that PFOS acts as a peroxisome proliferator by causing increased expression of peroxisome proliferator-activated receptor alpha (PPAR α)-regulated genes in cultured primary chicken embryo hepatocytes. The present study examined whether PPAR α -regulated genes were dose-dependently affected in chicken embryos exposed *in ovo* to PFOS. White leghorn chicken eggs were injected with 0.1, 5.0 or 100.0 μg PFOS/g egg into the air cell prior to incubation. Embryos were incubated until pipping, after which the expression of PPAR α -regulated genes was measured in the liver tissue of surviving embryos using real-time reverse transcription polymerase chain reaction. A dose-dependent decrease in embryo pipping success was observed with an LD50 of 93 $\mu\text{g}/\text{g}$ (3.54 $\mu\text{g}/\text{g}$ -672,910 $\mu\text{g}/\text{g}$, 95% confidence interval). Hepatic PFOS concentrations increased concomitantly with dose. The PPAR α -regulated genes measured were peroxisomal acyl-CoA oxidase, bifunctional enzyme, liver fatty acid binding protein and peroxisomal 3-ketoacyl thiolase. PFOS exposure by egg injection prior to incubation did not affect the transcriptional

activity of any of the assayed PPAR α -regulated genes at any of the doses examined in day 21 chicken embryos.

2.2. Introduction

Perfluoroalkyl compounds (PFCs) are used in a variety of commercial, domestic and industrial products including additives for the production of fluorinated polymers for paper coatings, metal plating, photography and semi-conductors, as well as in hydraulic fluids, fire fighting foams, lubricants, adhesives, stain and soil repellents, pharmaceuticals and insecticides (Kissa, 2001; Lau *et al.*, 2007). Production and use of various classes of PFCs have increased over the last fifty years, especially within the last two decades. One particular PFC, perfluorooctane sulfonate (PFOS), has been a major constituent of commercial PFC products with production reaching 3500 metric tons by the year 2000 (Lau *et al.*, 2007).

PFCs consist of a completely fluorinated carbon backbone, generally four to fourteen atoms in length, and have varying functional groups. The strength of the carbon-fluorine bonds results in a fluorocarbon backbone that is highly stable. PFCs have exceptionally low surface tension and are both hydrophobic and oleophobic. Perfluorinated sulfonates (PFSAs) and perfluorinated carboxylates (PFCAs) are characterized as terminal PFCs as they are highly stable and resistant to degradation in the environment. PFOS, for example, has been shown to be the biodegradation endpoint of various volatile fluorinated compounds, such as N-ethyl-(2-hydroxyethyl)-perfluorooctane sulfonamide (N-EtFOSE), which may partly account for its world-wide distribution (Xu *et al.*, 2004).

Several PFCAs and PFSAs are globally distributed anthropogenic contaminants in the environment and in some cases at considerable levels in water, air and wildlife tissue (especially

in liver) (Houde *et al.*, 2006). Biomonitoring programs have identified PFOS in many wildlife samples at various locations around the world. Because PFOS has been detected in all trophic levels, including in algae and small invertebrates, there is concern that it can biomagnify up food chains (Lau *et al.*, 2007). Fish eating seabirds, waterfowl and terrestrial birds have been found to have particularly elevated levels of PFOS, presumably due to their high trophic level (Houde *et al.*, 2006). PFOS has also been detected in wild bird eggs, suggesting transfer of this contaminant during egg-laying (Holmstrom *et al.*, 2005; Kannan *et al.*, 2001; Verreault *et al.*, 2005).

The toxic effects of PFOS have been studied extensively in mammalian systems, but surprisingly few studies have investigated its toxicity in avian species. PFOS exposure to rodents and non-human primates caused various adverse effects including reduced body weight, increased liver mass, hepatocellular adenomas, Leydig cell and pancreatic tumors, reduced cholesterol levels and mortality (Lau *et al.*, 2007). Among the few avian studies, acute and chronic exposure resulted in decreased weight gain, increased liver mass and slight reductions in egg fertility and hatchling survivability (Newsted *et al.*, 2006; Newsted *et al.*, 2007), although LD₅₀ and LOAEL values were relatively high compared to mammalian studies. Decreased sensitivity to PFOS in avian species is believed to be due to faster elimination rates and thus shorter half-lives after exposure compared to mammals. One egg injection study showed a marked decline in hatchability and hepatic aberrations including hepatic duct hyperplasia, periportal inflammation and cellular necrosis with a reported LOAEL of 100 ng/g based on reduced hatchability (Molina *et al.*, 2006), which is substantially lower than concentrations found in egg samples collected during field studies. PFOS levels as high as 196, 220 and 669 ng/g were reported in glaucous gull, cormorant and guillemot eggs, respectively (Kannan *et al.*, 2001; Holmstrom *et al.*, 2005; Verreault *et al.*, 2005).

Much of the hepatotoxicity due to PFOS exposure in mammalian systems is believed to be induced via activation of the peroxisome proliferator activated receptor alpha (PPAR α) (Peraza *et al.*, 2006). PPAR α is a lipid sensing nuclear receptor that is responsible for regulating the expression of genes involved in fatty acid and cholesterol transportation and metabolism, DNA replication and cellular proliferation (Feige *et al.*, 2006). Due to the structural resemblance of PFOS to fatty acids, PFOS is thought to bind to PPAR α and disturb this regulatory activity (Vanden Heuvel *et al.*, 2006). Although the amino acid sequence of PPAR α is strongly conserved among species (Diot & Douaire, 1999), species-specific responses have been reported upon exposure to PPAR α agonists (Guo *et al.*, 2007; Keller *et al.*, 1997; Mukherjee *et al.*, 1994; Nagasawa *et al.*, 2004). Few studies have explored the role of PPAR α activation in avian toxicity. One study observed increased expression of PPAR α -regulated genes in hens when fed a diet containing chlofibrate, a known PPAR α agonist (Konig *et al.*, 2007). Another study looked at the expression profiles of 6-week old chickens exposed to PFOS by subcutaneous injection using microarray technology (Yeung *et al.*, 2007). Many genes were significantly affected by PFOS exposure including several involved in lipid metabolism. Recent work in our laboratory has shown that PPAR α -regulated endpoints can be significantly up-regulated in a dose dependent manner in primary chicken embryo hepatocyte cultures when exposed to PFOS (Cwinn *et al.*, 2008). Whether or not this up-regulation occurs in embryos exposed to environmentally relevant concentrations *in ovo* remains to be shown. To our knowledge there have been no studies that have investigated the role of PPAR α activation in avian embryo toxicity.

In this study, real-time reverse-transcription polymerase chain reaction (RT-PCR) was used to examine the transcriptional activity of PPAR α -regulated endpoints in chicken (*Gallus gallus domesticus*) embryos that were exposed *in ovo* to various concentrations of PFOS.

Endpoints measured were peroxisomal acyl-CoA oxidase (ACOX), bifunctional enzyme (BIEN), liver fatty acid binding protein (L-FABP), and peroxisomal 3-ketoacyl thiolase (PKT).

2.3. Materials and methods

2.3.1. Chemicals

Perfluorooctane sulfonate (PFOS, Wellington Laboratories, Guelph, ON, Canada, 87% pure, 70% linear, 30% branched) was dissolved in dimethyl sulfoxide (DMSO) at concentrations of 0.1 µg/µl, 5.0 µg/µl and 100 µg/µl. Compared to water and corn oil, PFOS was maximally soluble in DMSO at the concentrations required for this study. When used as a carrier solvent for previous cell culture studies in our laboratory DMSO did not appear to affect transcriptional endpoints (Cwinn *et al.*, 2008). The use of this solvent allows direct comparison of results from the present egg injection study with previous and on-going *in vitro* studies. Furthermore, injection of DMSO alone had no effect on embryo pipping success.

2.3.2. Egg injection and tissue collection

Sixty eight white leghorn chicken (*Gallus gallus domesticus*) eggs were obtained from the Canadian Food Inspection Agency (Ottawa, ON, Canada). Eggs were weighed and randomly distributed into five dose groups as follows; untreated control (n=12), DMSO vehicle (n=12), 0.1 µg PFOS/g egg (n=12), 5.0 µg PFOS/g egg (n=12), 100 µg PFOS/g egg (n=20). The eggs were candled to determine the location of the air cell, which was marked by pencil. A dental drill (X35 micromotor system; Buffalo Dental Manufacturing, Syosset, NY, USA) was used to make two small holes, approximately 1–2 mm in size, above the air cell. The injection volume used was 1.0 µl/g egg. The appropriate volume and concentration of solution was injected into one of the holes

using a pipette while the membrane of the second hole was held open using another pipette tip. After injection both holes were covered with AirPore tape (Qiagen). The eggs were left at room temperature overnight with the air cell pointed upwards. The next day, eggs were placed horizontally into an incubator (CK 900 professional; Curfew, Essex, UK) set to 37.5 °C and 65% humidity. Eggs were weighed and candled frequently (every 1–3 days) to check for dead or infertile embryos. Eggs containing dead embryos were removed and opened to determine the approximate developmental stage at which the embryo died. Those that showed no signs of development were removed and considered infertile. Remaining eggs were incubated in these conditions for 18 days. After 18 days rotation was stopped to allow the embryos to turn into pipping position. Eggs were removed for tissue collection from the incubator when a pipping star was observed in the shell of the egg (after approximately 20 days). A pipping star is a small crack in the egg shell that the embryo makes with its egg tooth. Pipping requires a lot of energy, so after this initial crack is made, the embryo rests for up to 10 hours before it continues to break open the egg shell. Therefore, to avoid the possibility of embryos hatching in the incubator, eggs were checked frequently for pipping stars (every 3–6 hours) during the final 3 days of incubation. Embryos that did not make a pipping star by day 22 were considered unfit and unable to hatch.

Once removed from the incubator, eggs were opened and the embryos were sacrificed by decapitation and livers were collected. A small 20–50 mg section of each liver was saved for nucleic acid applications and the remaining tissue was used to assess hepatic PFOS concentration by HPLC/MS/MS analysis. All samples were immediately flash frozen in liquid nitrogen and stored at –80 °C until needed.

2.3.3. Hepatic PFOS concentration

The method for the determination of PFOS was performed according to procedures published elsewhere (Chu & Letcher, 2008; Hansen *et al.*, 2001; Taniyasu *et al.*, 2005). A tissue amount of 0.1–0.2 g was weighed into a 15 ml polypropylene centrifuge tube. The sample was spiked with 100 µl of 1 ppm ¹³C₄-labelled PFOS (Wellington Laboratories Guelph, ON, Canada) in methanol. A volume of 3 ml of 10 mM KOH in 80% acetonitrile solution was added. The sample was extracted by homogenization in an Ultra-Turrax homogenizer (IKAWorks, Wilmington, USA) for 1 min then centrifuged for 10 min at 2500 g. The supernatant was collected into a pre-weighed glass test tube. Extraction in KOH solution was repeated two more times and the supernatants from each extraction were combined. The weight of the combined supernatants was recorded. 2 ml of the extract was transferred to a fresh test tube and the remaining sample was weighed again. Eight ml of Milli-Q filtered water was added to the 2 ml aliquot and the pH was adjusted to approximately 4 using 2% formic acid aqueous solution (approximately 60 µl). The sample was cleaned by solid phase extraction (SPE) using an Oasis WAX SPE (Waters Inc., Mississauga, ON, Canada) cartridge on a Visiprep SPE vacuum manifold (Supelco, Sigma-Aldrich, Oakville, ON, Canada). The final eluate was collected in a glass test tube, evaporated with nitrogen gas to dryness, and the residue reconstituted in 1 ml of methanol.

PFOS analysis was performed using a Waters Alliance 2695 HPLC system equipped with an ACE 3 C18 analytical column (50mmL×2.1mm i.d., 3 µm particle size) and an ACE 3 C18 guard column (100 mm L×2.1 mm i.d., 3 µm particle size) coupled to a Waters Microsmass, Quattro Ultima Triple Quadrupole mass spectrometer (MS) with electrospray ionization (ESI) and operated in the negative ion mode. HPLC separation was performed at 40 °C with a mixture

of water and methanol as the mobile phase, each containing ammonium acetate at a concentration of 2 mM. The mixture of water to methanol was 95% water and 5% methanol, increasing to 80% methanol over 10 min, then to 100% methanol over 10 min, held for 5 min then decreased once again to 5% methanol within 1 min and held for 14 min.

HPLC-ESI-MS/MS analysis of PFOS was done in the multiple reaction monitoring (MRM) mode. The MRM transition ions monitored were 499>80 for PFOS and 503>80 for $^{13}\text{C}_4$ -labelled PFOS. Quantification was performed by an isotope dilution method using $^{13}\text{C}_4$ PFOS as the internal standard, and a five point calibration curve spanning the range of anticipated analyte concentration. The recovery of the internal standard was checked by the external standard method and ranged from 55.6 to 97.0 %. To determine the method quantification limit (MQL), eight pork liver samples were spiked with PFOS at concentration of 1 ng/g and analyzed by the method described above. The method quantification limit (MQL) was defined as three times the standard deviation of the replicates processed through the entire method. The results showed that for PFOS the MQL was 3.1 ng/g ww. Data processing was performed using Masslynx software (v 4.0).

2.3.4. RNA extraction and cDNA preparation

RNA was extracted from 20–50 mg sections of each liver using 1 ml of TRIzol Reagent (Invitrogen) according to manufacturer's recommendations. RNA was then DNase treated with DNA-free (Ambion) following the manufacturer's instructions. DNase treated RNA was then quantified and assessed for purity by measuring the A_{260} and A_{280} ratio. Samples with an A_{260}/A_{280} ratio of less than 1.7 were not used.

cDNA was prepared using random primers (Invitrogen) and Superscript II RNase H- reverse transcriptase (Invitrogen) as described by the manufacturer. Each reaction contained 750 ng of DNase treated RNA and 150 ng of random primers. Reactions containing RNA template but lacking reverse transcriptase were run in parallel to verify the absence of contaminating genomic DNA (no-RT control).

2.3.5. Real-time RT-PCR

Real-time RT-PCR assays were performed using a Stratagene Mx3000, Stratagene Mx3005 or Stratagene Mx4000. Assays for peroxisomal acyl-CoA oxidase (ACOX), bifunctional enzyme (BIEN), and liver fatty acid binding protein (L-FABP) were conducted using TaqMan fluorogenic probes, whereas peroxisomal 3-ketoacyl thiolase (PKT) assays were done using SYBR Green chemistry. In all assays β -actin expression was used as the normalizing factor. In previous *in vitro* experiments β -actin expression was not affected by PFOS exposure (Cwinn *et al.*, 2008) nor were there any dose dependent changes in β -actin expression in the current study. In the case of ACOX and L-FABP, assays were duplexed with β -actin amplification. BIEN and PKT amplification was run separately from β -actin. The nucleotide sequence and final concentration of each primer and probe used for real-time RT-PCR are shown in Table 2.1. TaqMan reactions were performed using Stratagene Brilliant Q-PCR Core Reagent kits. Each 25 μ l reaction contained primers (Invitrogen), probes (Biosearch), 1 \times reaction buffer, 5 mM of MgCl₂, 800 nM of dNTPs, 8% glycerol, 60 nM of ROX reference dye, 1.25 U of SureStart Taq polymerase, 5 μ l of diluted cDNA and brought to volume using DEPC treated water. The thermal profile included a 10 min activation step at 95°C followed by 40 cycles of 30 s at 95°C and 1 min at 60°C. Fluorescence data were collected after the 60°C step.

SYBR green reactions were performed using Stratagene Brilliant SYBR Green Master Mix kits. Each 25 μ l reaction contained primers and probes, 1 \times master mix, 60 nM of Rox reference dye and 5 μ l of diluted cDNA and brought to volume using DEPC treated water. The thermal profile included 10 min at 95°C followed by 40 cycles of 30 s at 95°C, 30 s at 60°C and 1 min at 72°C. Fluorescence data were collected after the 72°C step.

Reaction efficiencies for each target gene were determined from 1:2 serial dilutions of cDNA. Primer and magnesium concentrations were optimized to ensure all reaction efficiencies were similar to that of β -actin. cDNA from 6 individual embryos per dose group were run in duplicate for each gene of interest. No-RT and no-template controls were included in each run to ensure the absence of genomic contamination. MxPro v3.00 software (Stratagene) was used to determine the relative quantities of cDNA by the comparative quantitation method. The fold-change was determined relative to the DMSO treated vehicle control group.

2.3.6. Statistical analysis

A stepwise exact comparison using the Cochran-Armitage test for trend was used in StatXact (Cytel Corp.) to determine differences in pipping success between dose groups. Pipping success data were fit to a probit curve with SAS v9.1 (SAS Institute Inc.) using the OPTC option to estimate background effects. The median lethal dose (LD_{50}) was approximated using the probit analysis program from the U.S. Environmental Protection Agency (v 1.5, <http://www.epa.gov/nerleerd/stat2.htm>). SigmaStat v2.03 (SPSS) was used to perform a one-way ANOVA followed by Bonferroni's t-test on log-transformed data to determine statistically significant differences in hepatic PFOS residue levels between exposed and vehicle treated embryos. Differences were considered significant at a level of $p < 0.05$.

2.4. Results

2.4.1. Effects on pipping success

Injection of PFOS into the air cell of eggs prior to incubation resulted in a dose-dependent reduction in embryo pipping success (Table 2.2). Correlation between a fit probit curve and the observed trend was statistically significant with a chi square value of 0.05. The calculated LD₅₀ was 93 µg/g with a 95% confidence interval of 3.5 µg/g-673,000 µg/g. Injection of DMSO had no effect on embryo pipping success compared to untreated embryos. Only the highest dose group of 100 µg/g egg had significantly lower pipping success compared to the control groups (p=0.005), although a 20% decrease in hatching success also observed in the 5 µg/g group. Very few overt abnormalities were observed in either dose group. Only one embryo from the 0.1 µg/g dose group had a grossly discoloured liver. Among the embryos that did not survive to day 22, PFOS exposure did not seem to affect the developmental stage at which they died.

2.4.2. Hepatic PFOS Concentrations

Hepatic PFOS concentrations increased in a dose-dependent manner (Table 2.2). Livers from all PFOS-exposed dose-groups had significantly higher PFOS levels compared to those from the untreated and vehicle control groups. PFOS concentrations in the livers were slightly higher than the initial whole-egg concentrations at the time of injection in the 0.1 and 5.0 µg/g dose groups, but lower in the 100 µg/g dose group.

2.4.3. PPAR α -regulated genes

The transcriptional activity of several PPAR α -regulated endpoints was monitored for changes due to PFOS exposure using real-time RT-PCR. Although some inter-individual variation in β -actin was observed, there was no dose dependent trend in β -actin transcriptional activity. None of the PPAR α -regulated genes assayed were significantly up or down-regulated by PFOS exposure (Figure 2.1). There was a 2-fold decrease in PKT mRNA expression between the untreated and DMSO dose groups, however, this difference was not statistically significant. Amplification was not detected in the no-RT and no-template controls for any of the assays.

2.5. Discussion

A dose-dependent decrease in pipping success was observed when embryos were exposed *in ovo* to PFOS. Although all PFOS treated groups had slightly lower pipping success compared to the control groups, only the highest dose-group was statistically significant. A probit curve was fitted to the data in response to PFOS exposure with a chi-square value of 0.05 indicating that the trend was statistically significant. A fully sigmoidal dose–response curve was not obtained as the highest dose group only resulted in 43% pipping success, leading to an LD₅₀ with a very broad 95% confidence limit. A more accurate estimation of LD₅₀ might have been possible if higher doses were included in this study; however, this was not experimentally possible, as an injection solution of higher concentration would exceed the solubility of PFOS in the vehicle solvent, DMSO. Furthermore, such high concentrations would far exceed concentrations that have been reported in wild bird eggs (Kannan *et al.*, 2001; Holmstrom *et al.*, 2005; Verreault *et al.*, 2005).

Dose-dependent embryo toxicity due to PFOS exposure was also reported in another study (Molina *et al.*, 2006) that used exposure and incubation conditions comparable to this study. Comparisons between the results of the present study and those of Molina and colleagues are shown in Table 2.2. Although Molina *et al.* (2006) also reported an LD₅₀ with a broad confidence interval, the toxicity of PFOS was observed to be more potent when compared to the present study. Several factors may contribute to the difference in the observed effect on embryo pipping success/hatchability. Molina *et al.* (2006) detected elevated concentrations of PFOS in livers from embryos belonging to both the control and low 0.1 µg/g dose groups. This suggests that the DMSO vehicle may have been contaminated or that the eggs were pre-exposed to PFOS, resulting in higher mortality in dosed eggs, and perhaps leading to an underestimation of LD₅₀. This is uncertain however, as an untreated dose group was not included in the study. In the present study, PFOS concentrations in livers from untreated and vehicle control groups were much lower and significantly different from any of the PFOS exposed groups. Several differences in experimental design may also account for the discrepancies in LD₅₀ among the two studies. One difference is the orientation in which eggs were placed in incubators. In the present study eggs were incubated in the horizontal position, whereas Molina *et al.* (2006) placed eggs in incubators in the vertical position. The toxicity of methyl mercury when injected in the air cell was shown to be higher in eggs incubated vertically compared to when eggs were incubated in a horizontal position (Heinz *et al.*, 2006). It was also demonstrated that when incubated horizontally, the toxicity of methyl mercury in injected eggs was similar to when the mother transfers the same concentration at the time of egg laying (Heinz *et al.*, 2006). This has also recently been observed in eggs exposed *in ovo* to 3,3',4,4',5-pentachlorobiphenyl (PCB 126) (McKernan *et al.*, 2007). It is possible that this phenomenon may also be true for other injected

chemicals such as PFOS. Finally, LD₅₀ calculations were based on embryo pipping success, as opposed to hatchability, as measured in the Molina *et al.* (2006) study.

One of the goals of the present study was to investigate the toxicity of PFOS in avian embryos at environmentally relevant levels. PFOS has been detected in eggs found in wildlife monitoring studies suggesting maternal transfer at the time of egg-laying. The highest concentration we were able to find in the literature was 669 ng/g (wet weight (ww)) in the eggs of guillemots from the Baltic Sea collected in 2003 (Holmstrom *et al.*, 2005). When extrapolated from our experimentally obtained dose–response curve, this concentration corresponds to an approximately 15% decrease in pipping success compared to the control dose. Higher levels have been reported in adult avian samples. Some of the highest concentrations we found in the literature include 1030 ng/g ww in great egret livers (Houde *et al.*, 2006), 1120 ng/g ww in the liver of white pelicans (Houde *et al.*, 2006) and 2570 ng/g ww in bald eagle plasma (Giesy & Kannan, 2001). To our knowledge, the concentration of PFOS in the eggs of these more highly contaminated populations has not been surveyed, though one study reported that PFOS levels in glaucous gull eggs collected from a colony from the Norwegian Arctic were similar to the PFOS concentrations in livers from adults collected from the same region (Verreault *et al.*, 2005). In the eggs of herring gulls collected in 2007 from seven sites across the Laurentian Great Lakes of North America, an approximate range of PFOS levels from 180 to 450 ng/g ww has recently been found (Gebbink *et al.*, 2009).

Hepatic PFOS concentrations in all exposed groups significantly increased compared to controls in a dose-dependent manner (Table 2.2). There was no significant difference in PFOS levels between untreated and vehicle treated samples. PFOS levels in the liver of embryos from the 0.1 and 5.0 µg/g dose groups were slightly higher than the initial whole egg concentrations at

the time of injection indicating a small degree of accumulation. This is in accordance with other studies that have shown PFOS to accumulate in the kidney, serum and liver, with liver concentrations often being the highest (Hundley *et al.*, 2006; Kannan *et al.*, 2001; Seacat *et al.*, 2002; Seacat *et al.*, 2003). In the liver it is believed that PFOS has a high binding affinity for fatty acid binding proteins, lipoproteins as well as albumin (Jones *et al.*, 2003; Luebker *et al.*, 2002). In the highest dose-group hepatic PFOS concentration was lower than the initial injection concentration, suggesting that a saturation point in this tissue had been reached.

Although there was considerable inter-individual variation, no trends in expression levels of PPAR α -regulated endpoints were apparent in response to PFOS exposure in developing chicken embryos. Few studies have demonstrated PPAR α -dependent transcriptional activity in response to PFOS in an avian model similar to that seen in mammalian models. A recent study in our laboratory showed increased expression of PPAR α -regulated transcripts in response to PFOS exposure in primary chicken embryonic hepatocytes (Cwinn *et al.*, 2008). *In vitro* systems, however, are not necessarily indicative of an *in vivo* response. Furthermore, the concentrations required to induce a transcriptional response were considerably higher than those used for this study and may not reflect concentrations found in wild eggs. One study has shown an activated PPAR α type response to chlofibrate, a known PPAR α agonist, in hens (Konig *et al.*, 2007). However, PPARs are known to have ligand-specific activity (Peraza *et al.*, 2006) and it cannot be assumed that chlofibrate and PFOS would invoke a similar transcriptional response. A gene array study showed the regulation of many genes to be perturbed by subcutaneous injection of PFOS in 6-week-old chickens. Although several genes involved in lipid metabolism were affected, no changes in PPAR α -related genes were detected (Yeung *et al.*, 2007). It may be possible that PPAR α exerts its effect at earlier stages of embryonic development that were not

investigated in the present study. Endpoint observations were only performed on day 21 embryos. It is possible that PPAR α activation occurs at earlier stages of development and that homeostatic mechanisms mask any receptor mediated effects at later stages. If this were the case, one would expect that there will be an increase in embryos mortality at early stages of development. This however was not observed. There was no correlation between PFOS exposure and the developmental stage at which embryos died. A recent murine study showed a reduction in neonate survivability in PPAR α knockout mice when exposed *in utero* to PFOS in only the last four days of gestation (Abbott *et al.*, 2009), suggesting that the mechanisms of PFOS embryotoxicity are still active in the late stages of development, and not dependent on the activation of PPAR α in mice. Knockout studies using an avian model species would greatly clarify the requirement of PPAR α activation to induce embryo toxicity in avian species. Adverse effects have also been observed in studies with *Cynomolgus* monkeys, which have been shown to have a refractory PPAR α response (Seacat *et al.*, 2002) as well as in PPAR α -null mice (Yang *et al.*, 2002a) suggesting alternate mechanisms of toxicity. Furthermore, in acute dose studies with rats, hepatotoxicity and carcinogenicity have been evident at exposures much lower than those required to induce peroxisome proliferation via PPAR α (Seacat *et al.*, 2003). These observations and the results from the present study do not support the hypothesis that activation of PPAR α is a common central mechanism of toxicity due to PFOS exposure.

Several mechanisms of PFOS toxicity independent of PPAR α have been suggested. Due to its amphipathic properties, it has been proposed that PFOS may integrate into the plasma membrane and increase membrane fluidity and alter membrane permeability (Hu *et al.*, 2003; Liu *et al.*, 2008; Starkov & Wallace, 2002). PFOS has also been shown to inhibit gap-junctional intercellular communication (Hu *et al.*, 2002), interfere with fatty-acid transportation (Luebker et

al., 2002) and perturb estrogen and thyroid hormone metabolism (Fuentes *et al.*, 2006; Liu *et al.*, 2007a; Martin *et al.*, 2007; Shi *et al.*, 2008; Thibodeaux *et al.*, 2003). These mechanisms need to be investigated further in the context of developmental toxicity at environmentally relevant concentrations in an avian model.

Due to the observed persistence of PFOS in humans and in the environment, the major manufacturer of PFOS and its precursors, 3M, phased out production in 2001 (Houde *et al.*, 2006 and references therein). Other PFC products are most likely being manufactured as replacements to fill the market demand. A further understanding of the mechanisms of PFOS toxicity will be useful for risk assessment of new PFC products as they reach the marketplace.

Table 2.1: Primer and probe nucleotide sequences and their final concentrations in each reaction for real-time reverse transcription polymerase chain reactions.

Name	Chemistry		Sequence (5'-3')	Accession number	Concentration (nM)
β-actin	TaqMan	Forward	AAATTGTGCGTGCATCAAGGA	AY045724	49.5 or 150*
	SYBR green	Reverse	GAGGCAGCTGTGGCCATCT		49.5
		Probe	TGCTACGTCGCACTGGATTTGGAGC		200
ACOX	TaqMan	Forward	GGAATTGCAGACCCAGAAGA	NM_001006205	75
		Reverse	CATGCCCAGATGAAGATCCA		75
		Probe	CATCGTGGACGGCCTGAGCC		200
BIEN	TaqMan	Forward	AGATTCATCTCTTTCCACCT	XM422690	300
		Reverse	GCACTGCTCTGAAGACCTAAG		300
		Probe	GCCACTGCCCACCC		200
L-FABP	TaqMan	Forward	CCCTCACACTGCACCTTATCC	AF380998	300
		Reverse	CAGTGCAAGAGCTTTCAGAAATTC		300
		Probe	CATAATGGCATTTCAGTGGCACCTGGCA		200
PKT	SYBR green	Forward	CAGCATACTAGCAGAGGATTAGCA	XM001232576	900
		Reverse	TCACAGCAGAAAGGGATGAA		900
		Probe	N/A		

*TaqMan reactions used 49.5 nM of β-actin forward primer whereas SYBR green reaction used 150 nM.

Table 2.2: The effect of injecting PFOS into the air cell of chicken embryos prior to incubation on pipping success and hepatic PFOS concentration.

Dose Group	This Study			Molina, <i>et al.</i> , 2006		
	# Pipped/ #Fertile eggs	Hepatic [PFOS]* µg/g	Pipping Success* (%)	# Hatched/ #Fertile eggs	Hepatic [PFOS]* µg/g	Hatchability* (%)
Untreated	11/12	0.04 +/- 0.01 ^A	91.7 ^A	nd	nd	nd
DMSO vehicle	8/9	0.07 +/- 0.03 ^A	88.9 ^A	42/49	1.10 +/- 0.54 ^A	85.7 ^A
0.1 µg/g	10/12	0.15 +/- 0.02 ^B	83.3 ^A	27/44	1.40 +/- 0.54 ^A	61.4 ^B
1.0 µg/g	nd	nd	nd	23/48	1.80 +/- 0.54 ^A	47.9 ^B
5.0 µg/g	6/9	7.80 +/- 0.90 ^C	66.7 ^{AB}	nd	nd	nd
10.0 µg/g	nd	nd	nd	20/50	3.20 +/- 0.54 ^B	40.0 ^C
20.0 µg/g	nd	nd	nd	17/46	4.80 +/- 0.54 ^B	37.0 ^C
100.0 µg/g	7/16	69.95 +/- 10.15 ^D	43.8 ^B	nd	nd	nd
	LD ₅₀ = 93 µg/g, 95% CI = 3.5 µg/g – 673,000 µg/g			LD ₅₀ = 4.9 µg/g, 95% CI = 0.28 µg/g – 297.12 µg/g		

nd = not done, *Values with the same letters within a column are statistically indistinguishable, p<0.05

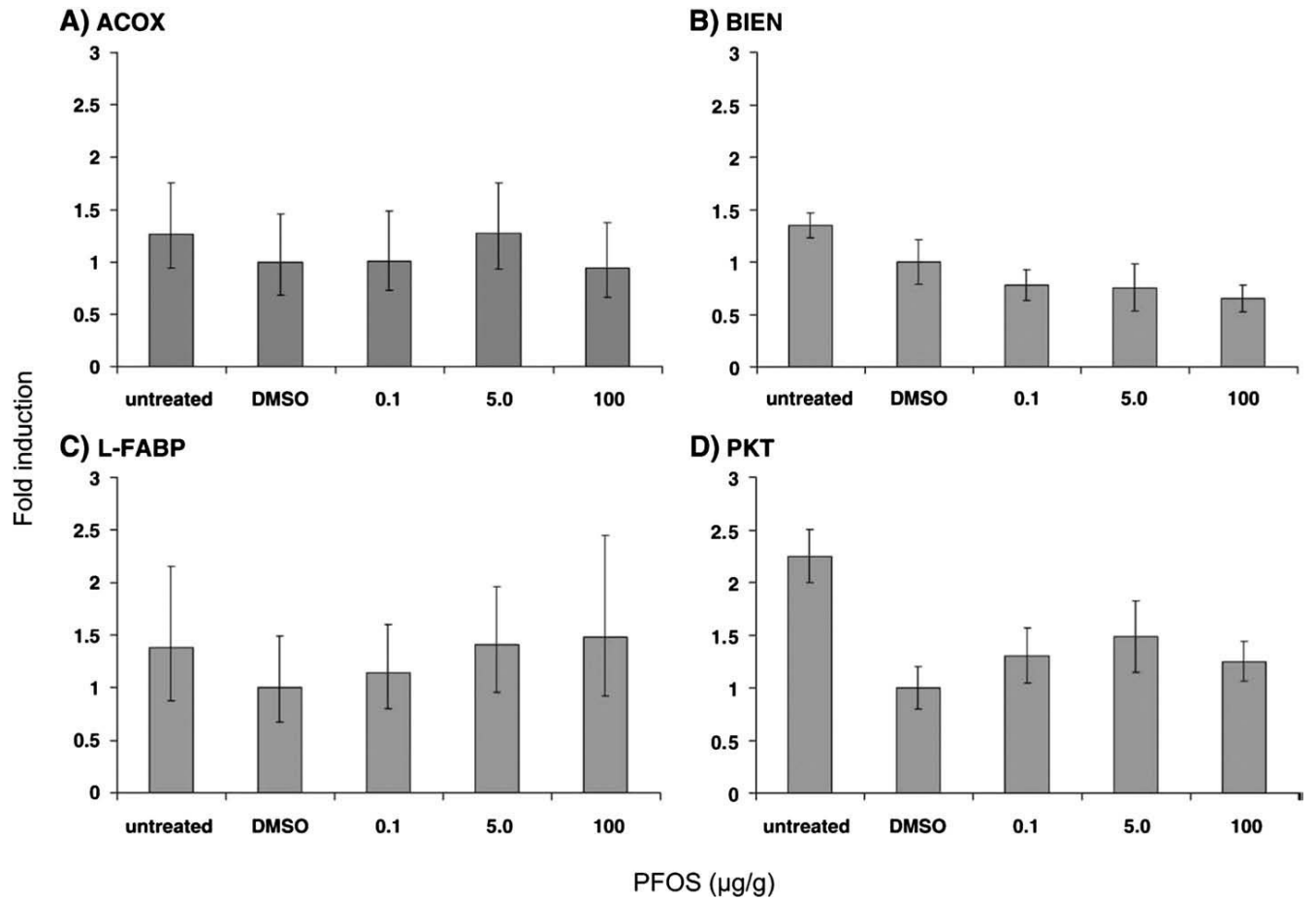


Figure 2.1: Mean fold induction of PPAR α regulated transcripts in chicken embryos exposed *in ovo* to PFOS prior to incubation +/- S.E.. Means were calculated using data from six individual embryos per dose group. A) ACOX, B) BIEN, C) L-FABP, D) PKT

Chapter 3

Pipping Success and Liver mRNA Expression in Chicken Embryos Exposed *in ovo* to C₈ and C₁₁ Perfluorinated Carboxylic Acids and C₁₀ Perfluorinated Sulfonate

(Modified from O'Brien, J.M., Crump, D., Mundy, L.J., Chu, S., McLaren, K.K., Vongphachan, V., Letcher, R.J. & Kennedy, S.W. 2009. *Toxicol. Lett.* **190**, 134-139)

3.1. Abstract

Several perfluoroalkyl compounds (PFCs) are ubiquitous environmental contaminants and may biomagnify in species at high trophic levels including wild birds. Perfluorooctane sulfonate (PFOS) and perfluorooctanoic acid (PFOA) have been detected in wild birds and are known to reduce hatching success of laboratory-exposed chicken embryos at environmentally relevant concentrations. Limited toxicity data are available regarding avian exposure to PFCs of chain lengths greater than C₈, which are of increasing environmental relevance following the recent phase-out of PFOS and PFOA. In this study, linear PFOA, perfluoroundecanoic acid (PFUdA) and perfluorodecane sulfonate (PFDS) were injected into the air cell of white leghorn chicken eggs (*Gallus gallus domesticus*) prior to incubation to determine effects on embryo pipping success. Furthermore, mRNA expression of key genes involved in pathways implicated in PFC toxicity was monitored in liver tissue. PFOA, PFUdA or PFDS had no effect on embryonic pipping success at concentrations up to 10 µg/g. All PFCs accumulated in the liver to concentrations greater than the initial whole-egg concentration as determined by HPLC/MS/MS. Hepatic accumulation was highest for PFOA (4.5 times) compared to PFUdA and PFDS. Cytochrome P450 1A4 and liver fatty acid binding protein mRNA expression increased after exposure to PFUdA but was only statistically significant at 10 µg/g; several orders of magnitude higher than levels found in wild bird eggs. Based on the present results for white leghorn

chickens, current environmental concentrations of PFOA, PFUDA and PFDS are unlikely to affect the hatching success of wild birds.

3.2. Introduction

Perfluoroalkyl compounds (PFCs) are used in the production of a variety of commercial and industrial products including stain-resistant and non-stick coatings, fire-fighting foams, lubricants and pesticides. Perfluorinated carboxylic acids (PFCAs) and sulfonates (PFSAs) are exceptionally resistant to environmental and biochemical degradation and bioaccumulate through food webs (Houde *et al.*, 2006). Numerous PFCAs and PFSAs have been identified in the serum and liver of various species of wild mammals, fish and birds (Houde *et al.*, 2006). Several of these are toxic to laboratory animals, with effects that include weight gain, hepatic aberrations, developmental abnormalities and mortality (reviewed in Lau *et al.*, 2007). Consequently, researchers and regulatory agencies have expanded their efforts to understand the global and biological fate of these compounds, as well as the associated hazards of exposure.

Perfluorooctanoic acid (PFOA), perfluorooctane sulfonate (PFOS), and their precursor compounds, have been or will soon be phased out of production due to their persistence in humans and wildlife (US EPA, 2002a; US EPA, 2002b). As the environmental release of PFOA and PFOS has declined in recent years, so too have their levels in tissue samples collected for wildlife monitoring studies (Butt *et al.*, 2007b; Verreault *et al.*, 2007). This decline has been accompanied by an increase in the detection of alternative PFCs (Butt *et al.*, 2007b; Verreault *et al.*, 2007) as manufactures turn to compounds with varying carbon chain lengths and functional groups in order to fill the market demand left behind by PFOA and PFOS.

Recent biomonitoring surveys of fish-eating birds demonstrated that the most elevated PFCA and PFSA besides PFOA and PFOS were the longer chained perfluoroundecanoic acid (PFUdA) and perfluorodecane sulfonate (PFDS), respectively (Bustnes *et al.*, 2008; Butt *et al.*, 2007a; Holmstrom and Berger, 2008; Houde *et al.*, 2006; Lofstrand *et al.*, 2008; Tao *et al.*, 2006; Verreault *et al.*, 2005; Verreault *et al.*, 2007; Wang *et al.*, 2008). PFUdA concentrations as high as 184 ng/g wet weight (ww) and 38.7 ng/g (ww) were reported in the plasma and eggs, respectively, of glaucous gulls (*Larus hyperboreus*) in the Norwegian Arctic (Verreault *et al.*, 2005). PFDS concentrations of 11 ng/g (ww.) in herring gull eggs (*L. argentatus*) from the North American Great Lakes (Gebbinck *et al.*, 2009) and 4.5 ng/g (ww.) in the liver of common guillemot chicks (*Uria aalge*) from the Baltic Sea have been reported (Holmstrom and Berger, 2008).

The toxicological effects of PFC exposure are diverse and in many cases compound- and species-dependent (Lau *et al.*, 2007; US EPA, 2002a; US EPA, 2002b). Many of these differences are believed to be the result of variable toxicokinetic properties between each compound and species (Andersen *et al.*, 2008; Lau *et al.*, 2007), although dissimilarities in species-specific biochemical responses may also account for some of this variation (Shipley *et al.*, 2004; Wolf *et al.*, 2008). While many studies have characterized the toxicity of various PFCs in mammalian species, few have investigated their effects in birds. Furthermore, most toxicity studies in birds have only been conducted with PFOA and PFOS. As such, studies on the effects of long chained PFCs in birds are warranted.

Recent research in our laboratory identified genes involved in xenobiotic metabolism, cholesterol synthesis and lipid transportation that were responsive to PFUdA and PFDS exposure in cultured chicken embryonic hepatocytes (CEH) (Hickey *et al.*, 2009). *In vitro* screening

techniques are useful tools for identifying potential biomarkers of toxic exposure as well as possible molecular modes of action (Crump *et al.*, 2008; Cwinn *et al.*, 2008; Kennedy *et al.*, 1996). As *in vitro* findings are not always consistent with an *in vivo* response, it is important to validate *in vitro* screening results in more biologically realistic situations (O'Brien *et al.*, 2009a).

In the present study, PFOA, PFUdA and PFDS were injected into white leghorn chicken (*Gallus gallus domesticus*) eggs prior to incubation to assess *in ovo* toxicity. PFC concentrations in liver were determined in day 20 embryos by HPLC/MS/MS. Genes that displayed altered mRNA expression in previous *in vitro* experiments (Hickey *et al.*, 2009) were also assayed for transcriptional changes in liver tissue of day 20 embryos. These genes were cytochrome P450s 1A4 and 1A5 (CYP1A4 and CYP1A5), 3-hydroxy-3-methyl-glutaryl-Coenzyme A reductase (HMGCR), and liver fatty acid binding protein (L-FABP) for embryos exposed to PFUdA and CYP1A4, CYP1A5, cytochrome P450 4B1 (CYP4B1), and L-FABP for embryos exposed to PFDS.

3.3. Materials and methods

3.3.1. Chemicals

Perfluoro-*n*-octanoic acid (PFOA), perfluoro-*n*-undecanoic acid (PFUdA), and sodium perfluoro-1-decane sulfonate (PFDS) used for egg injection were obtained from Wellington Laboratories (Guelph, ON, Canada). All injection compounds were the linear isomer (>98% purity). Injection solutions were made by dissolving the PFCs in dimethyl sulfoxide (DMSO) at concentrations of 10 ng/μl, 100 ng/μl, 1 μg/μl and 10 μg/μl. The actual concentrations of these solutions were determined by HPLC/MS/MS as described below and are indicated in Table 3.3.

PFOA, PFUdA and PFDS standard solutions for HPLC/MS/MS (50 µl/ml in methanol) as well as internal standard solutions of perfluoro-*n*-[1,2,3,4-¹³C₄]octanoic acid (MPFOA) (50 µg/ml), perfluoro-*n*-[1,2-¹³C₂]undecanoic acid (MPFUdA) (50 µg/ml) and sodium perfluoro-1-[1,2,3,4-¹³C₄]decane sulfonate (MPFDS) (50 µg/ml) were also purchased from Wellington Laboratories (Guelph, ON, Canada). Oasis WAX (3 ml, 60 mg) SPE cartridges were purchased from Waters (Mississauga, ON, Canada). All the solvents and reagents used in the experiment were HPLC grade or better.

3.3.2. Egg injection and tissue collection

White leghorn chicken (*Gallus gallus domesticus*) eggs were obtained from the Canadian Food Inspection Agency (Ottawa, ON, Canada). For each compound, eighty eggs were randomly distributed among four dose groups, with twenty eggs in each group; 10 ng PFC/g egg, 100 ng PFC/g egg, 1 µg/g and 10 µg PFC/g egg. Another twenty eggs were assigned to an untreated control group, and a final twenty to a DMSO vehicle control group. Eggs were candled to determine the location of the air cell, which was marked by pencil. A Dremel drilling tool (Dremel MultiPro, model 395) was used to make a small hole, approximately 1-2 mm in size, above the air cell. The injection volume was 1 µl/g egg, based on the average weight of all eggs in each exposure experiment (~50 µl). The appropriate volume and concentration of solution was injected into the air cell using an Eppendorf repeater pipette with a 2.5 ml tip. After injection the hole was covered with AirPore tape (Qiagen). The eggs were left at room temperature for one hour with the air cell pointed upwards. Eggs were then placed horizontally into an incubator (Petersime, Model XI) at 37.5°C and 58% humidity. Embryos were monitored and brought to pipping as previously described (O'Brien *et al.*, 2009a). Briefly, eggs were

candled frequently (every 1-3 days) to monitor for dead embryos. Eggs that showed no signs of development were considered infertile and removed. Embryos that did not make a pipping star by day 22 were considered unfit and unable to hatch. Pipping success was determined by dividing the number of embryos that pipped by day 22 by the number of total fertile eggs per dose group.

Once removed from the incubator, eggs were opened and the embryos were euthanized by decapitation. The weight of the embryo and excised liver tissue were determined. A few drops of blood, ~10-100 μ l, were collected from each embryo for genetic sex determination. A 20-50 mg section of each liver was saved for nucleic acid applications and the remaining tissue was used for PFC analysis by HPLC/MS/MS. All samples were immediately flash frozen in liquid nitrogen and stored at -80°C until needed.

3.3.3. Hepatic PFC concentration determination by HPLC/MS/MS

PFC analysis was performed using a previously described method (O'Brien *et al.*, 2009a) with modifications. Samples were spiked with 100 μ l of an internal standard solution containing 1000 ng/ml of MPFOA, MPFUdA and MPFDS prior to extraction. For PFC detection, a Waters Alliance 2695 HPLC system coupled to a Micromass Quattro Ultima triple quadrupole mass spectrometer equipped with electrospray ionization (ESI) interface was used. Analytes were separated chromatographically on an ACE 3 C₁₈ column (50 \times 2.1 mm i.d., 3 μ m particle size). The mobile phases were water (A) and methanol (B) both containing equal concentrations of 2 mM ammonium acetate. The elution gradient was as follows: initial mix of 95% mobile phase A and 5% mobile phase B, increasing to 100% mobile phase B within 6 min and held for 4 min, then decreasing to 5 % mobile phase B within 1 min and held for 4 min. The MS/MS was

operated in negative ion mode, with multiple reaction monitoring (MRM). The retention time, transitions and other compound dependent operation parameters for target compounds and internal standards are listed in Table 3.1. Quantitative analysis was performed by the isotope dilution method. MPFOA, MPFUdA and MPFDS were used as internal standards for PFOA, PFUdA and PFDS, respectively. The recovery of the internal standard was checked by the external standard method. The average recovery of internal standard for MPFOA, MPFUdA and MPFDS were 105, 113 and 89% respectively. To determine the method quantification limit (MQL), eight pork liver samples were spiked with PFOA, PFUdA and PFDS at concentration of 1 ng/g each and analyzed by the method described above. The method quantification limit (MQL) was defined as three times the standard deviation of the replicates processed through the entire method. The results showed that for PFOA, PFUdA and PFDS the MQL was 0.2, 0.1, and 0.2 ng/g ww, respectively. Data processing was performed using Masslynx software (v 4.0). Statistically significant differences in PFC concentration between embryo livers were identified by performing ANOVA to log-transformed data followed by a Tukey test.

3.3.4. Sex determination by PCR

The sex of each embryo was determined by PCR using the 1237L/1272H primer set as previously described (Kahn *et al.*, 1998) on DNA isolated from blood samples by chelex extraction as described elsewhere (Egloff *et al.*, 2009).

3.3.5. Real-time RT-PCR

RNA was extracted from 20-50 mg of each liver using 1 ml of TRIzol Reagent (Invitrogen) as per manufacturer's instructions, followed by DNase treatment using DNA-free

kits (Ambion). RNA was then quantified and assessed for purity by measuring the A_{260} and A_{280} ratio. Samples that had A_{260}/A_{280} ratios less than 1.7 were not used. cDNA was prepared using Superscript II RNase H-reverse transcriptase (Invitrogen) as directed by the manufacturer. Each reaction contained 750 ng of DNase treated RNA and 150 ng of random primers (Invitrogen). To assess the presence of contaminating genomic DNA, reactions containing template RNA but no reverse transcriptase were prepared in parallel (no-RT control).

Real-time reverse transcription PCR (real-time RT-PCR) reactions were performed using Mx3000, Mx3005 or Mx4000 instruments from Stratagene. All real-time RT-PCR assays were performed with TaqMan fluorogenic probes. β -actin was used as a normalizer. β -actin expression was not affected by exposure to either of the test PFCs. CYP4B1, HMGCR and L-FABP assays were each run in duplex with β -actin whereas CYP1A4 and CYP1A5 assays were triplexed with β -actin. Real-time RT-PCR reactions were performed using Stratagene Brilliant Q-PCR Core Reagent kits. Each 25 μ l reaction contained primers (Invitrogen), probes (Biosearch), 1x reaction buffer, 5 mM of $MgCl_2$, 800 nM of dNTPs, 8% glycerol, 60 nM of ROX reference dye, 1.25 U of SureStart Taq polymerase, 5 μ l of diluted cDNA and brought to volume using DEPC treated water. The nucleotide sequence of each primer and probe as well as their final reaction concentration can be found in Table 3.2. The thermal profile for each reaction included a 10 minute activation step at 95°C followed by 40 cycles of 30 seconds at 95°C and 1 minute at 60°C. Fluorescence data were collected after the 60°C step. Reaction efficiencies for each target gene were determined from eight-point standard curves constructed from 1:2 serial dilutions of cDNA. Reactions were optimized so that the amplification efficiency of each target was similar to that of β -actin ($\pm 5\%$). cDNA from 5 individual embryos per dose group were run in duplicate for each assay. No-RT and no-template controls were included in each assay to ensure the

absence of contamination. β -actin normalized gene expression was calculated using the $2^{-\Delta C_t}$ equation (Schmittgen and Livak, 2008) then expressed as fold induction relative to the DMSO vehicle control group. Statistically significant differences in gene expression were identified by performing ANOVA to $2^{-\Delta C_t}$ -transformed data followed by a Tukey comparison to the vehicle control.

3.4. Results

3.4.1. Effect of PFCs on pipping success

Concentration-dependent effects of PFOA, PFUdA and PFDS exposure on embryo pipping success (Figure 3.1) or frequency of gross abnormalities were not observed. The liver somatic index (LSI) was calculated for all surviving embryos. LSI was not affected by dose (data not shown). The developmental stage at which embryos died was also not affected by treatment nor were the times at which pipping occurred (data not shown). Pipping success was independent of embryo sex (data not shown).

3.4.2. Hepatic PFC concentrations

The concentration of PFCs in liver increased in a dose dependent fashion (Table 3.3). PFOA, PFUdA and PFDS levels were below the detection limit in all embryos from the untreated and vehicle control groups. In embryos exposed to PFOA, concentrations of PFOA were approximately 2.9-4.5 times higher than the initial whole-egg concentration of PFOA at the time of injection. PFUdA levels in the liver were up to 2-fold more concentrated while PFDS levels were not higher than the injection concentration except for a small increase in the lowest dose group. Hepatic PFC concentration was independent of embryo sex (data not shown).

3.4.3. mRNA expression

A concentration-dependent increase in the expression of CYP1A4 mRNA that was statistically significant in the highest group ($p < 0.1$) was observed in embryos exposed *in ovo* to PFUdA (Figure 3.2A). L-FABP mRNA expression increased significantly by approximately 2-fold ($p < 0.05$) in the highest dose group compared to DMSO treated embryos. L-FABP expression did not differ from the DMSO control group in any other dose group. CYP1A5 and HMGCR mRNA expression in embryonic liver tissue was not affected by PFUdA exposure. No significant changes in transcriptional activity were observed for CYP1A4, CYP1A5, CYP4B1 or L-FABP mRNA in the liver tissue of embryos exposed to PFDS (Figure 3.2B).

3.5. Discussion

All three PFCs were detected in chicken embryo livers at levels that were dependent upon injection concentration, indicating efficient uptake by the developing embryos. Despite the presence of these compounds, pipping success was not affected by *in ovo* exposure to PFOA, PFUdA or PFDS at any concentration up to 10 $\mu\text{g/g}$. Only two of the assayed genes, CYP1A4 and L-FABP, were affected by PFUdA exposure and were only up-regulated to a statistically significant level at the highest dose. All other genes were not affected.

PFCs can be manufactured by two distinct chemical processes: electrochemical fluorination (ECF) or fluoro-telomerization. Products of ECF yield mixtures of both linear (~70%) and branched (~30%) isomers, whereas telomerization products are almost purely linear (>98%) (Prevedouros *et al.*, 2006). In 2002, PFC production by the ECF process was discontinued by major PFC manufacturers. Most current operations use telomerization methods. PFCs that were released into the environment post-2002 are therefore expected to be mostly

linear in arrangement (Prevedouros *et al.*, 2006). Monitoring studies report a predominance of linear PFC isomers in the environment, wildlife and humans (De Silva *et al.*, 2009b; De Silva and Mabury, 2006; Karrman *et al.*, 2007). Branched isomers are also present, but their environmental presence appears to be declining since the phase out of ECF synthesis methods (De Silva and Mabury, 2004; Furdui *et al.*, 2008).

Two studies reported a dose-dependent decrease in embryo pipping or hatching success when environmentally relevant quantities of technical grade PFOS were injected into chicken eggs prior to incubation (Molina *et al.*, 2006; O'Brien *et al.*, 2009a). Technical grade PFOS, produced by the ECF method, is predominantly composed of the linear isomer but also contains a significant portion of branched impurities (15-30%) (Chu and Letcher, 2009). A third study reported no effects on hatching success when eggs were injected with PFOS (Peden-Adams *et al.*, 2009), although the isomeric content of the PFOS used in this study was not specified. Recent work in our laboratory showed that technical grade PFOS induced a more pronounced transcriptional response than linear PFOS in cultured CEH (Hickey *et al.*, 2009). In the present study, the linear form of the ten-carbon sulfonate, PFDS, had no effect on embryonic pipping success. The linear carboxylates, PFOA and PFUdA, also had no effect on chicken embryo pipping success. These results contrast with those of a recent injection study in which *in ovo* exposure to comparable concentrations of PFOA significantly impeded hatching success in all treatment groups (Yanai *et al.*, 2008). It was unspecified whether the PFOA was purely linear or a mixture containing branched isomers. Another possible explanation for this discrepancy may be the technical differences between studies. Yanai *et al.* (2008) injected PFOA into the pointed end of the egg (presumably into the albumin) whereas injections were made into the air cell in the present study. Furthermore, a vehicle control group was not included to determine if the

injection procedure had detrimental effects on hatching success. Incubation positions were also different between studies (horizontal in the present study vs. vertical) which can affect hatching success (Heinz *et al.*, 2006).

When rats were exposed to both linear and branched forms of the ammonium salt of PFOA, the branched isomers were less potent at inducing a toxic response (Loveless *et al.*, 2006). This might be explained by considering the difference in toxicokinetics between linear and branched PFCs in rats. Although branched PFCs may be more transcriptionally disruptive than the linear isomers, as suggested by *in vitro* studies (Hickey *et al.*, 2009), they are, in general, more easily eliminated than linear forms in rats (Benskin *et al.*, 2009; De Silva *et al.*, 2009a; De Silva *et al.*, 2009c; Loveless *et al.*, 2006). Because contaminants cannot be easily eliminated from enclosed eggs, developing avian embryos may be at higher risk to the toxic effects of branched PFCs compared to adult rats.

Although pipping success was not affected, exposure to PFCs *in ovo* may result in defects that are manifested post-hatch. Compromised immunological and neurological function, as well as reduced hatchling survivability has been reported in chicks exposed *in ovo* to PFOS (Newsted *et al.*, 2007; Peden-Adams *et al.*, 2009). Several other developmental toxicity studies have also demonstrated that some toxic effects of PFCs are only evident postpartum in rodents (Abbott *et al.*, 2009; Grasty *et al.*, 2005; Lau *et al.*, 2003).

PFOA, PFUdA and PFDS accumulated in the liver to concentrations that were higher than the initial whole-egg concentration at the time of injection. The degree of hepatic accumulation was highest for PFOA and was most pronounced in the lowest dose group for all injected compounds. Similar effects were reported in rats exposed to low and high doses of PFOA (Curran *et al.*, 2008; Kudo *et al.*, 2007). A comparable trend was also observed when

chicken embryos were exposed *in ovo* to PFOS, although the effect was less remarkable; PFOS concentrations only increased maximally to 1.5 times in the liver compared to whole-egg concentrations (O'Brien *et al.*, 2009a). The mechanism underlying the greater PFOA accumulation in the liver compared to other PFCs is unclear. PFCs are known to bind to fatty acid binding proteins, lipoproteins and albumin in the liver (Jones *et al.*, 2003; Luebker *et al.*, 2002). PFOA may have a stronger binding affinity to these proteins compared with other PFCs. Recent research has suggested that PFOA may bind to the murine L-FABP with an affinity similar to native fatty acids (Ellis *et al.*, 2008). The binding strength of other PFCs to L-FABP or other proteins has yet to be investigated.

In a recent *in vitro* study using cultured CEH, 18 different PFCs were screened for cytotoxicity and their ability to alter the transcription of genes from several pathways suspected of being affected by PFC exposure (Hickey *et al.*, 2009). Exposure to linear PFUdA caused significant increases in CYP1A4 and CYP1A5, genes involved in the metabolism of xenobiotic compounds, and in HMGCR, a rate limiting gene in the synthesis of cholesterol. PFUdA was also the strongest inducer of L-FABP mRNA expression, a protein involved in the transportation of fatty acids in liver tissue. Linear PFDS also affected the expression of CYP1A4, L-FABP and CYP4B1 mRNA in CEH. CYP4B1 is a gene involved in β -oxidation, the primary biochemical process during peroxisome proliferation. Peroxisome proliferation is a hallmark of exposure to PFOS and PFOA in rodents (Lau *et al.*, 2007). Interestingly PFDS did not affect the expression of acyl-CoA oxidase in CEH, the major rate limiting enzyme of β -oxidation (Hickey *et al.*, 2009). Exposure to linear PFOA did not affect the transcription of any of these genes in CEH. In the present study, only the alterations in CYP1A4 and L-FABP following exposure to linear PFUdA are in concordance with the *in vitro* screening study. These results show that, while *in*

in vitro screening techniques can be useful tools for identifying possible biomarkers of exposure or mechanisms of action, it is important to verify *in vitro* results in more biologically realistic situations. The observed changes in gene expression were only significant at the highest concentration administered in this study, which is several orders of magnitude higher than those detected in wild samples. It should be noted however that measurements were only taken at one time point and that it is possible that differential gene expression may occur at different developmental stages.

In the present study, the two lowest dose groups were chosen to reflect the highest concentrations of PFOA, PFUdA and PFDS found in wild bird tissues. PFC exposure at these concentrations, and those up to two orders of magnitude higher, had no effect on embryo pipping success. Only PFUdA caused statistically significant increases in the transcription of genes associated with PFC toxicity, but only in the highest dose group. These results demonstrate that at their current environmental levels, PFOA, PFUdA and PFDS do not pose a threat to the hatching success of the domestic chicken. However, in the environment, exposure is rarely limited to one PFC, but to a mixture of various PFCs and other environmental pollutants. Finally, species differences in toxic response to environmental contaminants are well documented in birds (Hoffman *et al.*, 1998; Head *et al.*, 2008) and, to our knowledge, the effects of PFC exposure in wild avian species have not yet been investigated.

Table 3.1: Retention time, transitions and compound dependent operation parameters for target compounds and internal standards.

Compound	Retention time	Transition	Cone Voltage (V)	Collision Energy (eV)	Dwell time (sec)
PFOA	13.56	412.8>368.9	35	8	0.5
PFUndA	15.28	562.8>518.9	35	10	0.5
PFDS	15.23	598.8>80.0	35	55	0.5
MPFOA	13.56	416.9>371.9	35	8	0.5
MPFUDa	15.28	564.9>519.9	35	10	0.5
MPFDS	14.21	502.8>80.0	35	40	0.5

Table 3.2: Nucleotide sequence and final reaction concentration of each primer and probe used for real-time RT-PCR assays.

Name		Sequence (5'-3')	Accession Number	Concentration (nM)
β-actin	Forward	AAATTGTGCGTGCATCAAGGA	AY_045724	50
	Reverse	GAGGCAGCTGTGGCCATCT		50
	Probe	TGCTACGTGCGACTGGATTTGGAGC		200
CYP1A4	Forward	TAAGGACGTCAATGCTCGTTTC	NM_205147	300
	Reverse	CGTCCCGAATGTGCTCCTTAT		300
	Probe	TGCCTTCGTACAGAAAATTGTCCAGAAC		200
CYP1A5	Forward	ACAGCTGTGGAAGAGCACTACCA	NM_205146	300
	Reverse	TCTCCACGCACTGCTCGAT		300
	Probe	CCGAGACGTCACCGACTCCCTCA		200
CYP4B1	Forward	ATCCCAAGCCTCCTGTACCT	XM_422455	300
	Reverse	AACGCTGGAGTGAGCAACTT		300
	Probe	TGGATTGGCAAAGGGTTGCTGG		200
HMGCR	Forward	TAGGTCCTACATTTACCCTGGATG	NM_204485	900
	Reverse	ATGATTTCAAGTTGTCGCACTCC		900
	Probe	CCAACGCCAATCACAAGACATTCCACAAGT		200
L-FABP	Forward	CCCTCACACTGCACCTTATCC	AF_380998	300
	Reverse	CAGTGCAAGAGCTTTCAGAAAATTC		300
	Probe	CATAATGGCATTTCAGTGGCACCTGGCA		200

Table 3.3: Hepatic concentration of PFOA, PFUdA and PFDS in day 20 chicken embryos that were exposed to PFCs via egg injection prior to incubation. Mean and standard error (S.E.) calculations are based on results from 4-5 individual embryos per group. Values with different capital letters are significantly different based on ANOVA followed by Tukey pairwise comparison ($p < 0.05$). Hepatic enrichment values indicate the fold increase in hepatic PFC concentration compared to the initial injection concentration. NA indicates dose groups that were not exposed to PFCs. BD indicates that the measured PFC was below the detection limit of the HPLC/MS/MS method.

Dose group	Actual Injection Concentration (ng/g)	Mean Hepatic Concentration (ng/g) \pm S.E.		Hepatic Enrichment
Embryos exposed to PFOA				
Untreated	NA	BD		-
DMSO	NA	BD		-
10 ng/g	8	38 \pm 7	A	4.5 x
100 ng/g	84	316 \pm 12	B	3.7 x
1000 ng/g	845	3384 \pm 362	C	4.0 x
10000 ng/g	8452	24492 \pm 1523	D	2.9 x
Embryos exposed to PFUdA				
Untreated	NA	BD		-
DMSO	NA	BD		-
10 ng/g	10	22 \pm 9	A	2.2 x
100 ng/g	96	171 \pm 6	B	1.8 x
1000 ng/g	967	1655 \pm 270	C	1.7 x
10000 ng/g	9676	14043 \pm 888	D	1.5 x
Embryos exposed to PFDS				
Untreated	NA	BD		-
DMSO	NA	BD		-
10 ng/g	9	16 \pm 14	A	1.7 x
100 ng/g	93	107 \pm 14	B	1.2 x
1000 ng/g	933	999 \pm 160	C	1.1 x
10000 ng/g	9326	6426 \pm 584	D	0.7 x

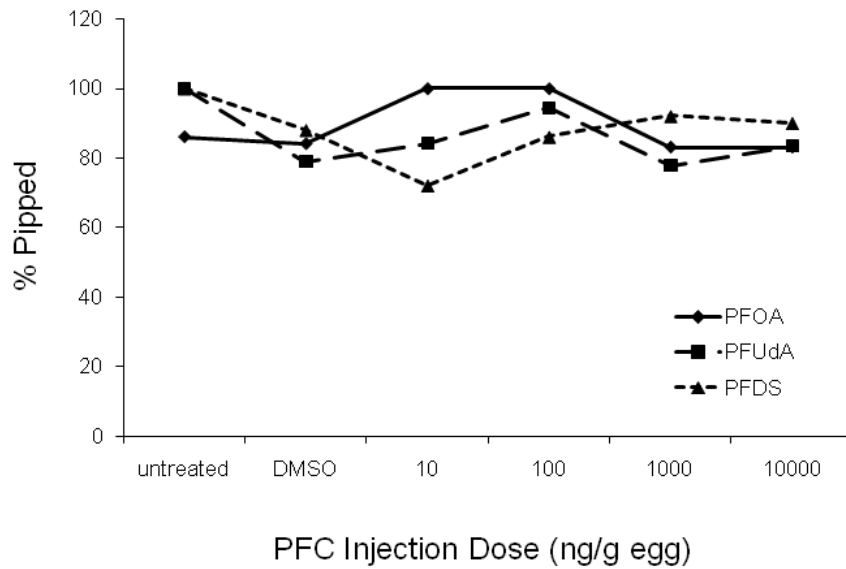


Figure 3.1: The effect of injecting PFOA, PFUdA and PFDS into chicken eggs prior to incubation on embryonic pipping success. Results are based on 13-20 fertile eggs per dose group.

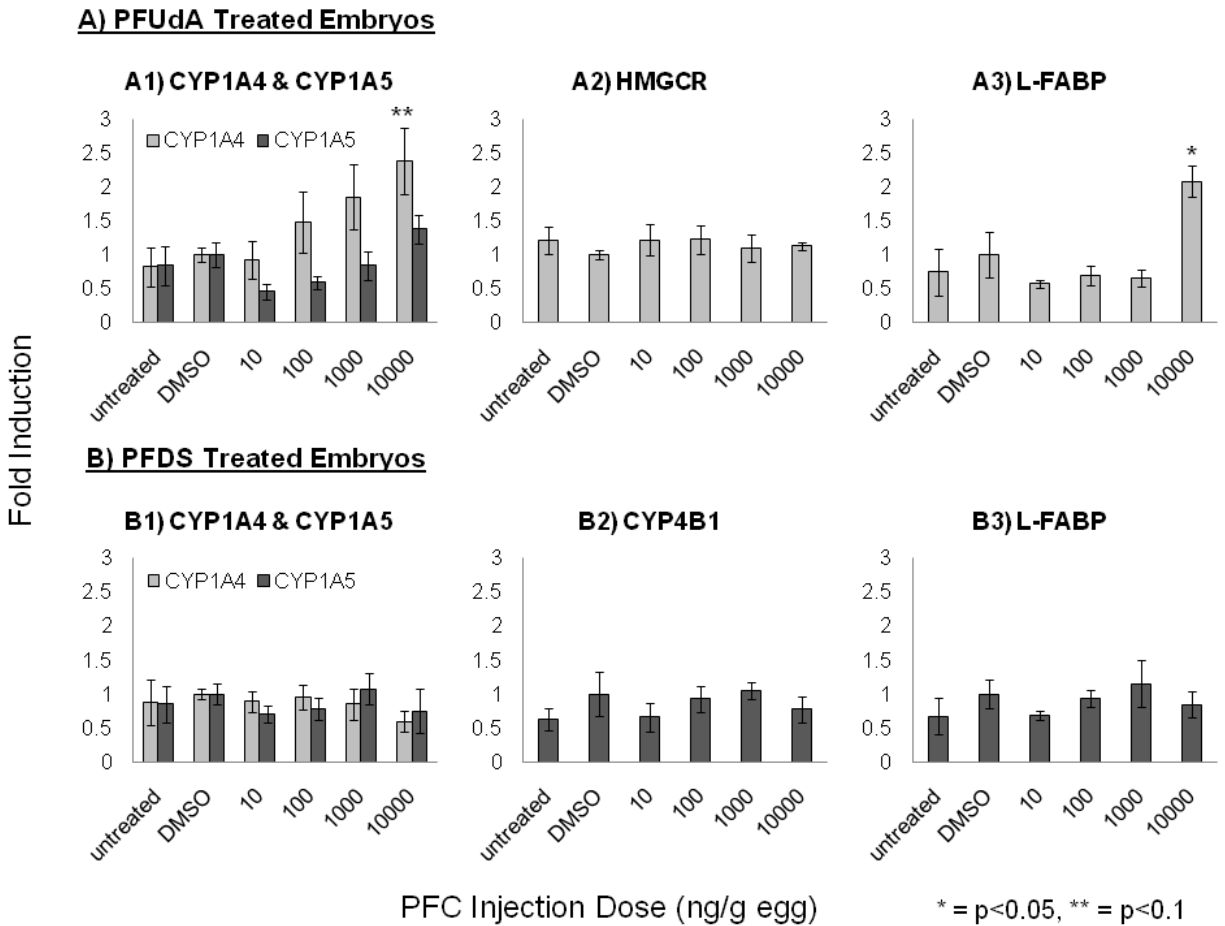


Figure 3.2: Expression of CYP1A4, CYP1A5, CYP4B1, HMGCR, and L-FABP mRNA in liver tissue of chicken embryos exposed to increasing concentrations of A) PFUdA and B) PFDS. Mean and standard error calculations are based on 5 individual embryos per dose group. p values were calculated by comparing values to the DMSO vehicle control group using ANOVA followed by Tukey pairwise comparison.

Chapter 4

Isomer-Specific Accumulation of Perfluorooctane Sulfonate in the Liver of Chicken Embryos Exposed *in ovo* to a Technical Mixture

(Modified from O'Brien, J.M., Kennedy, S.W., Chu, S. & Letcher, R.J. 2010. *Environ.Toxicol.Chem.*, **30**, 226-231)

4.1. Abstract

Prior to its recent phase-out, perfluorooctane sulfonate (PFOS) was produced by electrochemical fluorination processes, which yielded technical mixtures composed of linear isomer (~65-79%) and several branched isomers (~21-35%). Because it is suspected that PFOS can biomagnify in wildlife, birds that occupy higher trophic levels may be at increased risk of exposure. We hypothesized that the pharmacokinetic properties of PFOS are isomer-specific in developing chicken (*Gallus gallus domesticus*) embryos exposed to technical grade PFOS (T-PFOS). In the present study, T-PFOS was composed of 62.7% linear isomer (L-PFOS) and 37.3% branched isomer, including six mono(trifluoromethyl)-branched isomers and four bis(trifluoromethyl)-branched isomers. Concentrations of 0.1, 5, or 100 µg/g of T-PFOS were injected into the air cell of chicken eggs prior to incubation. After pipping, compared with T-PFOS, the PFOS isomer profile in embryonic liver tissue for the 0.1 µg/g dose-group showed 21% enrichment in the proportion of L-PFOS with a corresponding decrease in the proportion of branched isomers. Not all branched isomers were discriminated against at equal rates. The proportion of two mono(trifluoromethyl)-branched isomers and three bis(trifluoromethyl)-branched isomers decreased to a greater degree than other branched isomers. In contrast, the mono-branched isomer, P6MHpS, was overrepresented in the low-dose group. In the higher dose groups, L-PFOS was still enriched but only by approximately 10%, which indicated a dose-dependent change in isomer composition relative to T-PFOS. These results show that

accumulation of PFOS in chicken embryo livers is dependent on the presence and position of branches on the alkyl backbone. This supports the hypothesis that the pharmacokinetics of PFOS is isomer-specific in biota, and may help explain why wildlife PFOS burdens are dominated by L-PFOS relative to T-PFOS mixtures.

4.2. Introduction

Perfluoroalkyl compounds (PFCs) have unique chemical properties that make them ideal for a variety of applications including as industrial surfactants and oil and stain repellents (Kissa, 2001). Due to their large-scale use and their resistance to environmental and biological degradation, several PFCs have become persistent environmental contaminants. Concentrations of perfluorooctane sulfonate (PFOS) in the environment and in human tissue are the highest reported among PFCs. Consequently, the major manufacturers of PFOS phased-out its production by 2002. Although production has ceased, PFOS still remains the most environmentally abundant PFC and has been detected in a wide range of environmental niches including aquatic and arctic food webs (Houde *et al.*, 2006). Particularly high concentrations of PFOS (several parts per million) have been detected in animals at high trophic levels such as polar bears and fish eating birds (Houde *et al.*, 2006).

Prior to the phase-out of PFOS, it was primarily manufactured by industrial processes based on electrochemical fluorination (ECF), which yields impure mixtures composed of 2 to 20% non-PFOS impurities, with the remaining portion containing about 65 to 79% linear PFOS (L-PFOS) and 21 to 35% branched PFOS isomers (Arsenault *et al.*, 2008; Benskin *et al.*, 2007; Chu & Letcher, 2009). Although, theoretically, there are 89 possible geometric PFOS isomers, only eleven isomers have been detected in the technical product and environmental samples

(Rayne *et al.*, 2008). Most current PFC production is based on telomerization, a process that generates an almost purely linear product. While PFOS is known to be bioaccumulative (Conder *et al.*, 2008) and toxic to laboratory animals at environmentally relevant concentrations, including chickens (Lau *et al.*, 2007; Molina *et al.*, 2006; O'Brien *et al.*, 2009a; Peden-Adams *et al.*, 2008), the toxicology and kinetics of individual PFOS isomers is as of yet poorly characterized. This has mostly been due to the lack of methods for accurate isomer quantification. However, recent advances in analytical chemistry have allowed researchers to begin generating isomer-specific data for human and environmental samples (Benskin *et al.*, 2009; Chu & Letcher, 2009; De Silva & Mabury, 2004; De Silva & Mabury, 2006; De Silva *et al.*, 2009b; De Silva *et al.*, 2009c; Houde *et al.*, 2008).

The isomeric profile of PFOS in human serum was recently examined and was shown to have a high proportion of branched isomers, resembling ECF-produced PFOS (Karrman *et al.*, 2007). Interestingly though, the isomer profiles in wildlife samples had disproportionately low concentrations of branched isomers, compared to ECF produced PFOS. In many cases, over 90% of the total PFOS concentration was found to be L-PFOS (Chu & Letcher, 2009; Gebbink & Letcher, 2010; Houde *et al.*, 2008). The reason for these discrepancies is unclear as all environmental PFOS is believed to be of ECF origin. Possible explanations include differences in the sources of PFOS exposure, variable degradation or retention of PFOS isomers and its precursors, or biological mechanisms for selection.

In a two-part pharmacokinetic study, Benskin *et al.* (2009) and DeSilva *et al.* (2009a) found that, in general, most branched isomers had lower blood depuration half-lives in rats acutely or sub-chronically exposed to PFOS. Similarly, DeSilva *et al.* (2009b) showed a tendency for linear isomers of perfluorooctanoic acid (PFOA) and perfluorononanoic acid

(PFNA) to have higher half-lives in rainbow trout exposed via the diet to ECF produced mixtures of these compounds.

It is known, however, that PFCs have substantially different pharmacokinetic properties among species (Andersen *et al.*, 2008; Hundley *et al.*, 2006; Kudo *et al.*, 2001). It is therefore unclear if similar biological discrimination of PFC isomers occurs in avian species as it does in rats and trout. Given the high PFOS burden that many wild avian species bear, and their high trophic level in many aquatic and terrestrial food webs, PFOS isomer fate in birds is an important issue in environmental toxicology.

To investigate how PFOS isomers are accumulated in avian liver tissue, the PFOS content in the liver of laboratory-exposed chicken embryos, collected from a previously conducted egg injection study (O'Brien *et al.*, 2009a), was re-examined using a newly developed in-port derivatization gas-chromatography/mass spectrometry (GC-MS) method (Chu & Letcher, 2009). Hepatic isomer profiles were compared to that of the originally injected solution (technical grade PFOS, T-PFOS), to determine if changes in the PFOS isomer pattern had occurred.

4.3. Materials and methods

4.3.1. Chemicals

Technical grade perfluorooctane sulfonate (T-PFOS) for injection, standard solutions of the eleven individual branched and linear PFOS isomers, and $^{13}\text{C}_4$ -labeled PFOS were obtained from Wellington Laboratories (Guelph, ON, Canada). The abbreviations and chemical formulas for all eleven isomers identified in T-PFOS are shown in Table 4.1. Concentration and purity of all PFOS solutions were as previously described (Chu & Letcher, 2009). Solutions for injection

were prepared from a stock solution of T-PFOS dissolved in dimethyl sulfoxide (DMSO). Compared to water and corn oil, PFOS was maximally soluble in DMSO at the concentrations required for the present study. Injection of DMSO alone had no effect on embryo viability (measured as pipping success) (O'Brien *et al.*, 2009a). Tetrabutylammonium hydroxide 30 hydrate (TBAH), formic acid (98-100%) and ammonium hydroxide (28-30% w/v) were analytical grade and obtained from Sigma-Aldrich (Oakville, ON, Canada). All solvents used were high-performance liquid chromatography grade and purchased from Fisher Scientific (Ottawa, ON, Canada).

4.3.2. Tissues

Livers from embryos exposed in ovo to T-PFOS were obtained from a previously conducted egg injection study (O'Brien *et al.*, 2009a). Briefly, eggs were injected with T-PFOS dissolved in DMSO at concentrations of 0.1 µg PFOS/g egg, 5.0 µg/g and 100.0 µg/g prior to incubation. A vehicle control group was exposed solely to DMSO while another control group received no injection. Embryos were incubated until pipping, at which point embryos were euthanized by decapitation and liver tissues were collected. All procedures followed protocols approved by the Animal Care Committee at the National Wildlife Research Centre.

4.3.3. Isomer-specific PFOS determination

PFOS was extracted from the livers of 6 to 10 embryos per dose group then cleaned by solid-phase extraction (SPE) on Oasis[®] WAX cartridges (Waters Inc., Mississauga, ON, Canada). PFOS isomers were quantified in these extracts, as well as in two replicates, of the egg injection solution (T-PFOS dissolved in DMSO) according to the method of Chu and Letcher

(2009). Briefly, the methanol extracts for liquid chromatography-tandem mass spectrometry (which already contained the $^{13}\text{C}_4$ -labeled PFOS as internal standard) were evaporated to dryness and dissolved in 100 μl water. A volume of 100 μl TBAH solution (0.5 g of TBAH in 5 ml diethyl ether) was added to each sample. The tubes were capped and the solution was vortexed. Subsequently 100 μl of diethyl ether was added and mixed again. The samples were centrifuged and frozen at -20°C . The diethyl ether phase was separated from the aqueous layer (ice) and transferred into another tube. The samples were evaporated to dryness, redissolved in 100 μl of diethyl ether and transferred to a vial with 100 μl insert for gas chromatography-mass spectrometry (GC-MS) analysis.

The in-port derivatization and GC-MS analysis (Chu & Letcher, 2009) were performed using an Agilent 6890 gas chromatograph (GC) coupled to an Agilent-5973N quadrupole mass spectrometer (MS) detector (Mississauga, ON, Canada). The GC was equipped with a 30 m \times 0.25 mm inner diameter DB-5 capillary column with a film thickness of 0.25 μm . Helium was used as carrier gas at a constant flow of 1 ml/min. Five μl of sample solution were injected with splitless mode, and a double taper deactivated splitless inlet liner was used. The injector temperature was 300°C ; the oven temperature was programmed as follows: 50°C , hold for 2 min, then at $5^\circ\text{C}/\text{min}$ to 120°C . Ionization was performed in electron capture negative ionization mode using methane as reagent gas. The transfer line, source, and quadrupole temperatures were 280, 180, and 150°C , respectively. Selected ion-monitoring mode was used for quantitative analysis.

Quantification of the individual isomers was done using an isotope dilution method with five point calibration curves using T-PFOS as standard, for which the concentrations of the individual branched and L-PFOS isomers were previously determined using individual branched

or L-PFOS isomers standards (Chu & Letcher, 2009). There is currently no standard reference material of any kind for PFOS isomers. A pool of herring gull egg samples collected in 1989 from the Laurentian Great Lakes (North America) colonies was used as an in-house reference sample. For total PFOS (branched and linear), reproducibility was acceptable with a relative standard deviation of 20%. The method detection limits (MDL) for the branched PFOS isomers ranged between 0.17 to 0.46 ng/g wet weight, and for L-PFOS was 6.71 ng/g wet weight. For branched isomers, the most abundant, and thus the most sensitive MS ions were chosen for quantitative analysis. However, for L-PFOS an anion of m/z 499 atomic mass units (amu) was chosen for quantitative analysis, rather than the most abundant anion of m/z 137 amu. This resulted in a difference in MDL for L-PFOS compared to the branched isomers. The reason is that we used an internal standard method and the ^{13}C -enriched L-PFOS surrogate, sodium perfluoro-1-[1,2,3,4- $^{13}\text{C}_4$]octane sulfonates, was used as internal standard. As the relatively less abundant (and thus less sensitive) anion of m/z 449 amu was used for quantitative analysis, the MDL for L-PFOS was higher than branched isomers.

4.3.4. Statistics

Statistical differences in isomer proportions were identified by analysis of variance followed by Bonferroni's pairwise comparisons using normalized data. Isomer data were normalized to total PFOS/g sample, or to total branched PFOS isomers/g sample.

4.4. Results

Low levels of PFOS were detected in the untreated and vehicle control chicken embryos (as reported in O'Brien *et al.*, 2009a). Upon GC analysis it was determined that all PFOS

detected in these groups was of the linear form (data not shown). Total PFOS concentrations in liver tissue of exposed embryos increased in a dose dependent fashion as previously demonstrated (data presented in O'Brien *et al.*, 2009a).

Eleven different PFOS isomers, including L-PFOS, six mono(trifluoromethyl)-branched isomers and four bis(trifluoromethyl)-branched isomers, were detected in most treated samples. The PFOS isomer profiles in the liver tissue of exposed embryos and that of the original T-PFOS solution used for injection are compared in Figure 4.1. Technical grade PFOS was predominantly comprised of the linear isomer followed by P6MHpS > P3MHpS > P5MHpS > P4MHpS. The remaining two mono(trifluoromethyl)-branched isomers, P1MHpS and P2MHpS, and all bis(trifluoromethyl)-branched isomers each contributed less than 1% to total PFOS concentration in the technical mixture.

The proportion of L-PFOS in the liver of all treated embryos was significantly higher than in T-PFOS. The degree of difference was inversely proportional to dose, with the largest increase, approximately 20%, occurring in the 0.1 µg/g dose group. Concordantly, liver tissue from all treatment groups had lower proportions of branched isomers. Again, this difference was most evident in the lowest dose-group and lessened as a function of increasing dose. This general trend was observed for most individual branched isomers with two exceptions. Both P1MHpS and P2MHpS were over-represented up to 2-fold in the 100.0 and 5.0 µg/g dose groups compared to T-PFOS, but only significantly for P1MHpS at 100.0 µg/g. These two isomers were proportionally lower in the 0.1 µg/g dose group, although not significantly.

From an alternate perspective, when the isomer-specific concentration data were normalized to total branched isomer concentration, it was more evident that all branched forms were not equally discriminated against (Figure 4.2). Two mono(trifluoromethyl)-branched

isomers, P3MHpS, P4MHpS, and three of the bis(trifluoromethyl)-branched isomers, P44DMHxS, P45DMHxS and P55DMHxS, had lower representation in the 0.1 µg/g dose group, compared to other branched isomers in T-PFOS. In contrast, P6MHps was proportionately higher in the low dose group. In Supplementary Figure S4.1 (Appendix) we also show the portion of each PFOS isomer that was recovered in the liver relative to the administered dose of T-PFOS, where the percent recovery of each isomer was normalized to the percent recovery of total PFOS concentrations for a given dose group. From this figure, we further illustrate that L-PFOS is recovered at a higher rate in all dose groups, and that 1- and 2- branched isomers are recovered at higher rates in the 5 and 100 µg/g dose groups. Furthermore, among the branched isomers, the 2- and 6- branched isomers had lower recoveries, and that the remaining isomers and particularly the bis-branched isomers have the lowest recovery rate.

4.5. Discussion

The present study shows that the hepatic accumulation of PFOS in the developing avian embryo is isomer-specific. An enrichment of the linear isomer was observed in all embryonic dose groups relative to the dosed technical mixture. Similarly, all branched isomers were proportionately lower in all treatment groups relative to T-PFOS, and the degree to which individual branched isomers were affected also appeared to be isomer-specific.

Benskin *et al.* (2009) and DeSilva *et al* (2009a) also noted isomer-specific accumulation and elimination of PFOS isomers in rats exposed orally to T-PFOS. Most of these differences, however, were observed for accumulation of PFOS in blood. Accumulation constants in liver tissue were not determined but hepatic depuration half-lives for the various PFOS isomers were not statistically different in rats. In the present study, the extent to which differential

accumulation of isomers occurred was inversely proportional to dose, with the most dramatic differences occurring in the 0.1 $\mu\text{g/g}$ dose group. This dose corresponded to a hepatic PFOS burden of 0.15 (± 0.02) $\mu\text{g/g}$ in the embryos (O'Brien *et al.*, 2009a). The acute dose used in Benskin *et al.* (2009) resulted in a hepatic burden of 4.2 $\mu\text{g/g}$ of L-PFOS alone, which is approximately thirty-fold higher than the lowest exposure used in the present study. If differential accumulation of PFOS isomers in rat liver is dose dependent, as observed in developing chickens in the present study, differences may not be as discernable at the exposure levels employed by Benskin *et al.* (2009). However, isomer concentrations in chicken embryos exposed to concentrations as high as 100 $\mu\text{g/g}$ were statistically distinguishable from T-PFOS in the present study. Nevertheless, the overall discrimination of PFOS isomer patterns between rat blood and chicken embryo liver were similar.

In addition to a strong selection for L-PFOS, the mono(trifluoromethyl)-branched isomer, P1MHpS, was three times more persistent than L-PFOS in rat blood (Benskin *et al.*, 2009). This is consistent with the results from the present study. The proportion of P1MHpS increased relative to T-PFOS in both the 5.0 and 100 $\mu\text{g/g}$ dose groups. The proportion of P2MHpS also increased at these dose levels although not significantly. It was suggested that P1MHpS, and perhaps to a lesser degree P2MHpS, may be more resistant to elimination than other branched isomers as a function of the trifluoromethyl branch substitution being on alkyl chain positions closer to the sulfonate moiety. This trend however was only evident in the high dose groups of the present study.

Although all branched isomers were proportionately lower compared to T-PFOS at 0.1 $\mu\text{g/g}$, the degree to which all isomers were affected was not equal. When data were normalized to total branched isomer burden (Figure 4.2), it became evident that P3MHpS, P4MHpS,

P44DMHxS, P45DMHxS, and P55DMHxS contributed less to the sum of all branched isomers compared to T-PFOS. This suggests that there is a strong selection against the accumulation of these particular isomers in the liver. In contrast, the terminally branched P6MHpS was proportionately higher than other branched isomers, relative to T-PFOS. This indicates that, while there is a selection against the accumulation of this isomer in liver tissue, the degree is not as strong as for other branched isomers.

A recent biomonitoring study characterized the PFOS isomer profiles in herring gull eggs collected from several colonies in the Laurentian Great Lakes (North America) (Gebbinck & Letcher, 2010). L-PFOS consistently dominated the isomer pattern in all eggs, comprising between 95.0 to 98.3% of the total PFOS concentration. Also in all gull eggs studied, comparable to T-PFOS, the percentage of the mono(trifluoromethyl) isomer to total PFOS concentration was much lower than L-PFOS, and decreased as the branch substitution was located in the alkyl chain backbone closer to the sulfonate group, i.e., P6MHpS (0 - 2.5%), P5MHpS (0.43 - 1.18%), P4MHpS (0.25 - 0.69%) and P3MHpS (0.32 - 0.74%). It was suggested that the apparent dilution/degradation of the mono(trifluoromethyl) isomers from environmental processes that occur prior to final accumulation in herring gull eggs is independent of the mono(trifluoromethyl) isomer structure. It is important to distinguish that these observations were made in whole egg homogenates as opposed to the present study that looked specifically at embryo livers. It is likely that the observed isomer profiles in the wild gull eggs are representative of the isomer profile of the female gulls that laid them. The maternal isomer profile is in turn affected by her own metabolism of PFOS isomers as well as the profile in the food she eats. What the present study does show is that there are biological mechanisms in the chicken that cause selective accumulation of PFOS isomers. As both the rat and chicken appear

to have some mechanisms for the preferential accumulation of the linear isomer or elimination of branched isomers, it is likely that similar mechanisms are conserved in a broad range of species. Selection for the linear isomer at various points in the food web may partially explain why there is such a large bias for the linear isomer in wild gulls. Chu and Letcher (2009) also showed that polar bear blood and liver from the Norwegian Arctic and Northern Canada, respectively, had proportionately high levels of L-PFOS relative to what is found in T-PFOS. The most abundant branched isomer in polar bear liver was also P6MHpS. In a study of a Lake Ontario food web, Houde *et al.* (2008) found that L-PFOS had a very high trophic magnification factor compared to mono(trifluoromethyl)-branched isomers, and that bis(trifluoromethyl)-branched isomers did not accumulate at all through the food web.

Although unlikely, the present study provides no evidence against chemical transformation between isomeric structures as a mechanism for differential accumulation. Because of the strength of the C-F bond, fully fluorinated hydrocarbons are extremely resistant to degradation by acids, bases, or oxidizing agents (Prescher *et al.*, 1985). The conditions required to break and rearrange the carbon-fluorine backbone occur only in very rare situations (Chen & Zhang, 2006; Hori *et al.*, 2006). Recent evidence has emerged that suggests branched PFOS isomers could be microbially defluorinated in anaerobic conditions (Ochoa-Herrera *et al.*, 2008). This mechanism may partially explain isomer patterns in environmental samples, but cannot account for the results obtained in this or similar animal dosing studies. The use of DMSO as a vehicle solvent could have also affected the distribution of isomers in embryo tissue. Although DMSO is generally evenly distributed through the body (Kaye *et al.*, 1983), it is possible that DMSO may differentially affect partitioning of PFOS isomers into tissues. However, because our results were comparable to those from animal feeding studies (Benskin *et*

al., 2009; De Silva *et al.*, 2009a), and environmental samples (Chu & Letcher, 2009; De Silva *et al.*, 2009b; Gebbink & Letcher, 2010; Houde *et al.*, 2008) we feel the effects of DMSO were minimal. It is more likely that the change in profiles was due to a mechanism involving selective uptake and elimination of PFOS isomers. In their rat studies, Benskin *et al.* (2009) and DeSilva *et al.* (2009a) discovered that most branched isomers were preferentially eliminated via urinary excretion. It is likely that branched isomers are similarly excreted in the developing chicken embryo and would thus be stored within the chorioallantoic membrane; an extraembryonic membrane used to improve the diffusion of oxygen and to store liquid waste. Unfortunately, isomers profiles in this tissue could not be determined for the present study. Measurements were performed on archived samples from which chorioallantoic membrane tissue was not collected. The exact mechanisms of PFOS isomer differentiation remain to be elucidated but it is likely to involve differential binding to transport proteins. Perfluoroalkyl compounds have been shown to bind to fatty acid binding proteins in the liver and lipoproteins and albumin in blood (Jones *et al.*, 2003; Luebker *et al.*, 2002) although the binding strength of individual isomers to these proteins remains to be investigated. The observation that isomer discrimination was dose dependent suggests that all isomers accumulate through a similar mechanism, but at high doses, these mechanisms are saturated and cannot discriminate between branched arrangements.

Several studies have shown that PFCs will differentially affect toxicological endpoints (molecular or physiological) depending on its isomeric content (Hickey *et al.*, 2009; Loveless *et al.*, 2006; Vanden Heuvel *et al.*, 2006). In light of these findings, and others previously discussed, the environmental relevance of results from toxicological studies using T-PFOS need to be carefully assessed. Effects elicited by exposure to T-PFOS in the laboratory may not necessarily be pertinent to wild animals, which are mainly exposed to L-PFOS. This is

particularly important for in vitro studies, when there is little to no selective accumulation or elimination of isomers.

Table 4.1: Abbreviations and chemical formulas of all eleven isomers identified in technical grade PFOS

Abbreviation	Reading	Chemical Formula
L-PFOS	<i>n</i> -Perfluoro-1-octanesulfonate	CF ₃ CF ₂ CF ₂ CF ₂ CF ₂ CF ₂ CF ₂ CF ₂ SO ₃ H
P1MHpS	Perfluoro-1-methyl-heptane sulfonate	CF ₃ CF ₂ CF ₂ CF ₂ CF ₂ CF ₂ CF(CF ₃)SO ₃ H
P2MHpS	Perfluoro-2-methyl-heptane sulfonate	CF ₃ CF ₂ CF ₂ CF ₂ CF ₂ CF(CF ₃)CF ₂ SO ₃ H
P3MHpS	Perfluoro-3-methyl-heptane sulfonate	CF ₃ CF ₂ CF ₂ CF ₂ CF(CF ₃)CF ₂ CF ₂ SO ₃ H
P4MHpS	Perfluoro-4-methyl-heptane sulfonate	CF ₃ CF ₂ CF ₂ CF(CF ₃)CF ₂ CF ₂ CF ₂ SO ₃ H
P5MHpS	Perfluoro-5-methyl-heptane sulfonate	CF ₃ CF ₂ CF(CF ₃)CF ₂ CF ₂ CF ₂ CF ₂ SO ₃ H
P6MHpS	Perfluoro-6-methyl-heptane sulfonate	CF ₃ CF(CF ₃)CF ₂ CF ₂ CF ₂ CF ₂ CF ₂ SO ₃ H
P35DMHxS	Perfluoro-3,5-dimethyl-hexane sulfonate	CF ₃ CF(CF ₃)CF ₂ CF(CF ₃)CF ₂ CF ₂ SO ₃ H
P44DMHxS	Perfluoro-4,4-dimethyl-hexane sulfonate	CF ₃ CF ₂ C(CF ₃) ₂ CF ₂ CF ₂ CF ₂ SO ₃ H
P45DMHxS	Perfluoro-4,5-dimethyl-hexane sulfonate	CF ₃ CF(CF ₃)CF(CF ₃)CF ₂ CF ₂ CF ₂ SO ₃ H
P55DMHxS	Perfluoro-5,5-dimethyl-hexane sulfonate	CF ₃ C(CF ₃) ₂ CF ₂ CF ₂ CF ₂ CF ₂ SO ₃ H

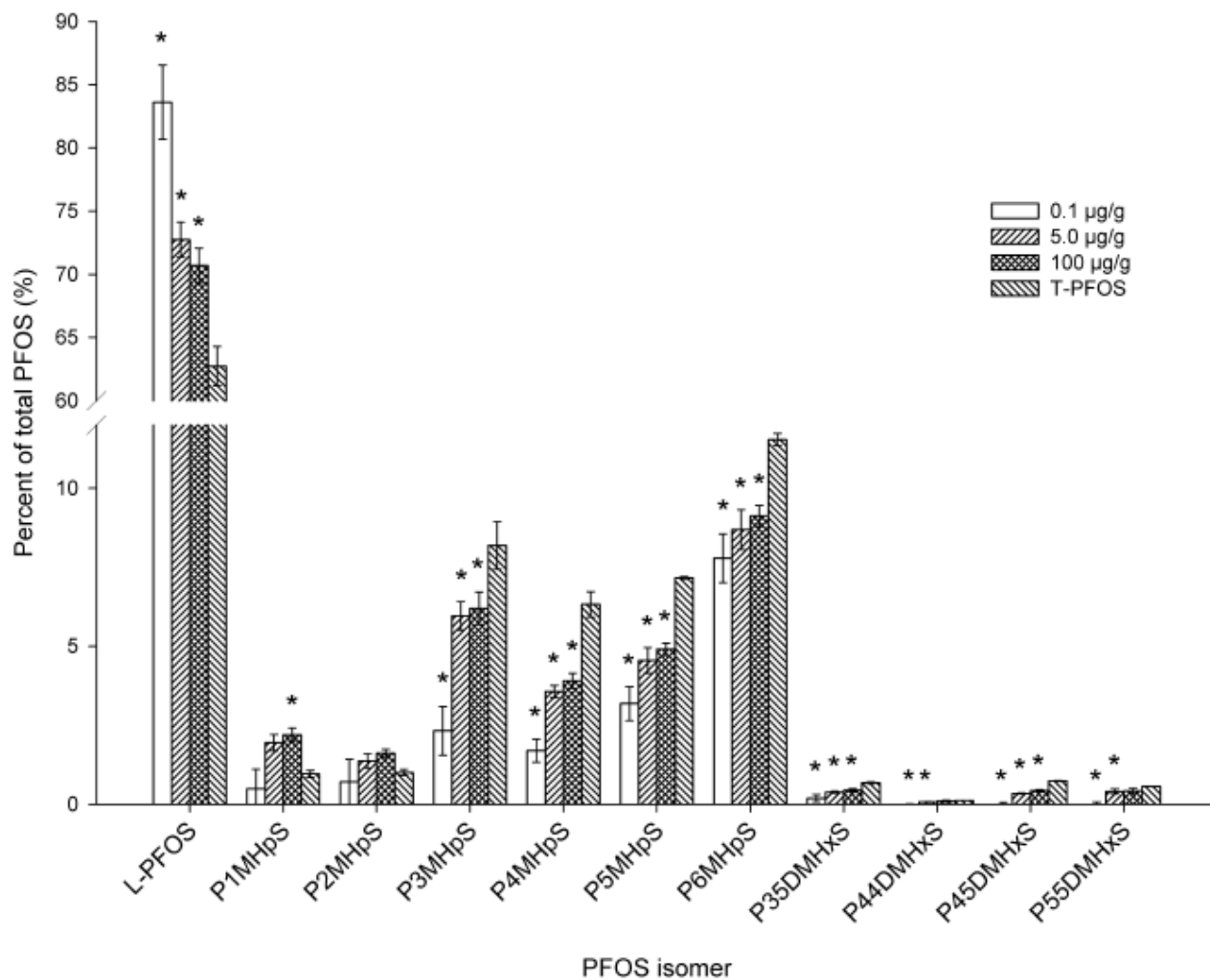


Figure 4.1: Perfluorooctane sulfonate (PFOS) isomer profiles in liver tissue from chicken embryos exposed prior to incubation to various concentrations of technical grade PFOS (T-PFOS). Data were normalized to total PFOS burden and represent the mean and standard deviation of 6-10 individual birds. The T-PFOS profile represents the mean and standard deviation of 2 replicates. (*) denotes significantly different from T-PFOS.

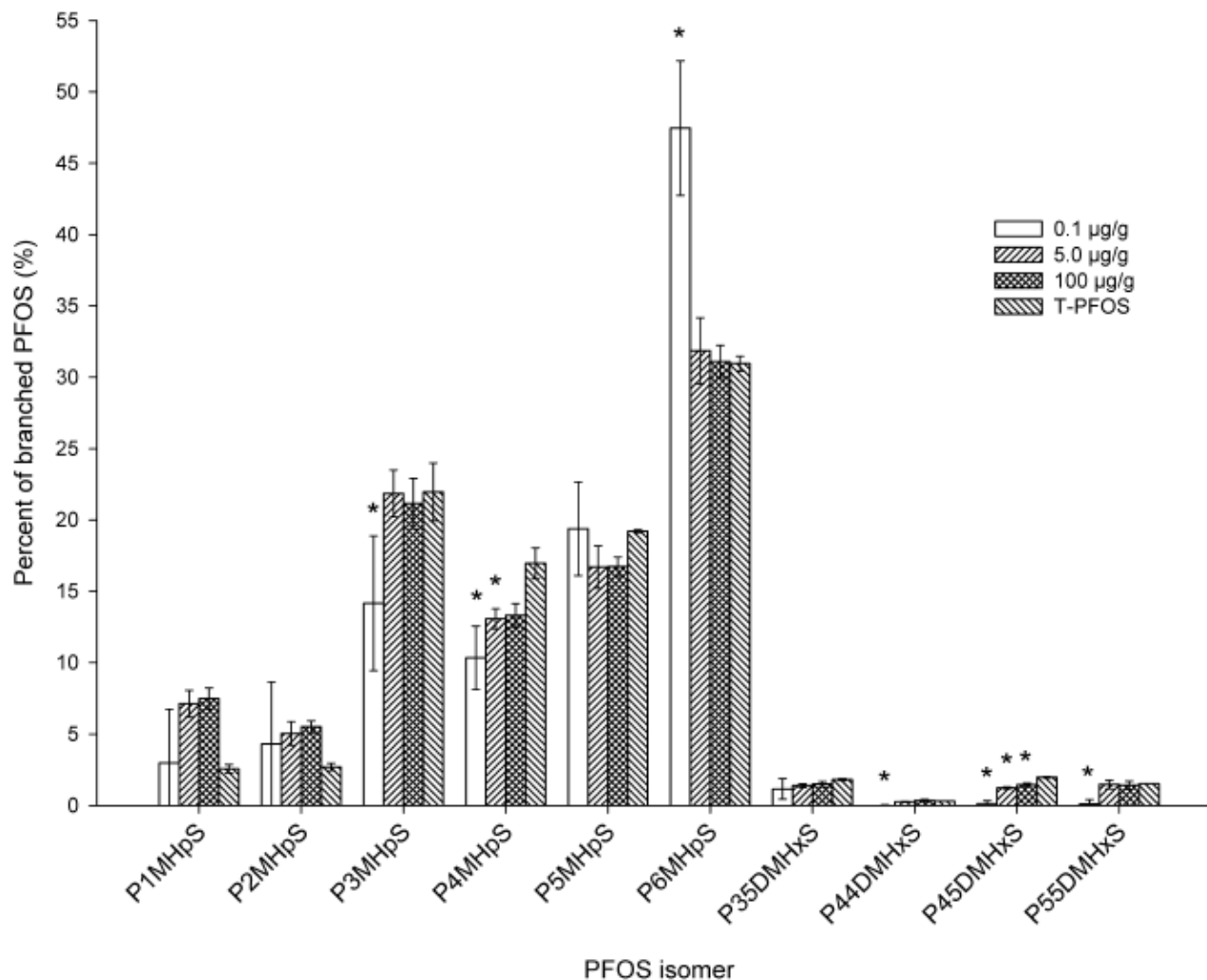


Figure 4.2: Profile of branched perfluorooctane sulfonate (PFOS) isomers normalized to total branched isomer content in chicken embryos exposed to various concentrations of technical grade PFOS (T-PFOS). Data represent the mean and standard deviation of 6 to 10 individual birds. The T-PFOS profile represents the mean and standard deviation of 2 replicates. (*) denotes significantly different from T-PFOS.

Chapter 5

Technical grade PFOS is more transcriptionally Disruptive in cultured chicken embryonic hepatocytes than linear PFOS

5.1. Abstract

Perfluorooctane sulfonate (PFOS) is a persistent environmental pollutant. Recently it was discovered that the PFOS detected in wildlife, such as polar bears and fish-eating birds, had a much greater proportion of linear PFOS (L-PFOS) than the commercially produced technical product (T-PFOS), which contains linear and branched isomers. Prior to this knowledge, most studies that investigated the possible toxicological effects of PFOS exposure used T-PFOS as the test compound. Such studies do not consider the environmental kinetics of the various PFOS isomers and results may lead to a less accurate assessment of the potential risk to wildlife. This is especially true for *in vitro* exposures where isomer-selective processes do not occur. In this study we compared the transcriptional profiles of cultured chicken embryonic hepatocytes (CEH) exposed to either L-PFOS or T-PFOS using Agilent 4x44k Chicken (V2) Gene Expression microarrays. At equal concentrations (10 μ M), T-PFOS altered the expression of significantly more genes (340 genes, >1.5 fold change, false discovery rate adjusted $p < 0.05$) compared to L-PFOS (130 genes). Functional enrichment analysis showed that L-PFOS and T-PFOS affected genes involved in lipid metabolism, cellular growth and proliferation, and cell-cell signalling. Pathway and interactome analysis suggested that genes may be affected through RXR binding partners, oxidative stress response, TP53 signalling, MYC signalling, Wnt/ β -catenin signalling and PPAR γ and SREBP receptors. In all functional categories and pathways examined, the response elicited by T-PFOS was much greater than L-PFOS. These data show that T-PFOS elicits a significantly greater transcriptional response in CEH than L-PFOS alone. These results

suggest that the branched isomers may account for a large proportion of the reported toxicological effects of PFOS, and that environmental assessments based on data from laboratory studies using T-PFOS may overestimate risk to wildlife as it is L-PFOS that is primarily found in wild liver tissues.

5.2. Introduction

Perfluoroalkyl compounds (PFCs) are a synthetic class of compounds that have been produced over the last half century for their use in non-stick and stain resistance applications, (Kissa, 2001). Because of their recent increase in production and use, and their inherent resistance to environmental and biological degradation (Prescher *et al.*, 1985), some PFCs have become persistent environmental contaminants (Giesy and Kannan, 2001; Houde *et al.*, 2006). Structurally, PFCs are composed of a completely fluorinated carbon chain, ranging from 4 to 14 carbon atoms long, with a functional group at the terminal end of the molecule. Depending on the production method employed, the carbon backbone can be completely linear or in various branched arrangements. Perfluorooctane sulfonate (PFOS), the most environmentally prevalent PFC, was mainly produced using an electrochemical fluorination process (ECF) that resulted in a technical product (T-PFOS) composed of approximately 60-70% linear isomer (L-PFOS) with the remaining 30-40% in different branched configurations (Arsenault *et al.*, 2008; Benskin *et al.*, 2007; Chu and Letcher 2009).

Although the majority of PFOS detected in the environment is thought to be of ECF origin, recent biomonitoring surveys found that the PFOS burden in wildlife, especially in animals at high trophic levels such as polar bears and fish-eating birds, had a much greater proportion of L-PFOS compared to manufactured T-PFOS (Chu & Letcher 2009; Gebbink and

Letcher 2010; Houde *et al.*, 2008). For example, Chu and Letcher (2009) found that in the eggs of herring gulls collected from the North American Great Lakes, 95% of the PFOS burden was in the linear form. Pharmacokinetic studies suggest that this may be due to the selective elimination of branched isomers and retention of L-PFOS, especially in the liver where PFOS tends to accumulate (Benskin *et al.*, 2009; De Silva *et al.*, 2009a, O'Brien *et al.*, 2010).

Before the pharmacokinetic differences between PFOS isomers were recognized, most laboratory toxicology studies exposed test animals to T-PFOS obtained directly from manufacturers. Exposure effects from such studies include interference with lipid and carbohydrate metabolism, increased liver weight, hepatomegaly, disruption of the neuroendocrine system, and decreased reproductive success (Abbott *et al.*, 2009; Austin *et al.*, 2003; Lau *et al.*, 2003; Lau *et al.*, 2004). For birds, exposure to T-PFOS can cause hepatic lesions, reduced hatching success and reduced survivability of hatchlings (Molina *et al.*, 2006; Newsted *et al.*, 2006; Newsted *et al.*, 2007; O'Brien *et al.*, 2009a; Peden-Adams *et al.*, 2008). These experiments, however, may not accurately reflect natural exposure conditions experienced by wildlife because they do not consider PFOS isomer kinetics, and may therefore lead to poor estimations of exposure effects. This is of particular relevance for conclusions drawn from *in vitro* experiments where there is no selective distribution of PFOS isomers.

Several recent studies have shown that PFCs can elicit different molecular and physiological effects depending on the isomeric composition. Loveless *et al.* (2006) observed increased weight loss and lipid oxidation in rodents orally exposed to linear ammonium perfluorooctanoate compared to animals exposed solely to branched isomers. In contrast, Hickey *et al.* (2009) found that genes involved in lipid and xenobiotic metabolism had a more profound

transcriptional response in cultured chicken embryonic hepatocytes when exposed to T-PFOS than when exposed solely to L-PFOS.

The aim of this study was to further characterize the differences in transcriptional response between L-PFOS and T-PFOS in a cell culture model that is used routinely in our laboratory for screening chemicals for transcriptional effects in avian species: cultured chicken embryonic hepatocytes (CEH). We used DNA microarrays to identify system-wide differences in transcriptome response to L-PFOS or T-PFOS exposure with emphasis on pathways and functionally related genes associated with PFOS toxicity. We also examined the potential role of regulatory proteins in the CEH response to L-PFOS or T-PFOS.

5.3. Materials and methods

5.3.1. Chemicals

Technical grade perfluorooctane sulfonate (T-PFOS) was obtained from Wellington Laboratories (Guelph, ON, Canada). The T-PFOS used in the present study comprised 65% linear isomers and 35% branched isomers as determined previously by Chu and Letcher (2009). Pure linear PFOS (L-PFOS, >98% purity) was also obtained from Wellington Laboratories. Stock solutions for dosing were prepared by dissolving T-PFOS and L-PFOS in dimethyl sulfoxide (DMSO).

5.3.2. Preparation of hepatocyte culture and dosing

Primary chicken embryonic hepatocyte (CEH) cultures were prepared from fertilized White Leghorn chicken (*Gallus gallus domesticus*) eggs that were obtained from the Canadian Food Inspection Agency (CFIA, Ottawa, Canada) as previously described (Hickey *et al.*, 2009)

with minor modifications. Briefly, eggs were artificially incubated at 37.5 °C and 60% humidity for 19 days. On day 19, embryos were removed from their eggs and euthanized by decapitation. Livers were removed and pooled. CEH were then isolated from pooled livers by collagenase digestion as described in Hickey *et al.* (2009). CEH were cultured in 48-well plates and each well contained approximately 781 µg of hepatocytes in 525 µl of medium. Cultured cells were incubated for 24 hr at 37 °C and 5% CO₂. All procedures were conducted according to protocols approved by the Animal Care Committee at the National Wildlife Research Centre.

CEH cultures were dosed with a DMSO solvent control or working solutions of T-PFOS or L-PFOS dissolved in DMSO to yield final concentrations of 1, 10, 20, 30 and 40 µM and then incubated for an additional 24 hours. After incubation, medium was removed and cells were flash frozen on dry ice and stored at -80°C. The viability of cells exposed to T-PFOS and L-PFOS were not affected by any of the concentrations tested as determined using the Calcein-AM assay (as reported in Hickey *et al.*, 2009).

5.3.3. RNA isolation and quantification

Total RNA was isolated from treated cells using the Qiagen RNeasy 96 kit (Qiagen, Mississauga, ON, Canada), including the on-column DNase treatment, according to the manufacturer's instructions. Following isolation, a second DNase treatment was performed using an Ambion DNA-free kit (Ambion, Austin, TX) as per manufacturer's instructions. RNA was quantified with a NanoDrop 2000 spectrophotometer (Thermo Scientific). RNA quality was assessed using a BioAnalyzer (Agilent Technologies, Mississauga, ON). Samples with A₂₆₀/A₂₈₀ ratios <1.7 and RNA integrity number <8.0 were not used for downstream applications. A

reference pool of RNA for microarray hybridizations was prepared from equal parts of all samples used for microarray analysis.

5.3.4. Microarray hybridization

For each microarray hybridization 150 ng of total RNA was hybridized to Agilent 4X44k chicken whole genome arrays (design #015068) against 150 ng of the reference pool of RNA. RNA from experimental samples was labelled with Cy5 and reference RNA with Cy3 using Agilent Quick Amp labelling kits as per manufacturer's instructions. 825 ng each of labelled sample and reference cRNA was then fragmented and hybridized for 17 hours to Agilent 4x44k Chicken (V2) Gene Expression microarrays (Design #015068) using Agilent Hybridization Kits as per manufacturer's direction. Arrays were washed and scanned on an Agilent G2505B scanner at 5 μ m resolution. Data were acquired using Agilent Feature Extraction software version

9.5.3.1.

5.3.5. Microarray data analysis

A reference design was used to analyse gene expression microarray data (Kerr, 2003; Kerr and Churchill, 2007). The design was blocked on the slide, since the Agilent arrays contain 4 arrays per slide. Background fluorescence was measured using the (-)3xSLv1 probes. Probes with median signal intensities less than the trimmed mean (trim = 5%) plus three trimmed standard deviations of the (-)3xSLv1 probe were flagged as absent. Data were pre-processed using R (R Development Core Team, 2010). The median signal intensities were normalized using the global LOWESS method (Yang *et al.*, 2002b) using the transform.madata function in the MAANOVA library (Wu *et al.*, 2003). Ratio intensity plots, constructed using complete and

single linkages, were generated to identify arrays with poor quality. Differentially expressed genes were identified using the MAANOVA library. An ANOVA model included the main effect of treatment and the block effect of the microarray. The F_s statistic (Cui *et al.*, 2005), a shrinkage estimator, was used for the gene-specific variance components and the associated p-values for all the statistical tests were estimated using the permutation method (30,000 permutations with residual shuffling). These p-values were then adjusted for multiple comparisons by using the false discovery rate approach (FDR) (Benjamini & Hochberg 1995). The least-squares means (Goodnight & Harvey 1978; Searle *et al.*, 1980), a function of the model parameters, was used to estimate the fold changes for each pairwise comparison.

Principal Component Analysis (PCA) and hierarchical clustering were performed using GeneSpring GX ver. 11.0.2 (Agilent Technologies). Clustering was performed on both entities and conditions, using the Euclidian distance metric and the centroid linkage rule.

Before gene sets were analyzed in Ingenuity Pathway Analysis (IPA, ver. 8.6), the DAVID Gene ID Conversion Tool (<http://david.abcc.ncifcrf.gov/>) was used to optimize the number of microarray gene ID's that were mapped as human, rat or mouse orthologs in IPA. The Functional and Canonical Pathway Analysis performed in IPA identified the biological functions/diseases or pathways that were most significant to the dataset. Molecules from the dataset that: a) were recognized as human, mouse or rat orthologs; b) met the fold-change cut-off of 1.5 and FDR adjusted p-value cut-off of 0.05; and c) were associated with biological functions and/or diseases in Ingenuity's Knowledgebase were considered for the analysis. A right-tailed Fisher's exact test was used to calculate a p-value determining the probability that each biological function/disease or pathway assigned to that dataset was due to chance alone.

For interaction network generation in IPA, differentially expressed genes that mapped into IPA were overlaid onto a global molecular network developed from information contained in Ingenuity's proprietary Knowledgebase. Networks of differentially expressed genes were then algorithmically generated based on their connectivity. In the generated network diagrams, genes are represented as nodes and the biological relationship between two nodes is represented as an edge (line). All edges are supported by at least one reference from the literature, from a textbook, or from canonical information stored in the Ingenuity Knowledgebase. Nodes are displayed using various shapes that represent the functional class of the gene. The intensity of the node color indicates the degree of up- (red) or down- (green) regulation. White nodes are not differentially expressed, and are added to the network as bridging/connector molecules. Edges are displayed with various labels that describe the nature of the relationship between the nodes (A=activation, B=binding, E=expression, EC=enzyme catalysis, I=inhibition, L=proteolysis, LO=localization, M=biochemical modification, MB=member of group, P=phosphorylation/dephosphorylation, PD=protein-DNA binding, PP=protein-protein binding, PR=protein-RNA binding, RB=regulation of binding, RE=reaction, T=transportation, and TR=translocation).

5.3.6. Real-time RT-PCR

RNA was reverse transcribed to cDNA using SuperScript II reverse transcriptase and random hexamer primers (Invitrogen Canada, Burlington, ON) as per manufacturer's instructions. No-RT controls were prepared in tandem. cDNA was diluted and aliquoted for real-time RT-PCR. Real-time RT-PCR reactions were performed using a Stratagene Mx3000 or Eppendorf Mastercycler ep Realplex real-time PCR instrument. Assays were performed with

TaqMan fluorogenic probes. Probes for each gene of interest were labelled with FAM and run in duplex with β -actin labelled with HEX (Mx3000) or JOE (Realplex) as the normalizing gene. All assays were performed using Stratagene Brilliant Q-PCR Core Reagent kits. Each reaction contained primers (from Invitrogen), probes (from Biosearch), 1x reaction buffer, 5mM $MgCl_2$, 0.8 μ M dNTPs, 8% glycerol and 1.25 U of SureStart Taq and brought to volume with diethylpyrocarbonate-treated water. Reactions performed in the Mx3000 had a total volume of 25 μ l and contained 60nM ROX reference dye and 5 μ l diluted cDNA. Reactions performed in the Realplex instrument had a total volume of 12.5 μ l and contained 2.5 μ l diluted cDNA. The nucleotide sequence for each primer and probe can be found in Supplementary Table S5.1 (Appendix). The thermal profile included a 10 min activation step at 95°C followed by 40 cycles of 30 s at 95°C and 1 min at 60°C. Fluorescence was measured after the 60°C step. Amplification efficiencies for each gene target were determined by standard curves and optimized by adjusting primer concentration (ranging from 50-900 nM) and $MgCl_2$ concentrations (from 5-10 mM) so that efficiency was approximately 100% (\pm 5%) and similar to that of β -actin (\pm 5%).

The delta CT values were used to identify differentially expressed genes using a generalization of the REST (Pfaffl *et al.*, 2002) approach. Here, a bootstrap test (Higgins, 2003) was conducted for each dose versus control comparison assuming a common error distribution using the R software. The critical value of the test statistic was determined by bootstrapping (B=2000) the residuals from a one-way ANOVA model. For each gene, p-values were adjusted for multiple comparisons using the Bonferroni-Holm method (Holm, 1979).

5.4. Results and discussion

5.4.1. Differentially expressed genes

Agilent 4x44k Chicken (V2) Gene Expression microarrays were used to identify changes in gene transcription in CEH exposed for 24 hours to different isomeric mixtures of PFOS relative to a vehicle control group. Array hybridizations were performed using RNA from replicate cultures (n=5 per dose group) prepared from a single pool of 60 chicken embryo livers and exposed to various concentrations of PFOS. For microarray experiments, cells were exposed to 10 μ M L-PFOS, 10 μ M T-PFOS or a DMSO solvent control. A total of 386 genes were differentially expressed >1.5 fold (FDR $p < 0.05$) in CEH following exposure to either L-PFOS or T-PFOS relative to the DMSO control group. Of these, 320 genes were up-regulated and 66 were down-regulated. The number of genes up- and down-regulated in each treatment is summarized in Table 5.1. Among these genes, 46 unique genes were dysregulated (up- or down-regulated) by only L-PFOS, 256 were affected only by T-PFOS, and 84 genes were affected by both L-PFOS and T-PFOS (Figure 5.1). T-PFOS was much more transcriptionally disruptive, affecting the expression of almost three times as many genes as L-PFOS at an equal dose of 10 μ M. A detailed list of genes differentially expressed by L-PFOS and T-PFOS treated cells is presented in Supplementary Table S5.2 (Appendix).

The highest increase in expression was for myosin heavy chain 6 (*Myh6*)*, which was greater than 3-fold in both treatment groups. Typically *Myh6* is only expressed in ventricular and extraocular muscle (Rossi *et al.*, 2010). However, one expression sequence tag (EST), ChEST143b11, a possible splice variant consisting of *Myh6* intron and exon sequence (including the region that is complementary to the *Myh6* microarray probe), has been detected in chicken

* Throughout this chapter, italicized abbreviations of gene names refer to the mRNA transcript whereas capitalized abbreviations refer to the protein

liver tissue (Boardman *et al.*, 2002). The role of *Myh6* in the response to PFOS is unclear. It is a type II myosin usually associated with contractile activity. It may be involved in the contraction of bile canaliculi (Ueno *et al.*, 1988), which, if improperly regulated, can lead to intrahepatic cholestasis and interfere with lipid metabolism. Functional analysis revealed that several other genes associated with intrahepatic cholestasis were also dysregulated by PFOS (shown in functional analysis section).

The greatest transcript up-regulation detected that were unique to L-PFOS and T-PFOS were a 2.0- and 2.4-fold increase in transcriptional activity of the uncharacterized transcripts CR386428 (EST ChEST229g1) and TC197254, respectively. The second largest unique increase to T-PFOS was a 2.2-fold increase in the expression of type II iodothyronine deiodinase (*Dio2*), which converts thyroxine (T4) to its more active form, triiodothyronine (T3). This is consistent with observations of reduced serum T4 in animals exposed to PFOS (Chang *et al.*, 2008; Martin *et al.*, 2007). A significant increase in expression for a gene with high sequence similarity to thyroid hormone receptor beta 2 (gene ID: X62642) was also observed only in the T-PFOS dose group. The fact that *Dio2* and X62642 were only perturbed by T-PFOS, and not L-PFOS, suggests that interference with active thyroid hormone levels may be instigated by the branched isomers of PFOS. Despite the presence of T4 in the culture medium (1 µg/ml) and changes in *Dio2* and X62642 expression, an accompanying change in expression for other thyroid hormone receptor controlled genes was not observed.

The largest overall decrease in expression was an approximately 4-fold change in glutathione-S-transferase alpha 3 (*Gsta3*) mRNA in both L-PFOS- and T-PFOS-treated cells. Down-regulation of several other glutathione-S-transferases (GSTs) was observed, including the alpha 4 and omega 1 isozymes (*Gsta4* and *Gsto1*, respectively). GSTs comprise a class of

enzymes that detoxify reactive electrophilic compounds by catalyzing their conjugation to reduced glutathione (GSH). Liu *et al.* (2007b) observed a decrease in total GST activity in response to PFOS exposure in cultured tilapia hepatocytes as well as a decrease in GSH levels. It was suggested that GST activity may have been suppressed in response to the oxidative stress due to increased lipid metabolism in order to conserve unconjugated GSH. The decreased GST mRNA expression from the present study supports this hypothesis. In addition to its role in detoxification, the protein encoded by *Gsta3* also has steroid isomerase activity that is crucial for steroid hormone production, which consumes cholesterol (Tars *et al.*, 2010). Suppression of *Gsta3* expression may also serve to maintain cholesterol levels, which are known to decrease following PFOS exposure (Berthiaume & Wallace, 2002; Seacat *et al.*, 2002). This is supported in the present study by the up-regulation of several genes involved in cholesterol synthesis including 3-hydroxy-3-methylglutaryl-CoA reductase (*Hmgcr*), cytochrome P450 8B1 (*Cyp8B1*), and isopentenyl-diphosphate delta isomerase 1 (*Idi1*), although these three genes were only affected by T-PFOS, whereas *Gsta3* was affected by both L- and T-PFOS (Supplementary Table S5.2).

The largest decrease unique to T-PFOS was a 1.9-fold reduction in alpha-2-HS-glycoprotein mRNA (*Ahsg*) expression. The *Ahsg* encodes a cytokine-binding glycoprotein that is secreted by the liver and is involved in the acute-phase immune response (Szweras *et al.*, 2002). AHSG glycoprotein also tends to accumulate in mineralized bone and can affect bone development (Szweras *et al.*, 2002). This effect on *Ahsg* expression may be related to PFOS induced immunotoxicity (reviewed in Dewitt *et al.*, 2008) and the delayed bone ossification observed in neonates exposed maternally to high concentrations of PFOS (Lau *et al.*, 2004). The

largest decrease unique to L-PFOS was detected on a probe for the EST gonad_EST06605 (accession # CV859129) which, as of yet, has an uncharacterized function.

Validation of microarray results was done by performing real-time RT-PCR analysis for fourteen genes (Supplementary Table S5.3 in Appendix). Real-time RT-PCR results were directionally consistent for twenty-three of the twenty-eight conditions, resulting in a validation rate of 82%. To supplement the microarray results, the expression of four genes was also examined in a separate cell culture employing a different pooling method to increase the biological variability of the model system and to investigate dose-response relationships. Cells from this culture were prepared from sub-pooled livers (6 livers per sub-pool) and exposed to concentrations of PFOS ranging from 1 to 40 μ M. Assays were repeated for each dose using RNA isolated from 2-3 separate sub-pools of hepatocytes. The genes acyl-CoA synthetase long-chain family member 1 (*Acs11*), acyl-CoA synthetase bubble gum family member 2 (*Acsbg2*), amphiregulin (*Areg*) and *Gsta3* were selected for analysis because results for PCR validation matched the microarray data both in directionality and significance (see Supplementary Table S5.3). Both *Acs11* and *Acsbg2* are genes involved in fatty acid metabolism. *Areg* encodes a growth factor that is often associated with liver injury (Berasain *et al.*, 2007) while *Gsta3*, as previously mentioned, is involved in oxidative stress response. Profiles for all four genes had fold-changes in the same direction as determined by microarray analysis (Figure 5.2); however, the concentration at which significant effects were detected was higher. This is likely due to the increased variability introduced by sub-pooling. *Gsta3* was down-regulated by both L-PFOS and T-PFOS, which is consistent with the microarray analysis, although this effect was not apparent at higher concentrations of T-PFOS. T-PFOS significantly increased the expression of *Acs11*,

Acsbg2 and *Areg* whereas these genes were not affected by L-PFOS, as predicted from the microarray results.

5.4.2. PCA and clustering analysis

The expression profiles of all 15 samples (5 per dose group) were reduced to three principal components using the Principal Component Analysis function in GeneSpring GX (Figure 5.3). The first principal component (PC1) accounted for 70% of the variability among samples. Almost all differentially expressed genes (341/386), including all 84 genes affected by both L-PFOS and T-PFOS, had absolute PC1 loadings greater than 0.5 (data not shown). This shows that PC1 mostly characterized the difference between DMSO- and PFOS-treated samples. This is further demonstrated by the complete separation of DMSO samples on the PC1 axis. L-PFOS and T-PFOS samples were also completely separated along PC1, showing L-PFOS as being an intermediate between T-PFOS and DMSO on this principal component. The second principal component (PC2) accounted for 18% of inter-sample variability. Of the genes that had PC2 loadings greater than 0.5 (71 genes), 82% (59/71) were differentially expressed by either L-PFOS or T-PFOS, but not by both, demonstrating that PC2 mainly describes the variability between samples treated with different isomeric mixtures of PFOS. Again, this is exemplified by the almost complete separation of L-PFOS and T-PFOS samples along PC2. Genes that had loadings greater than 0.5 for the third principal component (PC3), which accounted for the remaining 12% of variability, also comprised a large proportion of genes exclusively expressed by only one treatment. However, L-PFOS and T-PFOS samples were only partially separated along PC3.

Hierarchical clustering using the differentially expressed gene set was also performed using GeneSpring GX. The expression profile of each sample was clustered based on gene expression and treatment (Figure 5.4). Cluster analysis separated DMSO-treated CEH from all PFOS-treated samples. Similar to PCA analysis, L-PFOS- and T-PFOS-treated samples clustered separately from each other, although one L-PFOS sample clustered with the DMSO samples. Similar conclusions can be drawn from both the PCA and hierarchical clustering. Both methods show that at equal concentrations, T-PFOS and L-PFOS illicit distinct transcriptional responses in CEH based on their expression profiles.

5.4.3. Mapping gene IDs to IPA

The DAVID Gene ID Conversion Tool was used to map microarray gene IDs to human, rat or mouse orthologs in IPA. For all genes on the array, 12615 out of 42034 genes (30%) were recognized by IPA as orthologs. Of all disregulated genes, 166 of 386 (43%) were recognized as orthologs in IPA. Genes that mapped to IPA are identified in the list of differentially expressed genes (Supplementary Table S5.1). The majority of unmapped IDs correspond to probes for hypothetical proteins and ESTs with unknown function. Several differentially expressed genes with known functions, however, did not map to orthologs in IPA such as liver fatty acid binding protein (ID: L-FAPB) and thyroid hormone receptor beta 2 (ID: X62642), and therefore could not be included in downstream functional, pathway, and interactome analysis.

5.4.4. Functional analysis

IPA was used to perform a functional enrichment analysis. The relevant functional categories are summarized in Table 5.2. The specific functions that were significantly enriched

in each category are shown in detail in Supplementary Tables S5.4A and S5.4B (Appendix). The top five functional categories were: lipid metabolism, cellular growth and proliferation, cancer, hepatic system disease, and cellular movement. Although a similar set of functional categories was enriched for both L-PFOS and T-PFOS, in almost all cases the number of genes affected in each category was much greater in T-PFOS treated cells.

In general, the functional profiles are consistent with similar gene expression studies for mammalian and avian models (Bjork *et al.*, 2008; Hu *et al.*, 2005; Martin *et al.*, 2007; Yeung *et al.*, 2007). Changes in genes associated with lipid metabolism and cellular proliferation are generally consistent with the activation of peroxisome proliferator activated receptors (PPARs), particularly the PPAR α and PPAR γ isotypes (Feige *et al.*, 2006). However, one important difference from mammalian PFOS studies is the lack of response of genes involved in the peroxisomal β -oxidation of fatty acids that are transcriptionally regulated by PPAR α . It is believed that much of the toxicity of PFCs is propagated through activation of PPAR α . Differential expression of the β -oxidation genes acyl-CoA oxidase (ACOX), enoyl-CoA hydratase, bifunctional enzyme (BIEN) and peroxisomal 3-ketoacyl-CoA thiolase has been reported in rat liver and cultured rat hepatoma cells following PFOS exposure (Bjork *et al.*, 2008; Hu *et al.*, 2005). Other avian gene expression studies however, reported no apparent correlation between PFOS exposure and β -oxidation (Nakayama *et al.*, 2008; O'Brien *et al.*, 2009a; Yeung *et al.*, 2007), although a pair of studies performed in our laboratory reported T-PFOS-induced changes in β -oxidation genes in cultured CEH (Cwinn *et al.*, 2008; Hickey *et al.*, 2009). These changes were significant only after 36 hours of exposure at ≤ 40 μ M, which is a longer exposure time and higher concentration than the present study. The results indicate that activation of PPAR α may occur as a secondary response or only at high concentrations of PFOS.

At 24 hours of exposure to 10 μ M T-PFOS, the results of Cwinn *et al.* are in concordance with the present study, including a 2-3 fold change in L-FABP, which was suggested to be independent of PPAR α . In the present study, most of the lipid metabolism functions that were enriched were not involved in β -oxidation, but rather in the synthesis, modification and transport of lipids, fatty acids, terpenoids, eicosanoids, steroids and cholesterol. The differential expression of a similar gene set was also reported in rat hepatic cells exposed to PFCs (Bjork *et al.*, 2008; Martin *et al.*, 2007) and may represent PPAR α -independent effects on lipid metabolism. The role of PPAR α in the avian hepatocyte response to PFOS exposure is addressed further below when the results of interactome analysis are discussed.

The large number of disregulated genes involved in cellular growth and proliferation, cancer and hepatic system disease is consistent with the hepatomegaly, hepatocellular adenoma and hyperplasia that has been observed in mammals (Lau *et al.*, 2003; Seacat *et al.*, 2002; Seacat *et al.*, 2003) and birds (Molina *et al.*, 2006; Newsted *et al.*, 2006; Newsted *et al.*, 2007; Peden-Adams *et al.*, 2008) exposed to PFOS. Several genes in the hepatic system and disease category were associated with intrahepatic cholestasis (Supplementary Tables S5.4A and S5.4B), which, as previously discussed, may be a result of *Myh6* over-expression. Although cellular movement was a significantly enriched functional category, many of the genes from this group are involved in tumor cell migration and cell-cell signalling. Changes in other cell-cell interaction genes such as gap junction proteins including gap junction protein beta 1 (*Gjb1* also known as *Cx32*), cell adhesion molecule 1 (*Cadm1*) and other cell-to-cell signalling genes is in agreement with impaired gap junction intercellular communication observed in liver tissue and cultured cells (Hu *et al.*, 2002).

5.4.5. Canonical pathway mapping

IPA was used to map significantly dysregulated genes to canonical pathways in Ingenuity's Knowledge Base. IPA analysis revealed that exposure to L-PFOS and T-PFOS differentially regulated genes belonging to several pathways. Canonical pathways that were significantly affected ($p < 0.05$) are summarized in Table 5.3. A more detailed description of all pathways affected by each dose group and the genes that were affected is shown in Supplementary Tables S5.5A and S.5.B (Appendix). Pathways that were most significantly disrupted by PFOS exposure included LPS/IL-1 mediated inhibition of RXR function, LXR/RXR activation, aryl hydrocarbon receptor signalling, metabolism of xenobiotics by cytochrome P450s, fatty acid metabolism, glutathione metabolism and NRF-mediated oxidative stress response. Although the LPS/IL-1 mediated inhibition of RXR function pathway was the most significantly affected, it was actually the downstream genes of this pathway, which are regulated by RXRs binding partners, CAR, PXR, and PPARs, that were disrupted, and not genes involved in the inhibition mechanism (Supplemental Figure S5.1 in Appendix). LXR/RXR activation was the second most significantly enriched pathway. These results suggest that PFOS may exert its effect through RXR and its binding partners. However, binding studies have shown that PFOS does not activate human, rat or mouse RXR (Vanden Heuvel *et al.*, 2006). PFOS may interfere with RXR heterodimer formation through its binding partners. PFOS does show weak binding to both PPAR α and PPAR γ (Vanden Heuvel *et al.*, 2006). Binding studies with CAR, PXR and LXR would also clarify this issue.

Although the aryl hydrocarbon receptor (AHR) signalling pathway was significantly enriched, up-regulation of cytochrome P450 isoforms 1A4 and 1A5 (paralogs to mammalian *Cyp1a1* and *Cyp1a2*, respectively), which typically accompanies AHR activation, was not

observed. Furthermore, three of the six genes perturbed in the aryl hydrocarbon receptor signalling pathway were glutathione-S-transferase isoforms that are transcriptionally regulated by several other receptors including CAR and PXR. This evidence suggests that AHR activation may not be a central mechanism of the PFOS response. Genes regulated by AHR were previously shown to be affected by PFC exposure in CEH (Hickey *et al.*, 2009), however, the relative potencies of the various PFCs tested were many orders of magnitude lower than traditional AHR agonists.

Overall, T-PFOS had a larger impact on known biochemical pathways. In the same fashion as the functional analysis, almost all pathways that were affected by L-PFOS had a greater number of perturbed genes following T-PFOS exposure. In addition, several canonical pathways such as biosynthesis of steroids, Wnt/ β -catenin signalling and p53 signalling were only affected by T-PFOS. These pathways may represent mechanisms that are unique to the branched isomers of PFOS.

5.4.6. Interaction networks and potential regulatory molecules

IPA was used to generate interaction networks, using mapped orthologs of differentially expressed genes, for all three treatment groups (Figure 5.5, Supplementary Figures S5.2 to S5.4 in Appendix). Only direct interactions with gene products that occur in the liver were considered for interaction network construction. An example of one of these networks is shown in Figure 5.5. A high resolution version of this figure, as well as all networks examined in this study, can be found in Supplementary Figures S5.2 to S5.4. This example is one of two networks generated using data from T-PFOS-treated cells. A functional analysis of all the molecules in each network was performed and is summarized in Table 5.4.

All network entities that had direct interactions with four or more disregulated genes were considered to have potential regulatory roles in the PFOS response. For example, in Figure 5.5 the nodes labelled HNF4A and PPARG have direct interactions with greater than four red or green nodes and were therefore considered to have potential regulatory activity. IPA was then used to identify all possible direct or indirect interactions between potential regulatory molecules and all disregulated genes in each dose group. All known interactions in the Ingenuity Knowledgebase were considered regardless of tissue type (example for TP53 is shown in Figure 5.6). These data are summarized in Table 5.5. A detailed list of potential regulatory molecules and the genes with which they interact can be found in Supplementary Table S5.6 (Appendix). The overall trend in the number of interactions between potential regulatory molecules and genes disregulated by PFOS was similar to the trend observed for functional and pathway enrichment analysis. All potential regulatory molecules had the highest number of interactions with disregulated genes when cells were exposed to T-PFOS. This supports our hypothesis that while L-PFOS and T-PFOS may affect similar regulatory machinery, the effect is much more prominent following T-PFOS exposure.

Many of the potential regulatory molecules identified through interactome analysis, such as tumor protein p53 (TP53), v-myc myelocytomatosis viral oncogene homolog (MYC), hepatocyte nuclear factor 4 α (HNF4A), and catenin beta 1 (CTNNB1), each play integral roles in the proper functioning of diverse cellular processes. The responsiveness of these proteins to PFOS exposure may represent secondary responses, although there is some evidence that PFOS may act more directly in some instances. Tumor suppressor protein TP53 is an important regulator of cell cycle. It is not surprising that the majority of PFOS-affected genes involved with cell cycle, proliferation or cancer have direct or indirect interactions with TP53. It may be

unlikely that PFOS exerts its effect directly on TP53. A typical TP53 response involves differential p21/WAF1 expression, which was not observed, and is induced by DNA damage. PFOS does not appear to be genotoxic (Erikson *et al.*, 2010; Jernbro *et al.*, 2007; Kawamoto *et al.*, 2010), although Liu *et al.* (2007b) did report DNA damage at high PFOS exposures, but concluded it was likely to be apoptosis related. Recent evidence has shown that lipid peroxidation products can activate TP53 (Shibata *et al.*, 2006), which may explain results from the present study. The fact that both murine double minute 2 (*mdm2*), a gene that inactivates TP53, and cyclin-dependent kinase inhibitor 2A (*Cdkn2A*), which modulates *mdm2* protein activity (Hollstein & Hainaut, 2010), were both over-expressed following PFOS exposure is further evidence that TP53 activity was perturbed.

MYC is a multifunctional transcription factor that is believed to regulate the expression of 10-15% of all cellular genes directly or indirectly, and is one of the most frequently affected genes in a variety of cancers (Hoffman & Liebermann, 2008). MYC exerts effects on many cellular processes including growth, differentiation and apoptosis in a TP53-dependent or -independent fashion (Hoffman & Liebermann, 2008). As such, many of the genes affected by PFOS that interact with MYC are also known to interact with TP53.

HNF4A is believed to be involved in the regulation of up to 40% of all genes expressed in the liver (Odom *et al.*, 2004) and plays an indispensable role in hepatocyte development and lipid metabolism as evidenced in HNF4A knockdown studies (Hayhurst *et al.*, 2001). HNF4A-null mice die during embryogenesis while mature mice that lack HNF4A expression accumulate lipid in the liver, have reduced serum cholesterol and increased serum bile levels (Hayhurst *et al.*, 2001). Many of the genes that were dysregulated by PFOS and interact with HNF4A (see Supplementary Table S5.6) are involved in lipid metabolism such as acetyl-Coenzyme A

acetyltransferase 1 (*Acat1*), *Acs11*, aldo-keto reductase family 1, member B1 (*Akr1b1*), apolipoprotein A-IV (*Apoa4*) and *Cyp8b1* or in cellular proliferation such as cyclin G2 (*Ccng2*), *Gjb1*, and inhibin, beta A (*Inhba*). Binding studies would be needed to determine if PFOS interferes directly with HNF4A. Alternatively, HNF4A might be affected indirectly through altered fatty acyl-CoA thioester levels (Hertz *et al.*, 1998) that may result by PFOS interference in other regulatory mechanisms of lipid metabolism (for example through interference with PPARs).

CTNNB1 is an important component of two cellular systems: Wnt signalling and adherens junctions. The Wnt signalling pathway is one of the most fundamental mechanisms that direct cell proliferation and fate during embryonic development and tissue homeostasis (Logan & Nusse, 2004). Defects in proper Wnt signalling are often linked to birth defects, cancer and other diseases (Clevers, 2006). Increased expression of one of the Frazzled Wnt receptors, *Fzd4*, as well as increased expression of *Wnt5b* glycoprotein following PFOS exposure indicates that the Wnt signalling pathway may be disrupted by PFOS. Wnt signalling is also linked to TP53 and MYC activity, while *Wnt5b* has been shown to activate PPAR γ (van Tienen *et al.*, 2009). CTNNB1 is also a key component in the adherens junction complex, a cell-cell junction complex that mechanically attaches adjacent cells and relays signals. Interference with CTNNB1 function may be involved with impaired cell-cell communication which has been demonstrated following PFOS exposure (Hu *et al.*, 2002).

The hepatocyte response to PFOS may be mediated more directly through the lipid sensing PPARs. Following interactome analysis, only PPAR γ was present in any of the networks generated by IPA for both L-PFOS and T-PFOS. Analysis revealed that it had many direct interactions with differentially expressed genes, most of which were expression-type interactions

(Figure 5.7A). In contrast, PPAR α did not occur in any of the interaction networks generated by IPA. When all possible interactions in the Ingenuity Knowledge Base with differentially expressed genes were considered (as was done for all potential regulatory molecules), PPAR α had fewer interactions with genes that were dysregulated by PFOS than PPAR γ (Figure 5.7B). Only two of these were expression-type interactions, suggesting that PPAR α had minimal influence on the expression profile of CEH in response to PFOS. Binding assays (Vanden Heuvel *et al.*, 2006) and expression profile studies (Martin *et al.*, 2007) support the hypothesis that PFOS may be a PPAR γ agonist. These same studies, however, also suggest that PFOS is a more potent activator of PPAR α in mammals. Given the lack of response of PPAR α -regulated genes in the present study and other avian studies (O'Brien *et al.*, 2009a; Yeung *et al.*, 2007), it is possible that PFOS is a more potent activator of PPAR γ in the chicken. Binding assays using chicken PPAR isoforms would help clarify this issue.

Another possible mechanism for the effects of PFOS exposure may be through activation of sterol regulatory element binding protein 1 (SREBP1), which enhances the transcription of genes involved in fatty acid and cholesterol metabolism. Cleavage activation of SREBP1 is upregulated in response to cellular cholesterol demand (Rawson, 2003). This may represent a secondary response to PFOS exposure, which as previously mentioned, can result in reduced cholesterol levels.

Of all potential regulatory molecules identified, the transcription of only three was affected by PFOS exposure: *Hdac1*, *Cdkn2A* and *mdm2*. *Cdkn2A*, which was differentially expressed in the L-PFOS 10 μ M and T-PFOS 10 μ M groups, indirectly modulates TP53 activity through *Mdm2*, as previously discussed. *Cdkn2A* can also directly affect cell cycle through inhibition of cyclin-dependent kinase 4 (CDK4) inhibition. Histone deacetylase 1 (HDAC1) is

involved in chromatin packaging, and coordinates how the transcriptional machinery accesses DNA (Brunmeir *et al.*, 2009). Perturbation of *Hdac1* by T-PFOS may play a role in the increased numbers of genes affected in this treatment group via effects on chromatin structure. Although the differential expression of HDAC1 was not verified by real-time RT-PCR, expression analysis in an independent culture prepared from sub-pooled livers showed a significant dose-dependent increase in HDAC1 in T-PFOS, which was absent in the L-PFOS treatment group (Supplementary Figure S5.5 in Appendix).

Given the diversity in the effects of PFOS exposure, it is unlikely that it has a single primary mode of action. The mechanism leading to PFOS toxicity is in all likelihood a complex interplay of various molecular events, many of which are presently proposed. The results from this study represent only a snapshot of the transcriptional response to PFOS after 24 hrs of exposure. Time-course experiments would be required to more thoroughly investigate the proposed mechanisms to obtain further understanding of their order of activation, how they interact, and how they are affected by different isomer mixtures.

5.5. Conclusions

The majority of PFOS released into the environment is believed to be the product of ECF processes that result in mixtures of linear and branched isomers. Once in the environment, the isomeric proportions are altered, possibly through selective uptake and elimination through the food web or other biotic or abiotic transformation processes (Benskin *et al.*, 2009; De Silva *et al.*, 2009a; O'Brien *et al.*, 2010). Regardless of the mechanism, the PFOS burden in exposed wild animals, especially those occupying high trophic positions, is skewed towards a much greater proportion of L-PFOS compared to the technical product (Chu & Letcher, 2009; Gebbink

& Letcher, 2010). Until recently, differences in environmental kinetics between PFOS isomers were undetectable and therefore not considered in many laboratory studies.

In this study we showed that both L-PFOS and T-PFOS elicited a transcriptional response in genes related to lipid metabolism and transport, oxidative stress response, and cellular growth and proliferation. This transcriptional profile is generally typical for PFOS exposure studies using mammalian *in vivo* and *in vitro* systems (Bjork *et al.*, 2008; Hu *et al.*, 2005; Martin *et al.*, 2007). One major difference, however, is the lack of response in β -oxidation genes, which suggests that PPAR α may not be a major target of PFOS in cultured CEH. Interactome analysis also suggested that PPAR γ plays a more integral role in the PFOS response than PPAR α . PFOS exposure also appeared to affect several systems that are fundamental to regular hepatocyte functions such as TP53 signalling, HNF4A transcription regulation and Wnt signalling.

In almost all functional categories, pathways, and interaction networks examined in the present study, the impact of T-PFOS was much greater than L-PFOS. The reason for this difference is likely due to the increased number of shapes presented by the branched isomers of T-PFOS. This broader selection of shapes may be able to interact with more cellular machinery, thereby interfering with more signalling cascades, activating more receptors and recruiting more transcription factors than the linear isomer of PFOS alone. Examples from the current study include interference with the TP53 pathway, PPAR γ signalling, and HNF4A activity, all of which appear to be more affected by T-PFOS exposure than L-PFOS.

This study demonstrates the importance of considering environmental isomer kinetics when assessing possible exposure effects on wildlife, especially when an *in vitro* system is employed, and shows that the environmental relevance of studies using T-PFOS may need to be re-evaluated. Furthermore, the effects of different PFOS isomer mixtures remain poorly

characterized in mammalian models. Research investigating effects of branched PFOS isomers in mammals should be prioritized, especially given that branched isomers appear to accumulate in human samples. Branched isomer proportions as high as 50% (Riddell *et al.*, 2009) have recently been reported in human serum.

Table 5.1: Number of genes that were differentially expressed (FC>1.5, p<0.05) in CEH exposed to L-PFOS or T-PFOS (10 μ M each).

Treatment	# of Genes	
	Upregulated	Downregulated
L-PFOS	104	26
T-PFOS	278	62

Table 5.2: Enriched functional categories for genes differentially expressed due to L-PFOS or T-PFOS exposure in CEH.

Rank	Category	L-PFOS		T-PFOS		# genes on chip
		p-value range	# genes	p-value range	# genes	
1	Lipid Metabolism	2.75E-03 - 4.93E-02	12	9.88E-07 - 1.09E-02	28	325
2	Cellular Growth and Proliferation	5.47E-03 - 3.68E-02	3	1.08E-06 - 1.09E-02	40	1685
3	Cancer	7.86E-03 - 9.33E-03	6	1.10E-05 - 1.01E-02	37	1517
4	Hepatic System Disease	2.28E-03 - 2.25E-02	3	1.72E-05 - 6.53E-03	17	126
5	Cellular Movement	2.32E-02 - 2.82E-02	4	1.16E-04 - 9.47E-03	21	605
6	DNA Replication, Recombination, and Repair	4.68E-03 - 4.13E-02	1	1.61E-04 - 1.09E-02	12	203
7	Cellular Development	9.33E-03 - 1.40E-02	3	5.19E-04 - 1.09E-02	25	1092
8	Carbohydrate Metabolism	9.33E-03 - 2.77E-02	6	1.06E-03 - 3.71E-03	6	227
9	Drug Metabolism	3.44E-03 - 2.77E-02	7	1.06E-03 - 1.09E-02	7	287
10	Cell-To-Cell Signaling and Interaction	4.68E-03 - 3.68E-02	3	2.64E-03 - 1.09E-02	13	434
11	Cellular Organization and Maintenance	4.68E-03 - 4.68E-03	1	3.15E-03 - 1.09E-02	4	456
12	Endocrine System Development and Function	4.68E-03 - 2.32E-02	3	3.15E-03 - 1.09E-02	3	282
13	Amino Acid Metabolism	4.68E-03 - 4.58E-02	5	8.47E-03 - 1.09E-02	3	71
14	Nucleic Acid Metabolism	4.68E-03 - 9.33E-03	2	1.09E-02 - 1.09E-02	1	657
15	Gene Expression	1.40E-02 - 1.40E-02	1	8.47E-03 - 1.09E-02	4	365
16	Post-Translational Modification		-	1.09E-02 - 1.09E-02	1	396
17	Protein Synthesis		-	1.09E-02 - 1.09E-02	1	90

Table 5.3: Significantly enriched ($p < 0.05$) canonical pathways for genes that were differentially expressed due to L-PFOS or T-PFOS exposure in CEH.

Ingenuity Canonical Pathways	L-PFOS		T-PFOS		# genes in pathway
	p-value	# genes	p-value	# genes	
LPS/IL-1 Mediated Inhibition of RXR Function	3.16E-02	3	1.95E-04	8	149
LXR/RXR Activation	2.39E-01	1	3.89E-04	5	59
Aryl Hydrocarbon Receptor Signaling	8.51E-02	2	8.91E-04	6	105
Cysteine Metabolism	1.19E-01	1	3.02E-03	3	28
Metabolism of Xenobiotics by Cytochrome P450	8.71E-03	3	3.16E-03	5	92
Fatty Acid Metabolism	3.77E-01	1	4.47E-03	5	100
Glutathione Metabolism	1.62E-02	2	1.05E-02	3	42
Bile Acid Biosynthesis	1.41E-02	2	6.76E-02	2	47
Xenobiotic Metabolism Signaling	2.19E-01	2	1.62E-02	6	188
NRF2-mediated Oxidative Stress Response	2.19E-02	3	5.13E-02	4	129
Glycerolipid Metabolism	2.36E-01	1	2.40E-02	3	58
Taurine and Hypotaurine Metabolism	2.75E-02	1	6.31E-02	1	9
Nicotinate and Nicotinamide Metabolism	2.95E-02	2	4.72E-01	1	59
PXR/RXR Activation	3.09E-02	2	4.78E-01	1	60
IGF-1 Signaling	2.70E-01	1	3.63E-02	3	67
Lysine Biosynthesis	3.72E-02	1	8.32E-02	1	8
Synthesis and Degradation of Ketone Bodies	4.17E-02	1	9.33E-02	1	10
Biosynthesis of Steroids			5.13E-04	3	22
Pyruvate Metabolism			1.26E-03	4	51
Bladder Cancer Signaling			1.38E-03	4	45
Pentose and Glucuronate Interconversions			3.02E-03	3	29
Pancreatic Adenocarcinoma Signaling			7.24E-03	4	71
Glycine, Serine and Threonine Metabolism			1.12E-02	3	50
Hepatic Fibrosis / Hepatic Stellate Cell Activation			1.58E-02	4	89
Wnt/ β -catenin Signaling			1.66E-02	4	90
Galactose Metabolism			3.02E-02	2	30
p53 Signaling			3.24E-02	3	64
Chronic Myeloid Leukemia Signaling			3.63E-02	3	67
Ovarian Cancer Signaling			3.80E-02	3	68
Melanoma Signaling			3.98E-02	2	29
Chondroitin Sulfate Biosynthesis			4.17E-02	2	30
Keratan Sulfate Biosynthesis			4.17E-02	2	30
Cell Cycle: G2/M DNA Damage Checkpoint Regulation			4.17E-02	2	30
Airway Pathology in Chronic Obstructive Pulmonary Disease			4.27E-02	1	4
Fructose and Mannose Metabolism			4.68E-02	2	35

Table 5.4: Functional enrichment of interaction networks generated for genes differentially expressed following exposure to L-PFOS or T-PFOS (10 μ M each).

Treatment	Network	# Disregulated genes	Enriched Functions
L-PFOS	1 of 1	19	Inflammatory response Lipid metabolism Molecular transport
T-PFOS	1 of 2	29	Lipid metabolism Molecular transport Small molecule biochemistry
	2 of 2	26	Cell cycle Cellular growth and proliferation Connective tissue development and function

Table 5.5: Molecules from IPA-generated networks that had interactions with four or more PFOS-disregulated genes and were considered to have potential regulatory activity (red boxes are FC>1.5, p<0.05, NP=probe not present on microarray)

Gene	Entrez Gene Name	treatment	fold change	p-value	protein interactions		
					direct	indirect	total
TP53	Tumor protein 53	L-PFOS	NP	NP	3	1	4
		T-PFOS	NP	NP	12	9	21
MYC	v-myc myelocytomatosis viral oncogene homolog (avian)	L-PFOS	1.16	0.422	4	3	7
		T-PFOS	1.33	0.078	13	5	18
HNF4A	hepatocyte nuclear factor 4, alpha	L-PFOS	1.09	0.686	5	1	6
		T-PFOS	-1.10	0.587	17	1	18
CTNNB1	catenin (cadherin-associated protein), beta 1, 88kDa	L-PFOS	1.99	0.096	2	1	3
		T-PFOS	1.12	0.722	8	7	15
PPARG	peroxisome proliferator-activated receptor gamma	L-PFOS	-1.01	0.849	4	2	6
		T-PFOS	-1.00	0.980	10	4	14
SP1	Sp1 transcription factor	L-PFOS	-1.14	0.468	3	1	4
		T-PFOS	1.02	0.911	11	0	11
SREBF1	Sterol regulatory element binding transcription factor 1	L-PFOS	1.00	0.989	3	1	4
		T-PFOS	-1.05	0.646	11	1	12
CEBPB	CCAAT/enhancer binding protein (C/EBP), beta	L-PFOS	-1.01	0.953	5	2	7
		T-PFOS	1.05	0.749	8	2	10
HDAC1	histone deacetylase 1	L-PFOS	1.40	0.188	1	0	1
		T-PFOS	1.58	0.019	8	0	8
CDKN2A	cyclin-dependent kinase inhibitor 2A (melanoma, p16, inhibits CDK4)	L-PFOS	1.30	0.148	0	1	1
		T-PFOS	1.63	0.000	6	1	7
ESRRA	estrogen-related receptor alpha	L-PFOS	NP	NP	1	0	1
		T-PFOS	NP	NP	6	0	6
MDM2	Mdm2 p53 binding protein homolog (mouse)	L-PFOS	1.33	0.254	1	0	1
		T-PFOS	1.75	0.008	4	2	6
MYCN	v-myc myelocytomatosis viral related oncogene, neuroblastoma derived (avian)	L-PFOS	-1.00	0.999	1	0	1
		T-PFOS	1.37	0.027	5	0	5

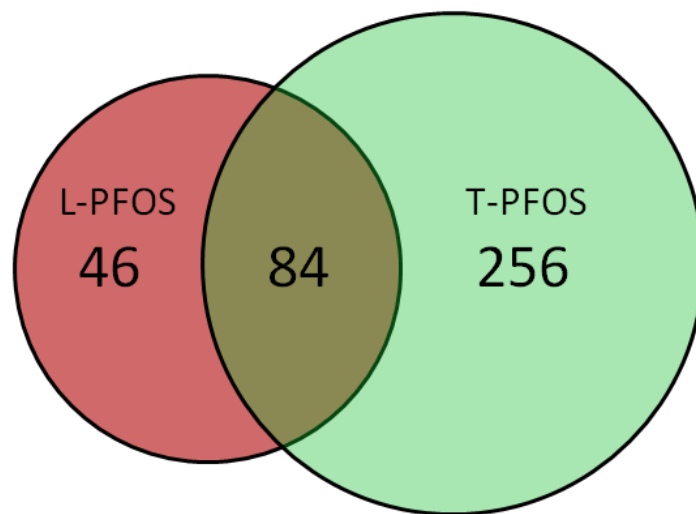


Figure 5.1: Venn diagram illustrating the number of genes that were uniquely disregulated (FC >1.5, $p < 0.05$) by either L-PFOS or T-PFOS or genes that were affected by both L-PFOS and T-PFOS.

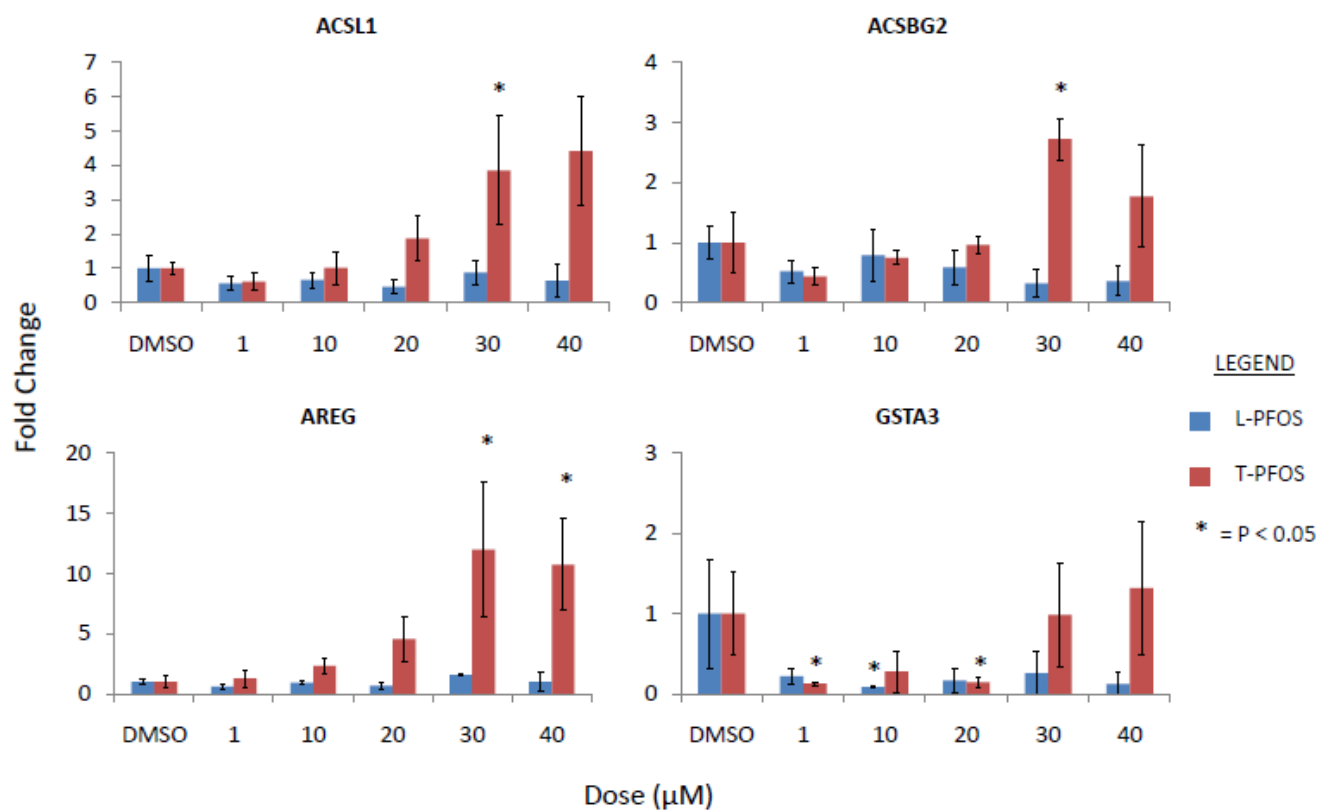


Figure 5.2: Expression of *Acs11*, *Acsbg2*, *Areg* and *Gsta3* in sub-pooled CEH (N=2-3 sub-pools, 6 livers/pool) following exposure to L-PFOS or T-PFOS.

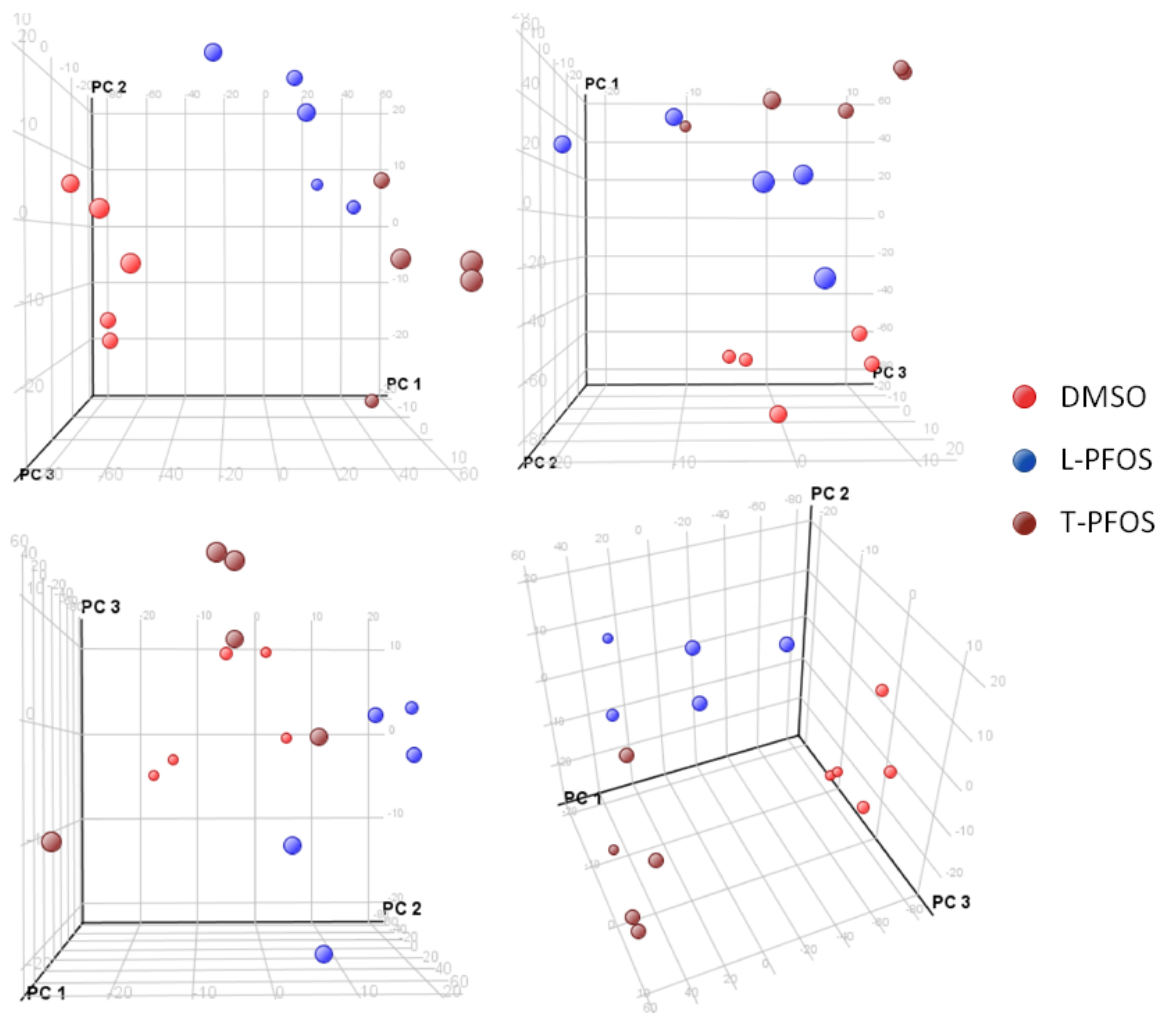


Figure 5.3: The expression profile of L-PFOS- and T-PFOS-treated samples plotted on three principal components compared to the DMSO control group viewed from various angles. PCA analysis was based on the expression profiles of 386 disregulated genes.

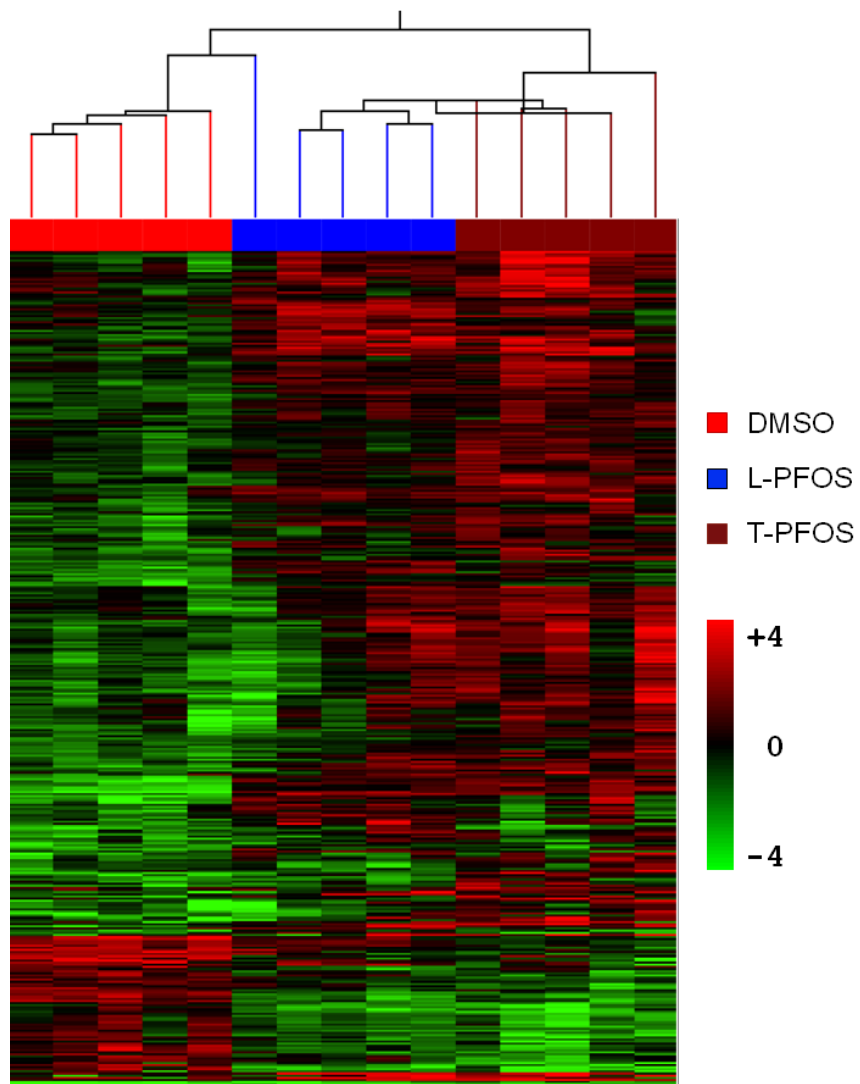
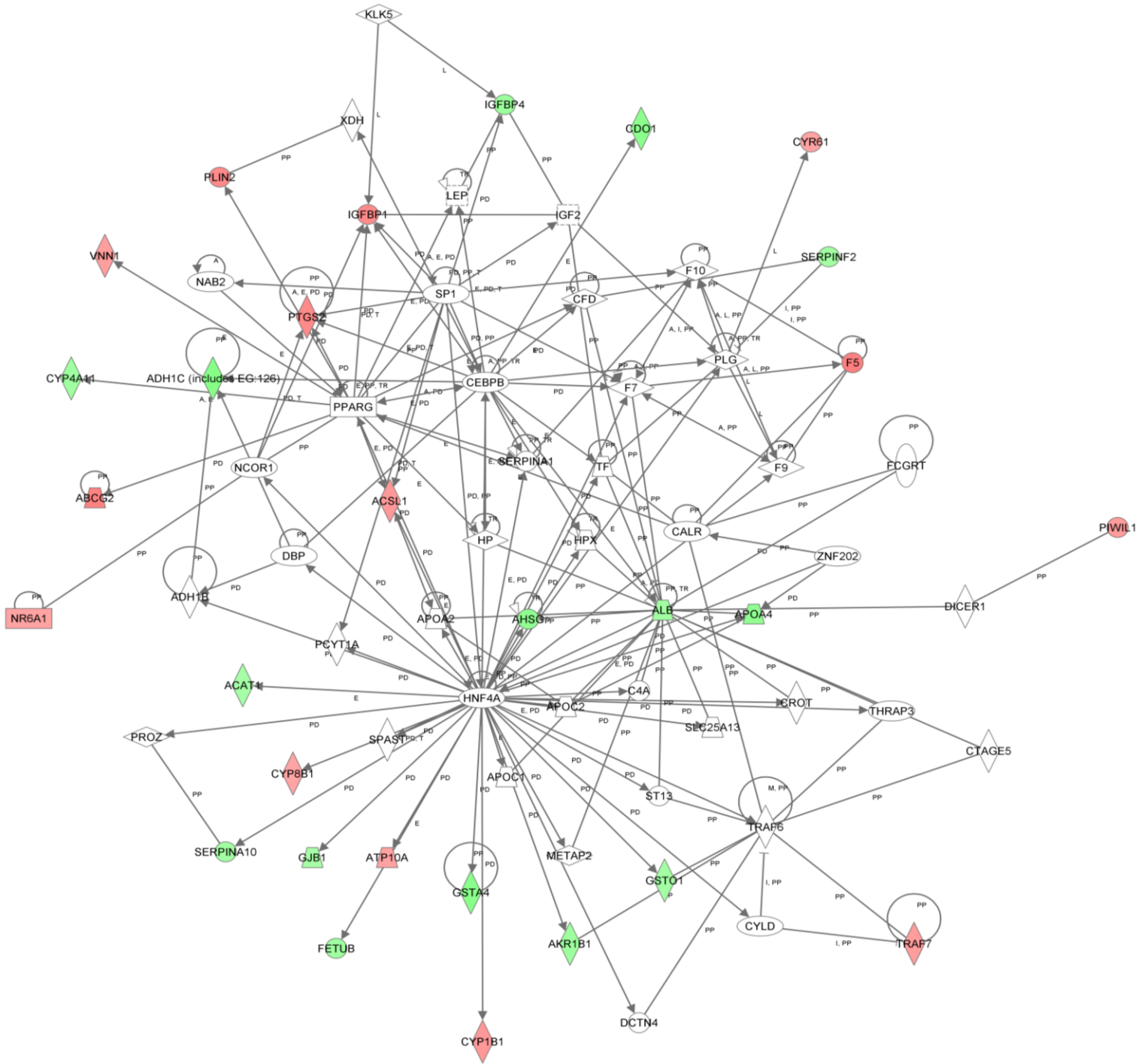
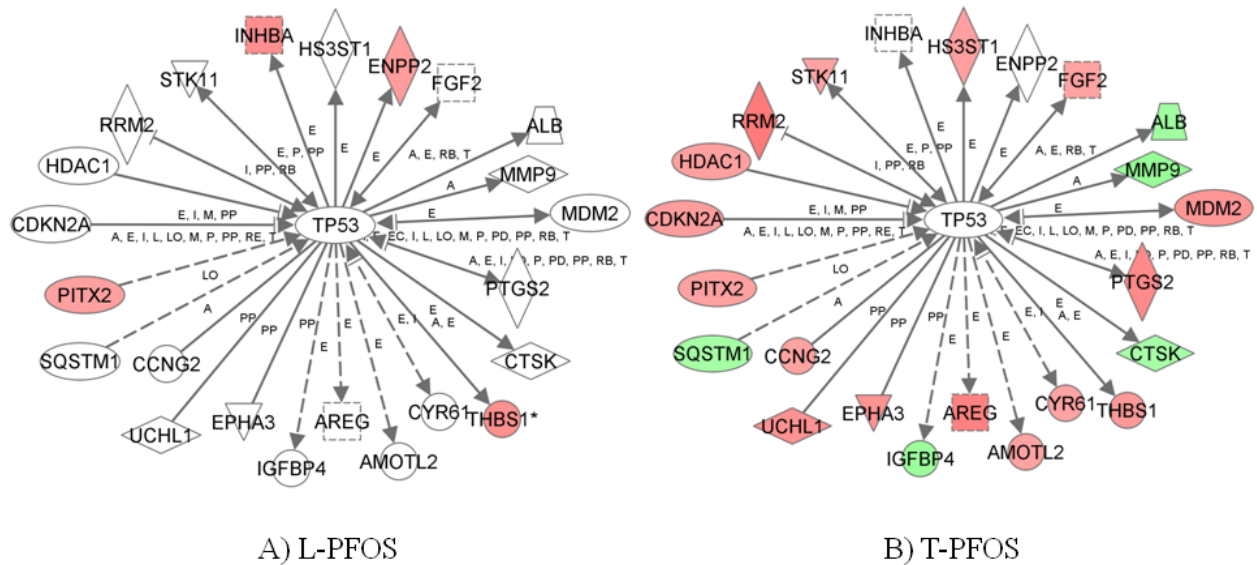


Figure 5.4: Hierarchical Clustering of expression profiles of CEH exposed to L-PFOS, T-PFOS or DMSO vehicle control. Clustering was based on 386 differentially expressed genes (FC >1.5, p<0.05).



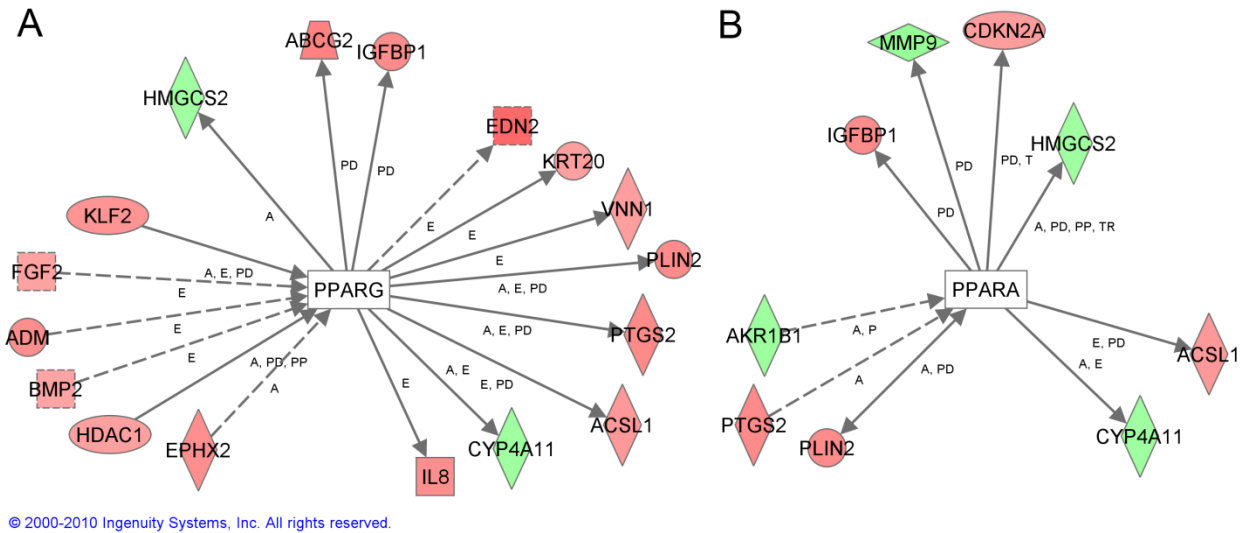
© 200-2010 Ingenuity Systems, Inc. All rights reserved.

Figure 5.5: One of two IPA-generated interaction networks for genes dysregulated by exposure to T-PFOS 10 μ M. Red shapes represent genes that were significantly up-regulated and green shapes represent genes that were down-regulated. Connecting lines represent interactions between genes that are documented in the Ingenuity Knowledge Base. White shapes are genes that were added to the network by IPA based on their connectivity to dysregulated genes.



© 2000-2010 Ingenuity Systems, Inc. All rights reserved.

Figure 5.6: All documented direct (solid line) and indirect (dashed line) interactions from Ingenuity’s Knowledgebase between TP53 and genes that were differentially expressed due to exposure to A) L-PFOS or B) T-PFOS at 10 μ M.



© 2000-2010 Ingenuity Systems, Inc. All rights reserved.

Figure 5.7: Direct (solid line) and indirect (dashed line) interactions between genes that were differentially expressed following exposure to PFOS and A) PPAR γ or B) PPAR α .

Chapter 6

General Conclusions and Future Directions

6.1. General conclusions

The results from this body of work help advance the current understanding of several aspects of PFC toxicology in avian species, although many challenges still remain in understanding the various biological processes that lead to PFC toxicity. First, in Chapter 2, it was shown that PFOS may affect the hatching success of the domestic chicken at environmentally relevant concentrations; an LD₅₀ of 93 µg PFOS/g egg was determined. While this LD₅₀ estimation was not very accurate (it had a very broad 95% confidence interval), it is within an order of magnitude of the highest PFOS concentrations reported in wild birds (~2.6 µg/g in bald eagle plasma) (Giesy & Kannan, 2001). Furthermore, the LOAEL of the egg injection study (5.0 µg PFOS/g egg) was also very comparable to PFOS concentrations in avian wildlife and resulted in an approximately 20% decrease in embryo pipping success. Only one study has investigated the reproductive toxicity of PFOS in avian species other than chicken. Newsted *et al.* (2007) observed that when bobwhite quail hens were exposed to PFOS via the diet there was a significant decrease in the survival of 14-day-old hatchlings. These hatchlings had corresponding PFOS liver burdens of approximately 5.5 µg/g, which are also near concentrations observed in the wild. Hatching success, however, was not significantly affected. In the same study, no adverse effects at all were observed in mallard hatchlings that were exposed to PFOS under similar conditions. Although the evidence is limited, these findings suggest that there may be species-specific differences in sensitivity to PFOS among birds. More investigation is required to confirm this possibility. An understanding of the molecular basis of

any possible species-specific difference in toxicity would undoubtedly be of great importance for the risk assessment of PFOS and perhaps other PFCs.

In contrast to what was observed for PFOS, *in ovo* exposure to the purely linear forms of PFOA, PFDS and PFUDA had no effect on hatching success of chicken embryos (Chapter 3). Whether or not exposure to these compounds can affect post-hatch survival, as Newsted *et al.* (2007) observed for PFOS in bobwhites, remains to be investigated. It is also unknown if mixtures containing branched isomers of these compounds can affect hatching success, nor is it known if *in ovo* exposure to purely linear PFOS (L-PFOS) can interfere with hatching or post-hatch survival.

In Chapters 4 and 5 the importance of considering the isomeric make-up of PFOS in the target tissue was demonstrated. A selective accumulation for the linear isomer (L-PFOS) in the liver of embryos exposed to a technical mixture of PFOS (T-PFOS, 63% linear, 37 % branched isomers) was observed in Chapter 4. This finding suggests that birds may have a mechanism for the isomer-specific accumulation of PFOS, and offers a possible explanation for why the PFOS burden in wild birds has such a high proportion of L-PFOS (Chu & Letcher, 2009; Gebbink & Letcher, 2010). Interestingly, the isomer accumulation pattern in chicken embryos was similar to what was observed in adult rats (Benskin *et al.*, 2009; De Silva *et al.*, 2009a), suggesting similar processes among these species. Although the mechanism for this selective accumulation is unclear, it may involve fatty acid binding proteins, lipoproteins or albumin, to which PFCs have a high affinity (Jones *et al.*, 2003; Luebker *et al.*, 2002). Recently, several organic anion transport proteins were implicated in species- and sex-specific differences in PFC kinetics (Han *et al.*, 2008; Katakura *et al.*, 2007) and may also be involved in the isomer-specific selection of PFOS.

The significance of PFOS isomer profiles diverging from that of the technical product in target tissues was apparent when examining the transcription profiles of cultured chicken embryonic hepatocytes (CEH) exposed to either L-PFOS or T-PFOS (Chapter 5). T-PFOS induced a much more disruptive transcriptional response than L-PFOS, perturbing more genes in several functional categories and biochemical pathways. These findings suggest that exposure to T-PFOS may have more toxicological ramifications than to L-PFOS alone. This has important implications for environmental risk assessments. Recent findings indicate that the isomer profiles in wild animals with heavy PFOS burdens tend to have highly elevated proportions of L-PFOS relative to T-PFOS, as high as 98% linear in herring gulls from the North American Great Lakes (Chu & Letcher, 2009; De Silva *et al.*, 2009b; Gebbink & Letcher, 2010; Houde *et al.*, 2008). Since branched PFOS isomers seem to be less prevalent in wildlife, results from laboratory studies that dose with T-PFOS need to be more critically evaluated for their environmental relevance, especially for *in vitro* studies. The consequences of T-PFOS's increased transcriptional disruption may also have more importance for human risk assessment. Recent studies have reported branched PFOS proportions in human serum ranging from 40-50% (Haug *et al.*, 2009; Karrman *et al.*, 2007; Riddell *et al.*, 2009). However I am not aware of any currently published studies that investigate whether or not T-PFOS is more transcriptionally disruptive than L-PFOS in a mammalian model.

The microarray CEH experiments showed that T-PFOS affected the expression of genes involved in several molecular functions including lipid metabolism, cellular growth and proliferation, intercellular communication, and oxidative stress response, and genes belonging to several biochemical pathways including RXR receptor signaling, TP53 and MYC signaling, Wnt/ β -catenin signaling and PPAR γ and SREBP receptor activation. While L-PFOS affected a

similar array of functions and pathways, the number of perturbed genes was much lower than T-PFOS. It is also of interest that the effects identified during mRNA profiling occurred at PFOS concentrations four-times lower than required for a typical PPAR α -type response in CEH (Cwinn *et al.*, 2008). The gene expression data from chicken embryos exposed to PFOS *in ovo* (Chapter 2) also suggest that PPAR α activation may not be the primary mode of action of PFOS reproductive toxicity in the chicken. Furthermore, several recent studies using PPAR α -knockout mice have demonstrated that the presence of PPAR α is not required for the developmental toxicity of PFOS (Abbott *et al.*, 2009), and that PPAR α -independent mechanisms of toxicity may involve the constitutive androstane receptor (CAR, a RXR binding partner), PPAR γ and PPAR β/δ (Rosen *et al.*, 2010). Although binding studies found that PFCs have low binding affinities for RXR, PPAR γ and PPAR β/δ (Vanden Heuvel *et al.*, 2006), studies using knockout animals for these receptors would further clarify the role of these receptors in PFOS toxicity. Despite accumulating mainly in the liver, PFC exposure appears to have effects in many target organs. Evidence suggests that PFCs may also be developmentally neurotoxic (Johansson *et al.*, 2008; Wang *et al.*, 2010), immunotoxic (De Witt *et al.*, 2008), and can cause tumors in several tissues including the pancreas and testes (Kennedy *et al.*, 2004). Whether the molecular events leading to these effects share common mechanisms with the hepatocyte PFOS response should be investigated.

It is uncertain how the concentrations of PFOS in CEH from this research compare to hepatic concentrations in experimentally exposed embryos or in wild birds and eggs. Because PFOS has both high water solubility and a high affinity to adsorb to proteins, it is unclear if the sum total of PFOS suspended in the culture medium was absorbed by the cultured cells. If entirely taken in by the cells, the PFOS concentration at which transcriptional effects were

observed in cultured CEH would surpass environmental levels by a factor of 1000 as shown in the following calculations:

Molecular weight of PFOS = 538 g/mol

Concentration of PFOS in medium = 10 μ M (10 μ mol/L)

Volume of medium = 0.5 ml (0.0005L)

Weight of cells in each well = 781.2 μ g

Total PFOS in medium = (538 g/mol) (10⁶ μ g/g) (10 μ mol/L) (10⁻⁶ mol/ μ mol) (0.0005 L medium)
= 2.69 μ g

Concentration of PFOS in cells = $\frac{\text{Total PFOS in medium}}{\text{Weight of cells in each well}}$
= $\frac{2.69 \mu\text{g}}{781.2 \mu\text{g}}$ (10⁶ μ g/g)
= 3443 μ g PFOS/g cell

Highest concentration reported in wild birds = 2.6 μ g/g ww
(in American bald eagle plasma; Giesy & Kannan, 2001)

It is most likely that only a fraction of the total PFOS was taken in by cells and that a large portion remained in solution, absorbed to the plastic walls of the culture vessel, or bound to albumin in the medium. However, partial absorption may still overestimate environmental levels. A useful exercise would be to determine how much PFOS is removed from the culture medium by cells so that more quantitative comparisons could be made between *in vitro* and *in vivo* studies. Nevertheless, the PFOS concentration used for these microarray experiments (10 μ M), to my knowledge, is lowest concentration reported at which significant effects have been observed in cultured avian hepatocytes. As with most *in vitro* screening studies, future studies should investigate whether the endpoints identified in CEH microarray experiments are also affected in developing embryos at lethal, sub-lethal and environmentally relevant concentrations of PFOS.

PFOS was phased-out of production by its major manufacturer (3M) in 2002 and recently listed in the Stockholm Convention as a persistent organic pollutant. However, being listed in annex B of the convention still permits the use of PFOS and its related precursor compounds for

several applications for which no suitable replacements have been found. For example PFOS is still used in semi-conductor coatings, aviation hydraulic fluids, medical devices, fire-fighting foams and insect baits (UNEP, 2009). Although no longer at the same levels prior to the 3M phase-out, global production of PFOS continues today. For example, a recent document from the Chinese government to the United Nation Environment Programme reported that in 2006, 15 different Chinese enterprises were producing a combined 200 tonnes of PFOS related compounds annually (MEP, 2008). The detection of PFOS emissions also suggests that PFOS is produced in several other countries. In 2007, aqueous PFOS emissions along the European river network were estimated to be approximately 20 tonnes annually (Pistocchi *et al.* 2009), although some of this PFOS may be of Chinese origin. Current sources of longer-chain PFCs such as PFUdA and PFDS, which have been detected in birds (Bustnes *et al.*, 2008; Butt *et al.*, 2007a; Holmstrom & Berger, 2008; Houde *et al.*, 2006; Verreault *et al.*, 2005; Verreault *et al.*, 2007; Wang *et al.*, 2008), are less clear. These compounds are likely impurities produced during the manufacture of eight- or nine-carbon PFCs via telomerization chemistries (Prevedouros *et al.*, 2006) that have elevated to detectable levels in wildlife due to their ability, as long-chain PFCs, to bioaccumulate and biomagnify (Conder *et al.*, 2008). Following the 3M phase-out of PFOS several fluorochemical companies, including 3M and DuPont, have turned to PFCs with four or six carbons to replace PFOS and PFOA (Lau, 2009). Although these compounds are expected to be less bioaccumulative than longer-chain PFCs, they have been detected in biota (Houde *et al.*, 2006), albeit at lower levels than the eight-carbon PFCs. The environmental presence of short-chain PFCs is expected to increase as industry continues to incorporate these compounds into more products and applications. Few studies have investigated the potential toxic effects of these replacement PFCs in avian species. One feeding study showed no signs of acute, chronic or

reproductive toxicity following an average daily intake of 87.8 mg PFBS/kg bw/d in mallards and quails (Newsted *et al.*, 2008). Another *in vitro* study reported no changes in the transcription of genes involved in lipid, cholesterol or xenobiotic metabolism in CEH following PFBS exposure (Hickey *et al.*, 2009). While this preliminary evidence suggests PFBS may be less toxic than its eight-carbon counterpart, more research is still need to assess the effects of these chemicals on the health of wild birds, animals and humans.

6.2. Future directions

Based on the results and discussions from this thesis, the specific recommendations for future PFCs research are as follows:

- While the results from Chapter 2 of this thesis suggests that PFOS is detrimental to the hatching success of the domestic chicken, Newsted *et al.* (2007) found that PFOS only affected post-hatch survival of quails and had no effect to mallards. Future work should address whether there are species-specific differences in reproductive toxicity towards PFOS and other PFCs and if so, what the biological basis of these differences might be. This is absolutely essential for the accurate extrapolation of laboratory test results for environmental risk assessment
- Injection of T- PFOS affected the hatching success of chickens (Chapter 2). But as discussed in Chapter 4, wildlife with high PFOS burdens tend to have higher proportions of L-PFOS relative to T-PFOS. In Chapter 5, it was demonstrated that T-PFOS can deregulate the transcription of many more genes than L-PFOS, although similar

biological functions and pathways are affected. In Chapter 3 it was shown that linear PFOA, PFDS, and PFUDa do not affect the hatching success of the chicken. An investigation into whether or not L-PFOS interferes with chicken reproduction is required.

- The pharmacokinetic properties of PFCs vary greatly between species, and in some cases even between sexes (Hundley *et al.*, 2006; Ohmori *et al.*, 2003). In Chapter 4, it was shown that the accumulation of PFOS isomers in the chicken liver was isomer specific. Whether there are species or sex differences in isomer accumulation patterns should be addressed.
- The observation that T-PFOS disrupts the regulation of more genes in cultured CEH than L-PFOS suggests that the branched isomers of PFOS are more biologically active than the linear isomer alone. This may have important consequences to human health as recent studies have shown higher proportions of branched isomers in human serum relative to T-PFOS. The effects of branched PFOS isomers in mammalian models need to be investigated to assess possible risk to human health.
- The results from the microarray experiments in Chapter 5 suggest several targets as mechanisms for PFOS toxicity. Hypotheses derived from these results should be used to design more targeted mechanistic investigations. Furthermore, time course experiments should be performed to dissect the various mechanisms and their interactions. In addition, these mechanisms will have to be validated in *in vivo* studies.

- In order to make more quantitative comparisons between *in vitro* and *in vivo* results, the amount of PFOS that is actually absorbed by cultured cells from the culture medium should be determined.
- While PFOS binding studies with LXR, RXR, and PPARs (Vanden Heuval *et al.*, 2006) have been performed with rat, mouse and human proteins, the binding affinity of PFOS to other implicated receptors, such as PXR and HNF4A, needs to be investigated. Binding studies using avian receptors would also be beneficial for species-species comparisons. Knockout studies for these various receptors would also clarify their requirement for PFOS toxicity.
- While PFOS does not appear to bind directly to RXR, whether or not PFOS can interfere with RXRs ability to form heterodimers with binding partners or to subsequently bind to regulatory DNA elements should be investigated.
- Finally, “replacement” PFCs need to be screened for their ability to interfere with any molecular targets identified from the PFOS research.

REFERENCES

- Abbott,B.D., Wolf,C.J., Das,K.P., Zehr,R.D., Schmid,J.E., Lindstrom,A.B., Strynar,M.J. & Lau,C. (2009) Developmental toxicity of perfluorooctane sulfonate (PFOS) is not dependent on expression of peroxisome proliferator activated receptor-alpha (PPARalpha) in the mouse. *Reprod.Toxicol.*, **27**, 258-265.
- Abbott,B.D., Wolf,C.J., Schmid,J.E., Das,K.P., Zehr,R.D., Helfant,L., Nakayama,S., Lindstrom,A.B., Strynar,M.J. & Lau,C. (2007) Perfluorooctanoic acid induced developmental toxicity in the mouse is dependent on expression of peroxisome proliferator activated receptor-alpha. *Toxicol.Sci*, **98**, 571-581.
- Andersen,M.E., Butenhoff,J.L., Chang,S.C., Farrar,D.G., Kennedy,G.L., Jr., Lau,C., Olsen,G.W., Seed,J. & Wallace,K.B. (2008) Perfluoroalkyl acids and related chemistries--toxicokinetics and modes of action. *Toxicol.Sci.*, **102**, 3-14.
- Arsenault,G., Chittim,B., McAlees,A., McCrindle,R., Riddell,N. & Yeo,B. (2008) Some issues relating to the use of perfluorooctanesulfonate (PFOS) samples as reference standards. *Chemosphere*, **70**, 616-625.
- Austin,M.E., Kasturi,B.S., Barber,M., Kannan,K., MohanKumar,P.S. & MohanKumar,S.M. (2003) Neuroendocrine effects of perfluorooctane sulfonate in rats. *Environ.Health Perspect.*, **111**, 1485-1489.
- Bao,J., Liu,W., Liu,L., Jin,Y., Dai,J., Ran,X., Zhang,Z. & Tsuda,S. (2010) Perfluorinated Compounds in the Environment and the Blood of Residents Living near Fluorochemical Plants in Fuxin, China. *Environ.Sci.Technol.*, epub.
- Benjamini,Y. & Hochberg,Y. (1995) Controlling the False Discovery Rate - A Practical and Powerful Approach to Multiple Testing. *J.Roy.Stat.Soc.BMeth.*, **57**(1), 289-300.
- Benskin,J.P., Bataineh,M. & Martin,J.W. (2007) Simultaneous characterization of perfluoroalkyl carboxylate, sulfonate, and sulfonamide isomers by liquid chromatography-tandem mass spectrometry. *Anal.Chem.*, **79**, 6455-6464.
- Benskin,J.P., De Silva,A.O., Martin,L.J., Arsenault,G., McCrindle,R., Riddell,N., Mabury,S.A. & Martin,J.W. (2009) Disposition of Perfluorinated Acid Isomers in Sprague Dawley Rats; Part 1: Single Dose. *Environ.Toxicol.Chem.*, **28**, 542-554.
- Berasin,C., Castillo,J., Perugorria,M.J., Prieto,J. & Avila, M. A. (2007) Amphiregulin: a new growth factor in hepatocarcinogenesis. *Cancer Lett.*, **254**(1), 30-41.
- Berthiaume,J. & Wallace,K.B. (2002) Perfluorooctanoate, perfluorooctanesulfonate, and N-ethyl perfluorooctanesulfonamido ethanol; peroxisome proliferation and mitochondrial biogenesis. *Toxicol.Lett.*, **129**, 23-32.

- Biegel, L.B., Liu, R.C., Hurtt, M.E. & Cook, J.C. (1995) Effects of ammonium perfluorooctanoate on Leydig cell function: in vitro, in vivo, and ex vivo studies. *Toxicol. Appl. Pharmacol.*, **134**, 18-25.
- Bjork, J.A., Lau, C., Chang, S.C., Butenhoff, J.L. & Wallace, K.B. (2008) Perfluorooctane sulfonate-induced changes in fetal rat liver gene expression. *Toxicology*, **251**(1-3), 8-20.
- Boardman, P.E., Sanz-Ezquerro, J., Overton, I.M., Burt, D.W., Bosch, E., Fong, W.T., Tickle, C., Brown, W.R., Wilson, S.A. & Hubbard, S.J. (2002) A comprehensive collection of chicken cDNAs. *Curr. Biol.*, **12**(22), 1965-1969
- Bookstaff, R.C., Moore, R.W., Ingall, G.B. & Peterson, R.E. (1990) Androgenic deficiency in male rats treated with perfluorodecanoic acid. *Toxicol. Appl. Pharmacol.*, **104**, 322-333.
- Boulanger, B., Vargo, J., Schnoor, J.L. & Hornbuckle, K.C. (2004) Detection of perfluorooctane surfactants in Great Lakes water. *Environ. Sci. Technol.*, **38**, 4064-4070.
- Brunmeir, R., Lagger, S. & Seiser, C. (2009) Histone deacetylase HDAC1/HDAC2-controlled embryonic development and cell differentiation. *Int. J. Dev. Biol.*, **53**(2-3), 275-289.
- Buist, S.C., Cherrington, N.J., Choudhuri, S., Hartley, D.P. & Klaassen, C.D. (2002) Gender-specific and developmental influences on the expression of rat organic anion transporters. *J. Pharmacol. Exp. Ther.*, **301**, 145-151.
- Bustnes, J.O., Borga, K., Erikstad, K.E., Lorentsen, S.H. & Herzke, D. (2008) Perfluorinated, brominated, and chlorinated contaminants in a population of lesser black-backed gulls (*Larus fuscus*). *Environ. Toxicol. Chem.*, **27**, 1383-1392.
- Butenhoff, J., Costa, G., Elcombe, C., Farrar, D., Hansen, K., Iwai, H., Jung, R., Kennedy, G., Jr., Lieder, P., Olsen, G. & Thomford, P. (2002) Toxicity of ammonium perfluorooctanoate in male cynomolgus monkeys after oral dosing for 6 months. *Toxicol. Sci.*, **69**, 244-257.
- Butt, C.M., Mabury, S.A., Muir, D.C. & Braune, B.M. (2007a) Prevalence of long-chained perfluorinated carboxylates in seabirds from the Canadian Arctic between 1975 and 2004. *Environ. Sci. Technol.*, **41**, 3521-3528.
- Butt, C.M., Muir, D.C., Stirling, I., Kwan, M. & Mabury, S.A. (2007b) Rapid response of Arctic ringed seals to changes in perfluoroalkyl production. *Environ. Sci. Technol.*, **41**, 42-49.
- Chang, S.C., Thibodeaux, J.R., Eastvold, M.L., Ehresman, D.J., Bjork, J.A., Froehlich, J.W., Lau, C., Singh, R.J., Wallace, K.B. & Butenhoff, J. L. (2008) Thyroid hormone status and pituitary function in adult rats given oral doses of perfluorooctanesulfonate (PFOS). *Toxicology*, **243**(3), 330-339.
- Chen, J. & Zhang, P. (2006) Photodegradation of perfluorooctanoic acid in water under irradiation of 254 nm and 185 nm light by use of persulfate. *Water Sci. Technol.*, **5**, 317-325.

- Chu,S. & Letcher,R.J. (2008) Analysis of fluorotelomer alcohols and perfluorinated sulfonamides in biotic samples by liquid chromatography-atmospheric pressure photoionization mass spectrometry. *J.Chromatogr.A*, **1215**, 92-99.
- Chu,S.G. & Letcher,R.J. (2009) Linear and branched perfluorooctane sulfonate isomers in technical product and environmental samples by in-port derivatization-gas chromatography-mass spectrometry. *Anal.Chem.*, **81**, 4256-4262.
- Clevers,H. (2006) Wnt/beta-catenin signaling in development and disease. *Cell*, **127**(3), 469-480.
- Conder,J.M., Hoke,R.A., De,W.W., Russell,M.H. & Buck,R.C. (2008) Are PFCAs bioaccumulative? A critical review and comparison with regulatory criteria and persistent lipophilic compounds. *Environ.Sci.Technol.*, **42**, 995-1003.
- Crump,D., Chiu,S., Egloff,C. & Kennedy,S.W. (2008) Effects of hexabromocyclododecane and polybrominated diphenyl ethers on mRNA expression in chicken (*Gallus domesticus*) hepatocytes. *Toxicol.Sci.*, **106**, 479-487.
- Cui,X., Hwang,J.T., Qiu,J., Blades,N.J. & Churchill,G.A. (2005) Improved statistical tests for differential gene expression by shrinking variance components estimates. *Biostatistics.*, **6**(1), 59-75.
- Curran,I., Hierlihy,S.L., Liston,V., Pantazopoulos,P., Nunnikhoven,A., Tittlemier,S., Barker,M., Trick,K. & Bondy,G. (2008) Altered fatty acid homeostasis and related toxicologic sequelae in rats exposed to dietary potassium perfluorooctanesulfonate (PFOS). *J.Toxicol.Environ.Health A*, **71**, 1526-1541.
- Cwinn,M.A., Jones,S.P. & Kennedy,S.W. (2008) Exposure to perfluorooctane sulfonate or fenofibrate causes PPAR-alpha dependent transcriptional responses in chicken embryo hepatocytes. *Comp Biochem.Physiol C.Toxicol.Pharmacol.*, **148**, 165-171.
- D'eon,J.C., Hurley,M.D., Wallington,T.J. & Mabury,S.A. (2006) Atmospheric chemistry of N-methyl perfluorobutane sulfonamidoethanol, C₄F₉SO₂N(CH₃)CH₂CH₂OH: kinetics and mechanism of reaction with OH. *Environ.Sci.Technol.*, **40**, 1862-1868.
- Dauwe,T., Van,d., V, De Coen,W. & Eens,M. (2007) PFOS levels in the blood and liver of a small insectivorous songbird near a fluorochemical plant. *Environ.Int.*, **33**, 357-361.
- De Silva,A.O., Benskin,J.P., Martin,L.J., Arsenault,G., McCrindle,R., Riddell,N., Martin,J.W. & Mabury,S.A. (2009a) Disposition of perfluorinated acid isomers in Sprague-Dawley rats; Part 2 subchronic dose. *Environ.Toxicol.Chem.*, **28**, 555-567.
- De Silva,A.O. & Mabury,S.A. (2004) Isolating isomers of perfluorocarboxylates in polar bears (*Ursus maritimus*) from two geographical locations. *Environ.Sci.Technol.*, **38**, 6538-6545.
- De Silva,A.O. & Mabury,S.A. (2006) Isomer distribution of perfluorocarboxylates in human blood: potential correlation to source. *Environ.Sci.Technol.*, **40**, 2903-2909.

- De Silva,A.O., Muir,D.C. & Mabury,S.A. (2009b) Distribution of perfluorocarboxylate isomers in select samples from the North American environment. *Environ.Toxicol.Chem.*, **28**, 1801-1814.
- De Silva,A.O., Tseng,P.J. & Mabury,S.A. (2009c) Toxicokinetics of perfluorocarboxylate isomers in rainbow trout. *Environ.Toxicol.Chem.*, **28**, 330-337.
- De Witt,J.C., Copeland,C.B. & Luebke,R.W. (2007) Dose-response of perfluorooctanoic acid-induced immunomodulation in adult C57BL/6 mice. *Toxicologist*, **96**, 13.
- De Witt,J.C., Shnyra,A., Badr,M.Z., Loveless,S.E., Hoban,D., Frame,S.R., Cunard,R., Anderson,S.E., Meade,B.J., Peden-Adams,M.M., Luebke,R.W. & Luster,M.I. (2008) Immunotoxicity of perfluorooctanoic acid and perfluorooctane sulfonate and the role of peroxisome proliferator-activated receptor alpha. *Crit.Rev.Toxicol.*, **39**, 76-94.
- Dimitrov,S., Kamenska,V., Walker,J.D., Windle,W., Purdy,R., Lewis,M. & Mekenyan,O. (2004) Predicting the biodegradation products of perfluorinated chemicals using CATABOL. *SAR QSAR.Environ.Res.*, **15**, 69-82.
- Dinglasan,M.J., Ye,Y., Edwards,E.A. & Mabury,S.A. (2004) Fluorotelomer alcohol biodegradation yields poly- and perfluorinated acids. *Environ.Sci.Technol.*, **38**, 2857-2864.
- Diot,C. & Douaire,M. (1999) Characterization of a cDNA sequence encoding the peroxisome proliferator activated receptor alpha in the chicken. *Poult.Sci.*, **78**, 1198-1202.
- Egloff,C., Labrosse,A., Hebert,C. & Crump,D. (2009) A nondestructive method for obtaining maternal DNA from avian eggshells and its application to embryonic viability determination in herring gulls (*Larus argentatus*). *Mol.Ecol.Resour.*, **9**, 19-27.
- Ehresman,D.J., Chang,S., Bjork,J.A., Hart,J.A., Lieder,P.H., Wallace,K.B. & Butenhoff,J.L. (2007) Increased acyl CoA oxidase activity in rats after five consecutive daily doses of perfluorobutanesulfonate, perfluorohexanesulfonate, and perfluorooctanesulfonate. *Toxicologist*, **96**, 179 (abstract).
- Elcombe,C.R., Elcomb,B.M., Foster,J.R. & Farrar,J.R. (2007) Characterization of the hepatomegaly induced by ammonium perfluorooctanoic acid (APFO) in rats. *Toxicologist*, **96**, 179 (abstract).
- Ellis,D.A., Martin,J.W., De Silva,A.O., Mabury,S.A., Hurley,M.D., Sulbaek Andersen,M.P. & Wallington,T.J. (2004) Degradation of fluorotelomer alcohols: a likely atmospheric source of perfluorinated carboxylic acids. *Environ.Sci.Technol.*, **38**, 3316-3321.
- Ellis,D.A., Woodcroft,M., March,R.E., Raffery,S., Yee,J., Burns,D. (2008) The interactions of fluorochemicals with liver fatty acid binding protein: potential mechanism for bioaccumulation and toxicity. SETAC North America 29th Annual Meeting. Tampa FL. Abstract #400. <http://www.setac.org/tampa/general/downloadable.php>. Platform presentation.

- Emmett,E.A., Shofer,F.S., Zhang,H., Freeman,D., Desai,C. & Shaw,L.M. (2006) Community exposure to perfluorooctanoate: relationships between serum concentrations and exposure sources. *J.Occup.Environ.Med.*, **48**, 759-770.
- Eriksen,K.T., Raaschou-Nielsen,O., Sorensen,M., Roursgaard,M., Loft,S. & Moller,P. (2010) Genotoxic potential of the perfluorinated chemicals PFOA, PFOS, PFBS, PFNA and PFHxA in human HepG2 cells. *Mutat.Res.*, **700**, 39-43.
- Fairley,K.J., Purdy,R., Kearns,S., Anderson,S.E. & Meade,B.J. (2007) Exposure to the immunosuppressant, perfluorooctanoic acid, enhances the murine IgE and airway hyperreactivity response to ovalbumin. *Toxicol.Sci.*, **97**, 375-383.
- Feige,J.N., Gelman,L., Michalik,L., Desvergne,B. & Wahli,W. (2006) From molecular action to physiological outputs: peroxisome proliferator-activated receptors are nuclear receptors at the crossroads of key cellular functions. *Prog.Lipid Res.*, **45**, 120-159.
- Fuentes,S., Colomina,M.T., Rodriguez,J., Vicens,P. & Domingo,J.L. (2006) Interactions in developmental toxicology: concurrent exposure to perfluorooctane sulfonate (PFOS) and stress in pregnant mice. *Toxicol.Lett.*, **164**, 81-89.
- Furdui,V.I., Helm,P.A., Crozier,P.W., Lucaciu,C., Reiner,E.I., Marvin,C.H., Whittle,D.M., Mabury,S.A. & Tomy,G.T. (2008) Temporal trends of perfluoroalkyl compounds with isomer analysis in lake trout from Lake Ontario (1979-2004). *Environ.Sci.Technol.*, **42**, 4739-4744.
- Gebbink,W.A., Hebert,C.E. & Letcher,R.J. (2009) Perfluorinated carboxylates and sulfonates and precursor compounds in herring gull eggs from colonies spanning the Laurentian Great Lakes of North America. *Environ.Sci.Technol.*, **43**, 7443-7449.
- Gebbink,W.A. & Letcher,R.J. (2010) Linear and branched perfluorooctane sulfonate isomers and patterns in herring gull eggs from colonial sites across the Laurentian Great Lakes. *Environ.Sci.Technol.*, **44**, 3739-3745.
- Giesy,J.P. & Kannan,K. (2001) Global distribution of perfluorooctane sulfonate in wildlife. *Environ.Sci.Technol.*, **35**, 1339-1342.
- Goodnight,J.H.,& Harvey,W.R. (1978) Least-Squares Means in the Fixed-Effects General Linear Models. Cary, NC, SAS Institute inc., SAS Technical Report R-103.
- Grasty,R.C., Bjork,J.A., Wallace,K.B., Wolf,D.C., Lau,C.S. & Rogers,J.M. (2005) Effects of prenatal perfluorooctane sulfonate (PFOS) exposure on lung maturation in the perinatal rat. *Birth Defects Res B Dev.Reprod.Toxicol.*, **74**, 405-416.
- Grasty,R.C., Wolf,D.C., Grey,B.E., Lau,C.S. & Rogers,J.M. (2003) Prenatal window of susceptibility to perfluorooctane sulfonate-induced neonatal mortality in the Sprague-Dawley rat. *Birth Defects Res.B Dev.Reprod.Toxicol.*, **68**, 465-471.

- Gutshall,D.M., Pilcher,G.D. & Langley,A.E. (1988) Effect of thyroxine supplementation on the response to perfluoro-n-decanoic acid (PFDA) in rats. *J.Toxicol.Environ.Health*, **24**, 491-498.
- Guo,Y., Jolly,R.A., Halstead,B.W., Baker,T.K., Stutz,J.P., Huffman,M., Calley,J.N., West,A., Gao,H., Searfoss,G.H., Li,S., Irizarry,A.R., Qian,H.R., Stevens,J.L. & Ryan,T.P. (2007) Underlying mechanisms of pharmacology and toxicity of a novel PPAR agonist revealed using rodent and canine hepatocytes. *Toxicol.Sci.*, **96**, 294-309.
- Han,X., Yang,C.H., Snajdr,S.I., Nabb,D.L. & Mingoia,R.T. (2008) Uptake of perfluorooctanoate in freshly isolated hepatocytes from male and female rats. *Toxicol.Lett.*, **181**, 81-86.
- Hansen,K.J., Clemen,L.A., Ellefson,M.E. & Johnson,H.O. (2001) Compound-specific, quantitative characterization of organic fluorochemicals in biological matrices. *Environ.Sci.Technol.*, **35**, 766-770.
- Hansen,K.J., Johnson,H.O., Eldridge,J.S., Butenhoff,J.L. & Dick,L.A. (2002) Quantitative characterization of trace levels of PFOS and PFOA in the Tennessee River. *Environ.Sci.Technol.*, **36**, 1681-1685.
- Haug,L.S., Thomsen,C. & Becher,G. (2009) Time trends and the influence of age and gender on serum concentrations of perfluorinated compounds in archived human samples. *Environ.Sci.Technol.*, **43**, 2131-2136.
- Hayhurst,G.P., Lee,Y.H., Lambert,G., Ward,J.M. & Gonzalez,F.J. (2001) Hepatocyte nuclear factor 4alpha (nuclear receptor 2A1) is essential for maintenance of hepatic gene expression and lipid homeostasis. *Mol.Cell Biol.*, **21**(4), 1393-1403.
- Head,J.A., Hahn,M.E. & Kennedy,S.W. (2008) Key amino acids in the aryl hydrocarbon receptor predict dioxin sensitivity in avian species. *Environ.Sci.Technol.*, **42**, 7535-7541.
- Heinz,G.H., Hoffman,D.J., Kondrad,S.L. & Erwin,C.A. (2006) Factors affecting the toxicity of methylmercury injected into eggs. *Arch.Environ.Contam Toxicol.*, **50**, 264-279.
- Hertz,R.J., Magenheim,J., Berman,I. & Bar-Tana,J. (1998) Fatty acyl-CoA thioesters are ligands of hepatic nuclear factor-4alpha. *Nature*, **392**, 512-516.
- Hickey,N.J., Crump,D., Jones,S.P. & Kennedy,S.W. (2009) Effects of 18 perfluoroalkyl compounds (PFCs) on mRNA expression in chicken embryo hepatocyte cultures. *Toxicol.Sci.*, **111**, 311-320.
- Higgins,J.J. (2003) An introduction to modern nonparametric statistics. Brooks/Cole, 2003. Pacific Grove, CA.
- Hoff,P.T., Van Campenhout,K., Van,d., V, Covaci,A., Bervoets,L., Moens,L., Huyskens,G., Goemans,G., Belpaire,C., Blust,R. & De Coen,W. (2005) Perfluorooctane sulfonic acid and organohalogen pollutants in liver of three freshwater fish species in Flanders

- (Belgium): relationships with biochemical and organismal effects. *Environ.Pollut.*, **137**, 324-333.
- Hoff,P.T., Van,d., V, Van Dongen,W., Esmans,E.L., Blust,R. & De Coen,W.M. (2003) Perfluorooctane sulfonic acid in bib (Trisopterus luscus) and plaice (Pleuronectes platessa) from the Western Scheldt and the Belgian North Sea: distribution and biochemical effects. *Environ.Toxicol.Chem.*, **22**, 608-614.
- Hoffman,B. & Liebermann,D.A. (2008) Apoptotic signaling by c-MYC. *Oncogene* **27**(50), 6462-6472.
- Hoffman,D.J., Melancon,M.J., Klein,P.N., Eisemann,J.D. & Spann,J.W. (1998) Comparative developmental toxicity of planar polychlorinated biphenyl congeners in chickens, American kestrels, and common terns. *Environ.Toxicol.Chem.*, **17**, 747-757.
- Hollstein,M. & Hainaut,P. (2010) Massively regulated genes: the example of TP53. *J.Pathol.*, **220**(2), 164-173.
- Holm,S. (1979) A simple sequentially rejective multiple test procedure. *Scand.J.Statist.*, **6**(2), 65-70.
- Holmstrom,K.E. & Berger,U. (2008) Tissue distribution of perfluorinated surfactants in common guillemot (Uria aalge) from the Baltic Sea. *Environ.Sci.Technol.*, **42**, 5879-5884.
- Holmstrom,K.E., Jarnberg,U. & Bignert,A. (2005) Temporal trends of PFOS and PFOA in guillemot eggs from the Baltic Sea, 1968--2003. *Environ.Sci.Technol.*, **39**, 80-84.
- Hori,H., Nagaoka,Y., Yamamoto,A., Sano,T., Yamashita,N., Taniyasu,S. & Kutsuna,S. (2006) Efficient decomposition of environmentally persistent perfluorooctanesulfonate and related fluorochemicals using zerovalent iron in subcritical water. *Environmental Science & Technology*, **40**, 1049-1054.
- Houde,M., Czub,G., Small,J.M., Backus,S., Wang,X., Alae,M. & Muir,D.C. (2008) Fractionation and bioaccumulation of perfluorooctane sulfonate (PFOS) isomers in a Lake Ontario food web. *Environ.Sci.Technol.*, **42**, 9397-9403.
- Houde,M., Martin,J.W., Letcher,R.J., Solomon,K.R. & Muir,D.C. (2006) Biological monitoring of polyfluoroalkyl substances: A review. *Environ.Sci.Technol.*, **40**, 3463-3473.
- Houde,M., Wells,R.S., Fair,P.A., Bossart,G.D., Hohn,A.A., Rowles,T.K., Sweeney,J.C., Solomon,K.R. & Muir,D.C. (2005) Polyfluoroalkyl compounds in free-ranging bottlenose dolphins (Tursiops truncatus) from the Gulf of Mexico and the Atlantic Ocean. *Environ.Sci.Technol.*, **39**, 6591-6598.
- Hu,W., Jones,P.D., Celius,T. & Giesy,J.P. (2005) Identification of genes responsive to PFOS using gene expression profiling. *Environ.Toxicol.Pharmacol.*, **19**, 57-70.

- Hu,W., Jones,P.D., DeCoen,W., King,L., Fraker,P., Newsted,J. & Giesy,J.P. (2003) Alterations in cell membrane properties caused by perfluorinated compounds. *Comp Biochem.Physiol C.Toxicol.Pharmacol.*, **135**, 77-88.
- Hu,W., Jones,P.D., Upham,B.L., Trosko,J.E., Lau,C. & Giesy,J.P. (2002) Inhibition of gap junctional intercellular communication by perfluorinated compounds in rat liver and dolphin kidney epithelial cell lines in vitro and Sprague-Dawley rats in vivo. *Toxicol.Sci.*, **68**, 429-436.
- Hundley,S.G., Sarrif,A.M. & Kennedy,G.L. (2006) Absorption, distribution, and excretion of ammonium perfluorooctanoate (APFO) after oral administration to various species. *Drug Chem.Toxicol.*, **29**, 137-145.
- Ikeda,T., Aiba,K., Fukuda,K. & Tanaka,M. (1985) The induction of peroxisome proliferation in rat liver by perfluorinated fatty acids, metabolically inert derivatives of fatty acids. *J.Biochem.*, **98**, 475-482.
- Jernbro,S., Rocha,P.S., Keiter,S., Skutlarek,D., Färber,H., Jones,P.D., Giesy,J.P., Hollert,H. & Engwall,M. (2007) Perfluorooctane sulfonate increases the genotoxicity of cyclophosphamide in the micronucleus assay with V79 cells. Further proof of alterations in cell membrane properties caused by PFOS. *Environ.Sci.Pollut.Res.Int.*, **14**, 85-87.
- Johansson,N., Fredriksson,A. & Eriksson,P. (2008) Neonatal exposure to perfluorooctane sulfonate (PFOS) and perfluorooctanoic acid (PFOA) causes neurobehavioural defects in adult mice. *Neurotoxicology*, **29**, 160-169.
- Jones,P.D., Hu,W., De Coen,W., Newsted,J.L. & Giesy,J.P. (2003) Binding of perfluorinated fatty acids to serum proteins. *Environ.Toxicol.Chem.*, **22**, 2639-2649.
- Kahn,N.W., St.John,J. & Quinn,T.W. (1998) Chromosome-specific intron size differences in the avian CHD gene provide an efficient method for sex identification in birds. *Auk* **115**, 1074-1078.
- Kannan,K., Choi,J.W., Iseki,N., Senthilkumar,K., Kim,D.H. & Giesy,J.P. (2002a) Concentrations of perfluorinated acids in livers of birds from Japan and Korea. *Chemosphere*, **49**, 225-231.
- Kannan,K., Franson,J.C., Bowerman,W.W., Hansen,K.J., Jones,P.D. & Giesy,J.P. (2001) Perfluorooctane sulfonate in fish-eating water birds including bald eagles and albatrosses. *Environ.Sci.Technol.*, **35**, 3065-3070.
- Kannan,K., Hansen,K.J., Wade,T.L. & Giesy,J.P. (2002b) Perfluorooctane sulfonate in oysters, *Crassostrea virginica*, from the Gulf of Mexico and the Chesapeake Bay, USA. *Arch.Environ.Contam Toxicol.*, **42**, 313-318.
- Kannan,K., Tao,L., Sinclair,E., Pastva,S.D., Jude,D.J. & Giesy,J.P. (2005) Perfluorinated compounds in aquatic organisms at various trophic levels in a Great Lakes food chain. *Arch.Environ.Contam Toxicol.*, **48**, 559-566.

- Karrman,A., Langlois,I., van Bavel,B., Lindstrom,G. & Oehme,M. (2007) Identification and pattern of perfluorooctane sulfonate (PFOS) isomers in human serum and plasma. *Environ.Int.*, **33**, 782-788.
- Katakura,M., Kudo,N., Tsuda,S., Hibino,Y., Mitsumoto,A. & Kawashima,Y. (2007) Rat organic anion transporter 3 and organic anion transporting polypeptide 1 mediate perfluorooctanoic acid transport. *J.Health Sci.*, **53**, 77-83.
- Kawamoto,K., Oashi,T., Oami,K., Liu,W., Jin,Y., Saito,N., Sato,I.,& Tsuda,S. (2010) Perfluorooctanoic acid (PFOA) but not perfluorooctane sulfonate (PFOS) showed DNA damage in comet assay on *Paramecium caudatum*. *J.Toxicol.Sci.*, **35**, 835-841.
- Kaye,T.S., Egorin,M.J., Riggs,C.E., Jr., Olman,E.A., Chou,F.T. & Salzman,M. (1983) The plasma pharmacokinetics and tissue distribution of dimethyl sulfoxide in mice. *Life Sci.*, **33**, 1223-1230.
- Keller,H., Devchand,P.R., Perroud,M. & Wahli,W. (1997) PPAR alpha structure-function relationships derived from species-specific differences in responsiveness to hypolipidemic agents. *Biol.Chem.*, **378**, 651-655.
- Kemper,R.A. & Jepson,G.W. (2003) Pharmacokinetics of perfluorooctanoic acid in male and female rats. *Toxicologist*, **72**, 148.
- Kennedy,G.L., Jr., Butenhoff,J.L., Olsen,G.W., O'Connor,J.C., Seacat,A.M., Perkins,R.G., Biegel,L.B., Murphy,S.R. & Farrar,D.G. (2004) The toxicology of perfluorooctanoate. *Crit Rev.Toxicol.*, **34**, 351-384.
- Kennedy,S.W., Lorenzen,A., Jones,S.P., Hahn,M.E. & Stegeman,J.J. (1996) Cytochrome P4501A induction in avian hepatocyte cultures: a promising approach for predicting the sensitivity of avian species to toxic effects of halogenated aromatic hydrocarbons. *Toxicol.Appl.Pharmacol.*, **141**, 214-230.
- Kerr,M.K. (2003) Design considerations for efficient and effective microarray studies. *Biometrics*, **59**(4): 822-828.
- Kerr,M.K. & Churchill,G.A. (2007) Statistical design and the analysis of gene expression microarray data. *Genet.Res.*, **89**(5-6): 509-514.
- Kissa,E. (2001) *Fluorinated Surfactants and Repellants, 2nd Ed.* Marcel Decker, New York.
- Konig,B., Kluge,H., Haase,K., Brandsch,C., Stangl,G.I. & Eder,K. (2007) Effects of clofibrate treatment in laying hens. *Poultry Science*, **86**, 1187-1195.
- Kudo,N., Bandai,N., Suzuki,E., Katakura,M. & Kawashima,Y. (2000) Induction by perfluorinated fatty acids with different carbon chain length of peroxisomal beta-oxidation in the liver of rats. *Chem.Biol.Interact.*, **124**, 119-132.

- Kudo,N., Sakai,A., Mitsumoto,A., Hibino,Y., Tsuda,T. & Kawashima,Y. (2007) Tissue distribution and hepatic subcellular distribution of perfluorooctanoic acid at low dose are different from those at high dose in rats. *Biol.Pharm.Bull.*, **30**, 1535-1540.
- Kudo,N., Suzuki,E., Katakura,M., Ohmori,K., Noshiro,R. & Kawashima,Y. (2001) Comparison of the elimination between perfluorinated fatty acids with different carbon chain length in rats. *Chem.Biol.Interact.*, **134**, 203-216.
- Lau,C. (2009) Perfluoroalkyl acids: recent activities and research progress. *Reprod.Toxicol.*, **27**, 209-211.
- Lau,C., Anitole,K., Hodes,C., Lai,D., Pfahles-Hutchens,A. & Seed,J. (2007) Perfluoroalkyl acids: a review of monitoring and toxicological findings. *Toxicol.Sci.*, **99**, 366-394.
- Lau,C., Butenhoff,J.L. & Rogers,J.M. (2004) The developmental toxicity of perfluoroalkyl acids and their derivatives. *Toxicol.Appl.Pharmacol.*, **198**, 231-241.
- Lau,C., Thibodeaux,J.R., Hanson,R.G., Rogers,J.M., Grey,B.E., Stanton,M.E., Butenhoff,J.L. & Stevenson,L.A. (2003) Exposure to perfluorooctane sulfonate during pregnancy in rat and mouse. II: postnatal evaluation. *Toxicol.Sci.*, **74**, 382-392.
- Liu,C., Du,Y. & Zhou,B. (2007a) Evaluation of estrogenic activities and mechanism of action of perfluorinated chemicals determined by vitellogenin induction in primary cultured tilapia hepatocytes. *Aquat.Toxicol.*, **85**, 267-277.
- Liu,C., Yu,K., Shi,X., Wang,J., Lam,P.K., Wu,R.S. & Zhou,B. (2007b) Induction of oxidative stress and apoptosis by PFOS and PFOA in primary cultured hepatocytes of freshwater tilapia (*Oreochromis niloticus*). *Aquat.Toxicol.*, **82**, 135-143.
- Liu,L., Liu,W., Song,J., Yu,H., Jin,Y., Oami,K., Sato,I., Saito,N. & Tsuda,S. (2009) A comparative study on oxidative damage and distributions of perfluorooctane sulfonate (PFOS) in mice at different postnatal developmental stages. *J.Toxicol.Sci.*, **34**, 245-254.
- Liu,W., Chen,S., Quan,X. & Jin,Y. (2008) Toxic effects of serial perfluorosulfonic and perfluorocarboxylic acids on the membrane system of a freshwater alga measured by flow cytometry. *Environ.Toxicol.Chem.*, **27**, 1597-1604.
- Lofstrand,K., Jorundsdottir,H., Tomy,G., Svavarsson,J., Weihe,P., Nygard,T. & Bergman,K. (2008) Spatial trends of polyfluorinated compounds in guillemot (*Uria aalge*) eggs from North-Western Europe. *Chemosphere*, **72**, 1475-1480.
- Logan,C.Y. & Nusse,R. (2004) The Wnt signaling pathway in development and disease. *Annu.Rev.Cell Dev.Biol.*, **20**, 781-810.
- Loveless,S.E., Finlay,C., Everds,N.E., Frame,S.R., Gillies,P.J., O'Connor,J.C., Powley,C.R. & Kennedy,G.L. (2006) Comparative responses of rats and mice exposed to linear/branched, linear, or branched ammonium perfluorooctanoate (APFO). *Toxicology* **220**, 203-217.

- Luebker,D.J., Hansen,K.J., Bass,N.M., Butenhoff,J.L. & Seacat,A.M. (2002) Interactions of fluorochemicals with rat liver fatty acid-binding protein. *Toxicology*, **176**, 175-185.
- Martin,M.T., Brennan,R.J., Hu,W., Ayanoglu,E., Lau,C., Ren,H., Wood,C.R., Corton,J.C., Kavlock,R.J. & Dix,D.J. (2007) Toxicogenomic study of triazole fungicides and perfluoroalkyl acids in rat livers predicts toxicity and categorizes chemicals based on mechanisms of toxicity. *Toxicol.Sci.*, **97**, 595-613.
- Martin,J.W., Ellis,D.A., Mabury,S.A., Hurley,M.D. & Wallington,T.J. (2006) Atmospheric chemistry of perfluoroalkanesulfonamides: kinetic and product studies of the OH radical and Cl atom initiated oxidation of N-ethyl perfluorobutanesulfonamide. *Environ.Sci.Technol.*, **40**, 864-872.
- Martin,J.W., Smithwick,M.M., Braune,B.M., Hoekstra,P.F., Muir,D.C. & Mabury,S.A. (2004a) Identification of long-chain perfluorinated acids in biota from the Canadian Arctic. *Environ.Sci.Technol.*, **38**, 373-380.
- Martin,J.W., Whittle,D.M., Muir,D.C. & Mabury,S.A. (2004b) Perfluoroalkyl contaminants in a food web from Lake Ontario. *Environ.Sci.Technol.*, **38**, 5379-5385.
- McKernan,M.A., Rattner,B.A., Hale,R.C. & Ottinger,M.A. (2007) Egg incubation position affects toxicity of air cell administered polychlorinated biphenyl 126 (3,3',4,4',5-pentachlorobiphenyl) in chicken (*Gallus gallus*) embryos. *Environ.Toxicol.Chem.*, **26**, 2724-2727.
- Ministry of Environmental Protection of China (MEP) (2008) Additional information on production and use of PFOS. http://chm.pops.int/Portals/0/Repository/comments_draftRME2008/UNEP-POPS-POPRC-DRME-08-CHI-SCCP.English.PDF accessed December 2010.
- Molina,E.D., Balander,R., Fitzgerald,S.D., Giesy,J.P., Kannan,K., Mitchell,R. & Bursian,S.J. (2006) Effects of air cell injection of perfluorooctane sulfonate before incubation on development of the white leghorn chicken (*Gallus domesticus*) embryo. *Environ.Toxicol.Chem.*, **25**, 227-232.
- Moody,C.A., Martin,J.W., Kwan,W.C., Muir,D.C. & Mabury,S.A. (2002) Monitoring perfluorinated surfactants in biota and surface water samples following an accidental release of fire-fighting foam into Etobicoke Creek. *Environ.Sci.Technol.*, **36**, 545-551.
- Mukherjee,R., Jow,L., Noonan,D. & McDonnell,D.P. (1994) Human and rat peroxisome proliferator activated receptors (PPARs) demonstrate similar tissue distribution but different responsiveness to PPAR activators. *J.Steroid Biochem.Mol.Biol.*, **51**, 157-166.
- Nagasawa,M., Ide,T., Suzuki,M., Tsunoda,M., Akasaka,Y., Okazaki,T., Mochizuki,T. & Murakami,K. (2004) Pharmacological characterization of a human-specific peroxisome proliferator-activated receptor alpha (PPARalpha) agonist in dogs. *Biochem.Pharmacol.*, **67**, 2057-2069.

- Nakayama,K., Iwata,H., Tao,L., Kannan,K., Imoto,M., Kim,E.Y., Tashiro,K. & Tanabe,S. (2008) Potential effects of perfluorinated compounds in common cormorants from Lake Biwa, Japan: an implication from the hepatic gene expression profiles by microarray. *Environ.Toxicol.Chem.*, **27**(11), 2378-2386.
- Newsted,J.L., Beach,S.A., Gallagher,S.P. & Giesy,J.P. (2006) Pharmacokinetics and acute lethality of perfluorooctanesulfonate (PFOS) to juvenile mallard and northern bobwhite. *Arch.Environ.Contam Toxicol.*, **50**, 411-420.
- Newsted,J.L., Beach,S.A., Gallagher,S.P. & Giesy,J.P. (2008) Acute and chronic effects of perfluorobutane sulfonate (PFBS) on the mallard and northern bobwhite quail. *Arch.Environ.Contam Toxicol.*, **54**, 535-545.
- Newsted,J.L., Coady,K.K., Beach,S.A., Butenhoff,J.L., Gallagher,S. & Giesy,J.P. (2007) Effects of perfluorooctane sulfonate on mallard and northern bobwhite quail exposed chronically via the diet. *Environmental Toxicology and Pharmacology*, **23**, 1-9.
- O'Brien,J.M., Carew,A.C., Chu,S., Letcher,R.J. & Kennedy,S.W. (2009a) Perfluorooctane sulfonate (PFOS) toxicity in domestic chicken (*Gallus gallus domesticus*) embryos in the absence of effects on peroxisome proliferator activated receptor alpha (PPARalpha)-regulated genes. *Comp.Biochem.Physiol.C.Toxicol.Pharmacol.*, **149**, 524-530.
- O'Brien,J.M., Crump,D., Mundy,L.J., Chu,S., McLaren,K.K., Vongphachan,V., Letcher,R.J. & Kennedy,S.W. (2009b) Pipping success and liver mRNA expression in chicken embryos exposed in ovo to C8 and C11 perfluorinated carboxylic acids and C10 perfluorinated sulfonate. *Toxicol.Lett.*, **190**, 134-139.
- O'Brien,J.M., Kennedy,S.W., Chu,S. & Letcher,R.J. (2010) Isomer-specific accumulation of perfluorooctane sulfonate in the liver of chicken embryos exposed in ovo to a technical mixture. *Environ.Toxicol.Chem.*, **30**, 226-231.
- Ochoa-Herrera,V., Sierra-Alvarez,R., Somogyi,A., Jacobsen,N.E., Wysocki,V.H. & Field,J.A. (2008) Reductive defluorination of perfluorooctane sulfonate. *Environ.Sci.Technol.*, **42**, 3260-3264.
- Odom,D.T., Zizlsperger,N., Gordon,D.B., Bell,G.W., Rinaldi,N.J., Murray,H.L., Volkert,T.L., Schreiber,J., Rolfe,P.A., Gifford,D.K., Fraenkel,E., Bell,G.I. & Young,R.A. (2004) Control of pancreas and liver gene expression by HNF transcription factors. *Science*, **303**(5662), 1378-1381.
- OECD (Organisation for Economic Co-operation and Development) (2002) Hazard assessment of perfluorooctane sulfonate (PFOS) and its salts. ENV/JM/RD(2002)17/FINAL. Joint Meeting of the Chemicals Committee and the Working Party on Chemicals, Pesticides, and Biotechnology, Environment Directorate, Organisation for Economic Co-operation and Development (Paris). <http://www.oecd.org/dataoecd/23/18/2382880.pdf> Accessed November, 2010.

- Ohmori,K., Kudo,N., Katayama,K. & Kawashima,Y. (2003) Comparison of the toxicokinetics between perfluorocarboxylic acids with different carbon chain length. *Toxicology*, **184**, 135-140.
- Onishchenko,N., Fischer,C., Wan Ibrahim,W.N., Negri,S., Spulber,S., Cottica,D. & Ceccatelli,S. (2010) Prenatal Exposure to PFOS or PFOA Alters Motor Function in Mice in a Sex-Related Manner. *Neurotox.Res.*, epub.
- Peden-Adams,M.M., Stuckey,J.E., Gaworecki,K.M., Berger-Ritchie,J., Bryant,K., Jodice,P.G., Scott,T.R., Ferrario,J.B., Guan,B., Vigo,C., Boone,J.S., McGuinn,W.D., Dewitt,J.C. & Keil,D.E. (2008) Developmental toxicity in white leghorn chickens following in ovo exposure to perfluorooctane sulfonate (PFOS). *Reprod.Toxicol.*, **27**, 307-318.
- Peraza,M.A., Burdick,A.D., Marin,H.E., Gonzalez,F.J. & Peters,J.M. (2006) The toxicology of ligands for peroxisome proliferator-activated receptors (PPAR). *Toxicol.Sci.*, **90**, 269-295.
- Pfaffl,M.W., Horgan,G.W. and Dempfle,L. (2002) Relative expression software tool (REST) for group-wise comparison and statistical analysis of relative expression results in real-time PCR. *Nucleic Acids Res.*, **30**(9), e36.
- Pinkas,A., Slotkin,T.A., Brick-Turin,Y., Van der Zee,E.A. & Yanai,J. (2010) Neurobehavioral teratogenicity of perfluorinated alkyls in an avian model. *Neurotoxicol.Teratol.*, **32**, 182-186.
- Prescher,D., Gross,U., Wotzka,J., Txcheu-Schlueter,M. & Stark,W. (1985) Environmental behavior of fluoro surfactants: Part 2. Study on biochemical degradability. *Acta Hydrochim.Hydrobiol*, **13**, 17-24.
- Prevedouros,K., Cousins,I.T., Buck,R.C. & Korzeniowski,S.H. (2006) Sources, fate and transport of perfluorocarboxylates. *Environ.Sci.Technol.*, **40**, 32-44.
- R Development Core Team (2010) R: A language and environment for statistical computing. R Foundation for Statistical Computing, Vienna, Austria. ISBN 3-900051-07-0, URL <http://www.R-project.org>.
- Rawson,R.B. (2003) The SREBP pathway--insights from Insigs and insects. *Nat.Rev.Mol.Cell Biol.*, **4**(8), 631-640.
- Rayne,S., Forest,K. & Friesen,K.J. (2008) Congener-specific numbering systems for the environmentally relevant C4 through C8 perfluorinated homologue groups of alkyl sulfonates, carboxylates, telomer alcohols, olefins, and acids, and their derivatives. *J.Environ.Sci.Health A Tox.Hazard.Subst.Environ.Eng*, **43**, 1391-1401.
- Ren,H., Vallanat,B., Nelson,D.M., Yeung,L.W., Guruge,K.S., Lam,P.K., Lehman-McKeeman,L.D. & Corton,J.C. (2009) Evidence for the involvement of xenobiotic-responsive nuclear receptors in transcriptional effects upon perfluoroalkyl acid exposure in diverse species. *Reprod.Toxicol.*, **27**, 266-277.

- Rhoads, K.R., Janssen, E.M., Luthy, R.G. & Criddle, C.S. (2008) Aerobic biotransformation and fate of N-ethyl perfluorooctane sulfonamidoethanol (N-EtFOSE) in activated sludge. *Environ.Sci.Technol.*, **42**, 2873-2878.
- Riddell, N., Arsenault, G., Benskin, J.P., Chittim, B., Martin, J.W., McAlees, A. & McCrindle, R. (2009) Branched perfluorooctane sulfonate isomer quantification and characterization in blood serum samples by HPLC/ESI-MS(/MS). *Environ.Sci.Technol.*, **43**, 7902-7908.
- Rosen, M.B., Schmid, J.R., Corton, J.C., Zehr, R.D., Das, K.P., Abbott, B.D. & Lau, C. (2010) Gene Expression Profiling in Wild-Type and PPARalpha-Null Mice Exposed to Perfluorooctane Sulfonate Reveals PPARalpha-Independent Effects. *PPAR.Res.*, **2010**.
- Rossi, A.C., Mammucari, C., Argentini, C., Reggiani, C. & Schiaffino, S. (2010) Two novel/ancient myosins in mammalian skeletal muscles: MYH14/7b and MYH15 are expressed in extraocular muscles and muscle spindles. *J.Physiol.*, **588**, 353-364.
- Ruch, R.J. & Trosko, J.E. (2001) Gap-junction communication in chemical carcinogenesis. *Drug Metab Rev.*, **33**, 117-124.
- Sato, I., Kawamoto, K., Nishikawa, Y., Tsuda, S., Yoshida, M., Yaegashi, K., Saito, N., Liu, W. & Jin, Y. (2009) Neurotoxicity of perfluorooctane sulfonate (PFOS) in rats and mice after single oral exposure. *J.Toxicol.Sci.*, **34**, 569-574.
- Seacat, A.M., Thomford, P.J., Hansen, K.J., Clemen, L.A., Eldridge, S.R., Elcombe, C.R. & Butenhoff, J.L. (2003) Sub-chronic dietary toxicity of potassium perfluorooctanesulfonate in rats. *Toxicology*, **183**, 117-131.
- Seacat, A.M., Thomford, P.J., Hansen, K.J., Olsen, G.W., Case, M.T. & Butenhoff, J.L. (2002) Subchronic toxicity studies on perfluorooctanesulfonate potassium salt in cynomolgus monkeys. *Toxicol.Sci.*, **68**, 249-264.
- Searle, S.R., Speed, F.M. & Milliken, G.A. (1980) Population Marginal Means in the Linear-Model - An Alternative to Least-Squares Means. *Am.Stat.*, **34**(4), 216-221.
- Schmittgen, T.D. & Livak, K.J. (2008) Analyzing real-time PCR data by the comparative C(T) method. *Nat.Protoc.*, **3**, 1101-1108.
- Shi, X., Du, Y., Lam, P.K., Wu, R.S. & Zhou, B. (2008) Developmental toxicity and alteration of gene expression in zebrafish embryos exposed to PFOS. *Toxicol.Appl.Pharmacol.*, **230**, 23-32.
- Shibata, T., Iio, K., Kawai, Y., Shibata, N., Kawaguchi, M., Toi, S., Kobayashi, M., Kobayashi, M., Yamamoto, K. & Uchida, K. (2006) Identification of a lipid peroxidation product as a potential trigger of the p53 pathway. *J.Biol.Chem.*, **281**(2), 1196-1204.
- Shiple, J.M., Hurst, C.H., Tanaka, S.S., DeRoos, F.L., Butenhoff, J.L., Seacat, A.M. & Waxman, D.J. (2004) trans-activation of PPARalpha and induction of PPARalpha target genes by perfluorooctane-based chemicals. *Toxicol.Sci.*, **80**, 151-160.

- Starkov,A.A. & Wallace,K.B. (2002) Structural determinants of fluorochemical-induced mitochondrial dysfunction. *Toxicol.Sci.*, **66**, 244-252.
- Szweras,M., Liu,D., Partridge,E.A., Pawling,J., Sukhu,B., Clokie,C., Jahnen-Dechent,W., Tenenbaum,H.C., Swallow,C.J., Grynopas,M.D. & Dennis,J.W. (2002) alpha 2-HS glycoprotein/fetuin, a transforming growth factor-beta/bone morphogenetic protein antagonist, regulates postnatal bone growth and remodeling. *J.Biol.Chem.*, **277**, 19991-19997.
- Taniyasu,S., Kannan,K., Horii,Y., Hanari,N. & Yamashita,N. (2003) A survey of perfluorooctane sulfonate and related perfluorinated organic compounds in water, fish, birds, and humans from Japan. *Environ.Sci.Technol.*, **37**, 2634-2639.
- Taniyasu,S., Kannan,K., So,M.K., Gulkowska,A., Sinclair,E., Okazawa,T. & Yamashita,N. (2005) Analysis of fluorotelomer alcohols, fluorotelomer acids, and short- and long-chain perfluorinated acids in water and biota. *J.Chromatogr.A*, **1093**, 89-97.
- Tao,L., Kannan,K., Kajiwara,N., Costa,M.M., Fillmann,G., Takahashi,S. & Tanabe,S. (2006) Perfluorooctanesulfonate and related fluorochemicals in albatrosses, elephant seals, penguins, and polar skuas from the Southern Ocean. *Environ.Sci.Technol.*, **40**, 7642-7648.
- Tars,K., Olin,B. & Mannervik, B. (2010) Structural basis for featuring of steroid isomerase activity in alpha class glutathione transferases. *J.Mol.Biol.*, **397**, 332-340.
- Thibodeaux,J.R., Hanson,R.G., Rogers,J.M., Grey,B.E., Barbee,B.D., Richards,J.H., Butenhoff,J.L., Stevenson,L.A. & Lau,C. (2003) Exposure to perfluorooctane sulfonate during pregnancy in rat and mouse. I: maternal and prenatal evaluations. *Toxicol.Sci.*, **74**, 369-381.
- Tomy,G.T., Budakowski,W., Halldorson,T., Helm,P.A., Stern,G.A., Friesen,K., Pepper,K., Tittlemier,S.A. & Fisk,A.T. (2004) Fluorinated organic compounds in an eastern Arctic marine food web. *Environ.Sci.Technol.*, **38**, 6475-6481.
- Trosko,J.E. & Ruch,R.J. (1998) Cell-cell communication in carcinogenesis. *Front Biosci.*, **3**, d208-d236.
- Ueno,T., Yasuura,S., Watanabe,S., Hirose,M., Sekine,T. & Namahisa,T. (1988) Immunocytochemical localization of myosin in rabbit liver cells. *J.Histochem.Cytochem.*, **36**, 803-806.
- United Nations Environment Programme (UNEP) (2009) Listing of perfluorooctane sulfonic acid, its salts and perfluorooctane sulfonyl fluoride.
<http://chm.pops.int/Portals/0/download.aspx?d=UNEP-POPS-COP.4-SC-4-17.English.pdf> accessed December 2010.

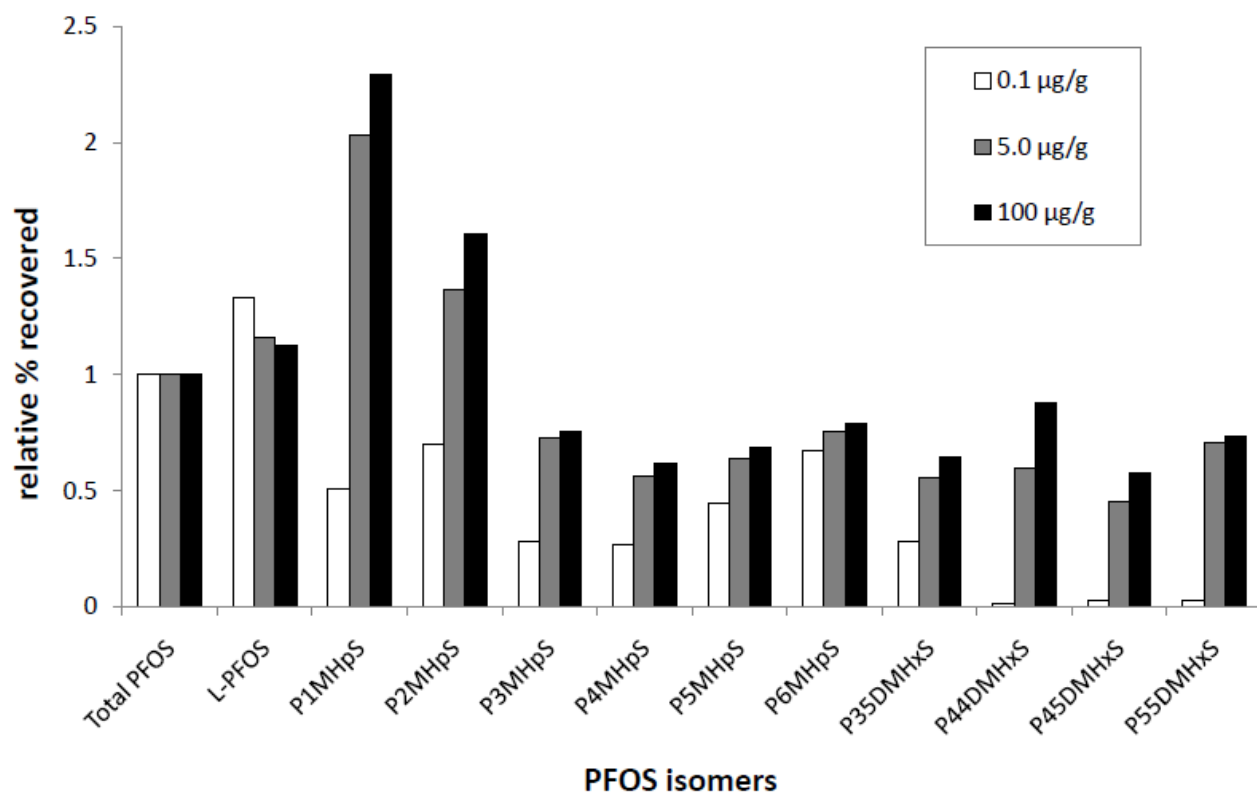
- United States Environmental Protection Agency (US EPA) (2002a) Co-operation on existing chemicals hazard assessment of perfluorooctane sulfonate (PFOS) and its salts. Document ID: EPA-HQ-OPPT-2005-0015-0016.
- United States Environmental Protection Agency (US EPA) (2002b) Revised draft hazard assessment of perfluorooctanoic acid (PFOA) and its salts. Document ID: EPA-HQ-OPPT-2002-0051-0030.
- Van de Vijver, K.I., Hoff, P., Das, K., Brasseur, S., Van Dongen, W., Esmans, E., Reijnders, P., Blust, R. & De Coen, W. (2005) Tissue distribution of perfluorinated chemicals in harbor seals (*Phoca vitulina*) from the Dutch Wadden Sea. *Environ.Sci.Technol.*, **39**, 6978-6984.
- Van de Vijver, K.I., Hoff, P.T., Van Dongen, W., Esmans, E.L., Blust, R. & De Coen, W.M. (2003) Exposure patterns of perfluorooctane sulfonate in aquatic invertebrates from the Western Scheldt estuary and the southern North Sea. *Environ.Toxicol.Chem.*, **22**, 2037-2041.
- van Tienen, F.H., Laeremans, H., van der Kallen, C.J. & Smeets, H.J. (2009) Wnt5b stimulates adipogenesis by activating PPAR γ , and inhibiting the beta-catenin dependent Wnt signaling pathway together with Wnt5a. *Biochem.Biophys.Res.Commun.*, **387**(1), 207-211.
- Vanden Heuvel, J.P., Thompson, J.T., Frame, S.R. & Gillies, P.J. (2006) Differential activation of nuclear receptors by perfluorinated fatty acid analogs and natural fatty acids: a comparison of human, mouse, and rat peroxisome proliferator-activated receptor- α , - β , and - γ , liver X receptor- β , and retinoid X receptor- α . *Toxicol.Sci.*, **92**, 476-489.
- Verreault, J., Berger, U. & Gabrielsen, G.W. (2007) Trends of perfluorinated alkyl substances in herring gull eggs from two coastal colonies in northern Norway: 1983-2003. *Environ.Sci.Technol.*, **41**, 6671-6677.
- Verreault, J., Houde, M., Gabrielsen, G.W., Berger, U., Haukas, M., Letcher, R.J. & Muir, D.C. (2005) Perfluorinated alkyl substances in plasma, liver, brain, and eggs of glaucous gulls (*Larus hyperboreus*) from the Norwegian arctic. *Environ.Sci.Technol.*, **39**, 7439-7445.
- Wang, F., Liu, W., Jin, Y., Dai, J., Yu, W., Liu, X. & Liu, L. (2010) Transcriptional effects of prenatal and neonatal exposure to PFOS in developing rat brain. *Environ.Sci.Technol.*, **44**, 1847-1853.
- Wang, Y., Yeung, L.W., Taniyasu, S., Yamashita, N., Lam, J.C. & Lam, P.K. (2008) Perfluorooctane sulfonate and other fluorochemicals in waterbird eggs from south China. *Environ.Sci.Technol.*, **42**, 8146-8151.
- Wolf, C.J., Takacs, M.L., Schmid, J.E., Lau, C. & Abbott, B.D. (2008) Activation of mouse and human peroxisome proliferator-activated receptor α by perfluoroalkyl acids of different functional groups and chain lengths. *Toxicol.Sci.*, **106**, 162-171.

- Wu,H., Kerr,M.K., Cui,X. & Churchill,G.A. (2003) MAANOVA: A Software Package for the Analysis of Spotted cDNA Microarray Experiments. In *The Analysis of Gene Expression Data: Methods and Software*. Springer-Verlag, pp. 313-431.
- Xu,L., Krenitsky,D.M., Seacat,A.M., Butenhoff,J.L. & Anders,M.W. (2004) Biotransformation of N-ethyl-N-(2-hydroxyethyl)perfluorooctanesulfonamide by rat liver microsomes, cytosol, and slices and by expressed rat and human cytochromes P450. *Chem.Res.Toxicol.*, **17**, 767-775.
- Yamashita,N., Kannan,K., Taniyasu,S., Horii,Y., Petrick,G. & Gamo,T. (2005) A global survey of perfluorinated acids in oceans. *Mar.Pollut.Bull.*, **51**, 658-668.
- Yanai,J., Dotan,S., Goz,R., Pinkas,A., Seidler,F.J., Slotkin,T.A. & Zimmerman,F. (2008) Exposure of developing chicks to perfluorooctanoic acid induces defects in prehatch and early posthatch development. *J.Toxicol.Environ.Health A*, **71**, 131-133.
- Yang,Q., Xie,Y., Alexson,S.E., Nelson,B.D. & DePierre,J.W. (2002a) Involvement of the peroxisome proliferator-activated receptor alpha in the immunomodulation caused by peroxisome proliferators in mice. *Biochem.Pharmacol.*, **63**, 1893-1900.
- Yang,Q., Xie,Y. & DePierre,J.W. (2000) Effects of peroxisome proliferators on the thymus and spleen of mice. *Clin.Exp.Immunol.*, **122**, 219-226.
- Yang,Y.H., Dudoit,S., Luu,P., Lin,D.M., Peng,V., Ngai,J. & Speed,T.P. (2002b) Normalization for cDNA microarray data: a robust composite method addressing single and multiple slide systematic variation. *Nucleic Acids Res.*, **30**(4), e15.
- Yeung,L.W., Guruge,K.S., Yamanaka,N., Miyazaki,S. & Lam,P.K. (2007) Differential expression of chicken hepatic genes responsive to PFOA and PFOS. *Toxicology*, **237**, 111-125.
- Yu,W.G., Liu,W. & Jin,Y.H. (2008) Effects of perfluorooctane sulfonate on rat thyroid hormone biosynthesis and metabolism. *Environ.Toxicol.Chem.*, **28**, 990-996.

APPENDIX

Supplementary Material

The following figures and tables contain data pertaining to Chapter 4



Supplementary Figure S4.1: Proportion of each perfluorooctane sulfonate (PFOS) isomer recovered in chicken embryo livers relative to the administered dose of technical grade PFOS (T-PFOS). Data are normalized to the % recovery of total PFOS concentrations for a given dose group.

The following figures and tables contain data pertaining to Chapter 5

Supplementary Table S5.1: List of genes examined for real-time RT-PCR and their gene symbols, accession numbers, and primer and probe sequences.

Gene Name	Symbol	Accession	Oligo	Sequence (5'-3')
Acyl-CoA synthetase long-chain family member 1	ACSL1	NM_001012578	fwd primer rev primer probe	TAAGAGGCTGGGCTATGCTG TGCTTAGAGGACCTGGCACT TCGTTTTCCCATGATGAATGTGGA
Acyl-CoA synthetase bubble gum family member 2	ACSL BG2	NM_001012846	fwd primer rev primer probe	CGCGTGTGTAACCTGTCTGT TCCCTGTCTCCACTCCAC AGGCAGGAGCACCCGGAGCT
Adipose differentiation-related protein	ADFP	NM_001031420	fwd primer rev primer probe	ACGAAGGTGAAGGGGAGAAA CTGCAGGGTACACACATGCT TCCAGCCAGGAAGACAAATAGCTTGA
Alcohol dehydrogenase 1C	ADH1C	X54612	fwd primer rev primer probe	CCCATGCTTATCTTCAGTGG AACTTTTCTTCATGTAATCAGCAAC CGCACCTGGAAAGGGTCCGT
alpha-2-HS-glycoprotein	AHSG	XM_422764.2	fwd primer rev primer probe	CCCTCACCCAGGTCAAGATA ATCATGCTGAGCAACCTCTG CCCAGCGCTGGACAAGGCTT
amphiregulin	AREG	NM_001031537	fwd primer rev primer probe	TATCTGCTTCAAAGAATTCATCTC CTACTGGGTTCAAGGACATAACC TGAATTGCAGGGTGTGGTGACA
β-actin	BA	X00182.1	fwd primer rev primer probe	AAATTGTGCGTGACATCAAGGA GAGGCAGCTGTGGCCATCT TGCTACGTCGCACTGGATTGGAGC
Cytochrome P450, family 4, subfamily B, polypeptide 1	CYP4A11	XM_422455	fwd primer rev primer probe	ATCCAAGCCTCTGTACCT AACGCTGGAGTGAGCAACTT TGGATTGGCAAAGGGTTGCTGG
Glutathione S-transferase alpha 3	GSTA3	NM_001001777	fwd primer rev primer probe	GGAAGAGTCGAAGCCTGATG GGGGATATTGCTTGTCTTTCG TGCAAAATTTCCCTCTTGCAGA
Histone deacetylase 1	HDAC1	NM_204156	fwd primer rev primer probe	TGAAAATCACCTGATGTGG CAAGTGCATAAAGATTCCATCC CGCTGTGCATCGCCCATAGG
3-hydroxy-3-methylglutaryl-CoA reductase	HMGCR	NM_204485	fwd primer rev primer probe	TAGGTCCTACATTTACCCTGGATG ATGATTTCAAGTGTGCGCACTCC CCAACGCCAATCACAAAGACATTCCACAAGT
Interleukin 1 receptor, type 1	IL1R1	NM_205485	fwd primer rev primer probe	CTCGGAAAGGTCACACTCAG GGGGAGAACCCTATCTTATG CCAGAAAAACCGGATCTTCATCAGGA
Sterol-C4-methyl oxidase-like	SC4MOL	NM_001006438	fwd primer rev primer probe	TTCCATCACATGAACTTTATTGG TTTCTTTATAGGCAATGAATTGAGAG CACGTGGTGGGACAGAATCTTTGG
Thrombospondin 1	THBS1	XM_421205	fwd primer rev primer probe	GCTGTTCTATAACACAGGACAAAAC CTGCATCTAACCAGGAAACAAA CAGCTTTGGGAGAACTGGGATTACAA
Ubiquitin carboxyl-terminal esterase L1	UCHL1	NM_001080212	fwd primer rev primer probe	CTGAAGAGAGAGCTAAGCGTTTT CAAAACAGGATGAAGTGGAAAGTT TGTCGGGTTGAGGACAACAGTGTG

Supplementary Table S5.2: Detailed list of genes that were differentially expressed following exposure to L-PFOS or T-PFOS

Legend:	FC > 1.5, p <0.05	FC > 1.3, p <0.01
	FC < -1.5, p <0.05	FC < -1.3, p <0.01

Probe ID	Gene ID	L-PFOS 10 uM		T-PFOS 10 uM		IPA
		FC	p-value	FC	p-value	
A_87_P009195	MYH15	3.34	0.000	3.42	0.000	mapped
A_87_P037650	LBFABP	1.51	0.027	2.91	0.000	
A_87_P016252	LOC419498	2.35	0.000	2.82	0.000	
A_87_P022766	EDN2	2.20	0.000	2.50	0.000	mapped
A_87_P005101	A_87_P005101	1.97	0.000	2.49	0.000	
A_87_P006127	A_87_P006127	2.00	0.000	2.38	0.000	
A_87_P035363	LOC417458	1.97	0.000	2.35	0.000	
A_87_P011824	CR523117	1.81	0.000	2.30	0.000	
A_87_P029108	BU358466	2.58	0.000	2.27	0.000	
A_87_P017222	CR385280	2.00	0.000	2.20	0.000	
A_87_P010960	CR524351	2.31	0.000	2.14	0.000	
A_87_P023505	BATF3	1.64	0.000	2.13	0.000	mapped
A_87_P014699	FKBP6	2.31	0.000	2.13	0.000	mapped
A_87_P016519	CR386379	1.51	0.007	2.12	0.000	
A_87_P032247	BU233875	1.74	0.000	2.09	0.000	
A_87_P008868	FABP7	2.01	0.000	2.09	0.000	mapped
A_87_P031283	ABCG2	1.94	0.000	2.09	0.000	mapped
A_87_P037767	FZD4	1.71	0.024	2.06	0.000	mapped
A_87_P023657	C21orf7	1.84	0.000	2.00	0.000	mapped
A_87_P035063	BMPER	1.67	0.000	2.00	0.000	mapped
A_87_P013596	CR391257	2.23	0.000	1.96	0.000	
A_87_P028015	BU401424	2.08	0.000	1.96	0.000	
A_87_P041822	A_87_P041822	1.54	0.000	1.95	0.000	
A_87_P035114	IGFBP1	1.69	0.000	1.94	0.000	mapped
A_87_P011716	CORO2A	1.59	0.000	1.93	0.000	mapped
A_87_P020282	LOC771401	1.57	0.000	1.93	0.000	
A_87_P026763	LOC427201	1.68	0.000	1.89	0.000	mapped
A_87_P008211	DR420410	2.31	0.000	1.88	0.000	
A_87_P018040	CR353283	1.56	0.007	1.87	0.000	
A_87_P013441	CR391462	1.64	0.000	1.87	0.000	
A_87_P004585	A_87_P004585	2.15	0.000	1.87	0.000	
A_87_P006556	A_87_P006556	1.73	0.000	1.82	0.000	
A_87_P020842	CN218805	1.63	0.007	1.81	0.000	
A_87_P037387	FMO6P	1.51	0.035	1.81	0.000	mapped
A_87_P023859	VIPR2	1.70	0.007	1.78	0.000	mapped
A_87_P022637	TPPP	1.63	0.000	1.74	0.000	mapped
A_87_P016670	XM_417488	2.04	0.000	1.74	0.000	mapped
A_87_P015937	ARHGEF4	1.99	0.000	1.73	0.000	mapped
A_87_P032648	BU223512	1.70	0.000	1.73	0.000	
A_87_P012140	LOC418543	2.16	0.000	1.71	0.000	
A_87_P014025	CR390630	1.74	0.000	1.70	0.006	
A_87_P003507	THBS1	1.81	0.000	1.70	0.008	mapped
A_87_P035058	WNT5B	1.64	0.000	1.69	0.000	mapped
A_87_P012121	CR407373	1.78	0.000	1.68	0.000	
A_87_P015426	PIWIL1	1.73	0.000	1.65	0.000	mapped
A_87_P007639	A_87_P007639	1.51	0.000	1.64	0.000	
A_87_P038686	A_87_P038686	1.87	0.000	1.64	0.000	
A_87_P011085	CR524168	1.56	0.000	1.63	0.000	
A_87_P035936	RCJMB04_35g11	1.53	0.007	1.62	0.003	mapped
A_87_P038173	PDGFB	1.65	0.000	1.61	0.003	mapped
A_87_P024549	XM_417636	1.57	0.000	1.61	0.003	mapped
A_87_P013727	XM_414038	1.50	0.000	1.60	0.000	
A_87_P012518	CR406806	1.90	0.000	1.60	0.018	
A_87_P018403	CR352731	1.82	0.000	1.59	0.000	
A_87_P014688	CR389639	1.62	0.000	1.59	0.000	
A_87_P015946	TPD52L1	1.73	0.000	1.58	0.000	mapped
A_87_P022338	XM_001231706	1.93	0.000	1.57	0.013	mapped
A_87_P030057	SCN5A	1.58	0.000	1.57	0.000	mapped
A_87_P022287	PITX2	1.54	0.000	1.57	0.000	mapped

Supplementary Table S5.2: Continued

Probe ID	Gene ID	L-PFOS 10 uM		T-PFOS 10 uM		IPA
		FC	p-value	FC	p-value	
A_87_P022287	PITX2	1.54	0.000	1.57	0.000	mapped
A_87_P031301	BU265263	1.65	0.000	1.52	0.000	
A_87_P030916	BU276723	1.53	0.000	1.51	0.003	
A_87_P031365	XM_416362	1.51	0.019	1.51	0.006	mapped
A_87_P035067	AREG	1.47	0.000	2.10	0.000	mapped
A_87_P028998	A_87_P028998	1.39	0.007	1.83	0.000	
A_87_P006234	A_87_P006234	1.43	0.000	1.82	0.000	
A_87_P003155	A_87_P003155	1.39	0.000	1.69	0.000	
A_87_P017037	LOC421780	1.45	0.000	1.69	0.000	
A_87_P038502	A_87_P038502	1.41	0.000	1.66	0.000	
A_87_P020929	CK609072	1.40	0.007	1.65	0.000	
A_87_P026087	A_87_P026087	1.46	0.000	1.62	0.000	
A_87_P021865	LYPD6B	1.36	0.000	1.56	0.000	mapped
A_87_P013726	CR391100	1.48	0.000	1.55	0.000	
A_87_P005339	LOC424943	1.40	0.007	1.55	0.000	
A_87_P023072	BX933356	1.39	0.000	1.52	0.000	
A_87_P007209	TC197254	1.29	0.264	2.43	0.000	
A_87_P037642	DIO2	1.59	0.168	2.22	0.000	mapped
A_87_P017804	RRM2	1.55	0.063	2.22	0.000	mapped
A_87_P039915	A_87_P039915	1.12	0.561	2.20	0.000	
A_87_P012714	F5	1.35	0.454	2.11	0.039	mapped
A_87_P015167	CR388880	1.59	0.289	2.11	0.049	
A_87_P024423	FGFBP1	1.45	0.091	2.08	0.000	mapped
A_87_P010802	XM_001231832	1.36	0.019	2.07	0.000	
A_87_P017914	CR353477	1.37	0.320	2.06	0.003	
A_87_P014242	CR390305	1.15	0.310	2.04	0.000	
A_87_P012110	XM_429189	1.49	0.173	2.03	0.003	mapped
A_87_P015174	CR388868	1.44	0.281	2.01	0.008	
A_87_P030763	BU282264	1.23	0.313	1.99	0.000	
A_87_P026278	BU456580	1.48	0.024	1.97	0.000	
A_87_P009311	PTGS2	1.51	0.099	1.96	0.000	mapped
A_87_P012941	XR_027067	1.40	0.027	1.95	0.000	
A_87_P035719	ADFP	1.29	0.310	1.93	0.000	mapped
A_87_P020691	CN228414	1.51	0.275	1.92	0.040	
A_87_P038083	HMGCR	1.24	0.268	1.89	0.000	mapped
A_87_P016888	CR385841	1.26	0.203	1.89	0.000	
A_87_P022818	ADM	1.26	0.218	1.88	0.000	mapped
A_87_P035980	TMEM164	1.32	0.283	1.87	0.000	mapped
A_87_P000757	A_87_P000757	1.51	0.134	1.86	0.003	
A_87_P017264	PKHD1	1.49	0.050	1.86	0.000	mapped
A_87_P040681	A_87_P040681	1.50	0.224	1.86	0.020	
A_87_P009715	DN929793	1.57	0.118	1.86	0.006	
A_87_P031940	A_87_P031940	-1.01	0.977	1.86	0.000	
A_87_P017419	CR354290	1.44	0.312	1.84	0.048	
A_87_P016497	CR386405	1.32	0.104	1.84	0.000	
A_87_P011662	XM_001233953	1.74	0.114	1.84	0.029	mapped
A_87_P009302	ALCAM	1.37	0.126	1.82	0.000	mapped
A_87_P010754	CR733330	1.49	0.089	1.82	0.000	
A_87_P031455	BU259892	1.29	0.149	1.82	0.000	
A_87_P016665	CR386166	1.39	0.221	1.82	0.006	
A_87_P009307	EPHA3	1.17	0.600	1.82	0.023	mapped
A_87_P021615	UCHL1	1.13	0.467	1.81	0.000	mapped
A_87_P010279	A_87_P010279	1.43	0.075	1.81	0.000	
A_87_P003351	A_87_P003351	1.24	0.335	1.80	0.000	
A_87_P017598	CR354013	1.39	0.134	1.80	0.000	
A_87_P030075	JMJD2B	1.46	0.245	1.80	0.027	mapped
A_87_P018002	CR353341	1.25	0.168	1.79	0.000	
A_87_P007581	SECISBP2L	1.26	0.363	1.78	0.008	mapped
A_87_P029917	KLF2	1.17	0.362	1.78	0.000	mapped
A_87_P003173	A_87_P003173	1.18	0.523	1.78	0.015	
A_87_P011870	CR523055	1.31	0.065	1.77	0.000	
A_87_P022627	BX934358	1.47	0.165	1.76	0.008	mapped
A_87_P018772	CR338881	1.29	0.290	1.75	0.003	
A_87_P012068	DOCK9	1.38	0.173	1.75	0.000	mapped
A_87_P018392	CR352752	1.33	0.254	1.75	0.008	mapped

Supplementary Table S5.2: Continued

Probe ID	Gene ID	L-PFOS 10 uM		T-PFOS 10 uM		IPA
		FC	p-value	FC	p-value	
A_87_P018392	CR352752	1.33	0.254	1.75	0.008	mapped
A_87_P015166	CADM1	1.12	0.589	1.75	0.003	mapped
A_87_P012497	CR406830	1.33	0.265	1.74	0.012	
A_87_P015275	CR388731	1.36	0.093	1.74	0.000	
A_87_P000820	A_87_P000820	1.46	0.246	1.74	0.042	
A_87_P038082	HMGCR	1.53	0.067	1.74	0.000	mapped
A_87_P038322	A_87_P038322	1.39	0.277	1.73	0.023	
A_87_P010183	ZNF618	1.32	0.301	1.73	0.019	mapped
A_87_P015333	CR388640	1.45	0.079	1.73	0.003	
A_87_P026077	BU461661	1.34	0.302	1.73	0.019	
A_87_P036699	RCJMB04_9i11	1.13	0.362	1.72	0.000	mapped
A_87_P017246	CR385249	1.22	0.465	1.72	0.027	
A_87_P009290	IL1R1	1.30	0.217	1.71	0.000	mapped
A_87_P036902	SC4MOL	1.33	0.163	1.71	0.000	mapped
A_87_P036994	PKD2	1.21	0.444	1.71	0.008	mapped
A_87_P035745	ACSL1	1.38	0.019	1.70	0.000	mapped
A_87_P024831	A_87_P024831	1.27	0.304	1.70	0.003	
A_87_P001885	A_87_P001885	1.68	0.059	1.70	0.023	
A_87_P002797	A_87_P002797	1.33	0.294	1.70	0.019	
A_87_P010381	CYP1B1	1.34	0.265	1.69	0.010	mapped
A_87_P034140	LOC771012	1.07	0.763	1.69	0.010	
A_87_P010982	CR524314	1.23	0.254	1.69	0.000	
A_87_P036122	LSS	1.20	0.200	1.69	0.000	mapped
A_87_P017944	CR353427	1.36	0.128	1.69	0.000	
A_87_P003299	A_87_P003299	1.39	0.038	1.68	0.000	
A_87_P027517	BU421242	1.21	0.387	1.68	0.003	
A_87_P020945	CK608429	1.22	0.351	1.68	0.003	
A_87_P039559	A_87_P039559	1.44	0.063	1.68	0.000	
A_87_P006399	A_87_P006399	1.12	0.459	1.68	0.000	
A_87_P021799	KCNK5	1.37	0.268	1.67	0.031	mapped
A_87_P021078	LGALS2	1.39	0.035	1.67	0.000	mapped
A_87_P023712	SPON2	1.27	0.224	1.66	0.000	mapped
A_87_P004772	A_87_P004772	1.41	0.264	1.66	0.044	
A_87_P018881	TRAF7	1.40	0.041	1.65	0.000	mapped
A_87_P014702	CR389617	1.04	0.861	1.64	0.013	
A_87_P012786	CR406423	1.60	0.097	1.64	0.023	
A_87_P028650	BU375675	1.33	0.038	1.63	0.000	
A_87_P011304	CR523886	1.34	0.031	1.63	0.000	
A_87_P035265	CDKN2A	1.30	0.148	1.63	0.000	mapped
A_87_P004766	A_87_P004766	1.31	0.274	1.63	0.013	
A_87_P007811	A_87_P007811	1.19	0.404	1.63	0.000	
A_87_P013217	XM_421361	1.19	0.283	1.63	0.000	
A_87_P018049	HHIP	1.28	0.337	1.63	0.033	mapped
A_87_P023046	BX933401	1.38	0.013	1.63	0.000	
A_87_P014457	CR389969	1.26	0.373	1.63	0.026	
A_87_P007306	LOC424917	-1.05	0.774	1.62	0.000	
A_87_P032817	BU219679	1.13	0.467	1.62	0.003	
A_87_P038105	HS6ST1	1.29	0.215	1.62	0.000	mapped
A_87_P016176	SIK1	1.34	0.119	1.62	0.000	mapped
A_87_P004034	A_87_P004034	1.11	0.548	1.62	0.000	
A_87_P030562	BU291135	1.01	0.957	1.62	0.000	
A_87_P007289	A_87_P007289	1.15	0.407	1.61	0.000	
A_87_P004209	A_87_P004209	1.29	0.238	1.61	0.008	
A_87_P008998	GFRA2	-1.05	0.819	1.61	0.003	mapped
A_87_P013884	CR390863	1.25	0.367	1.61	0.024	
A_87_P037753	GATM	1.56	0.109	1.61	0.045	mapped
A_87_P004634	A_87_P004634	1.31	0.238	1.61	0.012	
A_87_P034161	KRT20	1.36	0.098	1.60	0.000	mapped
A_87_P023871	BX931565	1.37	0.067	1.60	0.000	
A_87_P028545	LOC424918	1.28	0.182	1.60	0.000	
A_87_P010869	CR732796	1.22	0.418	1.60	0.037	
A_87_P024595	LOC415531	1.41	0.106	1.60	0.003	
A_87_P041067	A_87_P041067	1.06	0.777	1.60	0.003	
A_87_P032929	A_87_P032929	1.32	0.155	1.60	0.000	
A_87_P022671	HS3ST1	1.33	0.013	1.60	0.000	mapped

Supplementary Table S5.2: Continued

Probe ID	Gene ID	L-PFOS 10 uM		T-PFOS 10 uM		IPA
		FC	p-value	FC	p-value	
A_87_P022671	HS3ST1	1.33	0.013	1.60	0.000	mapped
A_87_P013392	CR391530	1.29	0.326	1.59	0.044	
A_87_P004183	CHKA	1.20	0.313	1.59	0.000	mapped
A_87_P034194	DR419712	1.48	0.084	1.59	0.012	
A_87_P003109	A_87_P003109	1.09	0.568	1.59	0.000	
A_87_P013582	CR391274	1.47	0.100	1.59	0.018	
A_87_P036801	AJ719870	1.44	0.089	1.59	0.006	mapped
A_87_P007739	A_87_P007739	1.15	0.460	1.59	0.000	
A_87_P003901	HDAC1	1.40	0.188	1.58	0.019	mapped
A_87_P004654	A_87_P004654	1.20	0.282	1.58	0.000	
A_87_P020397	CN602443	1.14	0.464	1.58	0.003	
A_87_P015765	CR387518	1.34	0.201	1.58	0.010	
A_87_P021057	SHC4	1.29	0.180	1.58	0.000	mapped
A_87_P003795	OTUD1	1.42	0.097	1.58	0.003	mapped
A_87_P018318	CR352859	1.31	0.160	1.58	0.003	
A_87_P021486	IDII	1.25	0.202	1.58	0.003	mapped
A_87_P015712	CR387588	1.26	0.224	1.58	0.000	
A_87_P016501	STARD4	1.20	0.321	1.57	0.000	mapped
A_87_P034287	A_87_P034287	1.14	0.440	1.57	0.000	
A_87_P006832	A_87_P006832	1.27	0.320	1.57	0.033	
A_87_P001579	BX263805	1.21	0.035	1.57	0.000	
A_87_P003003	A_87_P003003	-1.07	0.729	1.56	0.008	
A_87_P008885	X62642	1.21	0.378	1.56	0.022	
A_87_P018305	CR352877	1.44	0.031	1.56	0.000	
A_87_P019970	A_87_P019970	1.23	0.365	1.56	0.022	
A_87_P029522	BU334777	1.39	0.063	1.56	0.000	
A_87_P022027	STK11	1.35	0.222	1.56	0.024	mapped
A_87_P014673	CR389661	1.22	0.273	1.56	0.000	mapped
A_87_P017076	CCNG2	1.09	0.715	1.55	0.040	mapped
A_87_P000073	A_87_P000073	1.12	0.542	1.55	0.000	
A_87_P015411	SCHIP1	1.33	0.057	1.55	0.000	mapped
A_87_P003051	ATP10A	1.16	0.302	1.55	0.000	mapped
A_87_P027930	DOCK9	1.32	0.133	1.55	0.000	mapped
A_87_P031238	BU267436	1.38	0.079	1.55	0.003	mapped
A_87_P033449	BU201627	1.26	0.167	1.55	0.000	
A_87_P018723	AMOTL2	1.26	0.229	1.55	0.000	mapped
A_87_P024440	BX930091	1.09	0.548	1.55	0.003	
A_87_P028874	BU368763	-1.13	0.354	1.55	0.000	
A_87_P027148	BU432792	1.37	0.197	1.55	0.025	
A_87_P003194	A_87_P003194	1.33	0.104	1.54	0.000	
A_87_P017298	CR385178	1.24	0.353	1.54	0.034	
A_87_P003799	RBPMS	1.37	0.227	1.54	0.045	mapped
A_87_P023525	BX932377	1.25	0.358	1.54	0.044	
A_87_P033424	BU202671	1.24	0.318	1.54	0.019	
A_87_P013623	CR391228	1.36	0.148	1.54	0.010	
A_87_P031259	BU266711	1.31	0.141	1.54	0.000	
A_87_P001338	A_87_P001338	1.26	0.276	1.54	0.008	
A_87_P015711	CR387589	1.03	0.898	1.54	0.034	
A_87_P017405	CR354307	1.38	0.027	1.54	0.000	
A_87_P027023	BU434950	1.21	0.426	1.54	0.045	
A_87_P016506	CR386394	1.05	0.728	1.54	0.000	
A_87_P015077	CR389026	1.18	0.069	1.54	0.000	
A_87_P018365	CR352790	1.13	0.362	1.53	0.000	
A_87_P017672	CR353877	1.31	0.218	1.53	0.000	
A_87_P016344	XM_426585	1.18	0.378	1.53	0.008	mapped
A_87_P015170	CR388877	1.24	0.232	1.53	0.000	
A_87_P014915	CR389302	1.22	0.401	1.53	0.044	
A_87_P014644	CR389702	1.51	0.059	1.53	0.013	
A_87_P009540	CYR61	1.47	0.075	1.53	0.012	mapped
A_87_P033858	RASSF8	1.13	0.372	1.53	0.000	mapped
A_87_P031423	NR6A1	1.10	0.590	1.53	0.010	mapped
A_87_P011368	CR523791	1.13	0.476	1.53	0.003	
A_87_P002092	A_87_P002092	1.26	0.094	1.53	0.000	
A_87_P041871	A_87_P041871	1.22	0.382	1.52	0.039	
A_87_P036328	AJ720554	1.07	0.775	1.52	0.041	mapped

Supplementary Table S5.2: Continued

Probe ID	Gene ID	L-PFOS 10 uM		T-PFOS 10 uM		IPA
		FC	p-value	FC	p-value	
A_87_P036328	AJ720554	1.07	0.775	1.52	0.041	mapped
A_87_P031750	BU246369	1.35	0.103	1.52	0.003	
A_87_P006824	A_87_P006824	1.33	0.050	1.52	0.003	
A_87_P038197	KRT19	1.44	0.064	1.52	0.006	mapped
A_87_P007704	A_87_P007704	1.13	0.352	1.52	0.000	
A_87_P035229	BMP2	1.34	0.192	1.52	0.019	mapped
A_87_P040015	A_87_P040015	1.18	0.430	1.52	0.038	
A_87_P014706	CR389611	1.32	0.086	1.52	0.000	
A_87_P017899	SLC9A3R1	1.20	0.326	1.52	0.008	mapped
A_87_P017543	IGF2BP3	1.42	0.146	1.51	0.035	mapped
A_87_P016194	CR386872	1.18	0.310	1.51	0.000	
A_87_P022383	CYP8B	1.08	0.597	1.51	0.000	mapped
A_87_P012255	XM_426415	1.11	0.468	1.51	0.000	mapped
A_87_P025276	A_87_P025276	1.43	0.013	1.51	0.000	
A_87_P001747	A_87_P001747	1.45	0.050	1.51	0.008	
A_87_P017416	CR354293	1.06	0.735	1.51	0.000	
A_87_P038119	TLE4	1.13	0.399	1.51	0.000	mapped
A_87_P036388	ASB9	1.36	0.035	1.51	0.000	mapped
A_87_P017660	CR353908	1.13	0.551	1.51	0.020	
A_87_P027231	BU427398	1.48	0.024	1.51	0.003	
A_87_P040893	A_87_P040893	1.29	0.211	1.51	0.013	
A_87_P015417	CR388515	1.14	0.452	1.51	0.008	
A_87_P024286	RASD1	-1.03	0.888	1.51	0.008	mapped
A_87_P004174	A_87_P004174	1.25	0.218	1.50	0.003	
A_87_P003427	A_87_P003427	1.37	0.167	1.50	0.023	
A_87_P007435	A_87_P007435	1.32	0.115	1.50	0.000	
A_87_P007474	A_87_P007474	1.23	0.298	1.50	0.020	
A_87_P027990	A_87_P027990	1.23	0.293	1.50	0.012	
A_87_P016481	CR386428	1.95	0.000	-1.05	0.817	
A_87_P035611	RCJMB04_17j13	1.89	0.000	1.25	0.312	mapped
A_87_P009114	INHBA	1.84	0.000	1.30	0.064	mapped
A_87_P027893	BU409872	1.84	0.007	1.25	0.312	
A_87_P024379	MUSTN1	1.81	0.000	1.11	0.421	mapped
A_87_P009498	IAPP	1.79	0.041	1.23	0.394	mapped
A_87_P009031	XM_417864	1.79	0.041	1.10	0.680	mapped
A_87_P000137	A_87_P000137	1.79	0.007	1.12	0.523	
A_87_P023801	CTorf187	1.74	0.000	1.17	0.277	mapped
A_87_P030140	BU307787	1.73	0.000	1.43	0.015	
A_87_P037238	CRHR2	1.70	0.000	1.45	0.034	mapped
A_87_P017167	FAM62B	1.67	0.000	1.09	0.587	mapped
A_87_P007613	ENPEP	1.67	0.013	1.20	0.361	mapped
A_87_P005173	A_87_P005173	1.67	0.000	1.36	0.085	
A_87_P010924	XM_417096	1.66	0.019	1.42	0.073	
A_87_P004165	A_87_P004165	1.64	0.000	1.49	0.006	
A_87_P013118	CR405912	1.64	0.027	1.16	0.425	
A_87_P021402	A_87_P021402	1.64	0.031	1.22	0.305	
A_87_P010677	A_87_P010677	1.63	0.000	1.24	0.207	
A_87_P012952	LYN	1.62	0.024	1.17	0.387	mapped
A_87_P024395	C13orf15	1.62	0.007	1.09	0.583	mapped
A_87_P014902	CR389319	1.62	0.047	1.31	0.210	
A_87_P008280	XM_418466	1.61	0.027	1.41	0.089	mapped
A_87_P035040	LGALS8	1.58	0.007	1.21	0.270	mapped
A_87_P009020	XM_421205	1.58	0.027	1.27	0.210	mapped
A_87_P022668	LOC770996	1.58	0.013	1.37	0.076	mapped
A_87_P016861	CR385871	1.58	0.007	1.47	0.024	
A_87_P038091	SNTB1	1.57	0.041	1.42	0.078	mapped
A_87_P034251	UROCI	1.56	0.000	1.38	0.000	mapped
A_87_P009462	IRF8	1.56	0.013	1.37	0.068	mapped
A_87_P022896	CAPSL	1.56	0.007	1.46	0.000	mapped
A_87_P009134	U17000	1.55	0.038	1.30	0.146	mapped
A_87_P026412	BU236694	1.55	0.000	1.30	0.022	
A_87_P024671	HKDC1	1.54	0.007	1.25	0.168	mapped
A_87_P034789	A_87_P034789	1.54	0.027	1.32	0.135	
A_87_P003793	A_87_P003793	1.53	0.035	1.26	0.216	
A_87_P003107	A_87_P003107	1.52	0.000	1.16	0.286	

Supplementary Table S5.2: Continued

Probe ID	Gene ID	L-PFOS 10 uM		T-PFOS 10 uM		IPA
		FC	p-value	FC	p-value	
A_87_P003107	A_87_P003107	1.52	0.000	1.16	0.286	
A_87_P009676	TNFAIP6	1.52	0.041	-1.01	0.945	mapped
A_87_P011521	XM_419602	1.52	0.000	1.19	0.240	mapped
A_87_P002695	A_87_P002695	1.51	0.000	1.25	0.098	
A_87_P000545	DR419173	1.50	0.000	1.18	0.259	
A_87_P022225	TTR	1.50	0.050	1.38	0.055	mapped
A_87_P009500	GSTA3	-4.04	0.000	-3.79	0.000	mapped
A_87_P003938	LOC769608	-2.29	0.000	-2.38	0.000	
A_87_P035104	GAL9	-1.75	0.000	-2.23	0.000	
A_87_P022374	XM_001232960	-2.08	0.000	-2.09	0.000	
A_87_P011731	CA4	-1.76	0.000	-2.04	0.000	mapped
A_87_P018183	CR353076	-1.64	0.013	-2.02	0.000	mapped
A_87_P016647	HSD3B7	-2.04	0.000	-1.98	0.000	mapped
A_87_P037870	GSTA4	-2.03	0.000	-1.96	0.000	mapped
A_87_P017727	CDO1	-1.65	0.035	-1.92	0.000	mapped
A_87_P008721	APOA4	-2.03	0.000	-1.87	0.000	mapped
A_87_P030224	BX266010	-1.74	0.000	-1.83	0.000	
A_87_P023998	METTL7A	-1.98	0.000	-1.80	0.000	mapped
A_87_P024917	BX273422	-1.56	0.000	-1.75	0.000	
A_87_P018648	CR352354	-1.92	0.000	-1.72	0.013	
A_87_P030375	BU298479	-1.80	0.000	-1.70	0.000	
A_87_P022462	XM_427511	-1.60	0.000	-1.68	0.000	
A_87_P035579	RCJMB04_23a5	-1.99	0.000	-1.66	0.000	
A_87_P015638	CR387689	-1.62	0.000	-1.64	0.000	
A_87_P022548	FTH1	-1.62	0.019	-1.62	0.010	mapped
A_87_P017067	CLEC3B	-1.60	0.000	-1.59	0.000	mapped
A_87_P015138	FTH1	-1.54	0.013	-1.52	0.022	mapped
A_87_P013618	LL	-1.78	0.000	-1.50	0.000	
A_87_P037769	MMP9	-1.45	0.000	-1.75	0.000	mapped
A_87_P031687	CYP4B1	-1.36	0.000	-1.60	0.000	mapped
A_87_P002295	A_87_P002295	-1.49	0.000	-1.58	0.000	
A_87_P022419	BX934784	-1.39	0.000	-1.51	0.000	
A_87_P034235	BU122133	-1.41	0.000	-1.51	0.000	
A_87_P034122	AHSG	-1.28	0.258	-1.87	0.000	mapped
A_87_P008735	MGP	-1.59	0.064	-1.86	0.000	mapped
A_87_P015747	HPS5	-1.48	0.072	-1.84	0.000	mapped
A_87_P019426	A_87_P019426	-1.33	0.268	-1.79	0.003	
A_87_P036128	NMRAL1	-1.24	0.372	-1.79	0.003	mapped
A_87_P020473	CN236254	-1.34	0.144	-1.74	0.000	
A_87_P000465	A_87_P000465	-1.43	0.147	-1.73	0.006	
A_87_P031792	BU244314	-1.34	0.142	-1.72	0.000	
A_87_P006143	A_87_P006143	-1.31	0.100	-1.68	0.000	
A_87_P028117	A_87_P028117	-1.47	0.080	-1.68	0.003	
A_87_P035232	IGFBP4	-1.36	0.134	-1.68	0.000	mapped
A_87_P022033	XM_416402	-1.42	0.075	-1.66	0.000	mapped
A_87_P022242	XM_001232828	-1.45	0.013	-1.63	0.000	mapped
A_87_P036825	NEURL	-1.12	0.397	-1.62	0.000	mapped
A_87_P022786	FETUB	-1.46	0.061	-1.61	0.010	mapped
A_87_P024364	KCTD12	-1.21	0.210	-1.60	0.000	mapped
A_87_P008897	ALB	-1.40	0.024	-1.60	0.000	mapped
A_87_P038159	IL1RL1	-1.29	0.180	-1.59	0.003	mapped
A_87_P037459	AKR1B10	-1.54	0.088	-1.59	0.024	mapped
A_87_P030900	A_87_P030900	-1.42	0.044	-1.58	0.000	
A_87_P022312	SERPINF1	-1.09	0.510	-1.55	0.000	mapped
A_87_P029081	A_87_P029081	-1.11	0.538	-1.55	0.000	
A_87_P023211	SERPINA10	1.08	0.761	-1.55	0.040	mapped
A_87_P027779	BU413402	-1.40	0.114	-1.55	0.010	
A_87_P009319	MDK	-1.14	0.432	-1.54	0.003	mapped
A_87_P022622	GSTO1	-1.38	0.153	-1.53	0.022	mapped
A_87_P010672	A_87_P010672	-1.19	0.221	-1.53	0.000	
A_87_P021162	A_87_P021162	-1.32	0.080	-1.52	0.000	
A_87_P022703	SQSTM1	-1.24	0.346	-1.52	0.044	mapped
A_87_P003418	A_87_P003418	-1.50	0.027	-1.52	0.010	
A_87_P028131	TLCD1	-1.22	0.399	-1.51	0.047	mapped
A_87_P021767	GJB1	-1.27	0.222	-1.51	0.006	mapped

Supplementary Table S5.2: Continued

Probe ID	Gene ID	L-PFOS 10 uM		T-PFOS 10 uM		IPA
		FC	p-value	FC	p-value	
A_87_P021767	GJB1	-1.27	0.222	-1.51	0.006	mapped
A_87_P009087	CTSK	-1.40	0.109	-1.51	0.020	mapped
A_87_P019836	DPT	-1.24	0.110	-1.51	0.000	mapped
A_87_P024251	ACAT1	-1.12	0.601	-1.50	0.047	mapped
A_87_P010485	CV859129	-1.72	0.000	-1.31	0.133	
A_87_P031965	HMGCS2	-1.65	0.024	-1.42	0.052	mapped
A_87_P016902	XM_413811	-1.57	0.007	-1.04	0.787	mapped
A_87_P025005	REG4	-1.54	0.019	-1.28	0.141	mapped

Supplementary Table S5.3: Comparison of real-time RT-PCR results for changes in mRNA transcription in cultured chicken embryonic hepatocytes for genes determined by microarray analysis to be significantly affected by exposure to L-PFOS or T-PFOS (10 μ M each, N=2-4, MA FC=microarray fold change, RT-PCR FC=real-time RT-PCR fold change, bold and underlined values are FC>1.5, p<0.05)

Gene	Treatment	MicroArray FC	RT-PCR FC
ACSBG2	L-PFOS	1.13	1.31
	T-PFOS	<u>1.72</u>	<u>2.49</u>
ACSL1	L-PFOS	1.38	0.52
	T-PFOS	<u>1.70</u>	<u>7.36</u>
AREG	L-PFOS	1.47	0.89
	T-PFOS	<u>2.10</u>	<u>1.43</u>
GSTA3	L-PFOS	<u>0.49</u>	<u>0.09</u>
	T-PFOS	<u>0.51</u>	<u>0.13</u>
ADFP	L-PFOS	1.29	1.32
	T-PFOS	<u>1.93</u>	1.40
HMGCR	L-PFOS	1.24	1.44
	T-PFOS	<u>1.89</u>	2.53
IL1R1	L-PFOS	1.30	1.39
	T-PFOS	<u>1.71</u>	2.49
AHSG	L-PFOS	0.78	<u>0.58</u>
	T-PFOS	<u>0.53</u>	0.53
CYP4B1	L-PFOS	0.74	0.18
	T-PFOS	<u>0.63</u>	0.26
ADH1C	L-PFOS	<u>0.61</u>	<u>0.30</u>
	T-PFOS	<u>0.50</u>	0.71
THBS	L-PFOS	<u>1.81</u>	4.11
	T-PFOS	<u>1.70</u>	2.53
SC4MOL	L-PFOS	1.33	1.79
	T-PFOS	<u>1.71</u>	1.69
HDAC1	L-PFOS	1.40	0.97
	T-PFOS	<u>1.58</u>	0.51
UCHL1	L-PFOS	1.13	0.58
	T-PFOS	<u>1.81</u>	<u>0.44</u>

Supplementary Table S5.4A: Detailed list of functional enrichment categories, function and their genes, for genes differentially expressed following exposure to L-PFOS 10 μ M

Rank	Category	Sub-Category	Function	Function Annotation	p-value	# genes	genes
1	Lipid Metabolism	-	metabolism	metabolism of retinol	2.75E-03	2	ADH1C, DHRS3
1	Lipid Metabolism	-	metabolism	metabolism of terpenoid	5.01E-03	4	ADH1C, APOA4, DHRS3, HSD3B7
1	Lipid Metabolism	-	metabolism	metabolism of lipid	4.93E-02	5	ADH1C, APOA4, DHRS3, EDN2, HSD3B7
1	Lipid Metabolism	-	excretion	excretion of beta-estradiol	4.68E-03	1	ABCG2
1	Lipid Metabolism	-	synthesis	synthesis of retinaldehyde	4.68E-03	1	ADH1C
1	Lipid Metabolism	-	synthesis	synthesis of retinoic acid	1.86E-02	1	ADH1C
1	Lipid Metabolism	-	synthesis	synthesis of lipid	3.63E-02	4	ADH1C, APOA4, EDN2, HSD3B7
1	Lipid Metabolism	-	quantity	quantity of lipid	8.79E-03	6	ABCG2, APOA4, ENPP2, GULO, LGALS8, TTR
1	Lipid Metabolism	-	quantity	quantity of retinol	2.32E-02	1	TTR
1	Lipid Metabolism	-	accumulation	accumulation of all-trans-retinyl esters	9.33E-03	1	DHRS3
1	Lipid Metabolism	-	accumulation	accumulation of progesterone	1.86E-02	1	EDN2
1	Lipid Metabolism	-	biosynthesis	biosynthesis of ketone body	9.33E-03	1	HMGCS2
1	Lipid Metabolism	-	biosynthesis	biosynthesis of fatty acid	2.42E-02	2	APOA4, EDN2
1	Lipid Metabolism	-	biosynthesis	biosynthesis of bile acid	4.13E-02	1	HSD3B7
1	Lipid Metabolism	-	biosynthesis	biosynthesis of lipid	4.39E-02	3	APOA4, EDN2, HSD3B7
1	Lipid Metabolism	-	clearance	clearance of vitamin A	9.33E-03	1	ADH1C
1	Lipid Metabolism	-	concentration	concentration of retinaldehyde	9.33E-03	1	ADH1C
1	Lipid Metabolism	-	concentration	concentration of retinoic acid	9.33E-03	1	ADH1C
1	Lipid Metabolism	-	conversion	conversion of phosphatidylserine	9.33E-03	1	ENPP2
1	Lipid Metabolism	-	conversion	conversion of choline-phospholipid	1.40E-02	1	ENPP2
1	Lipid Metabolism	-	conversion	conversion of lysophosphatidic acid	1.40E-02	1	ENPP2
1	Lipid Metabolism	-	conversion	conversion of phosphatidylethanolamine	1.40E-02	1	ENPP2
1	Lipid Metabolism	-	reduction	reduction of monohydroperoxy-linoleic acid	9.33E-03	1	GSTA4
1	Lipid Metabolism	-	toxicity	toxicity of retinol	9.33E-03	1	ADH1C
1	Lipid Metabolism	-	modification	modification of polyunsaturated fatty acids	1.27E-02	2	ADH1C, GSTA4
1	Lipid Metabolism	-	modification	modification of 20-hydroxyeicosatetraenoic acid	1.86E-02	1	ADH1C
1	Lipid Metabolism	-	production	production of lysophosphatidic acid	1.40E-02	1	ENPP2
1	Lipid Metabolism	-	production	production of retinoic acid	1.40E-02	1	ADH1C
1	Lipid Metabolism	-	production	production of lipid	3.26E-02	3	ADH1C, EDN2, ENPP2

Supplementary Table S5.4A: Continued

Rank	Category	Sub-Category	Function	Function Annotation	p-value	# genes	genes
1	Lipid Metabolism	-	transport	transport of cerivastatin	1.86E-02	1	ABCG2
1	Lipid Metabolism	-	oxidation	oxidation of eicosanoid	3.23E-02	1	ADH1C
2	Cellular Growth and Proliferation	Cellular Growth and Proliferation	stimulation	stimulation of fibroblast cell lines	3.68E-02	1	EDN2
2	Cellular Growth and Proliferation	Cell Death	necrosis	necrosis of liver	5.47E-03	2	IGFBP1, IRF8
2	Cellular Growth and Proliferation	Cell Death	necrosis	necrosis of hepatocytes	3.23E-02	1	IGFBP1
3	Cancer	-	adenocarcinoma	adenocarcinoma	7.86E-03	5	ADH1C, C13ORF15, ENPEP, FTH1, TTR
3	Cancer	-	metastasis	metastasis of fibroblast cell lines	9.33E-03	1	ENPP2
4	Hepatic System Disease	-	intrahepatic cholestasis	intrahepatic cholestasis	2.28E-03	3	ABCG2, ADH1C, HSD3B7
4	Hepatic System Disease	-	progressive familial intrahepatic cholestasis type 1	progressive familial intrahepatic cholestasis type 1	2.25E-02	2	ABCG2, ADH1C
5	Cellular Movement	-	mobility	mobility of fibroblast cell lines	2.32E-02	1	ENPP2
5	Cellular Movement	-	migration	migration of tumor cell lines	2.82E-02	4	ARHGEF4, EDN2, ENPP2, IGFBP1
6	DNA Replication, Recombination, and Repair	-	conversion	conversion of DNA	4.68E-03	1	FTH1
6	DNA Replication, Recombination, and Repair	-	nicking	nicking of DNA	4.13E-02	1	FTH1
7	Cellular Development	Cellular Development	maturation	maturation of progenitor cells	9.33E-03	1	IRF8
7	Cellular Development	Cellular Development	transdifferentiation	transdifferentiation of tissue	4.68E-03	1	VNN1
7	Cellular Development	Cellular Development	epithelial-mesenchymal transition	epithelial-mesenchymal transition of liver cell lines	1.40E-02	1	FTH1
8	Carbohydrate Metabolism	-	conversion	conversion of phosphatidylserine	9.33E-03	1	ENPP2
8	Carbohydrate Metabolism	-	conversion	conversion of choline-phospholipid	1.40E-02	1	ENPP2
8	Carbohydrate Metabolism	-	conversion	conversion of lysophosphatidic acid	1.40E-02	1	ENPP2
8	Carbohydrate Metabolism	-	conversion	conversion of phosphatidylethanolamine	1.40E-02	1	ENPP2
8	Carbohydrate Metabolism	-	biosynthesis	biosynthesis of ascorbic acid	1.40E-02	1	GULO
8	Carbohydrate Metabolism	-	modulation	modulation of D-glucose	1.40E-02	1	IGFBP1

Supplementary Table S5.4A: Continued

Rank	Category	Sub-Category	Function	Function Annotation	p-value	# genes	genes
8	Carbohydrate Metabolism	-	production	production of lysophosphatidic acid	1.40E-02	1	ENPP2
8	Carbohydrate Metabolism	-	sequestration	sequestration of doxorubicin	1.40E-02	1	ABCG2
8	Carbohydrate Metabolism	-	signaling	signaling of inositol phosphate	1.40E-02	1	EDN2
8	Carbohydrate Metabolism	-	quantity	quantity of carbohydrate	1.49E-02	4	ENPP2, GULO, IGFBP1, LGALS8
8	Carbohydrate Metabolism	-	quantity	quantity of ascorbic acid	2.77E-02	1	GULO
9	Drug Metabolism	-	conjugation	conjugation of glutathione	3.44E-03	2	GSTA3, GSTA4
9	Drug Metabolism	-	accumulation	accumulation of topotecan	4.68E-03	1	ABCG2
9	Drug Metabolism	-	accumulation	accumulation of mitoxantrone	9.33E-03	1	ABCG2
9	Drug Metabolism	-	accumulation	accumulation of progesterone	1.86E-02	1	EDN2
9	Drug Metabolism	-	efflux	efflux of mitoxantrone	4.68E-03	1	ABCG2
9	Drug Metabolism	-	efflux	efflux of thyroxine	1.86E-02	1	TTR
9	Drug Metabolism	-	excretion	excretion of beta-estradiol	4.68E-03	1	ABCG2
9	Drug Metabolism	-	excretion	excretion of mitoxantrone	4.68E-03	1	ABCG2
9	Drug Metabolism	-	transport	transport of cladribine	4.68E-03	1	ABCG2
9	Drug Metabolism	-	transport	transport of mitoxantrone	4.68E-03	1	ABCG2
9	Drug Metabolism	-	transport	transport of pantoprazole	4.68E-03	1	ABCG2
9	Drug Metabolism	-	transport	transport of cimetidine	9.33E-03	1	ABCG2
9	Drug Metabolism	-	transport	transport of topotecan	1.40E-02	1	ABCG2
9	Drug Metabolism	-	transport	transport of cerivastatin	1.86E-02	1	ABCG2
9	Drug Metabolism	-	transport	transport of methotrexate	2.77E-02	1	ABCG2
9	Drug Metabolism	-	turnover	turnover of folic acid	4.68E-03	1	FTH1
9	Drug Metabolism	-	uptake	uptake of topotecan	4.68E-03	1	ABCG2
9	Drug Metabolism	-	clearance	clearance of methotrexate	9.33E-03	1	ABCG2
9	Drug Metabolism	-	concentration	concentration of retinoic acid	9.33E-03	1	ADH1C
9	Drug Metabolism	-	production	production of retinoic acid	1.40E-02	1	ADH1C
9	Drug Metabolism	-	sequestration	sequestration of doxorubicin	1.40E-02	1	ABCG2
9	Drug Metabolism	-	synthesis	synthesis of retinoic acid	1.86E-02	1	ADH1C
9	Drug Metabolism	-	quantity	quantity of folic acid	2.77E-02	1	FTH1
10	Cell-To-Cell Signaling and Interaction	-	contact growth inhibition	contact growth inhibition of embryonic cell lines	4.68E-03	1	ABCG2

Supplementary Table S5.4A: Continued

Rank	Category	Sub-Category	Function	Function Annotation	p-value	# genes	genes
10	Cell-To-Cell Signaling and Interaction	-	adhesion	adhesion of hepatoma cell lines	2.32E-02	1	LGALS8
10	Cell-To-Cell Signaling and Interaction	-	stimulation	stimulation of fibroblast cell lines	3.68E-02	1	EDN2
11	Cellular Organization and Maintenance	Cellular Function and Maintenance	contact growth inhibition	contact growth inhibition of embryonic cell lines	4.68E-03	1	ABCG2
12	Endocrine System Development and Function	-	excretion	excretion of beta-estradiol	4.68E-03	1	ABCG2
12	Endocrine System Development and Function	-	accumulation	accumulation of progesterone	1.86E-02	1	EDN2
12	Endocrine System Development and Function	-	metabolism	metabolism of thyroid hormone	2.32E-02	1	TTR
13	Amino Acid Metabolism	-	release	release of neutral amino acid	4.68E-03	1	ENPEP
13	Amino Acid Metabolism	-	release	release of L-aspartic acid	9.33E-03	1	ENPEP
13	Amino Acid Metabolism	-	release	release of basic amino acid	1.40E-02	1	ENPEP
13	Amino Acid Metabolism	-	release	release of sulfur amino acid	1.86E-02	1	ENPEP
13	Amino Acid Metabolism	-	release	release of essential amino acids	2.32E-02	1	ENPEP
13	Amino Acid Metabolism	-	turnover	turnover of folic acid	4.68E-03	1	FTH1
13	Amino Acid Metabolism	-	biosynthesis	biosynthesis of taurine	9.33E-03	1	CDO1
13	Amino Acid Metabolism	-	biosynthesis	biosynthesis of sulfur amino acid	4.13E-02	1	CDO1
13	Amino Acid Metabolism	-	clearance	clearance of methotrexate	9.33E-03	1	ABCG2
13	Amino Acid Metabolism	-	catabolism	catabolism of L-cysteine	1.40E-02	1	CDO1
13	Amino Acid Metabolism	-	efflux	efflux of L-triiodothyronine	1.86E-02	1	TTR
13	Amino Acid Metabolism	-	efflux	efflux of thyroxine	1.86E-02	1	TTR
13	Amino Acid Metabolism	-	metabolism	metabolism of taurine	1.86E-02	1	CDO1
13	Amino Acid Metabolism	-	quantity	quantity of folic acid	2.77E-02	1	FTH1
13	Amino Acid Metabolism	-	quantity	quantity of L-triiodothyronine	4.58E-02	1	TTR

Supplementary Table S5.4A: Continued

Rank	Category	Sub-Category	Function	Function Annotation	p-value	# genes	genes
13	Amino Acid Metabolism	-	transport	transport of methotrexate	2.77E-02	1	ABCG2
13	Amino Acid Metabolism	-	cleavage	cleavage of amino acids	3.23E-02	1	ENPEP
14	Nucleic Acid Metabolism	-	clearance	clearance of imatinib	4.68E-03	1	ABCG2
14	Nucleic Acid Metabolism	-	penetration	penetration of imatinib	4.68E-03	1	ABCG2
14	Nucleic Acid Metabolism	-	transport	transport of cladribine	4.68E-03	1	ABCG2
14	Nucleic Acid Metabolism	-	transport	transport of imatinib	4.68E-03	1	ABCG2
14	Nucleic Acid Metabolism	-	trapping	trapping of ATP	4.68E-03	1	ABCG2
14	Nucleic Acid Metabolism	-	separation	separation of nucleotide	9.33E-03	1	APOA4
15	Gene Expression	-	activation	activation of HAF1/HAF1a binding site	1.40E-02	1	IRF8

Supplementary Table S5.4B: Detailed list of functional enrichment categories, function and their genes, for genes differentially expressed following exposure to T-PFOS 10 μ M

Rank	Category	Sub-Category	Function	Function Annotation	p-value	# genes	genes
1	Lipid Metabolism	-	synthesis	synthesis of lipid	9.88E-07	14	ACAT1, ACSL1, ADH1C, APOA4, CHKA, CYP4A11, CYP8B1, EDN2, FGF2, HMGCR, HSD3B7, IDI1, LSS, PTGS2
1	Lipid Metabolism	-	synthesis	synthesis of terpenoid	1.12E-05	8	ACAT1, ADH1C, CYP8B1, FGF2, HMGCR, HSD3B7, IDI1, LSS
1	Lipid Metabolism	-	synthesis	synthesis of steroid	4.94E-05	7	ACAT1, CYP8B1, FGF2, HMGCR, HSD3B7, IDI1, LSS
1	Lipid Metabolism	-	synthesis	synthesis of sterol	3.05E-04	5	ACAT1, CYP8B1, HMGCR, IDI1, LSS
1	Lipid Metabolism	-	synthesis	synthesis of cholesterol	1.27E-03	4	CYP8B1, HMGCR, IDI1, LSS
1	Lipid Metabolism	-	synthesis	synthesis of fatty acid	5.12E-03	5	ACSL1, APOA4, CYP4A11, EDN2, PTGS2
1	Lipid Metabolism	-	metabolism	metabolism of lipid	1.28E-05	16	ACSL1, ADH1C, AKR1B10, APOA4, CHKA, CYP1B1, CYP4A11, DHRS3, EDN2, FGF2, HMGCR, HSD3B7, IDI1, LSS, PTGS2, SC4MOL
1	Lipid Metabolism	-	metabolism	metabolism of terpenoid	3.33E-05	9	ADH1C, AKR1B10, APOA4, CYP1B1, DHRS3, HMGCR, HSD3B7, IDI1, LSS
1	Lipid Metabolism	-	metabolism	metabolism of steroid	3.90E-04	7	AKR1B10, APOA4, CYP1B1, HMGCR, HSD3B7, IDI1, LSS
1	Lipid Metabolism	-	metabolism	metabolism of retinol	7.58E-04	3	ADH1C, CYP1B1, DHRS3
1	Lipid Metabolism	-	metabolism	metabolism of fatty acid	9.88E-04	7	ACSL1, APOA4, CYP1B1, CYP4A11, EDN2, PTGS2, SC4MOL
1	Lipid Metabolism	-	metabolism	metabolism of eicosanoid	1.27E-03	4	CYP1B1, CYP4A11, EDN2, PTGS2
1	Lipid Metabolism	-	metabolism	metabolism of cholesterol	6.26E-03	4	APOA4, HMGCR, IDI1, LSS
1	Lipid Metabolism	-	metabolism	metabolism of arachidonic acid	9.81E-03	2	CYP1B1, PTGS2
1	Lipid Metabolism	-	biosynthesis	biosynthesis of lipid	1.31E-05	10	APOA4, CHKA, CYP4A11, EDN2, FGF2, HMGCR, HSD3B7, IDI1, LSS, PTGS2
1	Lipid Metabolism	-	biosynthesis	biosynthesis of steroid	3.32E-04	5	FGF2, HMGCR, HSD3B7, IDI1, LSS
1	Lipid Metabolism	-	biosynthesis	biosynthesis of eicosanoid	1.44E-03	3	CYP4A11, EDN2, PTGS2
1	Lipid Metabolism	-	biosynthesis	biosynthesis of fatty acid	2.37E-03	4	APOA4, CYP4A11, EDN2, PTGS2

Supplementary Table S5.4B: Continued

Rank	Category	Sub-Category	Function	Function Annotation	p-value	# genes	genes
1	Lipid Metabolism	-	biosynthesis	biosynthesis of cholesterol	4.09E-03	3	HMGCR, IDI1, LSS
1	Lipid Metabolism	-	biosynthesis	biosynthesis of prostaglandin	7.21E-03	2	EDN2, PTGS2
1	Lipid Metabolism	-	modification	modification of polyunsaturated fatty acids	4.44E-05	5	ADH1C, ALB, CYP4A11, GSTA4, PTGS2
1	Lipid Metabolism	-	modification	modification of eicosanoid	3.27E-04	4	ADH1C, ALB, CYP4A11, PTGS2
1	Lipid Metabolism	-	modification	modification of fatty acid	1.03E-03	7	ACSL1, ADH1C, ALB, CYP4A11, GSTA4, HMGCR, PTGS2
1	Lipid Metabolism	-	modification	modification of hydroxyeicosatetraenoic acid	1.71E-03	2	ADH1C, ALB
1	Lipid Metabolism	-	modification	modification of lipid	3.08E-03	9	ACAT1, ACSL1, ADH1C, ALB, CYP1B1, CYP4A11, GSTA4, HMGCR, PTGS2
1	Lipid Metabolism	-	modification	modification of oleic acid	9.81E-03	2	ACSL1, CYP4A11
1	Lipid Metabolism	-	quantity	quantity of lipid	7.20E-05	14	ABCG2, ACAT1, ACSL1, AKR1B1, ALB, APOA4, CHKA, CYP8B1, GFRA2, HMGCR, IL1R1, PLIN2, PTGS2, STARD4
1	Lipid Metabolism	-	quantity	quantity of steroid	1.26E-04	9	ACAT1, ALB, APOA4, CHKA, CYP8B1, HMGCR, IL1R1, PTGS2, STARD4
1	Lipid Metabolism	-	quantity	quantity of cholesterol ester	2.51E-04	4	ACAT1, CHKA, CYP8B1, STARD4
1	Lipid Metabolism	-	quantity	quantity of sterol	3.36E-04	7	ACAT1, APOA4, CHKA, CYP8B1, HMGCR, PTGS2, STARD4
1	Lipid Metabolism	-	quantity	quantity of cholesterol	7.28E-03	5	ACAT1, APOA4, CYP8B1, HMGCR, STARD4
1	Lipid Metabolism	-	steroidogenesis	steroidogenesis	8.31E-05	5	FGF2, HMGCR, IDI1, IGFBP4, LSS
1	Lipid Metabolism	-	accumulation	accumulation of all-trans-retinyl esters	1.17E-04	2	DHRS3, PLIN2
1	Lipid Metabolism	-	clearance	clearance of vitamin A	1.17E-04	2	ADH1C, PLIN2
1	Lipid Metabolism	-	production	production of lipid	2.14E-04	8	ADH1C, ALB, CYP1B1, CYP4A11, EDN2, FGF2, IGFBP4, PTGS2
1	Lipid Metabolism	-	production	production of beta-estradiol	3.15E-03	2	CYP1B1, IGFBP4
1	Lipid Metabolism	-	production	production of eicosanoid	7.28E-03	4	ALB, CYP4A11, EDN2, PTGS2
1	Lipid Metabolism	-	production	delay in production of prostaglandin E2	1.09E-02	1	PTGS2
1	Lipid Metabolism	-	reduction	reduction of fatty acid	3.29E-04	3	GSTA4, HMGCR, PTGS2

Supplementary Table S5.4B: Continued

Rank	Category	Sub-Category	Function	Function Annotation	p-value	# genes	genes
1	Lipid Metabolism	-	reduction	reduction of lipid peroxide	1.15E-03	2	GSTA4, PTGS2
1	Lipid Metabolism	-	transport	transport of fatty acid	9.70E-04	4	ABCG2, ACSL1, ALB, PLIN2
1	Lipid Metabolism	-	transport	transport of lipid	1.37E-03	6	ABCG2, ACSL1, ALB, APOA4, CHKA, PLIN2
1	Lipid Metabolism	-	phospholipid flip-flop	phospholipid flip-flop of phosphatidylserine	1.06E-03	3	ABCG2, CDKN2A, PTGS2
1	Lipid Metabolism	-	conversion	conversion of arachidonic acid	2.38E-03	2	ALB, PTGS2
1	Lipid Metabolism	-	conversion	conversion of lipid	3.31E-03	5	ALB, CYP1B1, CYP4A11, HMGCR, PTGS2
1	Lipid Metabolism	-	conversion	conversion of fatty acid	4.09E-03	3	ALB, HMGCR, PTGS2
1	Lipid Metabolism	-	conversion	conversion of 5(S)-HETE	1.09E-02	1	ALB
1	Lipid Metabolism	-	oxidation	oxidation of eicosanoid	2.38E-03	2	ADH1C, PTGS2
1	Lipid Metabolism	-	efflux	efflux of lipid	4.50E-03	4	ACAT1, ACSL1, APOA4, LSS
1	Lipid Metabolism	-	induction	induction of lipid	8.47E-03	2	FGF2, PTGS2
1	Lipid Metabolism	-	concentration	concentration of arachidonic acid	1.09E-02	1	PTGS2
1	Lipid Metabolism	-	concentration	concentration of palmitic acid	1.09E-02	1	PTGS2
1	Lipid Metabolism	-	concentration	concentration of phosphatidylserine	1.09E-02	1	PTGS2
1	Lipid Metabolism	-	crystallization	crystallization of cholesterol	1.09E-02	1	ALB
1	Lipid Metabolism	-	excretion	excretion of beta-estradiol	1.09E-02	1	ABCG2
1	Lipid Metabolism	-	flux	flux of long chain fatty acid	1.09E-02	1	ACSL1
1	Lipid Metabolism	-	formation	formation of 5,8,11,14,17-eicosapentaenoic acid	1.09E-02	1	PTGS2
1	Lipid Metabolism	-	formation	formation of 6-keto-prostaglandin F1 alpha	1.09E-02	1	PTGS2
1	Lipid Metabolism	-	formation	formation of prostanoid	1.09E-02	1	PTGS2
1	Lipid Metabolism	-	generation	generation of 5,8,11,14,17-eicosapentaenoic acid	1.09E-02	1	PTGS2
2	Cellular Growth and Proliferation	Cellular Growth and Proliferation	proliferation	proliferation of tumor cell lines	1.08E-06	18	ACAT1, AKR1B10, CCNG2, CDKN2A, CHKA, CYP1B1, CYR61, FGF2, HDAC1, IGFBP1, IGFBP4, KLF2, MDM2, MMP9, PIWIL1, PTGS2, SLC9A3R1, TLE4
2	Cellular Growth and Proliferation	Cellular Growth and Proliferation	proliferation	proliferation of cell lines	2.75E-06	21	ACAT1, AKR1B1, AKR1B10, CCNG2, CDKN2A, CHKA, CYP1B1, CYR61, FGF2, HDAC1, HMGCR, IGFBP1, IGFBP4, KLF2, MDM2, MMP9, PIWIL1, PTGS2, SERPINF1, SLC9A3R1, TLE4

Supplementary Table S5.4B: Continued

Rank	Category	Sub-Category	Function	Function Annotation	p-value	# genes	genes
2	Cellular Growth and Proliferation	Cellular Growth and Proliferation	proliferation	proliferation of cells	1.29E-05	30	ABCG2, ACAT1, AKR1B1, AKR1B10, CADM1, CCNG2, CDKN2A, CHKA, CYP1B1, CYR61, EDN2, FGF2, FTH1, GJB1, HDAC1, HMGCR, HS6ST1, IGFBP1, IGFBP4, IL1R1, KLF2, MDM2, MMP9, NR6A1, PIWIL1, PTGS2, SERPINF1, SLC9A3R1, TLE4, UCHL1
2	Cellular Growth and Proliferation	Cellular Growth and Proliferation	proliferation	proliferation of eukaryotic cells	8.42E-05	25	ABCG2, ACAT1, AKR1B1, AKR1B10, CADM1, CCNG2, CDKN2A, CHKA, CYP1B1, CYR61, FGF2, HDAC1, HMGCR, HS6ST1, IGFBP1, IGFBP4, IL1R1, KLF2, MDM2, MMP9, PIWIL1, PTGS2, SERPINF1, SLC9A3R1, TLE4
2	Cellular Growth and Proliferation	Cellular Growth and Proliferation	proliferation	proliferation of tumor cells	4.90E-04	6	ABCG2, AKR1B1, CDKN2A, CYR61, FGF2, IL1R1
2	Cellular Growth and Proliferation	Cellular Growth and Proliferation	proliferation	arrest in proliferation of fibroblast cell lines	6.94E-04	2	AKR1B1, CDKN2A
2	Cellular Growth and Proliferation	Cellular Growth and Proliferation	proliferation	proliferation of fibroblast cell lines	1.16E-03	7	ACAT1, AKR1B1, CDKN2A, FGF2, IGFBP1, KLF2, MDM2
2	Cellular Growth and Proliferation	Cellular Growth and Proliferation	proliferation	proliferation of stem cells	2.05E-03	4	CDKN2A, CYR61, FGF2, HDAC1
2	Cellular Growth and Proliferation	Cellular Growth and Proliferation	proliferation	proliferation of epithelial cell lines	2.37E-03	4	CDKN2A, CYR61, FGF2, PTGS2
2	Cellular Growth and Proliferation	Cellular Growth and Proliferation	proliferation	proliferation of embryonic cell lines	2.70E-03	3	CDKN2A, FGF2, PTGS2
2	Cellular Growth and Proliferation	Cellular Growth and Proliferation	proliferation	proliferation of normal cells	5.93E-03	16	AKR1B1, CADM1, CCNG2, CDKN2A, CYR61, FGF2, HDAC1, HS6ST1, IGFBP1, IGFBP4, IL1R1, KLF2, MDM2, MMP9, PTGS2, SERPINF1
2	Cellular Growth and Proliferation	Cellular Growth and Proliferation	proliferation	proliferation of cancer cells	5.94E-03	4	ABCG2, AKR1B1, FGF2, IL1R1
2	Cellular Growth and Proliferation	Cellular Growth and Proliferation	growth	growth of cells	2.70E-05	26	AHSG, AKR1B1, ALB, ALCAM, CDKN2A, CHKA, CYR61, FGF2, FTH1, GFRA2, HDAC1, HMGCR, HSD3B7, IGFBP1, IGFBP4, IL1R1, KLF2, MDM2, MMP9, NEURL, PLIN2, PTGS2, SERPINF1, SLC12A4, SLC9A3R1, UCHL1

Supplementary Table S5.4B: Continued

Rank	Category	Sub-Category	Function	Function Annotation	p-value	# genes	genes
2	Cellular Growth and Proliferation	Cellular Growth and Proliferation	growth	growth of cancer cells	1.44E-03	5	CDKN2A, FGF2, HMGCR, IGFBP1, IL1R1
2	Cellular Growth and Proliferation	Cellular Growth and Proliferation	growth	growth of eukaryotic cells	2.10E-03	17	AHSG, AKR1B1, ALB, CDKN2A, CHKA, CYR61, FGF2, FTH1, HMGCR, IGFBP1, IGFBP4, IL1R1, KLF2, MDM2, PTGS2, SERPINF1, UCHL1
2	Cellular Growth and Proliferation	Cellular Growth and Proliferation	growth	growth of carcinoma cell lines	6.26E-03	4	AHSG, KLF2, MDM2, UCHL1
2	Cellular Growth and Proliferation	Cellular Growth and Proliferation	growth	growth of embryonic stem cells	7.21E-03	2	FGF2, SERPINF1
2	Cellular Growth and Proliferation	Cellular Growth and Proliferation	growth	growth of tumor cell lines	7.30E-03	11	AHSG, CDKN2A, CYR61, FGF2, FTH1, IGFBP1, IGFBP4, KLF2, MDM2, PTGS2, UCHL1
2	Cellular Growth and Proliferation	Cellular Growth and Proliferation	growth	arrest in growth of cells	8.42E-03	5	ALCAM, CDKN2A, IGFBP1, IL1R1, MDM2
2	Cellular Growth and Proliferation	Cellular Growth and Proliferation	colony formation	colony formation of carcinoma cell lines	4.15E-04	3	CADM1, CYR61, IGFBP4
2	Cellular Growth and Proliferation	Cellular Growth and Proliferation	colony formation	colony formation of tumor cell lines	4.50E-04	7	CADM1, CCNG2, CDKN2A, CYR61, FGF2, IGFBP4, PTGS2
2	Cellular Growth and Proliferation	Cellular Growth and Proliferation	colony formation	colony formation of eukaryotic cells	4.23E-03	8	CADM1, CCNG2, CDKN2A, CYR61, FGF2, IGFBP4, MMP9, PTGS2
2	Cellular Growth and Proliferation	Cellular Growth and Proliferation	expansion	expansion of embryonic stem cells	1.09E-02	1	FGF2
2	Cellular Growth and Proliferation	Cellular Growth and Proliferation	generation	generation of adipocytes	1.09E-02	1	PTGS2
2	Cellular Growth and Proliferation	Cell Death	survival	survival of carcinoma cell lines	8.19E-05	4	ABCG2, CADM1, MDM2, PTGS2
2	Cellular Growth and Proliferation	Cell Death	apoptosis	apoptosis of carcinoma cell lines	1.61E-03	5	CDKN2A, KLF2, MDM2, PTGS2, UCHL1
2	Cellular Growth and Proliferation	Cell Death	apoptosis	apoptosis of tumor cell lines	3.61E-03	15	ABCG2, CDKN2A, CHKA, CYP1B1, CYR61, FGF2, HDAC1, IGFBP1, IGFBP4, KLF2, MDM2, MMP9, PIWIL1, PTGS2, UCHL1
2	Cellular Growth and Proliferation	Cell Death	apoptosis	apoptosis of cell lines	7.52E-03	17	ABCG2, CDKN2A, CHKA, CYP1B1, CYR61, FGF2, FTH1, HDAC1, IGFBP1, IGFBP4, KLF2, MDM2, MMP9, PIWIL1, PTGS2, SERPINF1, UCHL1

Supplementary Table S5.4B: Continued

Rank	Category	Sub-Category	Function	Function Annotation	p-value	# genes	genes
2	Cellular Growth and Proliferation	Cell Death	necrosis	necrosis of hepatocytes	2.38E-03	2	IGFBP1, PTGS2
2	Cellular Growth and Proliferation	Cell Death	necrosis	necrosis of normal cells	2.54E-03	4	IGFBP1, KLF2, MMP9, PTGS2
2	Cellular Growth and Proliferation	Cell Death	necrosis	necrosis	6.62E-03	6	ALB, IGFBP1, IL1R1, KLF2, MMP9, PTGS2
2	Cellular Growth and Proliferation	Cell Death	cell death	cell death of tumor cell lines	2.83E-03	17	ABCG2, ALB, CDKN2A, CHKA, CYP1B1, CYR61, FGF2, FTH1, HDAC1, IGFBP1, IGFBP4, KLF2, MDM2, MMP9, PIWIL1, PTGS2, UCHL1
2	Cellular Growth and Proliferation	Cell Death	loss	delay in loss of cells	1.09E-02	1	SERPINF1
2	Cellular Growth and Proliferation	Cell Cycle	S phase	S phase of normal cells	2.05E-03	4	CCNG2, CDKN2A, FGF2, MDM2
2	Cellular Growth and Proliferation	Cell Cycle	S phase	S phase of cancer cells	2.38E-03	2	CDKN2A, FGF2
2	Cellular Growth and Proliferation	Cell Cycle	S phase	arrest in S phase of cancer cells	1.09E-02	1	CDKN2A
2	Cellular Growth and Proliferation	Cell Cycle	interphase	arrest in interphase of tumor cell lines	3.71E-04	7	CDKN2A, CHKA, CYP1B1, CYR61, FGF2, MDM2, MMP9
2	Cellular Growth and Proliferation	Cell Cycle	interphase	arrest in interphase of carcinoma cell lines	4.15E-04	3	CDKN2A, CYR61, MDM2
2	Cellular Growth and Proliferation	Cell Cycle	interphase	interphase of normal cells	6.48E-04	6	CCNG2, CDKN2A, CHKA, FGF2, MDM2, PTGS2
2	Cellular Growth and Proliferation	Cell Cycle	interphase	interphase of tumor cell lines	7.27E-04	8	CCNG2, CDKN2A, CHKA, CYP1B1, CYR61, FGF2, MDM2, MMP9
2	Cellular Growth and Proliferation	Cell Cycle	interphase	delay in interphase of fibroblast cell lines	1.15E-03	2	CDKN2A, HDAC1
2	Cellular Growth and Proliferation	Cell Cycle	interphase	interphase	1.26E-03	11	CCNG2, CDKN2A, CHKA, CYP1B1, CYR61, FGF2, HDAC1, MDM2, MMP9, PTGS2, TPD52L1
2	Cellular Growth and Proliferation	Cell Cycle	interphase	interphase of eukaryotic cells	1.37E-03	10	CCNG2, CDKN2A, CHKA, CYP1B1, CYR61, FGF2, HDAC1, MDM2, MMP9, PTGS2
2	Cellular Growth and Proliferation	Cell Cycle	interphase	interphase of cell lines	1.54E-03	9	CCNG2, CDKN2A, CHKA, CYP1B1, CYR61, FGF2, HDAC1, MDM2, MMP9
2	Cellular Growth and Proliferation	Cell Cycle	G0/G1 phase transition	arrest in G0/G1 phase transition of tumor cell lines	1.06E-03	3	CDKN2A, CHKA, MMP9

Supplementary Table S5.4B: Continued

Rank	Category	Sub-Category	Function	Function Annotation	p-value	# genes	genes
2	Cellular Growth and Proliferation	Cell Cycle	cell division process	arrest in cell division process of cell lines	2.84E-03	8	CCNG2, CDKN2A, CHKA, CYP1B1, CYR61, FGF2, MDM2, MMP9
2	Cellular Growth and Proliferation	Cell Cycle	cell division process	entry into cell division process of tumor cells	4.02E-03	2	CDKN2A, FGF2
2	Cellular Growth and Proliferation	Cell Cycle	cell division process	cell division process of hepatoma cell lines	7.21E-03	2	AHSG, CDKN2A
2	Cellular Growth and Proliferation	Cell Cycle	cell division process	cell division process of tumor cell lines	7.25E-03	9	AHSG, CCNG2, CDKN2A, CHKA, CYP1B1, CYR61, FGF2, MDM2, MMP9
2	Cellular Growth and Proliferation	Cell Cycle	cell division process	arrest in cell division process	8.65E-03	9	CCNG2, CDKN2A, CHKA, CYP1B1, CYR61, FGF2, MDM2, MMP9, PKD2 (includes EG:5311)
2	Cellular Growth and Proliferation	Cell Cycle	cell stage	entry into cell stage of tumor cells	2.38E-03	2	CDKN2A, FGF2
2	Cellular Growth and Proliferation	Cell Cycle	G1 phase	G1 phase of tumor cell lines	6.75E-03	5	CCNG2, CDKN2A, CYR61, FGF2, MDM2
2	Cellular Growth and Proliferation	Cell Cycle	G1 phase	arrest in G1 phase of tumor cell lines	1.01E-02	4	CDKN2A, CYR61, FGF2, MDM2
2	Cellular Growth and Proliferation	Cell Cycle	G2 phase	arrest in G2 phase of carcinoma cell lines	3.15E-03	2	CDKN2A, MDM2
2	Cellular Growth and Proliferation	Cell Cycle	G2 phase	G2 phase	7.28E-03	5	CCNG2, CDKN2A, HDAC1, MDM2, TPD52L1
2	Cellular Growth and Proliferation	Cell Cycle	G2 phase	arrest in G2 phase of tumor cells	1.09E-02	1	CDKN2A
2	Cellular Growth and Proliferation	Cell Cycle	checkpoint control	checkpoint control	4.49E-03	3	CCNG2, CDKN2A, MDM2
2	Cellular Growth and Proliferation	Cell Cycle	mitogenesis	mitogenesis	5.78E-03	5	AHSG, CDKN2A, CYR61, FGF2, PTGS2
2	Cellular Growth and Proliferation	Cell Cycle	senescence	senescence of tumor cell lines	9.81E-03	2	CDKN2A, FGF2
2	Cellular Growth and Proliferation	Cell Cycle	senescence	delay in senescence of fibroblasts	1.09E-02	1	CDKN2A
2	Cellular Growth and Proliferation	Cell Cycle	G2/M phase transition	delay in G2/M phase transition of fibroblast cell lines	1.09E-02	1	HDAC1
2	Cellular Growth and Proliferation	Cell Cycle	mitosis	entry into mitosis of tumor cells	1.09E-02	1	CDKN2A

Supplementary Table S5.4B: Continued

Rank	Category	Sub-Category	Function	Function Annotation	p-value	# genes	genes
3	Cancer	-	neoplasia	neoplasia	1.10E-05	37	ABCG2, ACAT1, ADH1C, AHSG, AKR1B1, AKR1B10, ALB, ALCAM, C9ORF150, CDKN2A, CYP1B1, CYP4A11, CYR61, F5, FGF2, FTH1, GJB1, GSTA4, GSTO1, HDAC1, HMGCR, IDI1, IGFBP1, IGFBP4, IL1R1, MDM2, MMP9, NEURL, PKD2 (includes EG:5311), PLIN2, PTGS2, RBPMS, SC4MOL, SERPINF1, SLC9A3R1, TPD52L1, UCHL1
3	Cancer	-	neoplasia	neoplasia of mice	1.01E-02	4	CDKN2A, CYP1B1, MMP9, PKD2 (includes EG:5311)
3	Cancer	-	carcinoma	carcinoma	1.67E-05	23	ACAT1, ADH1C, AHSG, AKR1B10, ALB, CDKN2A, CYP1B1, CYR61, FGF2, FTH1, GJB1, GSTA4, GSTO1, HDAC1, HMGCR, IDI1, IGFBP1, IGFBP4, MDM2, MMP9, PTGS2, SERPINF1, UCHL1
3	Cancer	-	liver tumor	liver tumor	1.72E-05	9	AKR1B10, CDKN2A, FGF2, GJB1, GSTO1, HDAC1, MDM2, MMP9, PTGS2
3	Cancer	-	tumor	tumor	2.33E-05	30	ABCG2, ACAT1, ADH1C, AHSG, AKR1B1, AKR1B10, ALB, ALCAM, C9ORF150, CDKN2A, CYP1B1, CYR61, FGF2, FTH1, GJB1, GSTA4, GSTO1, HDAC1, HMGCR, IDI1, IGFBP1, IGFBP4, IL1R1, MDM2, MMP9, PKD2 (includes EG:5311), PTGS2, RBPMS, SERPINF1, UCHL1
3	Cancer	-	malignant tumor	malignant tumor	2.92E-05	25	ACAT1, ADH1C, AHSG, AKR1B10, ALB, C9ORF150, CDKN2A, CYP1B1, CYR61, FGF2, FTH1, GJB1, GSTA4, GSTO1, HDAC1, HMGCR, IDI1, IGFBP1, IGFBP4, MDM2, MMP9, PTGS2, RBPMS, SERPINF1, UCHL1

Supplementary Table S5.4B: Continued

Rank	Category	Sub-Category	Function	Function Annotation	p-value	# genes	genes
3	Cancer	-	adenocarcinoma	adenocarcinoma	3.11E-05	12	ACAT1, ADH1C, ALB, CDKN2A, FGF2, FTH1, GJB1, HMGCR, IGFBP4, MDM2, MMP9, PTGS2
3	Cancer	-	clear-cell adenocarcinoma	clear-cell adenocarcinoma	3.54E-05	4	ACAT1, HMGCR, MDM2, MMP9
3	Cancer	-	hepatocellular carcinoma	hepatocellular carcinoma	5.37E-05	8	AKR1B10, CDKN2A, FGF2, GJB1, GSTO1, MDM2, MMP9, PTGS2
3	Cancer	-	cancer	cancer	6.02E-05	35	ABCG2, ACAT1, ADH1C, AHSG, AKR1B1, AKR1B10, ALB, ALCAM, C9ORF150, CDKN2A, CYP1B1, CYP4A11, CYR61, FGF2, FTH1, GJB1, GSTA4, GSTO1, HDAC1, HMGCR, IDI1, IGFBP1, IGFBP4, IL1R1, MDM2, MMP9, NEURL, PLIN2, PTGS2, RBPMS, SC4MOL, SERPINF1, SLC9A3R1, TPD52L1, UCHL1
3	Cancer	-	metastasis	metastasis of tumor	1.04E-04	5	AHSG, CDKN2A, FGF2, MMP9, PTGS2
3	Cancer	-	metastasis	metastasis of carcinoma	4.99E-03	2	AHSG, CDKN2A
3	Cancer	-	metastasis	metastasis	9.47E-03	8	AHSG, CDKN2A, CYP1B1, FGF2, HDAC1, HMGCR, MMP9, PTGS2
3	Cancer	-	benign tumor	benign tumor	1.57E-04	13	ACAT1, ALB, ALCAM, CDKN2A, CYP1B1, CYR61, FGF2, FTH1, GSTA4, GSTO1, HMGCR, MMP9, PTGS2
3	Cancer	-	liver cancer	liver cancer	3.73E-04	10	AKR1B10, CDKN2A, FGF2, GJB1, GSTO1, HDAC1, MDM2, MMP9, PTGS2, UCHL1
3	Cancer	-	benign nerve tumor	benign nerve tumor	4.19E-04	4	ACAT1, CDKN2A, FGF2, HMGCR
3	Cancer	-	quantity	quantity of tumor	5.34E-04	5	CDKN2A, CYP1B1, GJB1, MDM2, MMP9
3	Cancer	-	quantity	quantity of malignant tumor	1.88E-03	3	CYP1B1, GJB1, MDM2
3	Cancer	-	disease	disease of tumor	2.39E-03	6	AHSG, CDKN2A, CYP1B1, FGF2, MMP9, PTGS2
3	Cancer	-	tumorigenesis	tumorigenesis of malignant tumor	2.54E-03	4	AHSG, CDKN2A, CYP1B1, PTGS2

Supplementary Table S5.4B: Continued

Rank	Category	Sub-Category	Function	Function Annotation	p-value	# genes	genes
3	Cancer	-	tumorigenesis	tumorigenesis of mice	4.18E-03	6	CDKN2A, CYP1B1, MDM2, MMP9, PKD2 (includes EG:5311), PTGS2
3	Cancer	-	tumorigenesis	tumorigenesis of carcinoma	9.20E-03	3	AHSG, CDKN2A, PTGS2
3	Cancer	-	growth	growth of tumor	3.02E-03	6	AKR1B10, CDKN2A, GJB1, HDAC1, MMP9, PTGS2
3	Cancer	-	hyperplasia	hyperplasia of tissue	5.37E-03	3	CDKN2A, FGF2, MMP9
3	Cancer	-	transformation	transformation of normal cells	6.50E-03	5	CDKN2A, CYR61, FGF2, MDM2, MMP9
4	Hepatic System Disease	-	liver tumor	liver tumor	1.72E-05	9	AKR1B10, CDKN2A, FGF2, GJB1, GSTO1, HDAC1, MDM2, MMP9, PTGS2
4	Hepatic System Disease	-	intrahepatic cholestasis	intrahepatic cholestasis	3.17E-05	6	ABCG2, ACSL1, ADH1C, GJB1, HMGCR, HSD3B7
4	Hepatic System Disease	-	hepatocellular carcinoma	hepatocellular carcinoma	5.37E-05	8	AKR1B10, CDKN2A, FGF2, GJB1, GSTO1, MDM2, MMP9, PTGS2
4	Hepatic System Disease	-	liver cancer	liver cancer	3.73E-04	10	AKR1B10, CDKN2A, FGF2, GJB1, GSTO1, HDAC1, MDM2, MMP9, PTGS2, UCHL1
4	Hepatic System Disease	-	progressive familial intrahepatic cholestasis type 1	progressive familial intrahepatic cholestasis type 1	2.05E-03	4	ABCG2, ACSL1, ADH1C, HMGCR
4	Hepatic System Disease	-	hepatic system disorder	hepatic system disorder	6.53E-03	10	ABCG2, ACSL1, ADH1C, ALB, GJB1, HMGCR, HSD3B7, MMP9, PLIN2, PTGS2
5	Cellular Movement	-	movement	movement of cell lines	1.16E-04	13	ALCAM, ARHGEF4, CADM1, CDKN2A, CYR61, EDN2, FGF2, IGFBP1, IGFBP4, KLF2, MMP9, PTGS2, SLC9A3R1
5	Cellular Movement	-	movement	movement of eukaryotic cells	9.39E-04	17	AHSG, ALB, ALCAM, ARHGEF4, CADM1, CDKN2A, CYR61, EDN2, FGF2, HMGCR, IGFBP1, IGFBP4, KLF2, MMP9, PTGS2, SERPINF1, SLC9A3R1
5	Cellular Movement	-	migration	migration of tumor cell lines	3.50E-04	10	ARHGEF4, CDKN2A, CYR61, EDN2, FGF2, IGFBP1, IGFBP4, MMP9, PTGS2, SLC9A3R1

Supplementary Table S5.4B: Continued

Rank	Category	Sub-Category	Function	Function Annotation	p-value	# genes	genes
5	Cellular Movement	-	migration	migration of cell lines	3.55E-04	12	ALCAM, ARHGEF4, CDKN2A, CYR61, EDN2, FGF2, IGFBP1, IGFBP4, KLF2, MMP9, PTGS2, SLC9A3R1
5	Cellular Movement	-	migration	migration of eukaryotic cells	2.19E-03	16	AHSG, ALB, ALCAM, ARHGEF4, CDKN2A, CYR61, EDN2, FGF2, HMGCR, IGFBP1, IGFBP4, KLF2, MMP9, PTGS2, SERPINF1, SLC9A3R1
5	Cellular Movement	-	migration	migration of fibroblast cell lines	4.77E-03	4	CDKN2A, FGF2, KLF2, PTGS2
5	Cellular Movement	-	release	release of cells	4.02E-03	2	CADM1, MMP9
5	Cellular Movement	-	invasion	invasion of eukaryotic cells	6.56E-03	9	ACAT1, CDKN2A, CYP1B1, FGF2, GJB1, HDAC1, MMP9, PTGS2, SLC9A3R1
5	Cellular Movement	-	invasion	invasion of cell lines	9.47E-03	8	ACAT1, CDKN2A, CYP1B1, FGF2, GJB1, MMP9, PTGS2, SLC9A3R1
6	DNA Replication, Recombination, and Repair	-	synthesis	synthesis of DNA	1.61E-04	10	CDKN2A, CYR61, EDN2, FGF2, HDAC1, IGFBP1, IGFBP4, KLF2, MDM2, PTGS2
6	DNA Replication, Recombination, and Repair	-	repair	delay in repair of DNA	2.38E-03	2	CDKN2A, MDM2
6	DNA Replication, Recombination, and Repair	-	checkpoint control	checkpoint control	4.49E-03	3	CCNG2, CDKN2A, MDM2
6	DNA Replication, Recombination, and Repair	-	aberration	aberration of chromosomes	9.81E-03	2	CDKN2A, MDM2
6	DNA Replication, Recombination, and Repair	-	conversion	conversion of DNA	1.09E-02	1	FTH1
7	Cellular Development	Cellular Development	developmental process	developmental process of cancer cells	5.19E-04	6	CDKN2A, FGF2, HMGCR, IGFBP1, IL1R1, SERPINF1
7	Cellular Development	Cellular Development	cell spreading	cell spreading of eukaryotic cells	8.12E-03	5	ALB, CDKN2A, CYR61, FGF2, MMP9
7	Cellular Development	Cellular Development	cell spreading	cell spreading of cell lines	1.01E-02	4	CDKN2A, CYR61, FGF2, MMP9
7	Cellular Development	Cellular Development	development	development of cells	2.60E-03	17	ALB, ARHGEF4, CADM1, CDKN2A, CYR61, F5, FGF2, FTH1, GFRA2, HDAC1, IL1R1, KLF2, MDM2, MMP9, PIWIL1, PTGS2, VNN1

Supplementary Table S5.4B: Continued

Rank	Category	Sub-Category	Function	Function Annotation	p-value	# genes	genes
7	Cellular Development	Cellular Development	growth	growth of cancer cells	1.44E-03	5	CDKN2A, FGF2, HMGCR, IGFBP1, IL1R1
7	Cellular Development	Cellular Development	growth	growth of carcinoma cell lines	6.26E-03	4	AHSG, KLF2, MDM2, UCHL1
7	Cellular Development	Cellular Development	growth	growth of embryonic stem cells	7.21E-03	2	FGF2, SERPINF1
7	Cellular Development	Cellular Development	growth	growth of tumor cell lines	7.30E-03	11	AHSG, CDKN2A, CYR61, FGF2, FTH1, IGFBP1, IGFBP4, KLF2, MDM2, PTGS2, UCHL1
7	Cellular Development	Cellular Development	sprouting	sprouting of normal cells	2.70E-03	3	CYR61, FGF2, IL1R1
7	Cellular Development	Cellular Development	differentiation	differentiation of tissue	1.05E-02	3	CDKN2A, FGF2, VNN1
7	Cellular Development	Cellular Development	shape change	shape change of normal cells	5.34E-03	5	ALB, CDKN2A, CYR61, FGF2, IL1R1
7	Cellular Development	Cellular Development	shape change	shape change of eukaryotic cells	6.34E-03	7	ALB, ARHGEF4, CDKN2A, CYR61, FGF2, IL1R1, MMP9
7	Cellular Development	Cellular Development	immortalization	immortalization of fibroblasts	6.05E-03	2	CDKN2A, HDAC1
7	Cellular Development	Cellular Development	cell flattening	cell flattening of cell lines	9.81E-03	2	ARHGEF4, CDKN2A
7	Cellular Development	Cellular Development	cell flattening	delay in cell flattening of fibroblasts	1.09E-02	1	CDKN2A
7	Cellular Development	Cellular Development	expansion	expansion of embryonic stem cells	1.09E-02	1	FGF2
7	Cellular Development	Cellular Development	senescence	delay in senescence of fibroblasts	1.09E-02	1	CDKN2A
7	Cellular Development	Cell Morphology	tubulation	tubulation of eukaryotic cells	1.27E-03	4	ALCAM, CYR61, FGF2, SERPINF1
7	Cellular Development	Cell Morphology	cell spreading	cell spreading of eukaryotic cells	8.12E-03	5	ALB, CDKN2A, CYR61, FGF2, MMP9
7	Cellular Development	Cell Morphology	cell spreading	cell spreading of cell lines	1.01E-02	4	CDKN2A, CYR61, FGF2, MMP9
7	Cellular Development	Cell Morphology	sprouting	sprouting of normal cells	2.70E-03	3	CYR61, FGF2, IL1R1
7	Cellular Development	Cell Morphology	shape change	shape change of normal cells	5.34E-03	5	ALB, CDKN2A, CYR61, FGF2, IL1R1
7	Cellular Development	Cell Morphology	shape change	shape change of eukaryotic cells	6.34E-03	7	ALB, ARHGEF4, CDKN2A, CYR61, FGF2, IL1R1, MMP9
7	Cellular Development	Cell Morphology	size	size of cell lines	7.41E-03	3	ARHGEF4, CDKN2A, KLF2
7	Cellular Development	Cell Morphology	cell flattening	cell flattening of cell lines	9.81E-03	2	ARHGEF4, CDKN2A
7	Cellular Development	Cell Morphology	cell flattening	delay in cell flattening of fibroblasts	1.09E-02	1	CDKN2A
7	Cellular Development	Cell Morphology	area	area of gap junction plaques	1.09E-02	1	GJB1

Supplementary Table S5.4B: Continued

Rank	Category	Sub-Category	Function	Function Annotation	p-value	# genes	genes
8	Carbohydrate Metabolism	-	phospholipid flip-flop	phospholipid flip-flop of phosphatidylserine	1.06E-03	3	ABCG2, CDKN2A, PTGS2
8	Carbohydrate Metabolism	-	reduction	reduction of hexose	1.15E-03	2	AKR1B1, AKR1B10
8	Carbohydrate Metabolism	-	modification	modification of hexose	3.71E-03	3	AKR1B1, AKR1B10, IGFBP1
9	Drug Metabolism	-	conjugation	conjugation of glutathione	1.06E-03	3	CYP1B1, GSTA3, GSTA4
9	Drug Metabolism	-	production	production of beta-estradiol	3.15E-03	2	CYP1B1, IGFBP4
9	Drug Metabolism	-	production	delay in production of prostaglandin E2	1.09E-02	1	PTGS2
9	Drug Metabolism	-	accumulation	accumulation of topotecan	1.09E-02	1	ABCG2
9	Drug Metabolism	-	binding	binding of ketoprofen	1.09E-02	1	ALB
9	Drug Metabolism	-	efflux	efflux of mitoxantrone	1.09E-02	1	ABCG2
9	Drug Metabolism	-	excretion	excretion of beta-estradiol	1.09E-02	1	ABCG2
9	Drug Metabolism	-	excretion	excretion of mitoxantrone	1.09E-02	1	ABCG2
10	Cell-To-Cell Signaling and Interaction	-	activation	activation of eukaryotic cells	2.64E-03	11	ALB, CADM1, CDKN2A, EDN2, F5, FGF2, IL1R1, KLF2, MMP9, PTGS2, SERPINF1
10	Cell-To-Cell Signaling and Interaction	-	activation	activation of carcinoma cell lines	1.09E-02	1	CADM1
10	Cell-To-Cell Signaling and Interaction	-	area	area of gap junction plaques	1.09E-02	1	GJB1
10	Cell-To-Cell Signaling and Interaction	-	communication	communication of gap junctions	1.09E-02	1	GJB1
10	Cell-To-Cell Signaling and Interaction	-	contact growth inhibition	contact growth inhibition of embryonic cell lines	1.09E-02	1	ABCG2
10	Cell-To-Cell Signaling and Interaction	-	coupling	coupling of hepatoma cell lines	1.09E-02	1	GJB1
10	Cell-To-Cell Signaling and Interaction	-	formation	formation of intercellular channels	1.09E-02	1	GJB1
11	Cellular Organization and Maintenance	Cellular Function and Maintenance	contact growth inhibition	contact growth inhibition of embryonic cell lines	1.09E-02	1	ABCG2
11	Cellular Organization and Maintenance	Cellular Function and Maintenance	cytostasis	delay in cytostasis of fibroblasts	1.09E-02	1	CDKN2A
11	Cellular Organization and Maintenance	Cellular Assembly and Organization	biogenesis	biogenesis of ribosome	4.02E-03	2	CDKN2A, FGF2
11	Cellular Organization and Maintenance	Cellular Assembly and Organization	communication	communication of gap junctions	1.09E-02	1	GJB1
11	Cellular Organization and Maintenance	Cellular Assembly and Organization	formation	formation of intercellular channels	1.09E-02	1	GJB1
11	Cellular Organization and Maintenance	Cellular Assembly and Organization	shortening	delay in shortening of telomeres	1.09E-02	1	CDKN2A

Supplementary Table S5.4B: Continued

Rank	Category	Sub-Category	Function	Function Annotation	p-value	# genes	genes
12	Endocrine System Development and Function	-	production	production of beta-estradiol	3.15E-03	2	CYP1B1, IGFBP4
12	Endocrine System Development and Function	-	excretion	excretion of beta-estradiol	1.09E-02	1	ABCG2
13	Amino Acid Metabolism	-	metabolism	metabolism of sulfur amino acid	8.47E-03	2	CDO1, GNMT
13	Amino Acid Metabolism	-	auto-oxidation	auto-oxidation of homocysteine	1.09E-02	1	ALB
14	Nucleic Acid Metabolism	-	clearance	clearance of imatinib	1.09E-02	1	ABCG2
15	Gene Expression	-	activation	activation of p53 response element	8.47E-03	2	MDM2, PTGS2
15	Gene Expression	-	activation	activation of FGF-inducible response element	1.09E-02	1	FGF2
15	Gene Expression	-	activation	activation of c-MYC response element	1.09E-02	1	HDAC1
15	Gene Expression	-	binding	binding of Ets1 like site	1.09E-02	1	FGF2
15	Gene Expression	-	binding	binding of Kruppel-like factor 5 binding site	1.09E-02	1	HDAC1
15	Gene Expression	-	binding	binding of Lef binding site	1.09E-02	1	FGF2
15	Gene Expression	-	binding	binding of e2f-1 binding site	1.09E-02	1	MDM2
15	Gene Expression	-	gene silencing	gene silencing of synthetic promoter	1.09E-02	1	HDAC1
16	Post-Translational Modification	-	auto-oxidation	auto-oxidation of homocysteine	1.09E-02	1	ALB
17	Protein Synthesis	-	frameshifting	frameshifting of ribosome	1.09E-02	1	HDAC1

Supplementary Table S5.5A: Detailed list of enriched canonical pathways for genes that were differentially expressed following exposure to L-PFOS 10 μ M

Ingenuity Canonical Pathways	p-value	# genes	Genes
Metabolism of Xenobiotics by Cytochrome P450	8.71E-03	3	GSTA3, GSTA4, ADH1C
Bile Acid Biosynthesis	1.41E-02	2	ADH1C, HSD3B7
Glutathione Metabolism	1.62E-02	2	GSTA3, GSTA4
NRF2-mediated Oxidative Stress Response	2.19E-02	3	GSTA3, GSTA4, FTH1
Taurine and Hypotaurine Metabolism	2.75E-02	1	CDO1
Nicotinate and Nicotinamide Metabolism	2.95E-02	2	VNN1, ENPP2
PXR/RXR Activation	3.09E-02	2	IGFBP1, HMGCS2
LPS/IL-1 Mediated Inhibition of RXR Function	3.16E-02	3	GSTA3, GSTA4, HMGCS2
Lysine Biosynthesis	3.72E-02	1	VNN1
Synthesis and Degradation of Ketone Bodies	4.17E-02	1	HMGCS2
Ascorbate and Aldarate Metabolism	5.89E-02	1	GULO
C21-Steroid Hormone Metabolism	6.76E-02	1	HSD3B7
Aryl Hydrocarbon Receptor Signaling	8.51E-02	2	GSTA3, GSTA4
Nitrogen Metabolism	1.15E-01	1	VNN1
Cysteine Metabolism	1.19E-01	1	CDO1
Reelin Signaling in Neurons	1.67E-01	1	ARHGEF4
Sphingolipid Metabolism	1.79E-01	1	VNN1
Butanoate Metabolism	1.91E-01	1	HMGCS2
Tyrosine Metabolism	1.98E-01	1	ADH1C
Starch and Sucrose Metabolism	2.02E-01	1	ENPP2
Arginine and Proline Metabolism	2.06E-01	1	VNN1
Glycolysis/Gluconeogenesis	2.09E-01	1	ADH1C
Valine, Leucine and Isoleucine Degradation	2.13E-01	1	HMGCS2
Androgen and Estrogen Metabolism	2.13E-01	1	HSD3B7
Xenobiotic Metabolism Signaling	2.19E-01	2	GSTA3, GSTA4
VDR/RXR Activation	2.21E-01	1	IGFBP1
Glycerolipid Metabolism	2.36E-01	1	ADH1C
LXR/RXR Activation	2.39E-01	1	APOA4
IGF-1 Signaling	2.70E-01	1	IGFBP1
Estrogen Receptor Signaling	3.18E-01	1	IGFBP1
Hepatic Cholestasis	3.77E-01	1	HSD3B7
Fatty Acid Metabolism	3.77E-01	1	ADH1C
Actin Cytoskeleton Signaling	3.97E-01	1	ARHGEF4
Phospholipase C Signaling	4.44E-01	1	ARHGEF4
Acute Phase Response Signaling	4.72E-01	1	TTR
Molecular Mechanisms of Cancer	6.21E-01	1	ARHGEF4
Riboflavin Metabolism	5.50E-02	1	ENPP2
Pantothenate and CoA Biosynthesis	5.89E-02	1	ENPP2
Histidine Metabolism	1.40E-01	1	UROC1
IL-12 Signaling and Production in Macrophages	2.77E-01	1	IRF8
Dendritic Cell Maturation	3.08E-01	1	IRF8
Production of Nitric Oxide and Reactive Oxygen Species in Macrophages	3.61E-01	1	IRF8
Thrombin Signaling	3.97E-01	1	ARHGEF4
Breast Cancer Regulation by Stathmin1	4.11E-01	1	ARHGEF4
Purine Metabolism	5.37E-01	1	ENPP2
Axonal Guidance Signaling	5.66E-01	1	ADAM28

Supplementary Table S5.5B: Detailed list of enriched canonical pathways for genes that were differentially expressed following exposure to T-PFOS 10 μ M

Ingenuity Canonical Pathways	p-value	# genes	Genes
LPS/IL-1 Mediated Inhibition of RXR Function	1.95E-04	8	GSTA3, HS6ST1, GSTA4, HS3ST1, IL1R1, CYP4A11, ACSL1, GSTO1
LXR/RXR Activation	3.89E-04	5	APOA4, IL1R1, PTGS2, HMGCR, MMP9
Biosynthesis of Steroids	5.13E-04	3	IDI1, LSS, HMGCR
Aryl Hydrocarbon Receptor Signaling	8.91E-04	6	CDKN2A, GSTA3, GSTA4, MDM2, GSTO1, CYP1B1
Pyruvate Metabolism	1.26E-03	4	AKR1B10, ACAT1, AKR1B1, ACSL1
Bladder Cancer Signaling	1.38E-03	4	CDKN2A, FGF2, MDM2, MMP9
Cysteine Metabolism	3.02E-03	3	HS6ST1, HS3ST1, CDO1
Pentose and Glucuronate Interconversions	3.02E-03	3	UCHL1, AKR1B10, AKR1B1
Metabolism of Xenobiotics by Cytochrome P450	3.16E-03	5	GSTA3, GSTA4, ADH1C, GSTO1, CYP1B1
Fatty Acid Metabolism	4.47E-03	5	ADH1C, ACAT1, CYP4A11, ACSL1, CYP1B1
Pancreatic Adenocarcinoma Signaling	7.24E-03	4	CDKN2A, MDM2, PTGS2, MMP9
Glutathione Metabolism	1.05E-02	3	GSTA3, GSTA4, GSTO1
Glycine, Serine and Threonine Metabolism	1.12E-02	3	GNMT, CHKA, GATM
Hepatic Fibrosis / Hepatic Stellate Cell Activation	1.58E-02	4	IGFBP4, FGF2, IL1R1, MMP9
Xenobiotic Metabolism Signaling	1.62E-02	6	GSTA3, HS6ST1, GSTA4, HS3ST1, GSTO1, CYP1B1
Wnt/ β -catenin Signaling	1.66E-02	4	CDKN2A, HDAC1, TLE4, MDM2
Glycerolipid Metabolism	2.40E-02	3	AKR1B10, ADH1C, AKR1B1
Galactose Metabolism	3.02E-02	2	AKR1B10, AKR1B1
p53 Signaling	3.24E-02	3	CDKN2A, HDAC1, MDM2
Chronic Myeloid Leukemia Signaling	3.63E-02	3	CDKN2A, HDAC1, MDM2
IGF-1 Signaling	3.63E-02	3	IGFBP4, IGFBP1, CYR61
Ovarian Cancer Signaling	3.80E-02	3	CDKN2A, PTGS2, MMP9
Melanoma Signaling	3.98E-02	2	CDKN2A, MDM2
Chondroitin Sulfate Biosynthesis	4.17E-02	2	HS6ST1, HS3ST1
Keratan Sulfate Biosynthesis	4.17E-02	2	HS6ST1, HS3ST1
Cell Cycle: G2/M DNA Damage Checkpoint Regulation	4.17E-02	2	CDKN2A, MDM2
Airway Pathology in Chronic Obstructive Pulmonary Disease	4.27E-02	1	MMP9
Fructose and Mannose Metabolism	4.68E-02	2	AKR1B10, AKR1B1
NRF2-mediated Oxidative Stress Response	5.13E-02	4	GSTA3, GSTA4, GSTO1, FTH1
Acute Phase Response Signaling	5.89E-02	4	ALB, AHSG, SERPINF1, IL1R1
Taurine and Hypotaurine Metabolism	6.31E-02	1	CDO1
Arachidonic Acid Metabolism	6.76E-02	3	PTGS2, CYP4A11, CYP1B1
Cell Cycle: G1/S Checkpoint Regulation	6.76E-02	2	CDKN2A, HDAC1
Bile Acid Biosynthesis	6.76E-02	2	ADH1C, HSD3B7
Lysine Biosynthesis	8.32E-02	1	VNN1
Propanoate Metabolism	8.51E-02	2	ACAT1, ACSL1
Cyclins and Cell Cycle Regulation	9.33E-02	2	CDKN2A, HDAC1
Parkinson's Signaling	9.33E-02	1	UCHL1
Synthesis and Degradation of Ketone Bodies	9.33E-02	1	ACAT1
Hepatic Cholestasis	9.55E-02	3	IL1R1, HSD3B7, CYP8B1

Supplementary Table S5.5B: Continued

Ingenuity Canonical Pathways	p-value	# genes	Genes
Tryptophan Metabolism	9.55E-02	3	ACAT1, PTGS2, CYP1B1
Arginine and Proline Metabolism	1.00E-01	2	VNN1, GATM
Glycolysis/Gluconeogenesis	1.03E-01	2	ADH1C, ACSL1
DNA Methylation and Transcriptional Repression Signaling	1.23E-01	1	HDAC1
Ascorbate and Aldarate Metabolism	1.33E-01	1	GSTO1
Extrinsic Prothrombin Activation Pathway	1.43E-01	1	F5
HIF1 α Signaling	1.47E-01	2	MDM2, MMP9
C21-Steroid Hormone Metabolism	1.52E-01	1	HSD3B7
HGF Signaling	1.66E-01	2	CDKN2A, PTGS2
FXR/RXR Activation	1.69E-01	2	FETUB, CYP8B1
PPAR Signaling	1.69E-01	2	IL1R1, PTGS2
Glioma Signaling	1.81E-01	2	CDKN2A, MDM2
Urea Cycle and Metabolism of Amino Groups	1.88E-01	1	GATM
Inhibition of Angiogenesis by TSP1	2.06E-01	1	MMP9
MIF-mediated Glucocorticoid Regulation	2.15E-01	1	PTGS2
Intrinsic Prothrombin Activation Pathway	2.15E-01	1	F5
Glioblastoma Multiforme Signaling	2.25E-01	2	CDKN2A, MDM2
Neuroprotective Role of THOP1 in Alzheimer's Disease	2.32E-01	1	MMP9
PI3K/AKT Signaling	2.37E-01	2	MDM2, PTGS2
Role of Oct4 in Mammalian Embryonic Stem Cell Pluripotency	2.40E-01	1	NR6A1
Nitrogen Metabolism	2.48E-01	1	VNN1
Clathrin-mediated Endocytosis Signaling	2.49E-01	2	FGF2, MDM2
MIF Regulation of Innate Immunity	2.57E-01	1	PTGS2
Nur77 Signaling in T Lymphocytes	2.57E-01	1	HDAC1
Coagulation System	2.65E-01	1	F5
Docosahexaenoic Acid (DHA) Signaling	2.65E-01	1	SERPINF1
NF- κ B Signaling	2.86E-01	2	HDAC1, IL1R1
ILK Signaling	2.94E-01	2	PTGS2, MMP9
Eicosanoid Signaling	2.96E-01	1	PTGS2
IL-8 Signaling	2.98E-01	2	PTGS2, MMP9
ATM Signaling	3.04E-01	1	MDM2
Calcium-induced T Lymphocyte Apoptosis	3.12E-01	1	HDAC1
Actin Cytoskeleton Signaling	3.27E-01	2	ARHGEF4, FGF2
Glioma Invasiveness Signaling	3.34E-01	1	MMP9
Reelin Signaling in Neurons	3.49E-01	1	ARHGEF4
IL-10 Signaling	3.70E-01	1	IL1R1
Sphingolipid Metabolism	3.70E-01	1	VNN1
Lysine Degradation	3.84E-01	1	ACAT1
Molecular Mechanisms of Cancer	3.85E-01	3	CDKN2A, ARHGEF4, MDM2
IL-17 Signaling	3.91E-01	1	PTGS2
Myc Mediated Apoptosis Signaling	3.91E-01	1	CDKN2A
FGF Signaling	3.91E-01	1	FGF2
Butanoate Metabolism	3.91E-01	1	ACAT1
Phospholipase C Signaling	3.94E-01	2	ARHGEF4, HDAC1
Caveolar-mediated Endocytosis Signaling	3.97E-01	1	ALB
Non-Small Cell Lung Cancer Signaling	4.04E-01	1	CDKN2A
Tyrosine Metabolism	4.04E-01	1	ADH1C

Supplementary Table S5.5B: Continued

Ingenuity Canonical Pathways	p-value	# genes	Genes
Role of MAPK Signaling in the Pathogenesis of Influenza	4.10E-01	1	PTGS2
Starch and Sucrose Metabolism	4.10E-01	1	UCHL1
Colorectal Cancer Metastasis Signaling	4.13E-01	2	PTGS2, MMP9
Atherosclerosis Signaling	4.17E-01	1	MMP9
Small Cell Lung Cancer Signaling	4.24E-01	1	PTGS2
TGF- β Signaling	4.24E-01	1	HDAC1
Hypoxia Signaling in the Cardiovascular System	4.30E-01	1	MDM2
Valine, Leucine and Isoleucine Degradation	4.30E-01	1	ACAT1
Androgen and Estrogen Metabolism	4.30E-01	1	HSD3B7
HER-2 Signaling in Breast Cancer	4.36E-01	1	MDM2
VDR/RXR Activation	4.43E-01	1	IGFBP1
Prostate Cancer Signaling	4.67E-01	1	MDM2
Nicotinate and Nicotinamide Metabolism	4.72E-01	1	VNN1
PXR/RXR Activation	4.78E-01	1	IGFBP1
Linoleic Acid Metabolism	4.84E-01	1	CYP1B1
Human Embryonic Stem Cell Pluripotency	4.84E-01	1	FGF2
IL-1 Signaling	4.84E-01	1	IL1R1
Corticotropin Releasing Hormone Signaling	5.06E-01	1	PTGS2
Cholecystokinin/Gastrin-mediated Signaling	5.06E-01	1	PTGS2
HMGB1 Signaling	5.12E-01	1	IL1R1
p38 MAPK Signaling	5.12E-01	1	IL1R1
TR/RXR Activation	5.16E-01	1	MDM2
IL-6 Signaling	5.16E-01	1	IL1R1
Protein Ubiquitination Pathway	5.21E-01	2	UCHL1, MDM2
Hereditary Breast Cancer Signaling	5.22E-01	1	HDAC1
Role of Tissue Factor in Cancer	5.22E-01	1	CYR61
Glycerophospholipid Metabolism	5.33E-01	1	CHKA
Type I Diabetes Mellitus Signaling	5.33E-01	1	IL1R1
Role of Macrophages, Fibroblasts and Endothelial Cells in Rheumatoid Arthritis	5.35E-01	2	FGF2, IL1R1
Relaxin Signaling	5.48E-01	1	MMP9
Calcium Signaling	5.48E-01	1	HDAC1
Estrogen Receptor Signaling	5.92E-01	1	IGFBP1
Type II Diabetes Mellitus Signaling	5.96E-01	1	ACSL1
AMPK Signaling	5.96E-01	1	HMGCR

Supplementary Table S5.6: Detailed list of potential regulatory molecules and their interactions with genes that were dysregulated (FC > 1.5, p < 0.05) by exposure to L-PFOS or T-PFOS

molecule	Entrez Gene Name	Interacting molecules	Entrez Gene Name	Interaction	Fold Change	
					L-PFOS 10 μ M	T-PFOS 10 μ M
TP53	Tumor protein 53	CCNG2	cyclin G2	DIRECT		1.55
		CDKN2A	cyclin-dependent kinase inhibitor 2A (melanoma, p16, inhibits CDK4)	DIRECT		1.63
		CTSK	cathepsin K	DIRECT		-1.51
		ENPP2	ectonucleotide pyrophosphatase/phosphodiesterase 2	DIRECT	1.61	
		EPHA3	EPH receptor A3	DIRECT		1.82
		HAS2	hyaluronan synthase 2	DIRECT		
		HDAC1	histone deacetylase 1	DIRECT		1.58
		HS3ST1	heparan sulfate (glucosamine) 3-O-sulfotransferase 1	DIRECT		1.60
		INHBA	inhibin, beta A	DIRECT	1.84	
		MDM2	Mdm2 p53 binding protein homolog (mouse)	DIRECT		1.75
		PTGS2	prostaglandin-endoperoxide synthase 2 (prostaglandin G/H synthase and cyclooxygenase)	DIRECT		1.96
		RRM2	ribonucleotide reductase M2	DIRECT		2.22
		STK11	serine/threonine kinase 11	DIRECT		1.56
		THBS1	thrombospondin 1	DIRECT	1.81	1.70
		UCHL1	ubiquitin carboxyl-terminal esterase L1 (ubiquitin thiolesterase)	DIRECT		1.81
		ALB	albumin	indirect		-1.60
		AMOTL2	angiomin like 2	indirect		1.55
		AREG	amphiregulin	indirect		2.10
		CYR61	cysteine-rich, angiogenic inducer, 61	indirect		1.53
		FGF2	fibroblast growth factor 2 (basic)	indirect		1.55
		IGFBP4	insulin-like growth factor binding protein 4	indirect		-1.68
MMP9	matrix metalloproteinase 9 (gelatinase B, 92kDa gelatinase, 92kDa type IV collagenase)	indirect		-1.75		
PITX2	paired-like homeodomain 2	indirect	1.54	1.57		
SQSTM1	sequestosome 1	indirect		-1.52		
			TOTAL=	4	21	
MYC	v-myc myelocytomatosis viral oncogene homolog (avian)	ADM	adrenomedullin	DIRECT		1.88
		ALCAM	activated leukocyte cell adhesion molecule	DIRECT		1.82
		CDKN2A	cyclin-dependent kinase inhibitor 2A (melanoma, p16, inhibits CDK4)	DIRECT		1.63
		CYR61	cysteine-rich, angiogenic inducer, 61	DIRECT		1.53
		FTHI	ferritin, heavy polypeptide 1	DIRECT	-1.62	-1.62
		HDAC1	histone deacetylase 1	DIRECT		1.58
		INHBA	inhibin, beta A	DIRECT	1.84	
		KLF2	Kruppel-like factor 2 (lung)	DIRECT		1.78
		MDM2	Mdm2 p53 binding protein homolog (mouse)	DIRECT		1.75
PITX2	paired-like homeodomain 2	DIRECT	1.54	1.57		

Supplementary Table S5.6: Continued

molecule	Entrez Gene Name	Interacting molecules	Entrez Gene Name	Interaction	Fold Change	
					L-PFOS 10 μ M	T-PFOS 10 μ M
MYC	v-myc myelocytomatosis viral oncogene homolog (avian)	RRM2	ribonucleotide reductase M2	DIRECT		2.22
		SQSTM1	sequestosome 1	DIRECT		-1.52
		THBS1	thrombospondin 1	DIRECT	1.81	1.70
		TLE4	transducin-like enhancer of split 4 (E(sp1) homolog, Drosophila)	DIRECT		1.51
		ACAT1	acetyl-Coenzyme A acetyltransferase 1	indirect		-1.50
		CHKA	choline kinase alpha	indirect		1.59
		IGFBP1	insulin-like growth factor binding protein 1	indirect	1.69	1.94
		LYN	v-yes-1 Yamaguchi sarcoma viral related oncogene homolog	indirect	1.62	
		PDGFB	platelet-derived growth factor beta polypeptide (simian sarcoma viral (v-sis) oncogene homolog)	indirect	1.65	1.61
		PTGS2	prostaglandin-endoperoxide synthase 2 (prostaglandin G/H synthase and cyclooxygenase)	indirect		1.96
			TOTAL=	7	18	
HNF4A	hepatocyte nuclear factor 4, alpha	ACAT1	acetyl-Coenzyme A acetyltransferase 1	DIRECT		-1.50
		ACSL1	acyl-CoA synthetase long-chain family member 1	DIRECT		1.70
		AHSG	alpha-2-HS-glycoprotein	DIRECT		-1.87
		AKR1B1	aldo-keto reductase family 1, member B1 (aldose reductase)	DIRECT		-1.66
		APOA4	apolipoprotein A-IV	DIRECT	-2.03	-1.87
		ATP10A	ATPase, class V, type 10A	DIRECT		1.55
		CCNG2	cyclin G2	DIRECT		1.55
		CYP1B1	cytochrome P450, family 1, subfamily B, polypeptide 1	DIRECT		1.69
		CYP8B1	cytochrome P450, family 8, subfamily B, polypeptide 1	DIRECT		1.51
		FETUB	fetuin B	DIRECT		-1.61
		GJB1	gap junction protein, beta 1, 32kDa	DIRECT		-1.51
		GSTA4	glutathione S-transferase alpha 4	DIRECT	-2.03	-1.96
		GSTO1	glutathione S-transferase omega 1	DIRECT		-1.53
		HPS5 (includes EG:11234)	Hermansky-Pudlak syndrome 5	DIRECT		-1.84
		INHBA	inhibin, beta A	DIRECT	1.84	
		MDM2	Mdm2 p53 binding protein homolog (mouse)	DIRECT		1.75
		SERPINA10	serpin peptidase inhibitor, clade A (alpha-1 antitrypsin, antitrypsin), member 10	DIRECT		-1.55
		TNFAIP6	tumor necrosis factor, alpha-induced protein 6	DIRECT	1.52	
		TTR	transthyretin	DIRECT	1.50	
		UCHL1	ubiquitin carboxyl-terminal esterase L1 (ubiquitin thiolesterase)	DIRECT		1.81
PKP2	plakophilin 2	indirect	1.51	1.51		
			TOTAL=	6	18	
CTNNB1	catenin (cadherin-associated protein), beta 1, 88kDa	CDKN2A	cyclin-dependent kinase inhibitor 2A (melanoma, p16, inhibits CDK4)	DIRECT		1.63
		CYR61	cysteine-rich, angiogenic inducer, 61	DIRECT		1.53

Supplementary Table S5.6: Continued

molecule	Entrez Gene Name	Interacting molecules	Entrez Gene Name	Interaction	Fold Change	
					L-PFOS 10 μ M	T-PFOS 10 μ M
CTNNB1	catenin (cadherin-associated protein), beta 1, 88kDa	FGFBP1	fibroblast growth factor binding protein 1	DIRECT		2.08
		HDAC1	histone deacetylase 1	DIRECT		1.58
		PITX2	paired-like homeodomain 2	DIRECT	1.54	1.57
		PKD2 (includes EG:5311)	polycystic kidney disease 2 (autosomal dominant)	DIRECT		1.71
		PKP2	plakophilin 2	DIRECT	1.51	1.51
		SLC9A3R1	solute carrier family 9 (sodium/hydrogen exchanger), member 3 regulator 1	DIRECT		1.52
		AREG	amphiregulin	indirect		2.10
		BMP2	bone morphogenetic protein 2	indirect		1.52
		DIO2	deiodinase, iodothyronine, type II	indirect		2.22
		FGF2	fibroblast growth factor 2 (basic)	indirect		1.55
		FZD4	frizzled homolog 4 (Drosophila)	indirect	1.71	2.06
		IL1R1	interleukin 1 receptor, type I	indirect		1.71
		MMP9	matrix metalloproteinase 9 (gelatinase B, 92kDa gelatinase, 92kDa type IV collagenase)	indirect		-1.75
			TOTAL=	3	15	
PPARG	peroxisome proliferator-activated receptor gamma	ABCG2	ATP-binding cassette, sub-family G (WHITE), member 2	DIRECT	1.94	2.09
		ACSL1	acyl-CoA synthetase long-chain family member 1	DIRECT		1.70
		CYP4A11	cytochrome P450, family 4, subfamily A, polypeptide 11	DIRECT		-1.60
		HDAC1	histone deacetylase 1	DIRECT		1.58
		HMGCS2	3-hydroxy-3-methylglutaryl-Coenzyme A synthase 2 (mitochondrial)	DIRECT	-1.65	
		IGFBP1	insulin-like growth factor binding protein 1	DIRECT	1.69	1.94
		KLF2	Kruppel-like factor 2 (lung)	DIRECT		1.78
		KRT20	keratin 20	DIRECT		1.60
		PLIN2	perilipin 2	DIRECT		1.93
		PTGS2	prostaglandin-endoperoxide synthase 2 (prostaglandin G/H synthase and cyclooxygenase)	DIRECT		1.96
		VNN1	vanin 1	DIRECT	1.53	1.62
		ADM	adrenomedullin	indirect		1.88
		BMP2	bone morphogenetic protein 2	indirect		1.52
		EDN2	endothelin 2	indirect	2.20	2.50
		EPHX2	epoxide hydrolase 2, cytoplasmic	indirect	1.58	
FGF2	fibroblast growth factor 2 (basic)	indirect		1.55		
			TOTAL=	6	14	
SP1	Sp1 transcription factor	ACSL1	acyl-CoA synthetase long-chain family member 1	DIRECT		1.70
		CDKN2A	cyclin-dependent kinase inhibitor 2A (melanoma, p16, inhibits CDK4)	DIRECT		1.63
		FGF2	fibroblast growth factor 2 (basic)	DIRECT		1.55

Supplementary Table S5.6: Continued

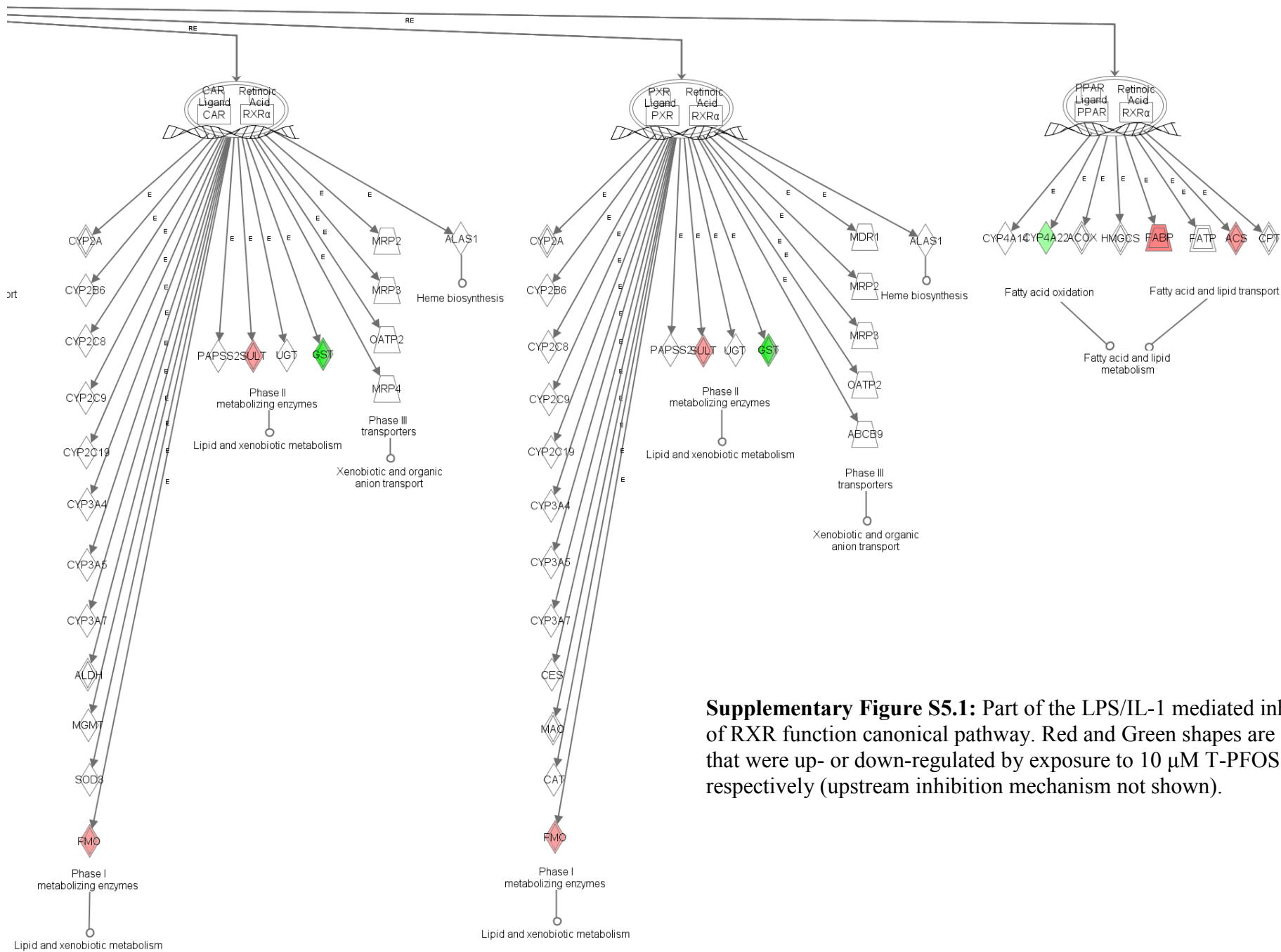
molecule	Entrez Gene Name	Interacting molecules	Entrez Gene Name	Interaction	Fold Change	
					L-PFOS 10 μ M	T-PFOS 10 μ M
SP1	Sp1 transcription factor	HDAC1	histone deacetylase 1	DIRECT		1.58
		IGFBP1	insulin-like growth factor binding protein 1	DIRECT	1.69	1.94
		IGFBP4	insulin-like growth factor binding protein 4	DIRECT		-1.68
		IRF8	interferon regulatory factor 8	DIRECT	1.56	
		KRT19	keratin 19	DIRECT		1.52
		MDM2	Mdm2 p53 binding protein homolog (mouse)	DIRECT		1.75
		MMP9	matrix metalloproteinase 9 (gelatinase B, 92kDa gelatinase, 92kDa type IV collagenase)	DIRECT		-1.75
		PDGFB	platelet-derived growth factor beta polypeptide (simian sarcoma viral (v-sis) oncogene homolog)	DIRECT	1.65	1.61
		PTGS2	prostaglandin-endoperoxide synthase 2 (prostaglandin G/H synthase and cyclooxygenase)	DIRECT		1.96
		INHBA	inhibin, beta A	indirect	1.84	
		TOTAL=	4	11		
SREPF1	Sterol regulatory element binding transcription factor 1	ACSL1	acyl-CoA synthetase long-chain family member 1	DIRECT		1.70
		ADH1C (includes EG:126)	alcohol dehydrogenase 1C (class I), gamma polypeptide	DIRECT	-1.64	-2.02
		CYP8B1	cytochrome P450, family 8, subfamily B, polypeptide 1	DIRECT		1.51
		HDAC1	histone deacetylase 1	DIRECT		1.58
		HMGCR	3-hydroxy-3-methylglutaryl-Coenzyme A reductase	DIRECT		1.89
		HMGCS2	3-hydroxy-3-methylglutaryl-Coenzyme A synthase 2 (mitochondrial)	DIRECT	-1.65	
		IAPP	islet amyloid polypeptide	DIRECT	1.79	
		IDI1	isopentenyl-diphosphate delta isomerase 1	DIRECT		1.58
		KLF2	Kruppel-like factor 2 (lung)	DIRECT		1.78
		LSS	lanosterol synthase (2,3-oxidosqualene-lanosterol cyclase)	DIRECT		1.69
		SC4MOL	sterol-C4-methyl oxidase-like	DIRECT		1.71
		SIK1	salt-inducible kinase 1	DIRECT		1.62
		STARD4	StAR-related lipid transfer (START) domain containing 4	DIRECT		1.57
		PDGFB	platelet-derived growth factor beta polypeptide (simian sarcoma viral (v-sis) oncogene homolog)	indirect	1.65	1.61
		TOTAL=	4	12		
CEBPB	CCAAT/enhancer binding protein (C/EBP), beta	ADH1C (includes EG:126)	alcohol dehydrogenase 1C (class I), gamma polypeptide	DIRECT	-1.64	-2.02
		ALB	albumin	DIRECT		-1.60
		BATF3	basic leucine zipper transcription factor, ATF-like 3	DIRECT	1.64	2.13
		CDO1	cysteine dioxygenase, type I	DIRECT	-1.65	-1.92
		HDAC1	histone deacetylase 1	DIRECT		1.58
		IGFBP1	insulin-like growth factor binding protein 1	DIRECT	1.69	1.94
		MGP	matrix Gla protein	DIRECT		-1.86

Supplementary Table S5.6: Continued

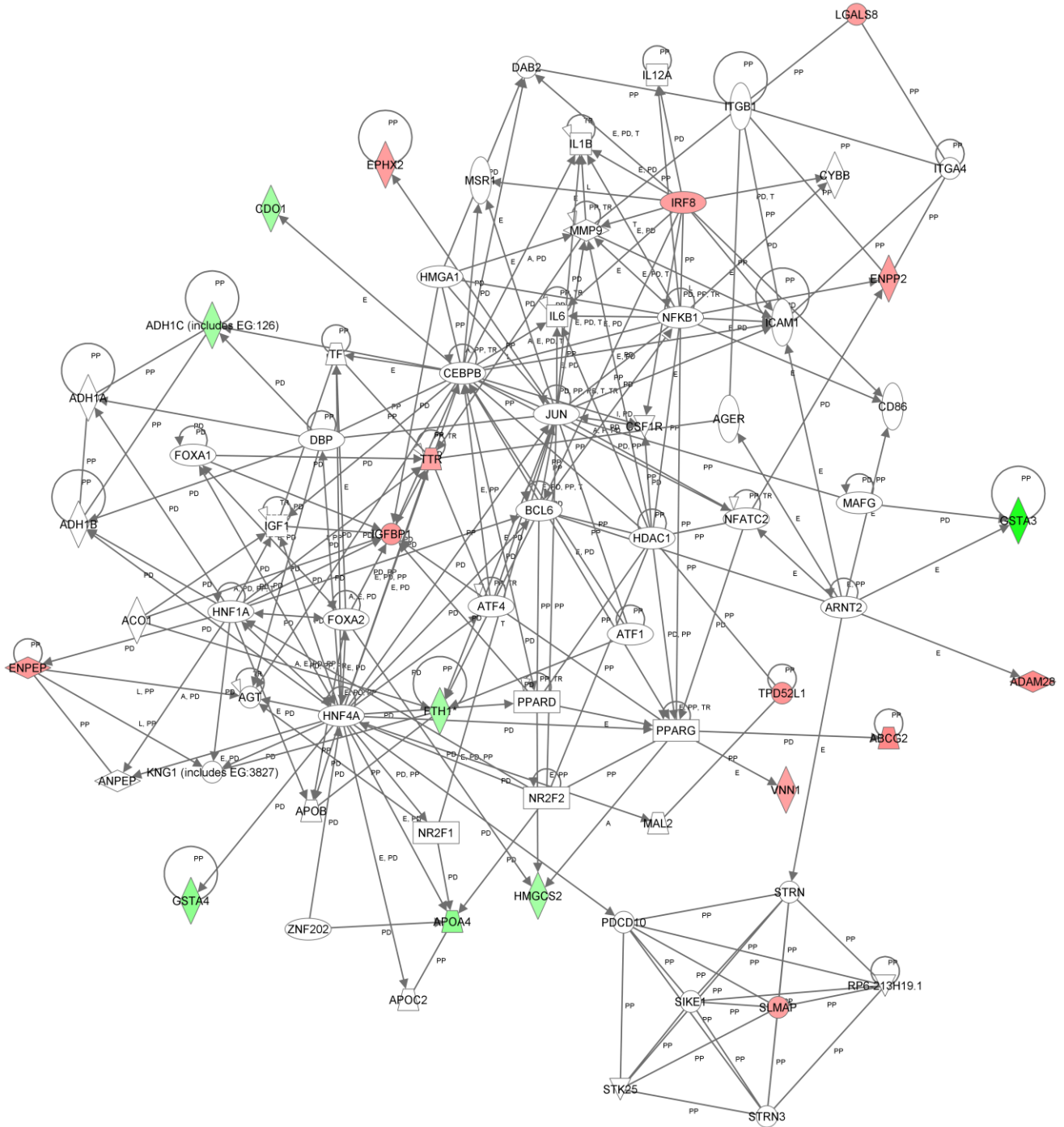
molecule	Entrez Gene Name	Interacting molecules	Entrez Gene Name	Interaction	Fold Change	
					L-PFOS 10 μ M	T-PFOS 10 μ M
CEBPB	CCAAT/enhancer binding protein (C/EBP), beta	PTGS2	prostaglandin-endoperoxide synthase 2 (prostaglandin G/H synthase and cyclooxygenase)	DIRECT		1.96
		TNFAIP6	tumor necrosis factor, alpha-induced protein 6	DIRECT	1.52	
		FGF2	fibroblast growth factor 2 (basic)	indirect		1.55
		FKBP6	FK506 binding protein 6, 36kDa	indirect	2.31	2.13
		LYN	v-yes-1 Yamaguchi sarcoma viral related oncogene homolog	indirect	1.62	
				TOTAL=	7	10
HDAC1	histone deacetylase 1	CDKN2A	cyclin-dependent kinase inhibitor 2A (melanoma, p16, inhibits CDK4)	DIRECT		1.63
		CTSK	cathepsin K	DIRECT		-1.51
		HDAC1	histone deacetylase 1	DIRECT		1.58
		MDM2	Mdm2 p53 binding protein homolog (mouse)	DIRECT		1.75
		MMP9	matrix metalloproteinase 9 (gelatinase B, 92kDa gelatinase, 92kDa type IV collagenase)	DIRECT		-1.75
		PTGS2	prostaglandin-endoperoxide synthase 2 (prostaglandin G/H synthase and cyclooxygenase)	DIRECT		1.96
		RRM2	ribonucleotide reductase M2	DIRECT		2.22
		TPD52L1	tumor protein D52-like 1	DIRECT	1.73	1.58
				TOTAL=	1	8
CDKN2A	cyclin-dependent kinase inhibitor 2A (melanoma, p16, inhibits CDK4)	CCNG2	cyclin G2	DIRECT		1.55
		EPHA3	EPH receptor A3	DIRECT		1.82
		HDAC1	histone deacetylase 1	DIRECT		1.58
		MDM2	Mdm2 p53 binding protein homolog (mouse)	DIRECT		1.75
		MYL12A	myosin, light chain 12A, regulatory, non-sarcomeric	DIRECT		1.56
		RRM2	ribonucleotide reductase M2	DIRECT		2.22
		CDKN2A	cyclin-dependent kinase inhibitor 2A (melanoma, p16, inhibits CDK4)	indirect		1.63
LYN	v-yes-1 Yamaguchi sarcoma viral related oncogene homolog	indirect	1.62			
				TOTAL=	1	7
ESRRA	estrogen-related receptor alpha	ACSL1	acyl-CoA synthetase long-chain family member 1	DIRECT		1.70
		CDKN2A	cyclin-dependent kinase inhibitor 2A (melanoma, p16, inhibits CDK4)	DIRECT		1.63
		CHKA	choline kinase alpha	DIRECT		1.59
		HMGCR	3-hydroxy-3-methylglutaryl-Coenzyme A reductase	DIRECT		1.89
		ID11	isopentenyl-diphosphate delta isomerase 1	DIRECT		1.58
		MYH6	myosin, heavy chain 6, cardiac muscle, alpha	DIRECT	3.34	3.42
				TOTAL=	1	6

Supplementary Table S5.6: Continued

molecule	Entrez Gene Name	Interacting molecules	Entrez Gene Name	Interaction	Fold Change	
					L-PFOS 10 μ M	T-PFOS 10 μ M
MDM2	Mdm2 p53 binding protein homolog (mouse)	CCNG2	cyclin G2	DIRECT		1.55
		CDKN2A	cyclin-dependent kinase inhibitor 2A (melanoma, p16, inhibits CDK4)	DIRECT		1.63
		HDAC1	histone deacetylase 1	DIRECT		1.58
		IRF8	interferon regulatory factor 8	DIRECT	1.56	
		MDM2	Mdm2 p53 binding protein homolog (mouse)	DIRECT		1.75
		FGF2	fibroblast growth factor 2 (basic)	indirect		1.55
		PTGS2	prostaglandin-endoperoxide synthase 2 (prostaglandin G/H synthase and cyclooxygenase)	indirect		1.96
				TOTAL=	1	6
MYCN	v-myc myelocytomatosis viral related oncogene, neuroblastoma derived (avian)	AMOTL2	angiomin like 2	DIRECT		1.55
		CDKN2A	cyclin-dependent kinase inhibitor 2A (melanoma, p16, inhibits CDK4)	DIRECT		1.63
		INHBA	inhibin, beta A	DIRECT	1.84	
		MDM2	Mdm2 p53 binding protein homolog (mouse)	DIRECT		1.75
		MYL12A	myosin, light chain 12A, regulatory, non-sarcomeric	DIRECT		1.56
		UCHL1	ubiquitin carboxyl-terminal esterase L1 (ubiquitin thiolesterase)	DIRECT		1.81
				TOTAL=	1	5

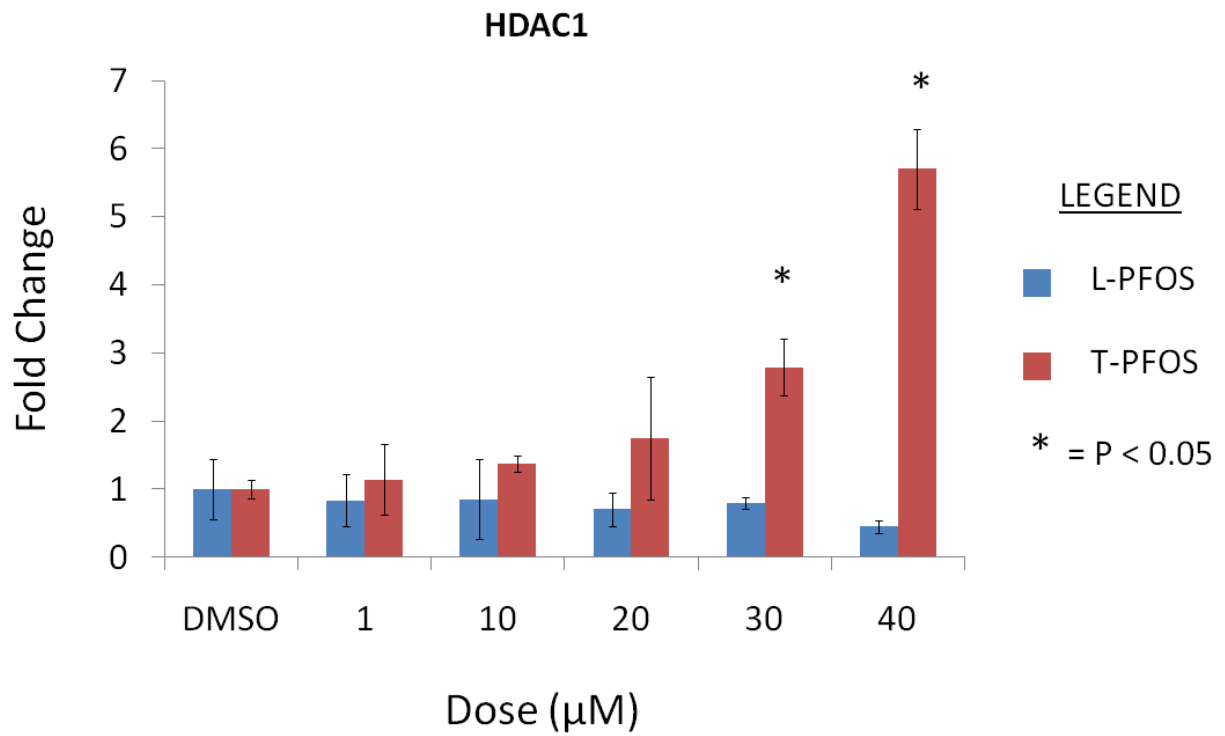


Supplementary Figure S5.1: Part of the LPS/IL-1 mediated inhibition of RXR function canonical pathway. Red and Green shapes are genes that were up- or down-regulated by exposure to 10 μM T-PFOS, respectively (upstream inhibition mechanism not shown).



© 2000-2010 Ingenuity Systems, Inc. All rights reserved.

Supplementary Figure S5.2: IPA generated interaction network for genes that were differentially expressed following L-PFOS 10 μ M.



Supplementary Figure S5.5: Expression of HDAC1 in sub-pooled CEH (N=2-3 sub-pools, 6 livers/pool) following exposure to L-PFOS or T-PFOS.